POTASSIUM CURRENT REGULATION AND INTRACELLULAR CALCIUM STORES IN RAT CEREBELLAR GRANULE NEURONS.

DAVID FRANK BOYD

A thesis submitted for the degree of Doctor of Philosophy

Department of Pharmacology,
Medawar Building,
University College London,
Gower Street,
London.
WC1E 6BT.

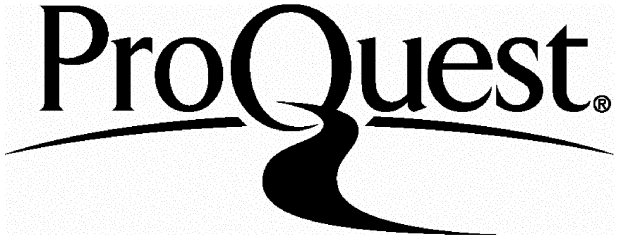

ACKNOWLEDGEMENTS

I would like to thank Dr Alistair Mathie, my PhD supervisor, for his support throughout the course of this project, not least in teaching me the necessary techniques and willingly proof reading this report.

In addition, I would like to express my gratitude to those who I have shared laboratory space with, Dr Kishani Ranatunga, Catherine Clarke, and in particular to Dr Julie Millar and Shuk Yin Yeung with whom the tissue culture duties where shared for the first two years.

I extend my thanks to include all those in the 'Dolphinarium' at UCL and in the Neuronal Excitability group at Imperial College, who have created a friendly atmosphere in which to work. In particular to Dr Brian Robertson who has seemingly undwindling supplies of the Journal of Physiology.

Finally I would like to thank my sponsors, the Medical Research Council and Merck Sharp and Dohme. Also to the physiological society for the travel grant which allowed me to present data in Chile.

ABSTRACT

Cerebellar granule neurons (CGNs) possess a standing outward potassium current (IK_{SO}) which shares many properties with the two-pore domain potassium channel TASK-1. This thesis extends the characterisation of IK_{SO} and considers its modulation by muscarinic M_3 receptor activation concentrating, in particular, on the role of intracellular calcium.

IK_{SO} was found to be permeable to other monovalent cations with a permeability sequence $Tl^+ = Rb^+ = K^+ >> Cs^+ > NH_4^+ > Li^+$. IK_{SO} was inhibited by muscarine (10μM; 70 ± 2%, n = 61) and histamine (30μM; 25.8 ± 7.3%, n = 6 out of 9).

Muscarine (10μM) was only able to evoke a rise in intracellular calcium concentration ($[Ca^{2+}]_i$) in a small proportion of CGN (9%). The thapsigargin sensitive, intracellular calcium stores in CGN were found to be depleted at rest and this may underlie the lack of calcium response to muscarine. In this respect, a prior depolarisation with potassium, which is shown to load calcium stores, increased the size of the calcium response and the proportion of CGN responding to muscarine (to 51%).

Raising $[Ca^{2+}]_i$ with ionomycin (1μM) elicited a small decrease in IK_{SO} (14 ± 4%, n=7). Thus, elevations in $[Ca^{2+}]_i$ do not appear to mediate muscarinic inhibition of IK_{SO}. Muscarinic inhibition of IK_{SO} was unaffected by the inhibitors of mitogen activated protein kinase kinase (MEK), PD 98059 and U 0126. While phorbol 12-myristate 13-acetate (PMA) had no effect on IK_{SO} amplitude, it did diminish muscarinic inhibition of IK_{SO}. Surprisingly, PD 98059 and U 0126 concentration dependently diminished IK_{SO} amplitude (at 30μM by 48 ± 1% (n = 10) and 46 ± 3% (n = 7), respectively) in a voltage insensitive manner. The mechanism of block by these compounds remains unknown but is not believed to be due to an action on MEK.

LIST OF CONTENTS

Chapter 1. General Introduction

Chapter 2 Materials and Methods

Chapter 3. Potassium current in cerebellar granule neurons

Chapter 4. Intracellular calcium regulation in cerebellar granule neurons

Chapter 5. Mitochondrial control of cytoplasmic calcium in cerebellar granule neurons

Chapter 6. Properties of intracellullar calcium stores in cerebellar granule neurons.

Chapter 7. Regulation of IK_{SO} by intracellular messengers.

LIST OF FIGURES

Chapter 1.

Chapter 2

Chapter 3

Chapter 4

Chapter 5

Chapter 6

Chapter 7

LIST OF TABLES

Chapter 1

Chapter 3

Abbreviations

The following abbreviations have been used in this report. Initially these have been cited in full after which only the abbreviation has been used.

$[Ca^{2+}]_i$	Intracellular calcium concentration
AMPA	α-amino-3-hydroxy-5-methyl-4-isoxazole propionic acid
ATP	Adenosine trisphosphate
BK_{Ca}	Large conductance calcium sensitive potassium channel
Ca^{2+}	Calcium
CCCP	Carbonyl cyanide *m*-chlorophenylhydrazone
CGN	Cerebellar granule neuron
CICR	Calcium induced calcium release
CIF	Calcium influx factor
CRAC	Calcium release activated channel
DAG	Diacylglycerol
DHP	Dihydropryidine
E_X	Reversal potential for the ion X
GABA	γ-aminobutyric acid
HVA	High voltage activated (voltage-gated calcium channel)
IP_3	Inositol 1,4,5-trisphosphate
IP_3R	Inositol 1,4,5-trisphosphate receptor
IVA	Intermediate activated (voltage-gated calcium channel)
K^+	Potassium
Kir	Inwardly rectifying potassium channel
Kv	Voltage-gated potassium channel
LVA	Low voltage activated (voltage-gated calcium channel)
MAPK	Mitogen activated protein kinase
NMDA	N-methyl D-aspartate
PKC	Protein Kinase C
PLC	Phospholipase C
PMA	Phorbolmyristate acetate
PMCA	Plasma membrane calcium ATPase

Ry	Ryanodine
RyR	Ryanodine receptor
SERCA	Sacro/endoplasmic reticulum calcium ATPase
SK_{Ca}	Small conductance calcium sensitive potassium channel
TASK	TWIK related acid sensitive potassium channel
TEA	Tetraethylammonium
TM	Transmembrane
TOK	Tandem-pore outward potassium channel
TRAAK	TWIK related arachadonic acid sensitive potassium channel
TREK	TWIK - related potassium channel
trp	Transient receptor potential
TTX	Tetrodotoxin
TWIK	Tandem pore weak inwardly rectifying potassium channel

Chapter 1.

General Introduction

1. INTRODUCTION

1.1 Organisation of the cerebellum.

The brain can be divided into three major anatomical regions, the fore, mid and the hindbrain, see figure 1.1. Each region can be further subdivided into distinct structures.

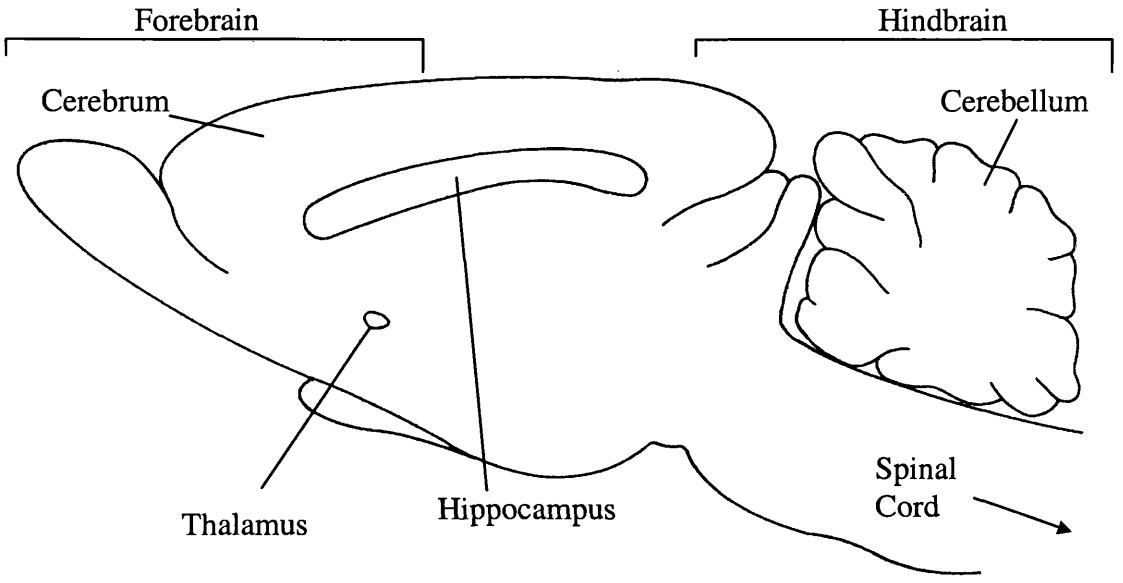

Figure 1.1 Basic anatomy of the rat brain.

The cerebellum is located at the back of the brain, dorsal to the midbrain and caudal to the corpus callosum and is divided into hemispheres, whose surfaces are highly convoluted, giving the cerebellum a characteristic laminated appearance. Each fold is known as a folium. The cerebellum is a highly ordered structure which contains more cells that the rest of the brain.

The cerebellum consists of five types of neuron, figures 1.2 & 1.3; Purkinje, granule, golgi, basket and stellate, and can be divided up into 'layers' according to its morphology. Towards the interior of the cerebellar cortex is the granule cell layer. The granule cell layer, consists of tightly packed granule neurons, golgi cells and the axons of Purkinje cells. Caudal to the granule cell layer is the Purkinje layer where the Purkinje cell and basket cell bodies reside. Beyond the Purkinje cell layer unmyelinated axonal projections of the granule cells extend to form parallel fibres. This region of grey matter contains comparatively few cell bodies.

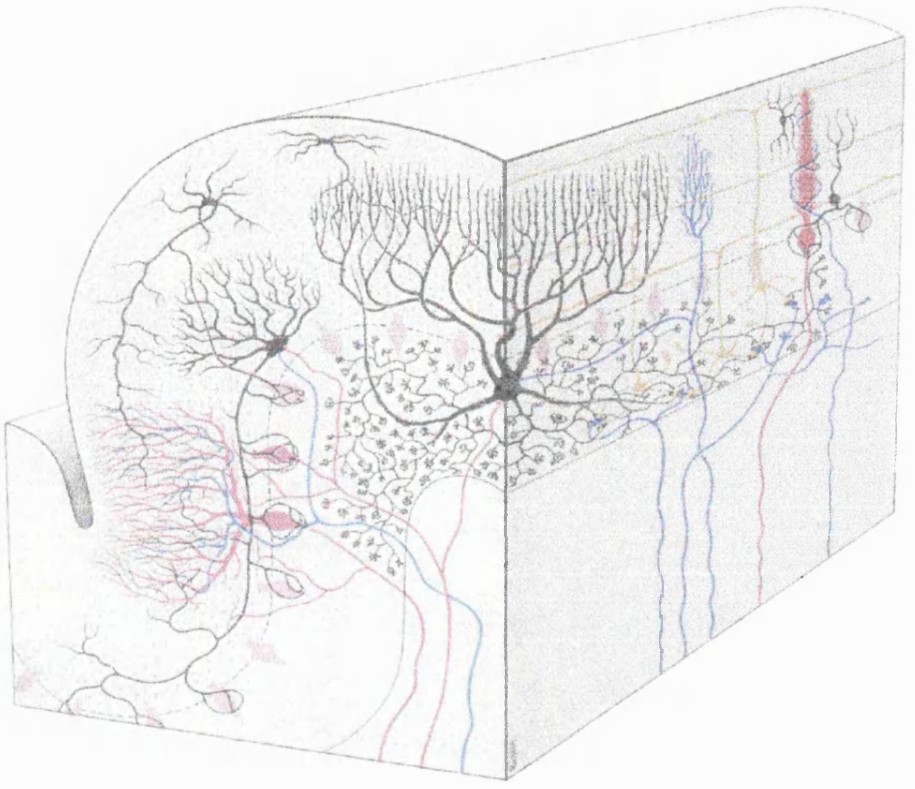

Figure 1.2. General organisation of the cerebellum.

Only one folium is shown in sagittal and transverse planes. The diagram shows the five neurons of the cerebellum. Granule cells are shown in yellow with axons forming the parallel fibres of the molecular layer. Large Purkinje neurons are shown in red. Inhibitory interneurons (golgi, stellate and basket) are shown in black and cerebellar inputs are shown in blue. Dotted lines represent the borders of the three layers of the cortex. Figure taken from Williams and Warwick, 1975.

Granule neurons are small glutaminergic interneurons which are by far the most numerous cell type in the brain. Some estimations suggest that, numbering in the region 10^{10} to 10^{11}, there are more cerebellar granule cells than there are all other neurons in the remained of the brain (Herrup and Kuemerle, 1997). Granule neurons receive inputs from mossy fibres which originate from an extracerebellar source, cerebellar nuclei or from the axons of brush cells which lie within the granule cell layer (Voogd & Glickstein 1998). Granule cell axons are unmyelinated and extend towards the superficial molecular layer. Bifurcation of the granule cell axon results in two projections that run in opposite directions perpendicular to the axon. These projections form the parallel fibres of the cerebellum and terminate on the dendrites of Purkinje neurons.

Purkinje neurons are large γ-aminobutyric acid (GABA) -ergic neurons with myelinated axons that extend through the granule cell layer to form the sole output of the cerebellum, terminating on cerebellar nuclei and certain brainstem nuclei.

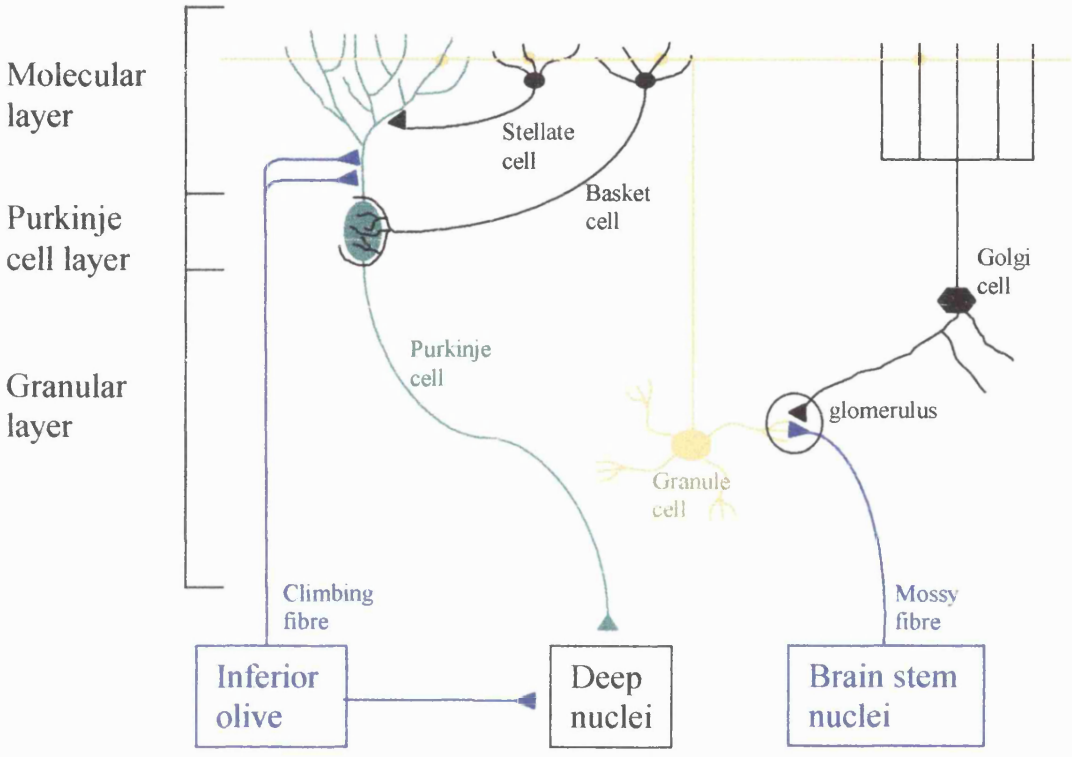

Figure 1.3. A schematic diagram indicating the major neuronal pathways in the cerebellar cortex.
Inputs to the cerebellum are shown in blue. Inhibitory interneurons are represented in black.

Purkinje cells receive inputs from the parallel fibres of granule neurons. The dendritic tree of a Purkinje neuron extends in one plane into the molecular layer where their distal branches are covered with many spines. It is onto these spines that the parallel fibres synapse. It has been estimated that a single Purkinje neuron can receive inputs from 80 000 granule neurons. Basket and stellate cells also synapse onto Purkinje neurons increasing the possible number of inputs.

The remaining neurons in the cerebellum are essentially inhibitory. Golgi cells are glycine and GABA-ergic (whereas stellate and basket are solely GABAergic) interneurons which receive inputs from the parallel fibres and provide negative

feedback to granule neurons. The cell bodies of the golgi neurons are found within the granule cell layer close to the Purkinje cell bodies. The large dendritic tree of a golgi cell is unlike other neurons of the cerebellum in that it expands in more than one plane. The axons of the golgi cells are also far reaching and extend throughout the granule cell layer to synapse on the dendrites of the granule neuron, see figures 1.2 and 1.3.
Stellate cells and basket cells also receive inputs from the parallel fibres of the granule cell but synapse onto the Purkinje cells. Stellate cells have small dendritic trees and shorter axons which synapse onto the spines of the Purkinje cell. The cell body of a stellate cell lies within the molecular layer of the cerebellum. Whereas basket cells are larger having their cell bodies in the lower third of the molecular layer. The axonal projections of the basket cell extend around the somata of the Purkinje cell resulting in their 'basket' like appearance.

Input to the cerebellum comes from sensory structures in muscles, skin and joints and from the visual and auditory cortices. The two major inputs are from climbing fibres and mossy fibres. Climbing fibres originate in the inferior olive and extend through the granule cell layer to synapse onto Purkinje neurons. Mossy fibres typically carry sensory and motor information and extend from brain stem nuclei to synapse onto the claw-like dendrites of the granule neuron. The convergence of the mossy fibres and granule cells, along with the terminals of the Golgi cell axons, form a characteristic structure known as a glomerulus.

The cerebellum as a whole is known to process information from various sensory inputs. It also plays a considerable role in motor function cerebellar dysfunction or lesion can strongly affect movement. Monkeys with damaged cerebellar cortices are unable to control eye movement during head movement (Optican & Robinson 1980). In man disorders of gait and eye movement have been attributed to damage of the cerebellum.

The cerebellar cortex also contains a variety of glial cells, in addition to type 1 astrocytes are oligodendrocytes, microglia and Bergmann glial cells (also known as golgi epithelial cells). This study will concentrate on the signalling properties of

cerebellar granule neurons as their vast interactions with all other cell types in the cerebellum dictates an importance in cerebellar function.

1.2 Cellular excitability, (Hille 1992).

Electrical information flows down the axon of neurons in the form of an action potential. Action potentials travel with a constant velocity and amplitude and are the result of highly organised and localised changes in the membranes permeability to ions, in particular sodium and potassium. In the cell soma and dendrites electrical processing occurs due to multiple ion channels.

A series of papers by Sidney Ringer in the 1880's identified the importance of ions in electrical excitability. Ringer showed that the solution perfusing a frog's heart must contain sodium, potassium and calcium salts in defined proportions if the heart was to continue beating.

The next major step towards understanding the dynamics of electrical excitability came from Bernstein's membrane theory in the early 1900s. It was already known that a potential difference existed between two solutions of same the salt if they were at different concentrations and separated by a membrane selectively permeable to one ion, figure 1.4.

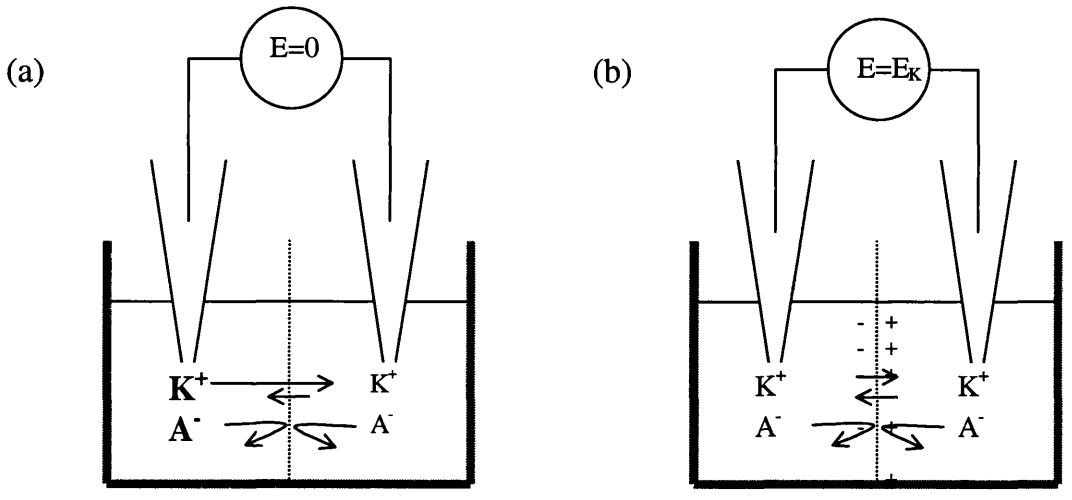

Figure 1.4 Diffusion potentials in pores.

(a) A vessel with a membrane that is selectively permeable to a cation K^+ separates two concentrations of a salt KA. K^+ ions start to diffuse down their concentration gradient and establish a potential difference across the membrane. (b) Net diffusion ceases when the potential across the membrane equals E_K.

All systems move toward equilibrium. If two different concentrations of salts were separated by a membrane that was selectively permeable to say the cation then the cation would attempt to move down its concentration gradient. However as the membrane is impermeable to its anion a potential difference is established and the cation is now subjected to an electrochemical gradient rather than just a chemical one. This potential difference grows as cations diffuse down their concentration gradient and exerts an electrical force in the opposite direction. Equilibrium is reached when the forces exerted by the chemical and the electrical gradient are equal and after that is reached there is no net diffusion of cations (see figure 1.4). This phenomenon is described by the Nernst equation:

$$E_A = \frac{RT}{z_A F} \ln \frac{[A]_o}{[A]_i}$$

Equation 1.1 The Nernst Equation.

E_A is the zero current potential for an ion A with charge z_A at a concentrations of $[A]_o$ (extracellular) and $[A]_i$ (intracellular). R is the gas constant, T the temperature in Kelvin and F Faraday's constant.

Calculations of resting membrane potential lead Bernstein to suggest that the membrane of a cell was, at rest, selectively permeable to potassium ions and that excitation was brought about by changes in the membrane permeability of other ions. The theories by Bernstein were greeted with much scepticism and even into the 1930's biophysicists were divided in their opinions of what causes action potentials. In the late 1940s Hodgkin observed that a depolarisation could spread past a patch of membrane that had been cold clamped to prevent the propagation of action potentials. This confirmed some early beliefs and showed that action potentials propagate electrically (Hille 1992).

When the action potential was recorded for the first time (Hodgkin and Huxley 1939, 1945; Curtis & Cole 1940, 1942) they found that the membrane potential instead of approaching zero during an action potential overshot by several tens of millivolts. Hodgkin and Katz (1949) showed that rather than the membrane becoming permeable to all ions during the action potential it was changing its permeability selectively to sodium ions (the reversal potential for sodium is about

+60mV, so any increase in membrane permeability to sodium from a resting state would bring about a sharp depolarisation, see equation 1.1).

A series of pioneering experiments by Hodgkin, Huxley and Katz between 1949 and 1952 used a newly developed technique, the voltage clamp. Used extensively ever since the voltage clamp allows the experimenter, with the aid of a high frequency feedback amplifier, to control the potential difference across the membrane whilst recording current movements. Using this technique Hodgkin and Huxley identified three components to the ionic current;

"Ionic current can be divided into components carried by sodium and potassium ions (I_{Na} and I_K) and a small leakage current (I_l) made up by chloride and other ions" (Hodgkin and Huxley, 1952).

As ions move down their electrochemical gradient it was proposed that sodium ions move inward at potentials negative to the equilibrium potential to sodium, E_{Na} (Equation 1.1) and outward at potentials positive to E_{Na}. The same theory applies to all other ions. Hodgkin and Huxley showed that the upstroke of the action potential was due to a selective increase in membrane permeability to sodium ions and the repolarisation was as a result of a change in potassium conductance. Further they suggested that these currents are controlled by membrane potential.

Since these early experiments were carried out, intense research has yielded a much improved understanding of the biophysical properties and molecular structure for many different types of ion channel.

The plasma membrane of an excitable cell contains a multitude of ion channels including chloride, sodium, calcium and potassium channels. This section will concentrate on those primarily involved in electrical excitability, sodium and potassium channels. Calcium channels will be introduced later with regard to their role in intracellular calcium homeostasis.

1.3 Sodium channels.

The rapid depolarisation associated with the upstroke of the action potential is due to an influx of sodium through voltage-gated sodium channels (Hille, 1992). The electric organ of the *electrophorus electricus* provided a rich source of sodium channels and the first was cloned in 1984 by Noda *et al.* The sodium channel α

subunit consists of 24 transmembrane spanning domains which are divided into 4 sets of 6, each with a voltage sensor and pore forming loop. To date 11 sodium channel α subunits have been cloned and two accessory β subunits. Intense work on sodium channel structure and function has ensued and a number of reviews on sodium channel structure and function now exist (Fozzard & Hanck, 1996; Roden & George, 1997; Voilley *et al.*, 1997; Marban *et al.*, 1998; Balser, 1999; Catterall, 2000) and their role in neuroprotection (Taylor & Meldrum, 1995; Obrenovitch, 1998), pain (Waxman *et al.* 1999; Waxman, 1999), local anaesthesiology (Courtney, 1988; Butterworth & Strichartz 1990), epilepsy (Ragsdale & Avoli, 1998; Catterall, 1999) and as target for insecticides (Narahashi, 1996).

1.4 Potassium Channels

This section addresses the properties of potassium channels; their diversity, structure and basic functional properties. The presence of native potassium currents in cerebellar granule neurons is reviewed in chapter 3.1.

Potassium channels are responsible for setting of the resting membrane potential as well as regulating the duration, threshold, waveform and frequency of action potentials, (Byrne, 1980; Hille, 1992).

Hodgkin and Huxley (1952) described a voltage-gated change in membrane permeability to potassium but due to a lack of a tissue rich source and selective high affinity ligands, potassium channels were not cloned until the late 1980s. Studies on the *Drosophila* mutant *Shaker* (so called because flies with this mutant shook their legs under ether anaesthesia) resulted in the first cloning of a potassium channel, which when expressed in *Xenopus* oocytes yielded currents similar to the A-current (Papazian *et al.* 1987, Tempel *et al.* 1987). Later a potassium channel from the rat cerebral cortex was cloned which also showed voltage dependence, activating at potentials between -35 and -30mV when expressed in oocytes (Stuhmer *et al.* 1988). Since these early discoveries there has been an explosion in the number of potassium channel genes discovered. Despite the large number of subtypes, potassium channels can be divided into three distinct subfamilies according to their molecular structure, figure 1.5 (see Coetzee *et al.* 1999). The voltage-gated family of potassium channels have six transmembrane domains (S1-S6) of which a pore

forming region (known as the p-domain, or H5-loop) exists between transmembrane domains S5 and S6 and confers potassium selectivity. The inwardly rectifying family of potassium channels are structurally similar to the C-terminus end of the voltage-gated potassium channels including two transmembrane domains (M1 and M2) and the p-domain, (Heginbotham *et al.* 1992). The final family has recently been discovered to consist of 4 transmembrane domains and 2 pore forming regions, akin to two inwardly rectifying potassium channels spliced together (Goldstein *et al.* 1998).

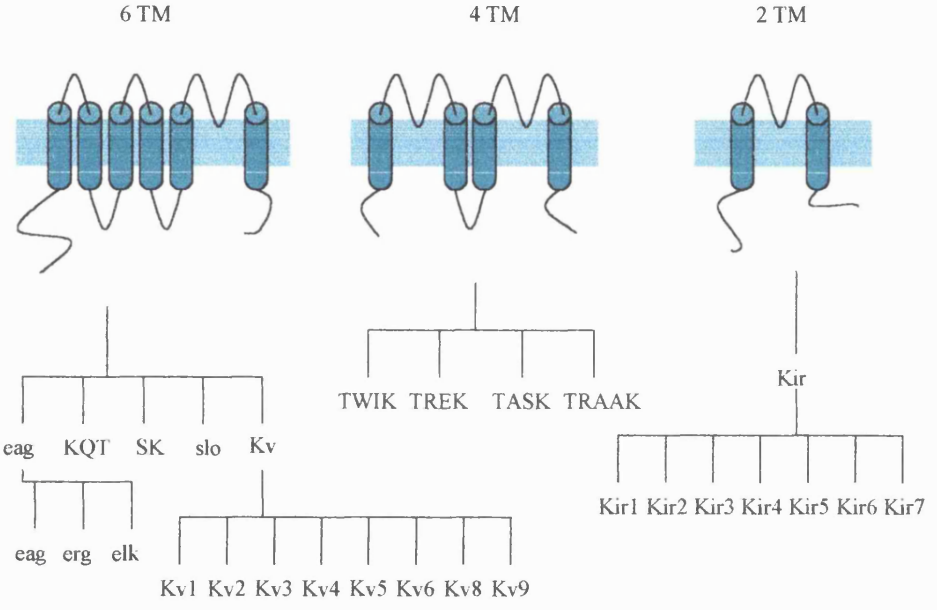

Figure 1.5. The molecular diversity of potassium channels.

Potassium channels can be separated into three distinct families depending on their molecular structure, the voltage-gated potassium channels having 6 TM domains and one pore forming loop, the inward rectifiers which have two TM domains and one pore forming loop and the leak channel which have two pore forming loops and four TM domains. Each family can be further divided as shown. Further divisions exist within many of the subfamilies shown, for example the Kv1 family consists of 7 channels (Kv1.1 - Kv1.7). Adapted from Coetzee *et al.* 1999.

1.4.1 Potassium Channel Structure.

The elucidation of the crystal structure of the KcsA potassium channel from *Streptomyces lividans* has given an indication of what the pore forming region is likely to look like.

KcsA is a potassium channel that has two transmembrane domains separated by a pore forming region, similar to the inward rectifiers (Schempf *et al.* 1995). However it has an amino acid sequence much more similar to that of the voltage-gated family of potassium channels especially in the pore forming region. Therefore when the crystal structure of KcsA was resolved (Doyle *et al.* 1998) comparisons were made between it and the voltage-gated potassium channels, in particular Shaker. The crystal structure of KcsA revealed that it resembled an inverted tepee with the potassium selectivity filter at the wide, extracellular end.

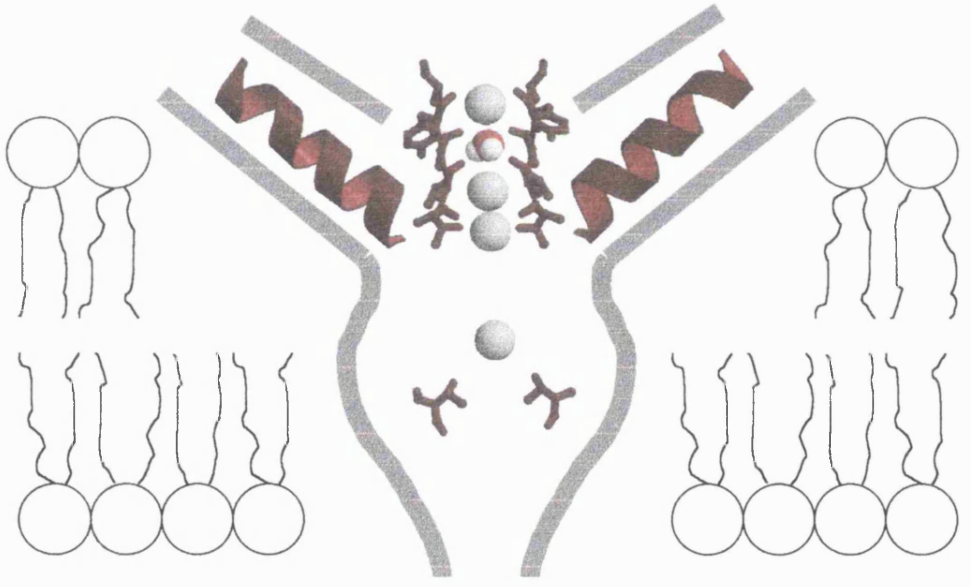

Figure 1.6 A view of the pore region of the KcsA channel.

Only two opposite subunit pore forming regions are included. The selectivity filter is represented in ball and stick format in which the helices are shown in ribbon format. Potassium ions are shown as grey spherical balls and a water molecule in red and grey. Three potassium ions and the water molecule are shown in the selectivity filter whilst the last is within the aqueous cavity towards the centre of the channel. Figure courtesy of Dr Kishani Ranatunga.

Intracellular to the selectivity filter the channel widens to 10Å. This forms a water filled cavity that acts to overcome the electrostatic destabilisation induced as the ion

passes through the point of the channel where the energy of the cation is highest, at the bilayer centre. The existence of a water filled pore rather than further binding pockets for potassium allows for high throughput of potassium ions. In fact this cavity, although being much longer than the 12Å selectivity filter accounts for only 20% of the potential difference across the membrane (Doyle *et al.* 1998). It is in this cavity that the classical potassium channel blocker, tetraethylammonium (TEA) binds (Doyle *et al.* 1998).

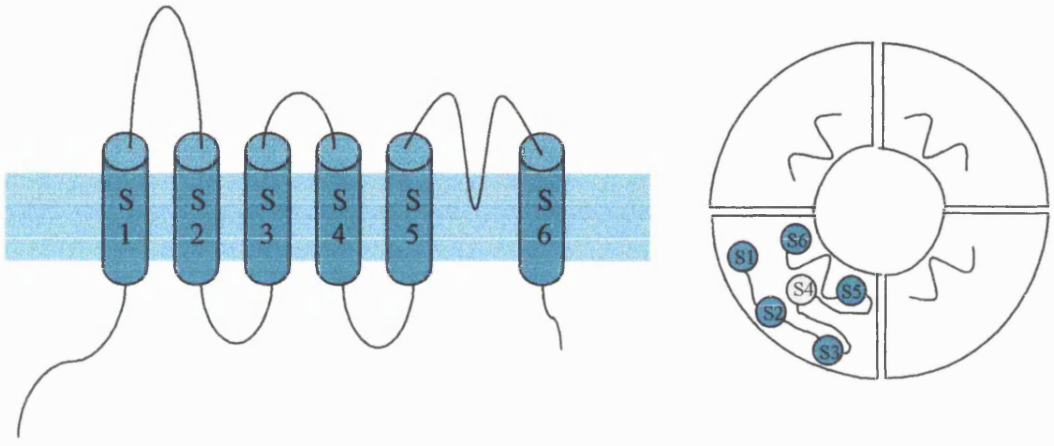

Figure 1.7. Subunit organisation of a K_v potassium channel.
The left hand side shows the six transmembrane domains of the K_v potassium channel subunit. The right hand side shows the organisation of the pore-forming loops around the channel duct.

1.4.2 The potassium channel selectivity filter

Potassium channels allow the passage of potassium at a rate of many ions per second but are ten thousand times more permeable to potassium compared to sodium, so how is this achieved?

Early studies suggested that the hydrated ion must lose all of its water molecules and come into close contact with the channel so that the ion can be sensed (Hille 1992). This gave a prediction that at the selectivity filter the channel can only be some 3Å in diameter. Despite their diversity potassium channels share a highly conserved sequence of eight amino acids (TXXTXGYG) see figure 1.8, (Heginbotham *et al.* 1994) and it was proposed that this region may make up the pore and confer potassium channel selectivity.

Early studies showed that mutating amino acids in the p-domain affected the biophysical properties of channel block by ions and toxins (MacKinnon & Miller 1989). Further Heginbotham *et al.* (1994) showed that some mutations of the amino acids in the signature sequence in *Shaker* render the channel unselective among monovalent cations.

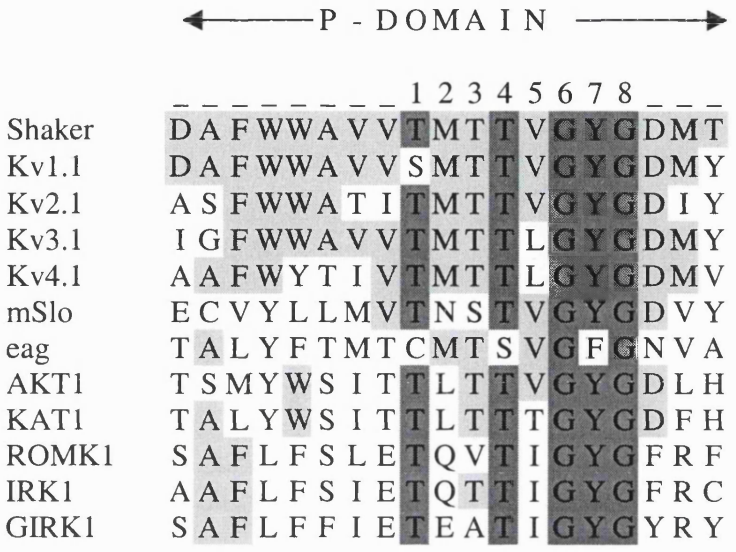

Figure 1.8 Sequence alignment of the pore forming region of different potassium channels.
Residues identical to those seen in Shaker are highlighted in light grey and those most highly conserved in dark grey. Adapted from Heginbotham *et al.* 1994. The numbered residues (1-8) make up the potassium channel signature sequence.

The determination of the crystal structure of the KcsA channel confirmed the role of the signature sequence in channel selectivity. The amino terminal portion of the p-domain forms an α helix which extends into the pore from the extracellular side. Unexpectedly five amino acids from this signature sequence (TXGYG) turn their carbonyls in towards the centre of the pore to form the selectivity filter (Doyle *et al.* 1998). The narrow carbonyl lined filter provides a 'pocket' for a potassium ion with much the same energy that it would have in water. Thus a potassium ion can become dehydrated and form electrostatic interactions with the oxygen atoms of the selectivity filter without the requirement of any extra energy. The selectivity filter was found to be only 12Å long and contained two potassium ions. These ions are proposed to repel each other overcoming the electrostatic interactions between ion and protein and thus increasing conduction rates (Doyle *et al.* 1998).

How then does the channel offer selectivity over sodium whose diameter is only 1.9Å compared to a selectivity filter diameter of 3Å. For the sodium ion to successfully permeate the potassium channel pore it too must lose its accompaniment of water molecules. However, the naked ion is too small to establish tight electrostatic coupling with the oxygens of the rigid carbonyls on the selectivity filter. It is therefore energetically unfavourable for the sodium ion to lose its water molecules and hence cannot permeate the channel (Armstrong, 1998).

1.4.3 Voltage-gated potassium channels.

Voltage-gated potassium channels were among the first ion channels identified by Hodgkin *et al.* (1949) in the squid giant axon. The voltage-gated family potassium channels is numerous and with many subtypes being highly localised their potential as pharmacological targets has resulted in intense research in recent years. Sequencing of the *Caenorhabditis elegans* genome (Bargmann, 1998) revealed that this organism, despite having only 302 neuronal cells, has about 20 voltage-gated 'like' genes giving some indication into their importance in multicellular organisms. Voltage-gated potassium channels, as their name suggests, respond to a change in membrane potential to change the permeability of the membrane to potassium.

1.4.4 Channel Assembly.

Voltage-gated potassium channels (Kvs) belong to the six transmembrane domain superfamily of potassium channels, (fig 1.5 & 1.7), and have a pore-forming loop between S5 and S6. Based on sequence homology the voltage-gated superfamily of potassium channels is divided into 8 subfamilies, Kv1-6, 8 and 9. α subunits of the voltage-gated potassium channel are numerous and many of the 8 subfamilies have multiple members, for example the Kv1 family consists of 7 individual channels named Kv1.1 - Kv1.7 (Coetzee *et al.* 1999).

Cloning of voltage-gated calcium and sodium channels (Noda *et al.* 1984) showed that these channels have four homologous (but not identical) units each containing a voltage sensor and a pore forming loop. When the potassium channel was cloned it was therefore prudent to suggest that the channel subunits formed tetramers (Tempel *et al.* 1987). In 1991 MacKinnon *et al.* showed that, as expected, potassium channel α subunits come together to form tetramers in functional channels. The vast number

of voltage-gated potassium channel genes in itself gives rise to a multitude of different channels, however channel diversity is further magnified by alternative splicing (Coetzee *et al.*1999). In addition it has been shown that potassium channels can form heterotetramers (Isacoff *et al.* 1990) and many native voltage-gated potassium channels are heterotetramers of different channel subtypes (Isacoff *et al.* 1990). The immense diversity that heterotetramers and alternative splicing bring to potassium channel suggests that they must be highly localised to different cellular locations depending on their unique electrical properties.

Native potassium currents are subjected to modulation by auxiliary or β subunits. Cloned in 1994 the Kvβ1 subunit was seen to change the properties of a Kv1 channel from a non-inactivating current that resembled the delayed rectifier to a rapidly inactivating, A-type current (Rettig *et al.*1994). This effect was mediated via an inactivating ball that contains positively charged amino acids and swings into the pore when the cell membrane is subjected to depolarisation.

1.4.5 The voltage sensor of the voltage-gated potassium channel

The fourth transmembrane domain (S4 domain) of the voltage-gated potassium channel is the voltage sensor. Hodgkin & Huxley (1952) suggested that there was a gating current that resulted from a change in membrane potential and that this movement of charge was responsible for increasing the permeability of the membrane to the ion. This current wasn't measured directly until 1973 when Armstrong and Bezanilla (1973) detected a movement of charge in response to membrane depolarisation.

Point mutations of positively charged amino acids in the S2 and S4 domains have shown that the S4 region is the voltage sensor but there is some contribution from positively charged residues in the S2 domain (Seoh *et al.* 1996). Positional changes of these positively charged residues has been observed directly using voltage-clamp fluorimetry (Mannuzzu *et al.* 1996) and confirms the belief that a conformational change in the channel protein underlies voltage sensitivity. Recently, it has been shown that a rotation in the S4 helix brings about the necessary conformational change and channel opening (Cha *et al.*, 1999).

1.4.6 Calcium activated potassium channels.

Excitable cells respond to external stimuli in a variety of ways but by far the two most prevalent signalling pathways are electrical excitability and an increase in intracellular calcium (see chapter1.2 and 1.5). When these two signalling pathways are used in conjunction it is of great importance that they are controlled and do not escalate to a point where they cause cell death. Outward potassium currents that are voltage dependent and activate in response to the elevated calcium concentrations created by an action potential provide a negative feedback mechanism preventing prolonged depolarisation and hence decrease the risk of calcium overload and cell death.

Two main types of calcium activated potassium current have been described, a large conductance (>100pS in symmetrical potassium concentrations, Sah 1996), voltage dependent current (MaxiK or BK_{Ca}) and a small conductance (5-20pS; SK_{Ca}) which is voltage independent. Rises in intracellular calcium cause an increased open probability causing hyperpolarisation.

(a) BK_{Ca} channels (slo).

Large conductance potassium channels were cloned from *Drosophila*. Because mutant flies could hardly fly at room temperature and shook their legs under ether anaesthesia - just as the Shaker mutants did (Atkinson *et al.* 1992)- the gene was termed slowpoke (slo). These channels are members of the six transmembrane domain super family of potassium channels but despite high sequence homology in the S1-S6, including the pore forming region, slo shows large structural differences to that voltage-gated family (see figure 1.9).

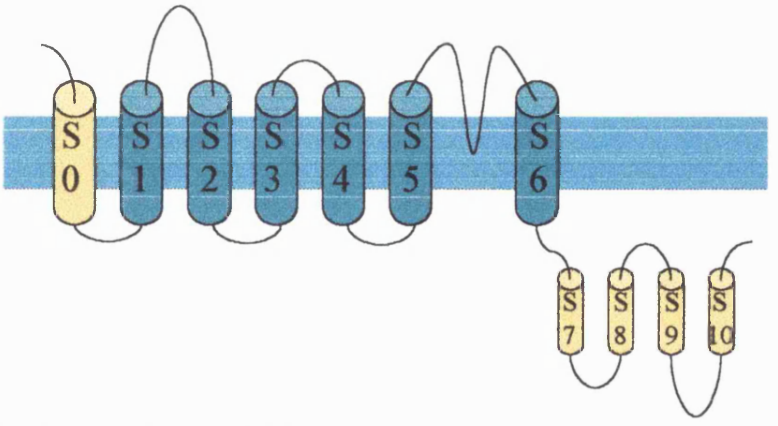

Figure 1.9 Proposed secondary structure of slo

At its N-terminal end slo has an additional hydrophobic region that is believed to be a transmembrane domain, termed S0 (Meera *et al.* 1997) resulting in an extracellular N-terminus. At the C-terminal end (after S6) slo has an additional four hydrophobic regions (S7-S10), this region is entirely cytosolic in its location (Meera *et al.* 1997). A series of negative charges between S9 and S10 are believed to come together to form a 'bowl' that makes up the calcium sensor, (Schreiber *et al.*1997).

BK_{Ca} channels open in response to membrane depolarisation and a rise in intracellular calcium. To open at the resting membrane potential BK_{Ca} channels require an intracellular concentration of calcium of 1-10μM (Sah, 1996). BK_{Ca} channels are proposed to activate rapidly during an action potential spike to bring about a hyperpolarisation and therefore could be key determinates in important processes such as neurotransmitter release.
An auxiliary subunit is often found with the BK_{Ca} channel. This β subunit has two transmembrane domains and intracellular N and C termini and interacts with S0 transmembrane domain of the channel. Presence of the β subunit causes a negative shift in the voltage range of activation (Vergara *et al.* 1998).

(b) SK_{Ca} channels

Small conductance potassium channels SK_{Ca} are responsible for the slow afterhyperpolarisation observed following an action potential (Sah 1996). The afterhyperpolarisation limits the ability of the cell to fire another action potential, so SK_{Ca} are important in regulating firing frequency as well as protecting the cell from continuous tetanic activity (Vergara *et al.* 1998). Three SK_{Ca} channels were cloned in 1996 by Köhler *et al.*, SK1 from human and SK2 and 3 from rat, and found, like BK_{Ca} channels, to be a member of the six transmembrane domain of potassium channels but has very little sequence homology with any other of the voltage-gated potassium channels.

1.4.7 Inwardly Rectifying Potassium Channels

A channel is said to rectify if its conductance changes with voltage. Inwardly rectifying potassium channels (Kirs) were first described by Katz (1949) in skeletal

muscle but have since been observed in many other tissue types. Kirs were originally believed to set the resting membrane potential by passing small outward currents at depolarised potentials and control cellular excitability.

Homology screening with Kv channel genes did not reveal any inwardly rectifying potassium channels and the first Kir was cloned comparatively recently by expression cloning from rat kidney (ROMK1 (Kir1.1a) Ho *et al.* 1993), from a mouse macrophage cell line (IRK1 (Kir2.1) Kubo *et al.* 1993) and from the heart (GIRK1 (Kir3.1) Dascal *et al.* 1993). Cloned Kir channels fall into 7 families based on their sequence identity (Coetzee *et al.* 1999) having up to 60% sequence homology within subfamilies and ~40% between them.

Cloning of Kir revealed a structure dissimilar to that of the voltage-dependent potassium channel family. Kir channels have just two transmembrane domains (M1 and M2) between which lies an H5 domain which has similar sequence identity to the H5 domain in the voltage-gated potassium channels (Heginbotham *et al.* 1994). Between families the Kirs exhibit varying properties, for example Kir1.1 is a weak inward rectifier which is inhibited by ATP (Leung *et al.* 2000) whereas the Kir3 subfamily exhibit strong rectification and are activated and inhibited by G-proteins (Velimirovic *et al.* 1995)

Like voltage-gated potassium channels Kirs come together to form tetramers in functional channels (Yang *et al.* 1995) and like voltage-gated potassium channels they can form heterotetramers (eg Kir3.1 and 3.4 Krapivinsky 1995). However unlike the voltage-gated potassium channels, Kir channels can co-assemble between families, Kir5.1 does not form functional channels as a homotetramer but will when expressed with Kir4.1 (Pessia *et al.* 1996). Further, properties of the Kir4.1 / Kir5.1 channel vary depending upon subunit position in the channel, when arranged 4.1-4.1-5.1-5.1 the channel behaves like a homotetramer of Kir4.1 subunits but when in a 4.1-5.1-4.1-5.1 arrangement the channel exhibits currents with larger conductances (Pessia *et al.* 1996). This reveals an interesting possibility that, perhaps in all potassium channels, the characteristics of the current may depend not only on the subunit composition but also on their position around the central pore.

Almost all potassium channels show some degree of inward rectification, so what underlies the strong rectification of the Kirs? Voltage dependent inactivation of other voltage-gated channels was known to involve blocking of the channel pore by

cations, in particular magnesium ions. Excised patches of Kir2.3 a strong inward rectifier showed that rectification decreased with time but could be restored by putting the patch close to the surface of a cell (Lopatin *et al.* 1994). The soluble factors determining the rectification were found to be polyamines. Spermine, spermidine and putrescine are all known to induce rectification. The polyamines are long narrow molecules who are believed to lie, in pairs, inside the Kir channel and bind to potassium binding pockets along the pore (Lopatin *et al.* 1994, Ficker *et al.* 1994). Mutation of a glutamate residue thought to line the pore, to a positive residue, results in intrinsic rectification. Like the voltage-gated potassium channels inward rectifiers are also subject to rectification by intracellular magnesium ions (e.g. Oliver *et al.* 2000).

1.4.8 Two-pore Domain Potassium Channels

Using computer searches of channel like motifs, Ketchum *et al.* (1995) identified a novel type of potassium channel from *Saccharomyces cerevisiae* that contained two p-domains in the same continuous peptide. When expressed in oocytes an outwardly rectifying potassium selective current was observed which was present at potentials positive of the equilibrium potential for potassium and was named TOK1 for tandem-pore outward potassium channel, (Ketchum *et al.* 1995). TOK1 has been found to be activated by volatile anaesthetics, such as halothane and isoflurane, which caused membrane hyperpolarisation (Gray *et al.* 1998) and fuelled intense research into whether two pore domain potassium channels were the site of action of many anaesthetics.

Since the recent discovery of TOK many more two-pore domain potassium channels have been cloned with diverse properties. Members of this family of potassium channels are still being discovered (e.g. recently TASK-3 Kim *et al.* 2000) and it remains to be seen how many mammalian genes encode two-pore domain potassium channels, although the sequencing of the entire genomic sequence in C. elegans revealed over 40 genes encoding two-pore domain potassium channels (Bargmann, 1998) and 11 were found in the *Drosophila* genome (Adams *et al.* 2000). At present 9 distinct mammalian two-pore domain potassium channels have been discovered (see table 1.1) and it remains to be seen whether any more will be uncovered. The real test now is to elucidate the native currents that result from the expression of these genes.

Channel subtype	Alternative name	Species	Reference
TWIK-1	KCNK1	Human	Lesage *et al.* 1996
TWIK-2		Human	Chavez *et al.*1999
		Rat	Patel *et al.* 2000
	KCNK6	Mouse	Salinas *et al.* 1999
	KCNK7	Human	Salinas *et al.*1999
TREK-1	KCNK2	Mouse	Fink *et al.*1996
		Human	Meadows *et al.* 2000
TREK-2	KCNK10	Human	Lesage *et al.* 2000
		Rat	Bang *et al.* 2000
TASK-1	KCNK3	Mouse	Duprat *et al.* 1997
TASK-2	KCNK5	Human	Reyes *et al.* 1998
rTASK		rat	Leonoudakis *et al.* 1998
TASK-3	KCNK9	Guinea-pig	Kim *et al.* 2000
		Human	Kim *et al.* 2000
TRAAK	KCNK4	Mouse	Fink *et al.* 1998

Table 1.1 Cloned two-pore domain potassium channels.

1.4.8.1 Structure of two-pore domain potassium channels.

The first described two-pore domain potassium channel, (TOK) had 8 transmembrane domains and two pore forming regions and resembled a voltage-gated and inward rectifier potassium channel spliced together. However, the mammalian channels described below and listed in table 1.1 all consist of 4 transmembrane spanning regions (M1 - M4) and two pore forming loops (P1, between M1 and M2 and P2, between M3 and M4) resembling two inward rectifier potassium channels spliced together, although it is worth noting that the two halves of these channels are not identical. Perhaps the most striking difference is that the selectivity filter is different from that of other potassium channels. The selectivity filters of the voltage-gated and inwardly rectifying potassium channels have the signature sequence -TXXTXGYG- (section 1.4.1) however the two-pore domain

family do not consistently adhere to this motif. For example the corresponding amino acids in TWIK-1 are -VXXTXGYG- in P1 and -SXXTXGLG- in P2 (Lesage *et al.*1996), and TASK-1 has -VXXTXGYG in P1 and -TXXTXGFG- in P2 (Duprat *et al.* 1997). In both cases the signature sequence is slightly altered from that seen in other families of potassium channels. The effects on conductance and ionic selectivity remains to be fully characterised (but see chapter 3). Two-pore domain potassium channels have short intracellular N-termini and a long C-terminus, that on some subtypes provides consensus sequences for phosphorylation by PKA and PKC (eg TASK-3; Kim *et al.* 2000).

1.4.9 Two-pore domain potassium channel subtypes.

1.4.9(a) TWIK

The first mammalian two-pore domain potassium channel was discovered by Lesage *et al.* (1996) from genetic screening of the human genomic sequence The channel, when expressed in oocytes, was found to be time independent and was a magnesium sensitive inward rectifier and was called TWIK-1 (for tandem pore weak inwardly rectifying potassium (K^+) channel). TWIK-1 can be up-regulated by phosphorylation by protein kinase C and down-regulated by intracellular acidification. A protein with a high sequence homology to TWIK-1 was cloned from the human cDNA library (Chavez *et al.* 1999). When expressed in oocytes this channel (TWIK-2) has similar biophysical properties to TWIK-1 but has slightly different pharmacology, being insensitive to quinidine and quinine, (TWIK-1 is inhibited by both quinidine and quinine (Lesage *et al.*1996). At a similar time to the publication of the TWIK-2 sequence, two non-functional channels were cloned from mouse and human, KCNK6 and KNCK7 which have a higher sequence similarity to TWIK-1 than any other known two-pore domain potassium channel (Salinas *et al.* 1999) although due to the similar time of publication these channels were not compared with TWIK-2.

1.4.9(b) TREK

TREK-1 (TWIK - related potassium channel) was cloned shortly after TWIK-1 by Fink *et al.* (1996) and was found to also have two-pore forming loops but had an overall sequence homology to TWIK-1 of only 28%. TREK-1 encodes channels that when expressed in oocytes are quite different from TWIK-1. TREK-1 is an outwardly rectifying potassium channel that is sensitive to quinidine and quinine but is strongly inhibited by agents that activate protein kinase A and C (Fink *et al.*1996).

TREK-1 channels are also opened by membrane stretch, intracellular acidification and arachidonic acid (Fink *et al.* 1996). TREK-1 channels have been implicated as thermoreceptors as they show an increase in temperature increases current amplitude and are extensively expressed in peripheral sensory neurones (Maingret *et al.* 2000). TREK-2 displays high sequence homology with TREK-1 (68%) shows less widespread tissue distribution (Bang *et al.* 2000) and is activated by intracellular acid pH, membrane stretch and arachidonic acid.

1.4.9(c) TASK

The TASK subfamily of two-pore potassium channels are sensitive to extracellular acidification. Three members of this family have been described thus far, TASK-1 to 3. TASK-1 was the first to be described from the mouse cDNA library and when expressed in oocytes, yielded currents that were potassium selective, instantaneous and non-inactivating. Further, TASK-1 appeared as an open rectifier which lacked voltage sensitivity (Duprat *et al.* 1997). For these reasons TASK-1 was described as a background or leak conductance. An outwardly rectifying two-pore domain potassium channel cloned from human kidney was found to have little sequence homology with the other know two-pore domain potassium channels. However, it was found to be strongly inhibited by extracellular acidification and was named TASK-2 (Reyes *et al.* 1998). TASK-2 is not found in the brain unlike many other two-pore domain potassium channels but is highly expressed in kidney. The recently cloned third member of this subfamily is TASK-3 (Kim *et al.* 2000). Cloned from rat cerebellum it has higher sequence homology to TASK-1 (54%) than with TASK-2 (<30%). As with other members of the TASK family TASK-3 is highly sensitive to extracellular acidification, it is also blocked by quinidine.

1.4.9(d) TRAAK

Cloned in 1998, TRAAK is an arachidonic acid stimulated two-pore domain potassium channel subfamily. TRAAK (TWIK related arachidonic acid sensitive potassium channel) which is found exclusively in central neurons and the retina, expresses currents that are instantaneous and non-inactivating (Fink *et al.* 1998)

Modulation of potassium channel function, in particular TASK, by intracellular messengers and by externally applied drugs, will be discussed further in chapters 3 and 7.

1.5 Intracellular calcium signalling

1.5.1 Calcium as a second messenger

Calcium is a ubiquitous second messenger with a multitude of diverse actions. Rises in intracellular calcium concentration ($[Ca^{2+}]_i$) are responsible for functions as diverse as cell proliferation, hormone and neurotransmitter release, apoptosis and muscle contraction. The ubiquitous nature of calcium as a signalling molecule has made it by far the most intensely researched element. Without calcium life is impossible but too much and cells die. How then has calcium evolved to be such an important messenger in all cells from prokaryotic to eukaryotic?

Calcium is an abundant element but only exists in an unbound, or free, form in very small concentrations (millimolar) in the environment, due to it forming complexes with multiple compounds many of which form a precipitate. In the early cytosolic 'soup', free calcium bound to elementary proteins reducing the local free calcium concentration further. It is thought that as evolution progressed and membranes formed, so the binding of calcium to negatively charged proteins created a free calcium concentration gradient across the membrane in the absence of complex calcium pumping mechanisms.
With time, cells developed ways to remove calcium from the cytoplasm and further increased the concentration gradient. Selective changes in membrane permeability could therefore bring about large changes in free calcium concentration in the cytoplasm and a large signal to noise ratio made calcium an ideal second messenger.

The importance of calcium as a key regulatory element has been known since the work of Ringer in the 1880s and due to its ubiquitous nature the mechanisms controlling calcium concentration have been the target of much work since then. Regulation of calcium influx and efflux is of immense importance to a cell, too little and a cell is unable to function, too much and it will die. The mechanisms of calcium storage, influx and efflux will be addressed separately here.

The importance of calcium as a second messenger is highlighted by the lengths cells have gone to provide themselves with diverse and adequate reserves of calcium. There are two major calcium stores, the extracellular space and the sarco-

endoplasmic reticulum. In addition the mitochondria, nucleus and golgi have all been implicated as having roles as calcium stores.

Calcium can enter the cell from the extracellular space via three major classes of channels, the ligand gated ion channels, the voltage-gated calcium channels and store-operated calcium channels.

1.6 Voltage-gated Calcium channels.

Voltage-gated calcium channels were first identified in crustacean muscle by Fatt & Katz in 1953. Since then voltage-gated calcium channels have been identified in almost every cell including plant cells. The high density of the skeletal muscle subtype (the L-type, see below) resulted in the first cloning of a calcium channel showing them to be hetero-oligomeric proteins consisting of a pore-forming or $\alpha 1$ subunit and a number of auxiliary subunits, see figure 1.10. The $\alpha 1$ subunit is a large (175kDa) protein exhibiting a pseudotetrameric structure. The $\alpha 1$ subunit consists of 24 transmembrane domains which can be divided into four distinct segments (I-IV) each contain 6 transmembrane domains S1-S6 the fourth of which contains a conserved sequence rich in the positively charged amino acids arginine and lysine. Between S5 and S6 lies a pore forming loop which extends into the channel and makes up the selectivity filter, as with the voltage-gated potassium channels already described.

A number of voltage-gated calcium channels have been described and $\alpha 1$ subunits cloned and, based upon biophysical and pharmacological characteristics, can be loosely divided into two subfamilies, the high voltage activated (HVA) and the low voltage activated (LVA). After pharmacological inhibition of HVA and LVA currents a residual or R-type current often remains, this current is often referred to as a intermediate voltage-activated (IVA) as it does not fall easily into either the HVAs or the LVAs.

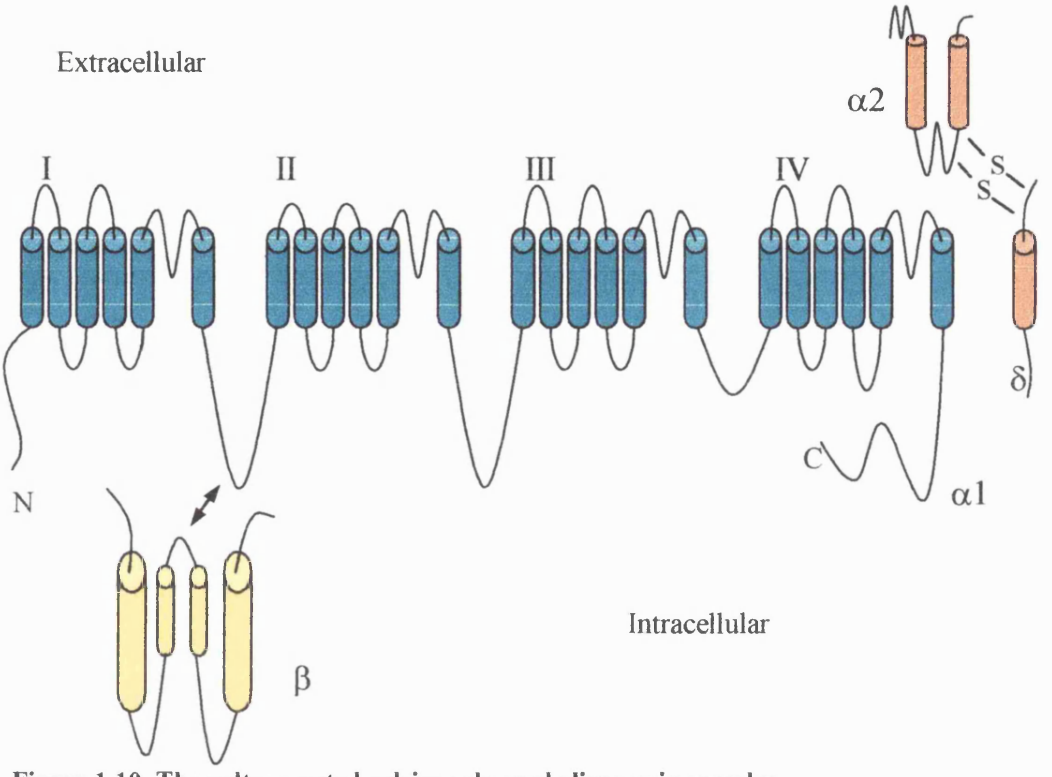

Figure 1.10 The voltage-gated calcium channel oligomeric complex.

The pore forming subunit, the α1 subunit consists of four repeating domains each containing 6 transmembrane segments and a pore forming loop. The α2 subunit is convalently linked to the δ subunit by the way of disulphide bridges. The β subunit is entirely intracellular and is believed to interact with the I - II loop of the α1 subunit.

Recently a new nomenclature of α1 subunits has been proposed to replace the α1A, α1B, ... etc. (Ertel *et al.*, 2000). The proposal is to rename α1 subunits as Ca_V subunits and then apply a number which is based upon amino acid identity, thus members of the L-type family of voltage-gated calcium channels will be referred to as $Ca_V1.1$ to $Ca_V1.4$. A similar nomenclature is successfully applied to both voltage-gated and inwardly rectifying potassium channels (figure 1.5 and table 1.2 below)

Voltage Dependence	Channel type	α1 subunit	Proposed nomenclature
HVA	L	α1S	Ca_V 1.1
		α1C	Ca_V 1.2
		α1D	Ca_V 1.3
		α1F	Ca_V 1.4
	N	α1B	Ca_V 2.2
	P	α1A	Ca_V 2.1
	Q	α1A	Ca_V 2.1

IVA	R	α1E	Ca_V 2.3
LVA	T	α1G	Ca_V 3.1
		α1H	Ca_V 3.2
		α1I	Ca_V 3.3

Table 1.2. Voltage-gated calcium channel α1 subunits.

1.6 (a) HVA voltage-gated calcium channels.

HVA channels are closed at the resting membrane potential and open in response to strong cellular depolarisation. HVA channels fall into several different subtypes depending on their biophysical and pharmacological properties.

L-type calcium channels were the first to be cloned from skeletal muscle and show slow inactivation hence they were termed L-type for long lasting. They are inactivated by increases in $[Ca^{2+}]_i$ which acts as a negative feedback loop (Eckert & Chad, 1984). L-type calcium channels are sensitive to the dihydropryidines, (DHPs, such as nifedipine). The α1 subunit of these channels can be either the α1C, α1D or α1S, i.e. the Ca_V1 family.

N-type calcium currents are characterised by their sensitivity to ω-conotoxin GVIA and are proposed to be due to calcium flux through α1B (Ca_V 2.2).

P -type calcium channels were originally discovered in Purkinje cells (Llinas *et al.*, 1989), and later the Q-type was described as being a different channel (Randall & Tsien 1995), however it is currently unknown whether P and Q-type currents result from different α1 subunits (table 1.2). P-type currents have been observed to vary considerably between studies and it remains to be seen whether these differences are the product of separate genes or sub-conductance states. Both P- and Q-type currents are inhibited by ω-agatoxin IVA but with different sensitivities. P-type channels are inhibited by funnel spider venom toxin (FTX) and by low concentrations of ω-agatoxin IVA (K_d 2-10nM) whereas Q-type channels show an IC_{50} of ~100nM. When the α1A ($Ca_V2.1$) was first cloned (Starr *et al.*, 1991; Mori *et al.*, 1991) it was deemed to underlie Q-type channels as the sensitivity to ω-agatoxin IVA was much lower than that expected for P-type. It is now believed that the differing properties of the native P- and Q-type channels may come about from different coupling of auxiliary subunits and perhaps other intracellular modulators (Sutton *et al.* 1999).

1.6 (b) LVA voltage-gated calcium channels

Low voltage activated calcium channels were discovered in the 1960s in dorsal root ganglia but it was only recently that they were cloned, (Perez-Reyes *et al.* 1998). LVA channels are inactive at the resting membrane potential and require a hyperpolarisation to remove inactivation because of this property they are believed to be involved in modulating the firing frequency of action potential. LVA currents are transient in nature, and have thus been referred to as T-type. Activating at about -60mV T-type currents have very low conductances, typically about 7-8pS. T-type currents in muscle and sensory neurons are DHP insensitive, whereas in brain neurons the DHPs may modulate cell firing. Altered developmental expression of the T-type channels may explain some inconsistencies between groups studying T-type channels. It has recently been shown that HVA channels can result in low-threshold, small conductance currents similar to native LVA channels (Meir & Dolphin 1998). This was attributed to an absence of the $\alpha 2\delta$ subunit in the expression system. It remains to be determined whether these findings are physiologically relevant.

1.6 (c) IVA voltage-gated calcium channels.

R-type currents are defined as the residual current left after all the other known channels have been blocked pharmacologically. They have similar biophysical properties to N- and Q-type channels and as far as inactivation constants T-type, but is insensitive to all know calcium channel blockers. In cerebellar granule neurons two components to this current have been shown to coexist in the same cell, named G1 and G2 (Forti *et al.*, 1994). The R-type calcium current is thought to be due to $\alpha 1E$ ($Ca_V2.3$). However, the biophysical and pharmacological properties of $\alpha 1E$ currents express considerable species differences. An unknown amount of the R-type current may be due to incomplete block of other calcium channels.

In combination with certain auxiliary subunits (see below) calcium channels can become more or less sensitive to antagonists. For example, ω-agatoxin IVA and FTX are unable to completely block currents from $\alpha 1A + \alpha 2\delta + \beta s$ in HEK293T cells. Until specific inhibitors for IVA current exist these questions regarding R-type currents are likely to remain unanswered.

1.6.1 Auxiliary Subunits

Voltage-gated calcium channels co-purify with several other proteins, see figure 1.10. The α1 subunits are capable of functioning as calcium channels in the absence of the auxiliary subunits but their properties, both biophysical and pharmacological can be radically altered by co-expression of β, α2δ or γ subunits. α2δ or γ have been shown to influence both voltage dependence and the time course of activation of α1C subunits (e.g. Singer *et al.*, 1991) but the β subunit appears to play the major role in calcium channel modification, (Birnbaumer *et al.* 1998). There are four subtypes of β receptor named β1-4 which are all subject to alternative splicing.

1.7 Ligand-gated ion channels.

Neurotransmitters act on three different types of receptor, tyrosine kinase, metabotropic and ionotropic receptors. Activation of tyrosine kinase receptors leads to receptor dimerisation and binding of protein complexes that initiate protein kinase signalling cascades, e.g. the mitogen activated protein kinase (MAPK) signalling cascade (appendix 1).

Metabotropic receptors represent a large family of structurally similar proteins all having seven transmembrane domains and coupling to the activation of G-proteins.

Ionotropic receptors are ion channels that open in response to neurotransmitters or hormones, examples include the nicotinic acetylcholine receptor, the AMPA, NMDA or kainate glutamate receptors, and the 5-HT_3 receptor. Ligand binding causes a conformational change in the protein structure resulting in channel opening.

1.7.1 AMPA receptors.

AMPA receptors are a good example of ligand gated ion channels. Glutamate was first shown to cause cellular depolarisation by increasing sodium conductance by Curtis *et al.* in 1972. Based upon the potencies of N-methyl D-asparate (NMDA), quisqualate and kainate glutamate channels were originally classified into two subgroups, NMDA and non-NMDA receptors. Further, classification by Collingridge & Lester (1989) led to the non-NMDA receptors being renamed as either AMPA or kainate based upon the relative potencies of these agonists. AMPA receptors are formed of either homo or heteromeric complexes made up of the AMPA receptor subunits, GluR1, 2, 3 or 4 (see Bleakman & Lodge 1998). They

were originally thought to be pentameric but recent evidence suggests that the subunits come together as tetramers to form functional channels (Mano & Teichberg 1998). Each GluR subunit consists of three transmembrane domains termed M1, M3 and M4. The M2 domain is believed to extend into the pore and make up the channel selectivity filter (Bettler & Mulle 1995). Ionic selectivity of AMPA receptors depends upon subunit composition. Heteromeric channels that possess the GluR2 subunit exhibit low calcium permeability, however, in the absence of GluR2 AMPA receptors are highly permeable to calcium (Hollmann *et al.*, 1991). The difference between ionic selectivity in GluR2 containing and GluR2 absent channels has been mapped to a single amino acid in the pore forming M2 region. In GluR2 an arginine exists where, in other GluR subunits, an aspartate normally resides (Hume *et al.*, 1991) and is a consequence of mRNA editing. This provides further evidence for the role of the pore-forming loop in ion selectivity.

A third calcium channel is important in calcium influx - the store operated calcium channel. This channel is activated via an unknown pathway which links emptying of the endoplasmic reticulum calcium stores to calcium influx and is discussed further in chapter 1.8.2.

1.8 Intracellular calcium stores.

For an intracellular organelle to be able to act as a calcium store it must be able to take up calcium, store it (usually with the aid of calcium buffering proteins) and release it in when required. There are two well characterised calcium stores, the sarco/endoplasmic reticulum and the mitochondria (see figure 1.11). In addition, the nuclear envelope and the golgi apparatus have also been implicated to play a role in calcium signalling.

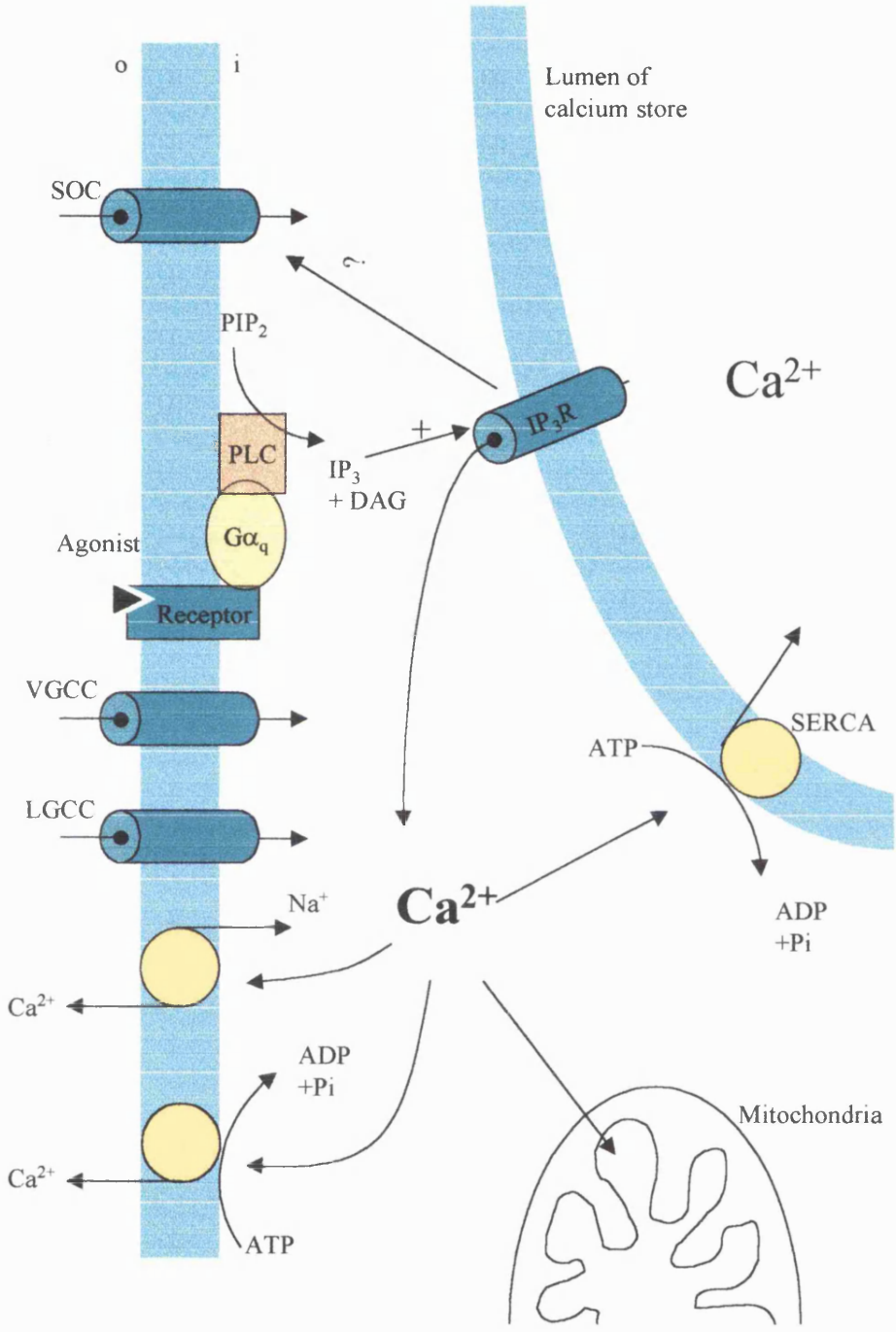

Figure 1.11 Elementary pathways of intracellular calcium signalling.

Calcium entry into the cytoplasm can be via voltage or ligand gated calcium channels (VGCC and LGCC) or from release from intracellular stores. Efflux is via Ca^{2+}ATPases on the endoplasmic reticulum or plasma membrane or via the sodium calcium exchanger.

1.8.1 Sarco/Endoplasmic reticulum calcium stores.

The endoplasmic reticulum is surrounded by the largest membrane system in eukaroytic cells. Virtually all proteins that are secreted from the cell and certain membrane proteins and organelle proteins are synthesised within the endoplamsic reticulum. The endoplasmic reticulum is comprised of two distinct types, the smooth and the rough. The smooth endoplasmic reticulum is responsible for the synthesis of many fatty acids and phospholipids and lacks ribosomes whereas the rough endoplasmic reticulum is enriched with ribosomes. Secretary cells often have large endoplasmic reticulum networks that take over most of the cytoplasm, (e.g. pancreatic acinar cells, Petersen *et al.*, 1991). However, it is their role as an intacellular store for calcium that has received the most attention.

Calcium specific pumps utilise the energy in ATP to pump calcium ions up their electrochemical gradient from the cytosol into the lumen of the endoplasmic reticulum. These pumps (sarco- endoplasmic reticulum Ca^{2+}-ATPases or SERCAs) are encoded by three genes, SERCA1 - SERCA3. SERCA1 is exclusively expressed in fast skeletal muscle, SERCA2 is ubiquitously expressed and SERCA3 is expressed most abundantly in large and small intestine, thymus, and cerebellum and at lower levels in spleen, lymph node, and lung. All subtypes are subjected to post-translation modification for example four different mRNA are known for SERCA2, classes 1-4, of which class 4, which encodes SERCA2b is ubiquitously expressed in the brain (Baba-Aissa et al., 1996).
Once in the lumen of the endoplasmic reticulum calcium binds to high affinity calcium binding proteins, such as calretulin and calsequestin. This enables the endoplasmic reticulum to store large concentrations of calcium without the danger of calcium phosphates precipitating.

Release of calcium from the endoplasmic reticulum follows activation of plasma membrane metabotropic receptors. Activation of plasma membrane receptors that are linked to $G\alpha_{q/11}$ cause the activation of phospholipase C. Phospholipase C catalyses the hydrolysis of PIP_2 to DAG and IP_3. DAG is a membrane bound activator of PKC (Liu, 1996) whereas IP_3 is water soluble and able to diffuse across the cytosol to the membrane of the endoplasmic reticulum. There, it binds to specific

IP_3 receptors on the surface of the endoplasmic reticulum causing channel opening and subsequent release of stored calcium (Berridge 1993).

The first, neuronal, IP_3 receptor (IP_3 type 1 or IP_3R1) was cloned over ten years ago by Furuichi *et al.* (1989) which led to a further two types being identified, (Furuichi *et al.* 1994). IP_3 receptor subunits come together to form either homo or heterotetrameric structures in functional channels. Each subunit consists of 6 transmembrane spanning segments, a pore forming loop, a large cytosolic N-terminus and a short cytosolic C-terminus, see figure 1.12. IP_3 binds to the N-terminus where positively charged amino acids, namely arg265, lys508, and arg511, facilitate ionic interaction with the negatively charged IP_3. The kinetics of IP_3-gated Ca^{2+} release are profoundly altered by Ca^{2+} ions. At low calcium concentrations (<1μM) calcium can be considered a co-agonist at the IP_3 receptors (Finch *et al.*, 1991). However, at higher concentrations calcium and IP_3 cause channel inactivation (Hajnóczky & Thomas 1994). This provides a negative feedback mechanism by which IP_3 receptors open only transiently.

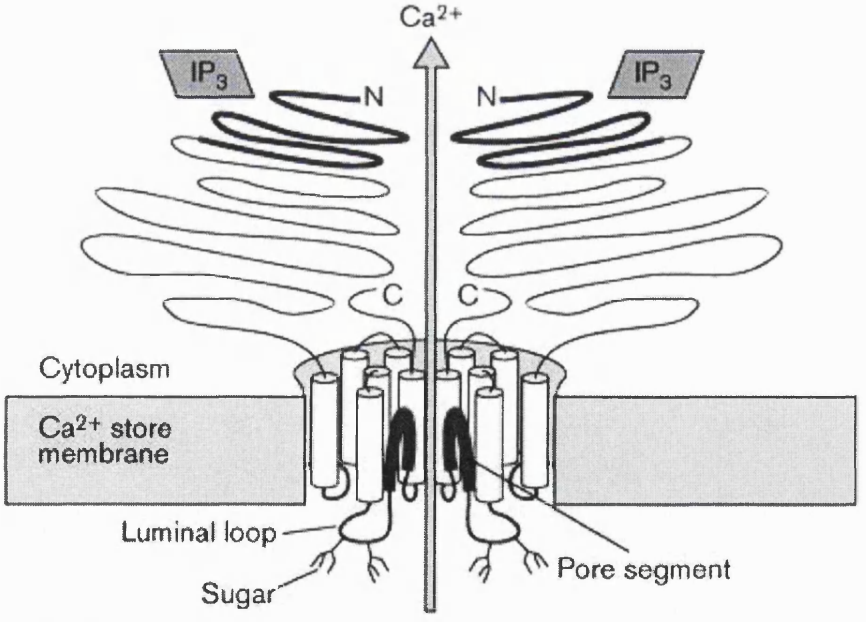

Figure 1.12 Schematic representation of an IP_3 receptor.

A cross section of an IP_3 receptor in the ER membrane. Two subunits have been removed for clarity. IP_3 receptors have a large N-terminus which is responsible for binding of IP_3 and calcium. Each subunit consists of 6 transmembrane domains and a pore forming loop that extends into the channel pore from the luminal side.

IP_3 receptors are subject to intensive modification. PKA, PKC and Ca^{2+}/calmodulin kinase II are all known to phosphorylate IP_3 receptors. In addition, type 1 and type 2 but not type 3 IP_3 receptors have been shown have consensus sequences for tyrosine kinase phosphorylation (Harnick *et al.*, 1995) and that phosphorylation of type 1 IP_3 receptors by non-receptor tyrosine kinases results in increased IP_3 induced calcium release (Jayaraman *et al.*, 1996).

In addition to IP_3 receptors ryanodine receptors (RyRs) also release calcium from the intracellular stores. Ryanodine receptors were first cloned from skeletal muscle (Marks *et al.*, 1989). There are three ryanodine receptor subtypes, RyR_{1-3}, sharing considerable sequence homology. Like IP_3 receptors ryanodine receptors come together to form tetrameric structures in functional channels. Ca^{2+} itself is the primary activating agent and although cyclic ADP ribose (cADPR) is known to be able to stimulate activation of ryanodine receptors (see Galione, 1991) their main function is thought to be in the mediation of calcium induced calcium release (CICR), a process whereby elevated cytosolic calcium causes release of calcium from intracellular stores, (Sitsapesan *et al.*, 1995).

1.8.2 Store-operated calcium influx.

In 1977 Putney showed that carbachol, phenylephrine and substance P were all able to induce a calcium influx into rat parotid gland cells. Subsequent work in a wide variety of cell types has shown that agents that induced calcium release from intracellular stores also evoke an influx of calcium across the plasma membrane. Such agents included calcium mobilising agonists (e.g. 5-HT, Parekh *et al.*, 1993), IP_3 itself (Bird *et al.*, 1991) and SERCA inhibitors (e.g. thapsigargin, Petersen & Berridge, 1994). This evidence indicated that release of calcium from intracellular stores induces a calcium influx. The calcium current induced by store depletion was first measured directly by Hoth & Penner (1992), who referred to it as I_{CRAC} (calcium release-activated calcium current). I_{CRAC} is a calcium current with a very low conductance, perhaps as low as 24fS (Zweifach & Lewis 1993) and is both activated by low and inactivated by high calcium concentrations.

The molecular identity of the store-operated (or CRAC) channel was not, until recently, known. It is now known to be a product of the transient receptor potential (trp) gene discovered in *Drosophila* photoreceptors (see Montell, 1997). *Drosophila* which contain a mutant trp gene become blind in bright light, but are

indistinguishable from wild type in the dark or in dim light, (Cosens & Manning 1969). Molecular identification of the trp gene realised it as a voltage-independent calcium channel (Montell *et al.*, 1985). Depletion of intracellular stores caused activation of trp identifying it as a store-operated channel (Vaca *et al.*,1994; Xu *et al.*, 1997). The existence of mammalian trp channels was shown simultaneously by two groups leading to complications in their nomenclature (Zhu *et al.*, 1995; Wes *et al.*, 1995). To date there are 6 known genes encoding trp channels (see Putney & McKay 1999) some of which are subjected to splice variations (e.g. TRP1, Zitt *et al.*, 1996).

Although the biophysical properties of the store-operated calcium channels are well understood the mechanisms underlying activation of the store operated calcium channels remain to be fully classified. A number of mechanisms have been proposed to explain how a depletion of endoplasmic stores results in the activation of a plasma membrane calcium channel (see Berridge, 1995), two of which are described below

(a) Diffusible messenger

This model proposes that as the intracellular calcium stores deplete they release a soluble diffusible second messenger that crosses the cytoplasm and activates the store-operated calcium channels on the plasma membrane. The proposed messenger has been termed calcium influx factor (CIF) and is thought to be a small highly phosphorylated compound (Randriamampita & Tsien 1995). The mechanism of action of several kinase and phosphatase inhibitors (which affect store-operated calcium entry) has been attributed to an action on CIF (Thomas & Hanley 1995). However, recent evidence suggests that store-operated calcium influx is not dependent on a diffusible second messenger (Yao *et al.*, 1999).

(b) A conformational coupling between IP_3 receptors and trp channels.

A tight coupling between IP_3 receptors and plasma membrane calcium channels was first proposed by Irvine (1990). A tight coupling between ryanodine receptors and L-type calcium channels is known to exist in skeletal muscle fibres (Berridge *et al.* 1997) and may be analogous to a coupling between IP_3 receptors and store-operated channels in other tissues. In HEK293 cells a functional interaction between IP_3 receptors and human TRP3 channels has been demonstrated (Kiselyov *et al.*, 1998). Kiselyov *et al.* showed that activation of TRP3 channels in patches, by calcium

mobilisation in intact cells, was lost upon extensive washing and subsequently restored by administration of IP_3-bound IP_3 receptors. Further experiments have shown that the N-terminal domain of the IP_3 receptor functions as a gate for human TRP3 channels (Kiselyov *et al.*, 1999). However, other studies have found that loss of all three IP_3 receptors does not affect thapsigargin induced calcium influx, (Sugawara *et al.*, 1997).

Despite the presence of some contradictions conformational coupling between endoplasmic and plasma membrane proteins remains the most likely mechanism which links store depletion to calcium influx. Many other proposals such as vesicular insertion of TRP channels into the plasma membrane have been largely discounted (e.g. Gregory & Barritt 1996).

1.9 Mitochondria

Mitochondria have long been known to be responsible for the process of oxidative phosphorylation which yields most of the ATP derived from the breakdown of carbohydrates and fatty acids. However, in recent years mitochondria have been shown to have a dramatic impact on the time course of calcium signalling, (Gunter *et al.* 1994; Babcock and Hille 1998; Duchen 1999).

The mitochondria are unlike other intracellular organelles, they contain their own DNA and are able to create their own mitochondrial proteins. They are surrounded by a double-membrane system, the outer of which is readily permeable to small molecules. The inner mitochondrial membrane forms numerous folds (cristae) which extent into the interior or matrix of the mitochondria. The space between the inner and outer mitochondrial membranes is called the intermembrane space. Glucose is broken down to pyruvate by glycolysis in the cytosol. Pyruvate is then transported into the matrix where it is converted to acetyl-CoA which joins the citric acid cycle that yields the bulk of the ATP manufactured from glucose and fatty acid metabolism. Oxidation of acetyl-CoA to CO_2 is coupled to the reduction of NAD^+ and FAD to NADH and $FADH_2$. Oxidative phosphorylation of NADH and $FADH_2$ results in high energy electrons being transferred through a series of carriers to molecular oxygen. The energy derived from the movement of the electrons is stored as potential energy in the form of a proton gradient. Protons are pumped out of the matrix across the inner mitochondrial membrane and into the intermembrane space.

This movement of protons creates a large membrane potential (often referred to as $\Delta\psi_m$) that is in the order of -150 to -200mV (Duchen 1999). Proton re-entry into the matrix occurs through the F_1F_0-ATPase (or -ATP synthase) which synthesises ATP by utilising the large electrochemical gradient for protons, see figure 1.13. Depolarisation of the inner mitochondrial membrane causes the F_1F_0-ATPase to pump protons out of the matrix consuming ATP. In this way uncoupling agents such as carbonyl cyanide *m*-chlorophenylhydrazone, (CCCP) that dissipate the potential across the inner mitochondrial membrane by making the membrane permeable to protons, can cause complete depletion of the cellular ATP (see figure 1.14). In a futile energy wasting process the F_1F_0-ATPase acts in reverse utilising ATP to pump protons out of the matrix causing ATP depletion within minutes (Leyssens *et al.*

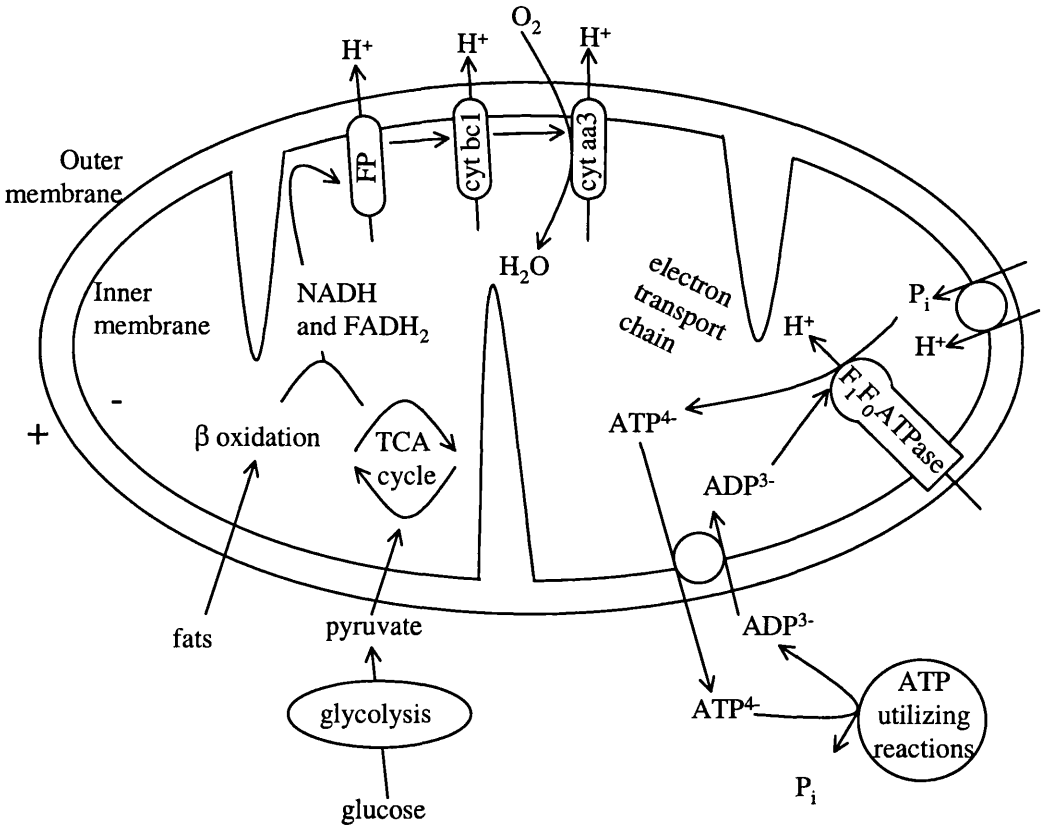

Figure 1.13 Metabolic pathways within a mitochondrion.

Products of metabolism of sugars, carbohydrates, amino acids, and lipids are used as carbon sources for the citric acid cycle (TCA cycle). NADH and $FADH_2$ supply reducing equivalents into the electron transport chain (ETC), in the inner mitochondria membrane. Protons are pumped across the inner mitochondrial membrane at three points in the ETC into the intermembrane space. Proton re-entry provides energy for the phosphorylation of ADP to ATP. FP, flavoprotein; cyt, cytochrome. Adapted from Gunter *et al.* 1994.

1996).

Studies on isolated mitochondria showed that mitochondrial calcium uptake occurs when $[Ca^{2+}]_i$ reaches a 'set point', above which mitochondria sequester calcium. This 'set point' has been shown to be in the order of 0.5 - 1μM in isolated mitochondria (Carafoli 1987) but may be different in intact cells. Calcium uptake into mitochondria is via a calcium selective channel, the mitochondrial calcium uniporter, and driven by the large electrical gradient across the inner mitochondrial membrane. Under normal circumstances the mitochondria would not be expected to take up calcium however, during repeated cell stimulation mitochondria have been shown to both buffer $[Ca^{2+}]_i$ and prolong the calcium signal, (Werth & Thayer 1994, Thayer & Millar 1990, Friel & Tsien 1994).

Driven by the large electrochemical gradient, calcium enters the mitochondria via a calcium selective uniporter. Extrusion of calcium from the matrix is an active one through an electrically neutral sodium calcium exchange. A more rapid extrusion can occur if mitochondrial calcium is sufficiently high by opening of the mitochondrial permeability transition pore which is a large channel ~3nm in diameter that is permeable to many ions and small molecules.

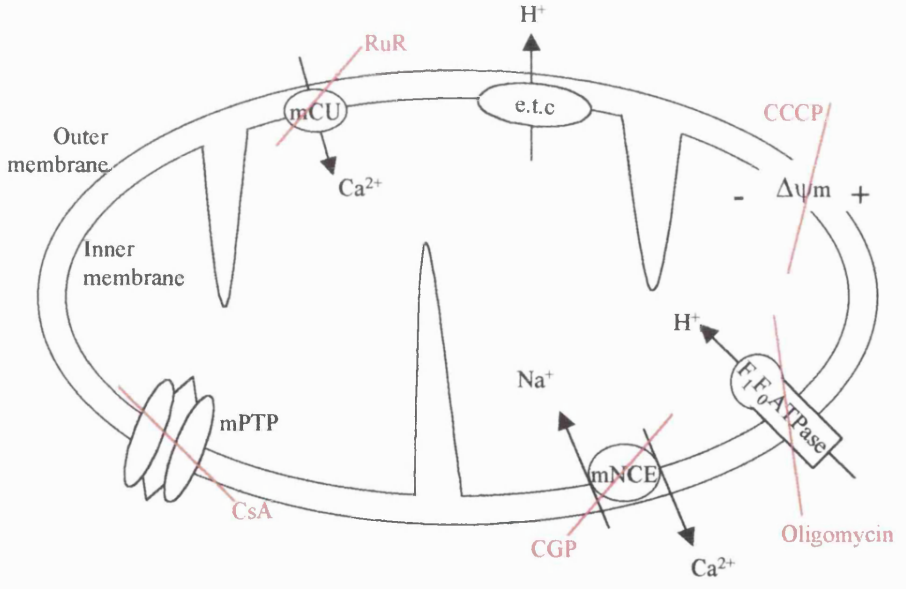

Figure 1.14 Ca^{2+} transport across the inner mitochondrial membrane.

Inhibitors are indicated in red. e.c.t., electron transport chain, mCU, mitochondrial calcium uniporter; mPTP, mitochondrial permeability tranisition pore; mNCE, mitochondrial sodium - calcium exchanger; RuR, ruthenium red; CsA, cyclosporin A, CGP, 7-choro-3,5-dihyro-5-phenyl-1H-4,1-benzothiazepine-2-on. Adapted from Babcock & Hille, 1998.

Electrical activity of the cell results in increased $[Ca^{2+}]_i$ which enters the mitochondria due to the large electrical gradient across the inner membrane. The subsequent mitochondrial depolarisation temporarily stops proton re-entry and hence ATP synthesis. Calcium oscillations in the cytoplasm bring about oscillations in mitochondrial calcium, these oscillations are particularly effective at activating a number of the dehydrogenases of the citric acid cycle and hence increase ATP production (Hajnóczky *et al.* 1995). Increased mitochondrial calcium concentration has also been shown to activate pyruvate dehydrogenase increasing the substrate supply for the citric acid cycle (Robb-Gaspers *et al.* 1998). In this way, the increased energy demand of the cell during times of cellular activity translate into increased ATP synthesis via increased mitochondrial calcium (McCormack *et al.* 1990; Duchen 1990). Recent evidence also suggests that rises in intramitochondrial calcium can lead to priming of the metabolic pathway leading to prolonged ATP production (Jouaville *et al.* 1999).

A more detailed account of the role of mitochondria as active participants in cellular calcium signalling can be found in chapter 5.

1.10 Nuclear Envelope and golgi as calcium stores.

The nuclear envelope has been shown to act as a calcium store, having both SERCAs to take up calcium and IP_3 and ryanodine receptors to release it. Calcium has been shown to be released by the nuclear envelope into the nucleoplasm in response to both IP_3 and cADPR, (Petersen *et al.*, 1998).

Also recently the golgi apparatus has been shown to act as a calcium store. In HeLa cells Pinton *et al.*, (1998) showed that stimulation with histamine, known to evoke a rise in IP_3 caused a decrease in calcium concentration within the golgi apparatus.

1.11 Organisation of the calcium signal.

Global increases in calcium are the net result of activation of some or all of the channels described above, however, beneath the global aspects of $[Ca^{2+}]_i$ cells have developed complex mechanisms to localise and control $[Ca^{2+}]_i$. Localised increases in $[Ca^{2+}]_i$ are achieved by restricted expression of the channels. For example, voltage-gated calcium channels are highly localised at points of exocytosis. There, membrane depolarisation results in a rise in $[Ca^{2+}]_i$ close to proteins associated with

vesicular release (such as syntaxin), resulting in exocytosis without the need for large global rises in $[Ca^{2+}]_i$ (Llinás *et al.*, 1992).

Recent advances in imaging technology have allowed for a more detailed analysis of the elementary events that underlie global rises in $[Ca^{2+}]_i$. Many studies on the fundamental aspects of calcium signalling have been performed on large cells to give the best signal to noise ratios.

Calcium imaging of *Xenopus* oocytes has revealed a series of elementary aspects to calcium signalling. Low concentrations of IP_3 result in a small rise in $[Ca^{2+}]_i$ due to the opening of a very few IP_3 receptors (Parker & Yao 1996). This elementary event is called a 'blip'. As the concentration of stimulating IP_3 increases 'blips' turn into 'puffs'. Puffs occur when sufficient calcium is released from IP_3 receptors to diffuse to neighbouring IP_3 or Ry receptors within a cluster and activate it. This process is known as calcium induced calcium release (CICR). Further increases in concentration of IP_3 activate sufficient IP_3 receptors that a puff can, by CICR, activate IP_3 or Ry receptors in a neighbouring cluster. As the process of CICR continues so a wave can be seen to spread from its point of origin through the cytoplasm of the cell, (Berridge, 1996).

1.12 Calcium Efflux

For efficient calcium signalling and to maintain a high signal to noise ratio cells must be able to remove calcium from the cytoplasm efficiently. As already mentioned mitochondria are able to remove calcium from the cytoplasm and in this way can act to terminate an intracellular response, (e.g. pancreatic acinar cells, Tinel *et al.*, 1999).

The endoplasmic reticulum calcium store has been shown to play an active part in the termination as well as initiation of a calcium signal. In cerebellar granule neurons calcium clearance following activation of voltage-gated calcium channels was slowed by the presence of thapsigargin which inhibits the Ca^{2+}-ATPases on the endoplasmic reticulum (Toescu 1998).

There are two mechanisms by which calcium is pumped across the plasma membrane and into the extracellular space. The plasma membrane calcium ATPases (PMCAs) are ubiquitously expressed proteins that couple the extrusion of calcium across the plasma membrane with the hydrolysis of ATP. There are four subtypes of

PMCAs all of which are subject to alternative splicing, (Garcia & Strehler 1999). The sodium-calcium exchanger was first cloned in 1990 by Nicoll *et al.*, and was termed NCX1. There are three known mammalian Na^{+}-Ca^{2+} exchangers, NCX1, NCX2, and NCX3 (Philipson & Nicoll 2000). The Na^{+}-Ca^{2+} exchanger is the major regulator of physiological response to calcium. and utilises the sodium concentration gradient to pump one calcium ion out of the cell for three sodium ions which flow down their electrochemical gradient into the cell, see also figure 1.11.

1.13 Aims

An outwardly rectifying, non-inactivating potassium current, IK_{SO}, has previously been identified in cerebellar granule neurons (Watkins & Mathie 1996) and is believed to be a member of the two-pore domain family of potassium channels (Millar *et al.*, 2000). IK_{SO} is strongly inhibited by activation of muscarinic M_3 receptors (Boyd *et al.*, 2000). This study aims to further investigate the properties of IK_{SO} and explore the regulatory mechanisms underlying muscarinic inhibition of IK_{SO}. In particular the role of calcium as a possible intracellular regulator of IK_{SO} will be investigated. This study also aims to investigate the properties of calcium signalling in cerebellar granule neurons.

Chapter 3 describes experiments classifying potassium currents in cerebellar granule neurons and in particular IK_{SO}, with emphasis on regulation by $G\alpha_q$ coupled receptors and ionic permeabilities. Chapter 4 investigates the basic aspects of calcium signalling in cerebellar granule neurons. The role of the mitochondria in modulating calcium responses is analysed and discussed in chapter 5. Chapter 6 investigates the properties of intracellular calcium stores. Chapter 7 describes calcium mediated regulation of IK_{SO} and also investigates alternative pathways that may serve as modulators of IK_{SO}.

Chapter 2.

Materials and Methods

2.0 METHODS

2.1. Tissue culture protocol.

All experiments described in this thesis were performed on primary cultures of cerebellar glial cells or granule neurons obtained from the cerebellum of neonatal Sprague-Dawley rats (6 - 9 days old; either sex). All procedures during tissue culture were performed using sterile implements and carried out in an horizontal laminar air-flow bench (BASSAIRE) which was swabbed with 70 % ethanol before and after use. Solutions were made up non-sterile and then sterile filtered through a 0.22μm pore filter. Metalware was flame sterilized and only sterile plastic-ware was used.

The cerebellum from one neonatal unanaesthetised decapitated rat was used per culture. The head of the rat was pinned to a Sylgard-lined petri dish ventral face down. Using a pair of fine surgical scissors the skin covering the skull was cut down the midline. The skin was peeled away exposing the skull and securely pinned down. The cerebellum was exposed by cutting the skull with a fine pair of scissors from the posterior end in an anterior direction to bregma. At the junction of the skull plates the bone was cut lateral both left and right. The skull plates were then carefully removed exposing the cerebellar cortex and brainstem.

Using a curved pair of forceps the cerebellum was removed and placed in a petri dish containing approximately 5ml of phosphate buffered saline (PBS) enriched with 0.32 % $MgSO_4$, 0.25 % glucose and 0.3 % bovine serum albumin (BSA). Under a dissection microscope (x6.4 magnification) the meningeal layers and connective tissue were removed. The tissue was then transplanted to a plate with a few drops of the enriched PBS solution to prevent drying and cross-chopped (200 × 200 μm) using a McIlwain tissue chopper (Mickle Laboratory Engineering Company, U.K.). The chopped tissue was transferred to a 50ml falcon tube containing 10mls of the enriched PBS solution with 0.025 % trypsin and incubated at 37°C for 20 minutes. Trypsinisation was ceased by addition of 10 mls of enriched PBS solution containing 1.78 mM $MgSO_4$, 8 μg ml^{-1} soyabean trypsin inhibitor (SBTI) and 10.24 Kunits ml^{-1} deoxyribose nucleotidase (DNase). The tissue was then agitated to prevent clumping and centrifuged at 1200 rpm for 3 minutes to pellet the cells. The supernatant was discarded and the cells re-suspended in enriched PBS containing 3

mM $MgSO_4$, 50 μg ml^{-1} SBTI and 64 Kunits ml^{-1} DNase. Using two fire-polished glass pipettes with varying bore sizes the tissue was gently titurated in this solution until all visible clumps had dissipated. The suspended cells were transferred to a 15ml falcon tube and underlayed with 2ml of 4 % BSA in Earle's salt solution (g l^{-1}: 6.8 NaCl, 2.2 $NaHCO_3$, 0.158 NaH_2PO_4, 0.4 KCl, 1 D-glucose, 0.01 phenol red). The tissue was then centrifuged at 1500 rpm for 5mins to remove any cell debris. The supernatant was discarded and using a sterile p1000 pipette tip the cells resuspended in 4-5 mls of minimum essential media (MEM: 2.5 % chick embryo extract, 39 mM D-glucose, 2 mM glutamine, 25 mM KCl, 50 IU penicillin and 50 μg ml^{-1} streptomycin) supplemented with 10 % foetal calf serum (FCS).

80μl aliquots of the suspended cells were allowed to settle on pre-prepared 13mm glass coverslips. Glass coverslips were sterilised in 70% ethanol and incubated in poly-L-lysine (15 mg l^{-1} in sterile water) for a minimum of 12hrs at room temperature. The coverslips were washed twice in sterile water and dried in four-well culture dishes before use. All coverslips were incubated in a humidified atmosphere of 5% CO_2 at 37°C. The following day cells were fed with 0.5mls of MEM +10% FCS per well.

Figure 2.1 shows a typical phase contrast image of a field of cerebellar granule neurons. Granule neurons are readily identifiable as small round cells that are typically phase dark and surrounded by a bright halo. They are by far the most abundant cell type in the culture. Cerebellar glial cells conversely appear phase dark.

All electrophysiological recordings were performed on cerebellar granule neurons that had been maintained in culture for 7-10 days. Calcium imaging experiments were performed on cells which had been in culture for between 5 and 10 days.

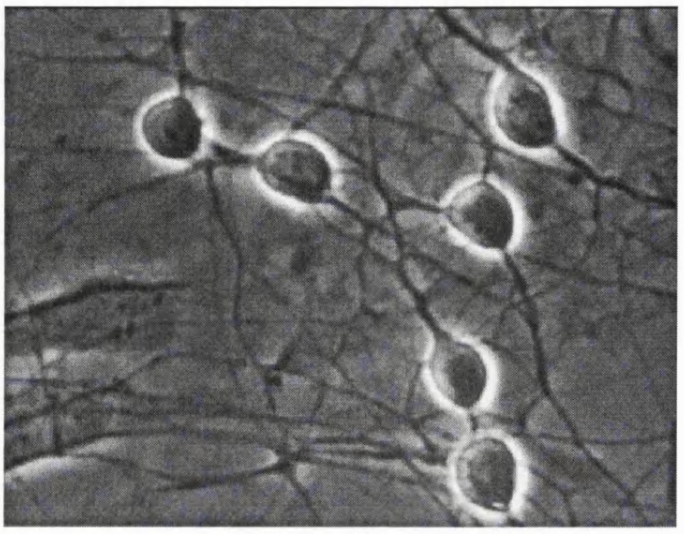

Figure 2.1. A typical phase contrast image of a field of cerebellar granule neurons.

Cerebellar granule neurons are the round cells that appear phase dark surrounded by a bright halo. Their projections are also clearly visible. Two glial cells can be seen on the left hand side and appear phase dark. Granule cell soma are in the order of 10μm in diameter.

2.2 Electrophysiology

The voltage clamp technique was developed by Cole (1949) and Hodgkin *et al.* (1952) and has resulted in experiments which have given us the bulk of our knowledge of ion channels and their behaviour in lipid membranes.

Electrophysiological recordings using patch electrodes require the formation of a high resistance seal (typically in the region of approximately 10GΩ; a 'gigaseal') between the pipette and the membrane. If the seal is not of sufficient resistance then leak can occur around the seal. This will lead to a lower signal to noise ratio.

Formation of a gigseal allows for the study of small numbers of channels under the pipette. If there are very few channels in the patch of membrane enclosed by the pipette single channel recordings can be observed.

However, a much more widespread technique is the whole cell configuration (Hamill *et al.* 1981). Once a gigaseal has formed additional negative pressure is applied to the interior of the pipette which causes the membrane in the patch to rupture. Rupturing of the membrane in the patch has two major consequences. Firstly, it creates an electrically continuous medium between the inside of the cell

and the pipette. Thus ionic current in the whole cell can be measured by the whole cell patch clamp technique, these currents are referred to as macroscopic currents. The second major consequence is that molecules in the pipette are free to diffuse into the cytoplasm of the cell and vice versa. This allows the experimenter to introduce mediators or fluorescent dyes, into the cell. However, it also means that intracellular nutrients can be diluted by the pipette solution which is many times the volume of cell interior. Pipette solutions for whole cell patch clamp recording must therefore contain essential molecules such as ATP and GTP.

The dilution of intracellular mediators is a major drawback in whole cell patch clamping. This report describes a current that undergoes considerable run-down under whole cell recording (Watkins & Mathie 1996). To study this current electrophysiologically it is necessary to use perforated patch recording.

2.2.1 Perforated patch recording

Perforated patch recording allows the experimenter to measure macroscopic currents without rupturing large areas of the plasma membrane which leads to dilution of diffusible intracellular nutrients and messengers, (see Rae *et al.* 1991). Perforated patch recording is achieved by including an antibiotic in the pipette solution. The antibiotic (such as amphotericin B) creates small pores in the plasma membrane that are permeable only to ions and uncharged molecules that are no larger than 0.8nm. Thus molecules such as glucose can not diffuse out into the pipette and the internal environment is maintained. As the number of pores created by the antibiotic increases so the access resistance decreases and allows electrical manipulation of the intracellular surface of the cell.

2.2.2 Principles of electrophysiology

The voltage clamp technique has two major advantages in that it allows the separation of capacitative and ionic currents and allows the membrane potential to be maintained at a constant, pre-determined voltage. As channels activate in the plasma membrane and ions flow down their electrochemical gradient they induce a change in the membrane potential. This change in potential can influence the properties of other channels in the membrane, complicating results. The voltage clamp will prevent this change in potential and will therefore increase the chances of ionic currents being studied in isolation.

The voltage clamp technique therefore requires the set up of a feedback system to maintain membrane potential at a constant level. Figure 2.2 shows the basic circuitry of the voltage clamp technique.

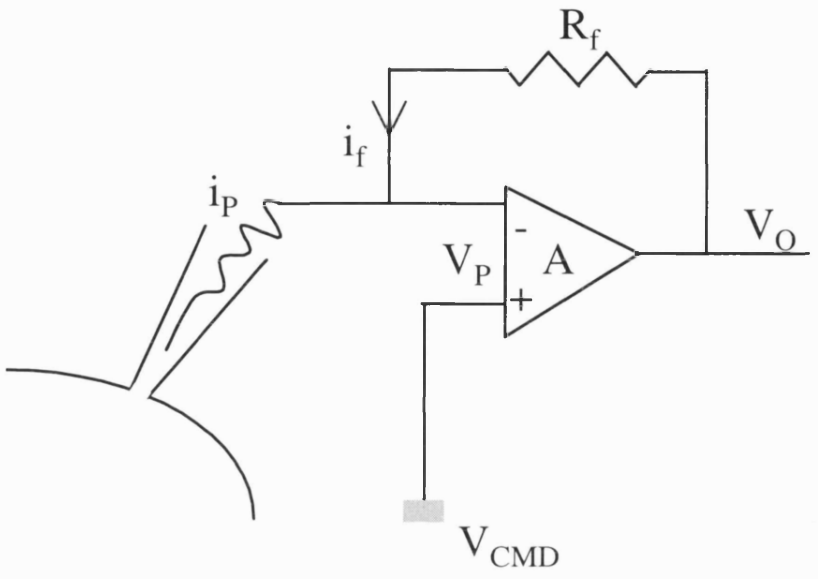

Figure 2.2 The basic circuitry of the voltage clamp.

Membrane potential is held or clamped by a negative feedback loop. The pipette potential (V_P) is fed into the inverting input on the amplifier (A), the command potential is connected to the non-inverting input (+). The amplifier output is fed back into the inverting input via a high resistance feedback resistor (R_f). This forces the inverting input to equal the non-inverting input, the command potential.

Activation of membrane currents in response to a change in V_{CMD} will cause a change in the pipette potential. This feeds into the amplifier which in turn injects a small current, via the feedback loop, into the cell which is of equal but opposite magnitude to the membrane current. In this way the amount of current required to hold V_p at V_{CMD} (i_P), and hence the membrane ionic current can be measured whilst continually clamping the membrane potential.

2.2.3 Capacitance measurement

Both the membrane of the cell and the pipette separate two conducting mediums and hence act as a capacitor. In most voltage clamp experiments the membrane potential is stepped rapidly from one potential to another. When this occurs capacitance spikes are often seen which may mask current with rapid kinetics. The capacitance of the pipette and membrane can be compensated. The current required to compensate for the charging of the capacitative surfaces can be removed from the trace leaving only the ionic currents. In this study, granule cell capacitance was between 2 and 4 pF.

2.2.4 Series Resistance.

As already mentioned a feedback loop supplies small amounts of current to maintain the membrane potential at a constant level. However, this current is subjected to a resistance known as the series resistance.

Series resistance is the sum of the access resistance and the external resistance. The access resistance is the resistance the current experiences when gaining access to the cell, this will be affected by the pipette geometry and the state of the ruptured or perforated membrane. External resistance is the resistance experience by the current in the external solution and the reference electrode. The most efficient way of reducing series resistance is by increasing the diameter of the electrode tip. However, larger pipette diameters reduce the likelihood of getting seals of sufficiently high resistance.

Injected current that is flowing across the membrane has to pass through the series resistance. Series resistance will therefore reduce the current amplitude and therefore the membrane will not be clamped at V_{CMD}. The effect is exaggerated when the amplifier is compensating for large ionic currents. Most conventional patch clamp amplifiers compensate for potential changes due to series resistance but none are entirely effective. Series resistance can also slow the changes in membrane potential. In cases where series resistance is high a second electrode solely for measuring membrane potential can be used.

In this study, even with perforated patch recordings, series resistance was generally $\leq 20M\Omega$, and therefore not compensated for.

2.2.5 Space clamp

Many ion channels are acutely sensitive to voltage, it is therefore necessary to be sure that the channels being examined are all being subjected to the same membrane potential. In single electrode recordings the area surrounding the electrode will be tightly voltage clamped, however, areas of membrane distant to the recording electrode may not be subject to the same membrane potential. Such errors may be observed as 'notches' of inward current which may occur a long time after the depolarising step. There is no way to compensate for a lack of isopotentiality without the use of several linked electrodes.

In this study cerebellar granule neurons are used. Cerebellar granule neurons are very small and spherical, making them ideal for voltage clamp experiments as good voltage control is possible. However, inputs from unclamped projections can not be completely ruled out.

2.2.6 Junction Potentials.

At the interface between two solutions of different composition a potential is established. Under voltage clamp the composition of bathing and pipette solutions are often changed by the experimenter depending on the experimental protocol. Therefore, liquid junction potentials exists between the solution in the pipette and the bathing solution. These are often compensated for by 'zeroing' the potential while the pipette is in the bath and before seal formation. However, the potential required to compensate for the junction potential persists after seal formation despite the solutions not being in contact any longer. Therefore the holding potential V_{CMD} may be affected by adjustments for junction potential.

Junction potentials also exist between the bathing solution and the pipette and reference electrodes. Junction potentials can be calculated both experimentally (e.g. Neher, 1992) and theoretically using the generalised Henderson equation (see Barry and Lynch, 1991).

2.2.7 Microelectrode manufacture.

Patch pipettes used during this thesis for recording whole-cell currents and membrane potential were fabricated from thick walled boroscilicate glass capillary tubing (o.d. 1.4-1.6 mm, i.d. 0.8-1.0 mm, with 2 mm fibre; Plowden and Thompson).

All pipettes were pulled on the day of the experiment using a vertical two stage Narashige PC-10, micropipette puller. Pipettes were firepolished to the desired shape and resistance using a Narashige MF-83 microforge. The resistance of filled electrodes was approximately 10 MΩ.

2.2.8 Intracellular (pipette) solution composition.

The pipette solution used was a KCl based solution, the composition of which was (in mM): 125 KCl, 5 4-(-2-hydroxyethyl)-1-piperazinethanesulphonic acid (HEPES), 5 $MgCl_2$, and 0.1 bis (2-aminophenoxy)-ethane-N, N, N' N' tetraacetate (BAPTA); titrated with KOH to pH 7.4. Solution was filtered using a 0.22 μm filter unit and warmed to room temperature prior to use. When not in use solution was kept refrigerated.

To enable perforated patch recordings to be made the pipette solution was supplemented with 320 μg ml^{-1} of amphotericin B. A stock solution of amphotericin B was made up in DMSO to a concentration of 8 mg ml^{-1}. Once made the stock solution was then stored at -20 °C and if made up at the beginning of the week remained potent for the duration of that week.

To obtain amphotericin B supplemented pipette solution for use in recordings, 8 μl of the stock solution was added to 2 ml of filtered pipette solution, giving a final concentration of 320 μg ml^{-1}. This solution was stored in the dark at room temperature, as amphotericin B is light sensitive, and used within 4 hours.
Once the amphotericin has been added to the pipette solution it cannot be filtered as amphotericin B will not pass through a 0.22 μm filter unit.

2.2.9 Extracellular solution composition

The extracellular solution contained: (mM) 120 NaCl, 2.5 KCl, 2 $MgCl_2$, 0.5 $CaCl_2$, 10 HEPES and 5 D-glucose; titrated with NaOH to pH 7.4. Extracellular solution was made up fresh on the day of the experiment.
In some experiments, described in chapter 3, potassium concentration was increased. To maintain a constant concentration of monovalent cations, sodium concentration was reduced. Solutions containing 25mM potassium (or 25mM of the test ion) had a

reduced sodium concentration of 97.5mM. In the experiment described in figure 3.5b potassium was replaced with thallium. However, thallium chloride is not soluble at concentrations > ~3mM. Here, Na_2SO_4 was used as a source of sodium ions, and $KC_2H_3O_2$ and $TlC_2H_3O_2$ as a source of potassium and thallium ions. Potassium (or thallium) was used at a concentration of 10mM and sodium concentration reduced to 112.5mM (56.25mM Na_2SO_4).

External solution was perfused over the cells throughout all experiments at rate of 4-6mls min^{-1}. Complete exchange of bathing solution occurred in approximately 30 seconds. Solution was removed from the bath by suction from a vacuum pump.

2.2.10 Experimental protocols

All experiments were performed at room temperature (20-23°C).

2.2.10.1 Seal Formation

Pipettes were back-filled with internal solution containing 320μg ml^{-1} amphotericin B, and any bubbles removed by gently tapping the pipette. The pipette was inserted onto the electrode holder with the silver wire immersed as much as possible in the internal solution.

The pipette was lowered, into the bath, towards a cerebellar granule neuron which was selected on the basis of accessibility, general state (health) and proximity to other neurons (cells whose somata appeared to touch another's were not used).

A 5 mV voltage step was applied to the interior of the pipette, which produced a square current pulse allowing the resistance of the pipette to be calculated using Ohm's Law. A typical value for the resistance of the pipettes when filled with electrolyte in response to the 5 mV test pulse was 10 MΩ.

The pipette was moved toward a cell. Contact between pipette tip and cell membrane was detected by an increase in the tip resistance, seen by a decrease in current amplitude.

Negative pressure was applied to the interior of the pipette and as the seal formed the current amplitude reduced further. As the space between the tip of the electrode and the membrane surface reduced to >1Å very little current could be observed to flow and the seal had a typical resistance of approximately 10GΩ.

The holding potential of the pipette was hyperpolarised to -60mV so as the membrane perforated the cell is held close to the resting membrane potential. Amphotericin B incorporation into the membrane occurs after between 2 and 4 minutes and can be observed as an enlargement of the width of the capacitive transients. Access into the cell was also visualised as an increase in potassium current amplitude. As access to the cell improved currents could be seen to gradually increase in magnitude, until the access resistance reaches its final value. At this point experiments were performed providing the access resistance was not unusually high (>20MΩ).

The electrophysiological recordings were performed using a Zeiss, Axioskop microscope, the micromanipulator was supplied by Narishige (Japan), the oscilloscope by Hameg (HM 205_{-2}) and the air table, to stop exogenous vibrations, by Technical Manufacturing Corporation (TMC). Axon instruments supplied the amplifier (Axopatch 1D), interface (digidata 1200) and electrode holder.

2.2.10.2 Voltage Protocols

1) A-current and delayed rectifier.

From a holding potential of -30mV cells were stepped to -120mV for 500ms. This served to remove the inactivation from the potassium channels responsible for the inactivating A-current. The cell was then stepped to a test potential of 0mV for 400ms, after which it was stepped back to the holding potential. This protocol was repeated once every 5 seconds.

2) IK_{SO}

Previous reports have measured IK_{SO} at -30mV (Watkins & Mathie 1996) and at -20mV (Millar *et al.* 2000). The experiments described in this report used the same procedure as Millar *et al.* (2000). Cells were held at -20mV for 150ms before stepping to -60mV for 800ms. The cell was then returned to the holding potential. This protocol was repeated every 5 seconds. IK_{SO} was measured as the mean current amplitude at -20mV after the cell had been at that potential for 4.6 seconds.

3) Voltage Ramps

Current voltage protocols were derived either using a varying step protocol (see 4 below) or a voltage ramp. A ramp protocol allows for a wide range of voltages to be examined. Cells were held at -20mV and ramped slowly to -100mV at a rate of $0.1mVms^{-1}$ (over 800ms), before stepping back to the holding potential. This protocol was repeated every 5 seconds.

4) Current voltage relationships

Here, cells were held at a holding potential of -30mV and stepped to potentials ranging from -10mV to -120mV in 10mV increments for 150ms before returning to the holding potential. The inter-episode duration was 5 seconds.

2.2.10.3 Data Analysis

All electrophysiological data were analysed using CLAMPFIT 6.0.2 software (Axon Instruments). The data were then transferred to and analysed in Microsoft Excel 97 and presented graphically using Microsoft Origin version 5.0.

Typically an example trace is shown for each experiment. Data presented in the text represent mean ± standard error of the mean (s.e.mean).

2.3 Calcium Imaging

Advances in calcium imaging have allowed physiologists to explore one of the most fundamental and important intracellular signalling pathways. The development of calcium sensitive dyes that are specifically targeted to intracellular membranes and organelles continues to enhance our understanding of the intricacies of calcium signalling. This report concentrates on global changes in calcium concentration in the soma of the cell. The calcium fluorophore fura-2 is used to monitor changes in cytoplasmic calcium concentration.

2.3.1 The Fluorescence Process

Fluorescence is the product of a series of processes that start with the absorption of a photon of one wavelength and finish with the emission of a photon of a different energy. The Jablonski diagram (figure 2.3) shows the three stage fluorescence process.

Excitation by a photon of energy $h\nu_{EX}$ from an external source (such as a lamp) results in a higher energy excited state, or singlet state (S_1') of the fluorophore. The excited state of the fluorophore has a limited half life that is typically in the region of $1\text{-}10^{-9}$ seconds). Whilst in this state the fluorophore is able to react or interact with its environment and in doing so loses energy yielding a relaxed singlet state (S_1). Finally, a photon of energy $h\nu_{EM}$ is emitted returning the fluorophore to its original state. Due to the energy lost between the excited singlet state and the relaxed singlet state the energy, and hence wavelength, of the emitted photon is different to the excitation photon.

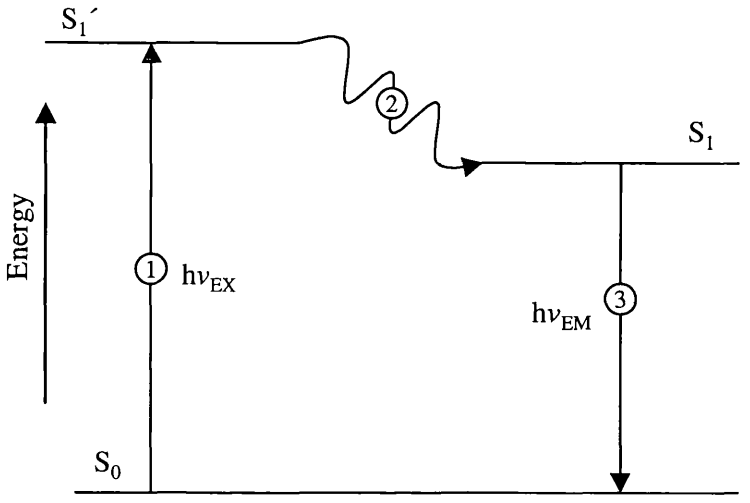

Figure 2.3 The Jablonski diagram

An illustration of the three processes involved in fluorescence of a fluorophore. 1. excitation, 2. excited state energy loss, and 3. fluorescence emission.

This report uses a ratiometric calcium indicator. Ratiometric dyes have different emission or excitation spectra depending on whether they are bound to ions. Fura-2 is a calcium sensitive ratiometric dye. The excitation energy required to excite fura-2 to its excited singlet state differs when it is bound to calcium, the emission spectrum however does not change upon calcium binding, see figure 2.4.

Thus, in the presence of calcium fluorescence emission (collected at 510nm) is greatest when the fluorophore is stimulated with light of wavelength approximately 340nm, and in the absence of calcium emission is greatest following stimulation with light at 380nm. Emission fluorescence is unchanged by the presence of calcium. Therefore, ratiometric calcium imaging with fura-2 is performed by

stimulating the fluorophore with light of 340nm followed by light of 380nm and emitted fluorescence is always collected at 510nm.

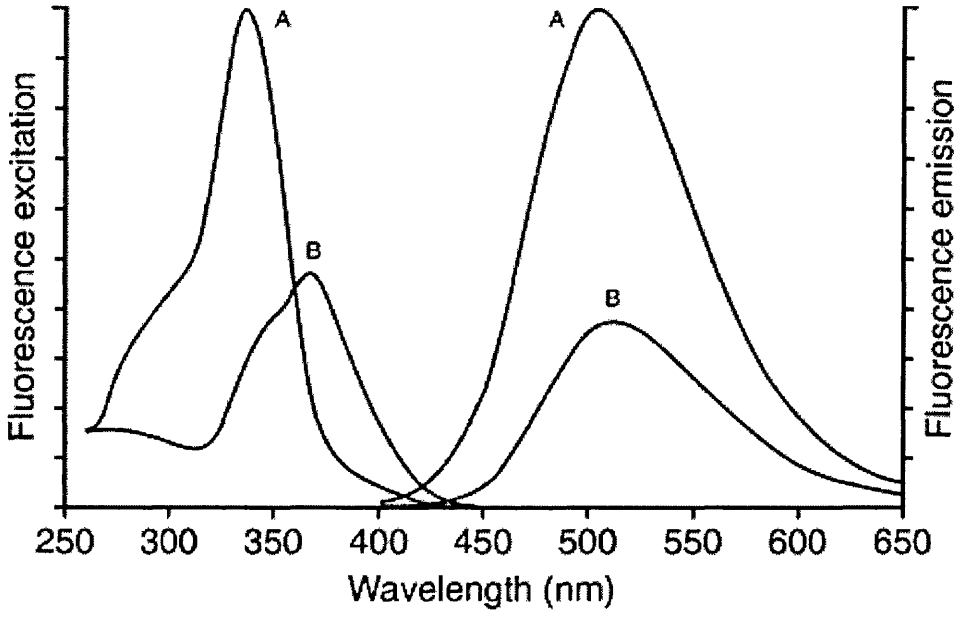

Figure 2.4 Excitation and Emission Spectra for fura-2.

Fluorescence excitation (left hand side; detected at 510 nm) and emission (right hand side; excited at 340 nm) spectra of Ca^{2+}-saturated (A) and Ca^{2+}-free (B) fura-2. Adapted from Molecular Probes product literature.

Emitted fluorescence following stimulation at 340nm is often of much less intensity than the emitted fluorescence emitted following stimulation at 380nm (see figure 2.4). Therefore to decrease the signal to noise ratio, it is customary to collect emission following 340nm stimulation for 3 times longer than 380nm stimulation.

Fura-2 forms a pentapotassium salt which is cell impermeant. To introduce fura-2 into the cytoplasm of the cell it is therefore necessary to either inject it artificially, which is highly invasive or to use the acetoxymethyl esters of fura-2 (fura-2AM). The AM ester of fura-2 is able to passively diffuse across lipid membranes. Once

inside the cell cytosolic esterases cleave the AM ester to release fura-2, which is unable to leak out of the cell across the plasma membrane. The presence of unhydrolysed fura-2 AM can complicate analysis. In the experiments reported here the fura-2 loaded cells are incubated for a further 10 minutes in control extracellular solution to allow unhydrolysed fura-2AM to diffuse out of the cell.

2.3.2 Fura-2 loading.

Fura-2 AM (Molecular probes) was dissolved in DMSO and diluted to a concentration of 10μM in extracellular solution. The Fura-2AM solution was stored at -20°C until required.

For imaging experiments cerebellar granule neurons were used from 5 day *in vitro*. Coverslips were removed from the MEM + 10% FCS solution and incubated in fura-2AM (10μM) in external solution for 20 minutes at 37°C. The coverslips were then washed twice in control external solution and incubated for a further 10 minutes.

On occasion drugs were added to the extracellular solution for the duration of the 10 minute incubation, see results text for details.

2.3.3 Extracellular solution composition.

The composition of the extracellular solution was: (in mM) 120 NaCl, 2.5 KCl, 2 $MgCl_2$, 2 $CaCl_2$, 10 HEPES and 5 D-glucose; titrated with NaOH to pH 7.4. Calcium free solutions contained no $CaCl_2$ and the $MgCl_2$ concentration was increased to 4mM to maintain a constant concentration of external divalent cations. Calcium free solution also contained 1mM (ethylene glycol-bis(β-aminoethyl ether)-N,N,N',N'-tetraacetic acid (EGTA) to buffer any residual calcium.

Sodium free extracellular solution was used in the experiment described in figure 4.2. In this experiment sodium was replaced by choline at the same concentration. During experimental recording cells were continually perfused with extracellular solution by a gravity driven perfusion system at a rate of 4-6mls min^{-1}. Solution was removed from the bathing solution by a vacuum pump.

2.3.4 Experimental Protocol

A suitable field of cells was selected so that it contained cerebellar granule neurons that were not in close proximity to each other or to cerebellar glial cells. The

fluorescence of cells that are touching or in close proximity can overlap and distort results.

Coverslips were secured to the bottom of a well and perfused with external solution as previously mentioned. If the field of cells appeared to move during the course of the experiment the data from that experiment were not used in the final analysis. Cells were exposed to light of 340nm and 380nm wavelengths for 600 and 200ms respectively, once every 1.4 seconds. The light source was a xenon lamp (Nikon) which passed through filters (Cairn) before being reflected onto the cells. Emitted fluorescence was collected at 510nm onto a Hamamatsu multi format CCD camera. The signal was relayed via an amplifier to a PC imaging package, Lucida analysis (Kinetic Imaging, UK). All drugs were perfused onto the cells in the extracellular solution and all experiments were performed in the dark with minimal interference from the light source.

2.3.5 Data analysis.

In Lucida analysis, fluorescent intensity following stimulation at 340nm was divided by emitted fluorescence following stimulation at 380nm. This was performed at each time point during the experiment. The resultant ratio is proportional to the concentration of cytosolic calcium, see calibration below.

This ratio (F_{340}/F_{380}) was plotted against time and the raw data for each cell imported into Microsoft Excel 97 for further analysis. Graphical representation was performed on Microsoft Origin 5.0. Data represented in this report gives either example traces or average data. Data in text and in some figures is given as mean ± s.e.mean, and n numbers represent number of cells. Stastical analysis was performed using the students *t* test for normal unpaired data.

Figure 2.5 shows divided fluorescent images of the field of cells shown in figure 2.1 when exposed to high concentrations of extracellular potassium. Fluorescent intensity is represented by a colour scheme where cold colours (blacks-blues) represent low calcium concentrations and progressively warmer colours (pink, red white) represent rising calcium concentrations. The intracellular calcium concentration can clearly be seen to rise in the presence of high extracellular potassium.

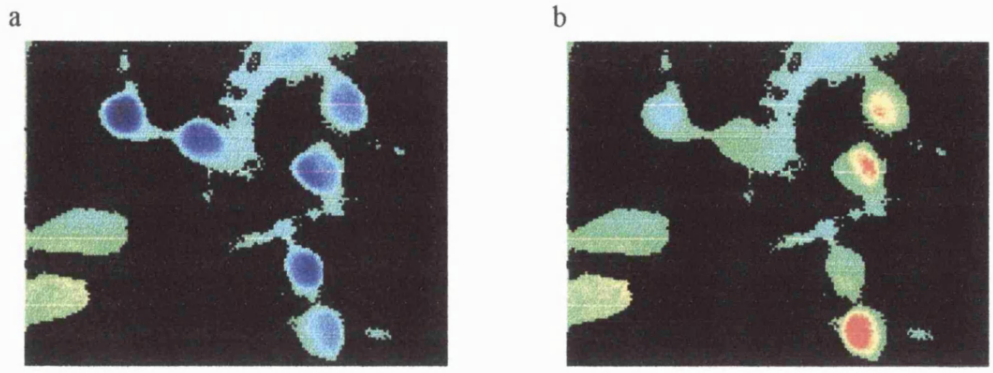

Figure 2.5 Pseudocolour images of fura-2 fluorescence of the field of cells in figure 2.1
Low F_{340}/F_{380} ratios (and hence low $[Ca^{2+}]_i$) are represented by the cold colours whereas higher ratios are represented by increasingly warmer colours. At rest (a) CGN have low resting a $[Ca^{2+}]_i$, exposure to high extracellular potassium (b) increases $[Ca^{2+}]_i$, as indicated by the warmer colours, (oranges and reds). See also chapter 4. The two glial cells on the left hand side do not respond to high potassium.

2.3.6 Calibration

To calibrate the F_{340}/F_{380} ratios into 'real' calcium concentrations a zero and maximum level of fluorescence must be found. Cells were incubated in fura-2AM as previously described. During imaging cells were exposed to ionomycin (5μM), CCCP (3μM) and thapsigargin (1μM) in calcium free extracellular solution (containing 1mM EGTA). This solution is made to release calcium from all intracellular space including intracellular compartments. Ionomycin is an ionophore which will make all membranes permeable to calcium, CCCP will dissipate the inner mitochondrial membrane allowing for the release of mitochondrial calcium and thapsigargin will facilitate the release of calcium from endoplasmic reticulum calcium stores. After 2 minutes the calcium (2mM) was re-introduced to the extracellular solution and the EGTA removed. The fluorescent intensities in the zero calcium concentration is referred to as zero calcium and in the presence of 2mM calcium the fluorescence is referred to as maximum calcium. Calcium concentration is calculated using the equation:

$$[Ca^{2+}]_i = K_d\left(\frac{R - R_{min}}{R_{max} - R}\right)\left(\frac{S_{f2}}{S_{b2}}\right)$$

Equation 2.1 Calibration equation (Grynkiewicz *et al.* 1985)

where R is the measured ratio of interest, R_{min} and R_{max} are the zero and maximum ratios, S_{f2} and S_{b2} the signals at 380nm in zero and 2mM calcium and K_d is the apparent dissociation constant for fura-2 (224nM).

Figure 2.6 shows a calibration curve for the fura-2 from experiments performed as described above.

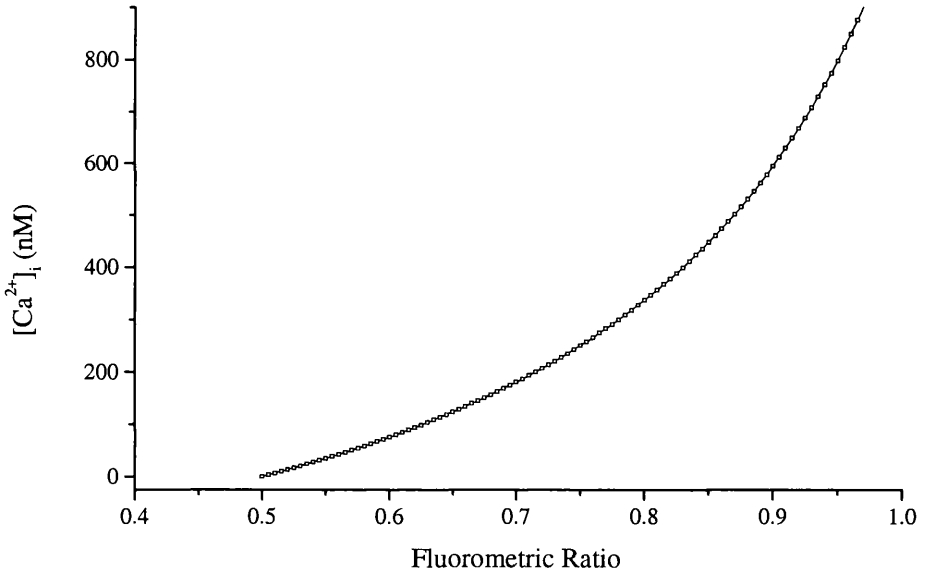

Figure 2.6 A calibration curve for fura-2 in CGN.

Cells were exposed to zero and maximum calcium concentrations as described in the text. A calibration curve was calculated using equation 2.1. n = 26.

The validity of using calibrated data in this system is discussed later in chapter 4.4.

2.4 Materials

2.4.1 Cell culture:

All enzymes and chemicals used during the isolation of CGNs were purchased from Sigma Chemicals Ltd. (UK), except for Earles salt's solution, chick embryo extract, glutamine, FCS and penicillin/streptomycin which were obtained from GIBCO BRL, Life Technologies, (UK).

2.4.2 Electrophysiology and calcium imaging: Salts used in the preparation of internal and external solutions were purchased from BDH, except for NaCl which was purchased from Sigma. Glucose, HEPES, BAPTA and DMSO were all obtained from Sigma.

Pharmacological agents were purchased from Sigma, except for thapsigargin and U73122 which were purchased from Research Biochemicals International (RBI). PD 98059 and U0125 were pucharsed from Calbiochem, U 0126 from Promega and PMA from Tocris. Fura-2AM was purchased from Molecular Probes.

Chapter 3. Results.

Potassium currents in cerebellar granule neurons.

3.1 INTRODUCTION

3.1.1 Voltage-gated currents in cerebellar granule neurons

Cerebellar granule neurons are numerous, one estimation suggests that their numbers exceed the combined total of other central neurons (Herrup and Kuemerle, 1997). However, despite their immense numbers early electrophysiologists were unable to record from them due to their small size, (< 10μm, Hirano *et al.* 1986). The advent of more sensitive patch clamp recording methods (Hamill *et al*, 1981) allowed the electrophysiologist to record electrical activity in these cells and because of their small size good voltage control is readily achieved. Cerebellar granule neurons are available in near pure cultures and their small size and high numbers have made them the neuron of choice for many studies (e.g. Bhave *et al.* 2000; Carlier *et al.*2000)

(a) Inward Currents

Using the newly developed patch clamp techniques several groups identified inward currents in cerebellar granule neurons in response to a depolarisation. Hirano *et al.* (1986) demonstrated the presence of an inward current in response to a depolarisation from a holding potential to potentials positive of -40mV. This early inward current has been seen in other studies since, (Cull-Candy *et al.* 1989, Hockburger *et al.* 1987, Jalonen *et al.* 1990), and due to its sensitivity to tetrodotoxin and the removal of extracellular sodium has been shown to be due to opening of voltage gated sodium channels. A further component to the inward current was discovered by Hirano *et al.* (1986). They showed that the residual current left after application of TTX was a calcium current. Shortly after several studies failed to identify calcium current in cerebellar granule neurons (Cull-Candy *et al.*1988; Hockberger *et al.* 1987). However, there are now several reports detailing the existence of calcium currents in cerebellar granule neurons. An inward current that could be carried by barium could be activated at -25mV and reversed at ~ +80mV (Marchetti *et al.*, 1991; Amico *et al.*, 1995). This current could be inhibited by the dihydropyridine nimodipine by ~25% and was also sensitive to omega-conotoxin GVIA (17%) and omega-agatoxin IVA (47%), (Amico *et al.*, 1995). Cerebellar granule neurons are known to possess L-, N- (Pearson *et al.*,

1995), P-, and Q- (Randall & Tsien, 1995) calcium currents and although there is still proportion (19%) of the calcium current that remains unclassified and is known as residual or R-type (Randall & Tsien 1995). As mentioned some early studies failed to identify the calcium component to the inward current (Cull-Candy *et al.*1988; Hockberger *et al.* 1987). This may have been due to incomplete removal of outward currents or a rundown of calcium current amplitude under whole cell recording. Marchetti *et al.*, (1991) showed that calcium current amplitude increased with days in vitro, so it remains a possibility that calcium currents alter with development.

(b) Outward Currents

A two-phase outward current is seen to follow the inward sodium current, (Hirano *et al.* 1986; Hockburger *et al.* 1987; Cull-Candy *et al.*1989). This current was shown to be due to voltage-gated potassium channels by it's sensitivity to caesium (Hirano *et al.* 1986), barium and quinine (Cull-Candy *et al.* 1989).

Depolarising the cells from -40mV to a test potential of greater that 0mV induced a slow rising sustained outward current, however if the cells were held at -80mV and stepped to -40mV a transient outward potassium current was observed preceding the sustained current, (Hirano *et al.* 1986, Hockburger *et al.* 1987).

The two components to the outward current in cerebellar granule neurons resemble potassium currents seen in other cell types. The slow activating sustained current is a delayed rectifier and the fast activating transient component the A-type (Rudy 1988). Jalonen *et al.* (1990) showed that the transient A-type current had a conductance of 20pS whereas the delayed rectifier was made up of two components of conductance 160 and 60pS.

Separation of the delayed rectifier and A-type potassium currents has been achieved using the appropriate voltage protocols. Stepping to more depolarised test potentials from a holding potential of -80mV elicits both A-type and delayed rectifier potassium currents. However, holding the cell at a potential of -50mV inactivates the A-type potassium current so stepping to more depolarised potentials results in pure delayed rectifier, (Carignani *et al.*1991). Digital subtraction of the two current recordings results in pure A-type current.

The components of the outward current can also be separated pharmacologically but the results appear less reproducible. Carignani *et al.* (1991) reported that tetraethylammonium (TEA) was a selective blocker of the delayed rectifier and that the A-current was selectivity inhibited by 4-aminopryidine. However, other reports suggest that although the delayed rectifier can be selectively inhibited by TEA, 4-AP also produces significant block (Cull-Candy *et al.* 1989; Bardoni & Belluzzi, 1993; Watkins & Mathie, 1994). In addition, the two components exhibited differing sensitivities to extracellular calcium. The delayed rectifier was not affected by removal of extracellular calcium whereas the A-current was fully inhibited in the absence of extracellular divalent cations (Carignani *et al.* 1991).

Later, Bardoni and Belluzzi (1993) showed that the sustained outward current was composed of calcium sensitive and calcium insensitive components. Blocking calcium influx with calcium channel blockers inhibited the calcium sensitive component suggesting that this component was a calcium-activated potassium channel, probably BK.

3.1.2 Other potassium conductances.

Potassium currents that are sensitive to the classical L-type calcium channel inhibitors, the dihydropyridines have been described in patches from cerebellar granule neurons (Fagni *et al.*1994). These currents are likely to be due to the large conductance calcium activated potassium channels BK^+.

mRNA for Kir2.2 and Kir3.1-3 has been identified in the cerebellum (Karschin *et al.*1996) but to date studies on functional inward rectifiers in cerebellar granule neurons are limited.

3.1.3 Leak Currents

Using the perforated patch technique Watkins and Mathie (1996) discovered that the resting membrane potential of a cerebellar granule neuron decreased with time in culture. Cells that had been in culture for 48 hours exhibited a resting membrane potential of -29 ± 2mV however, after 7 days in culture V_m had dropped to -91 ± 7mV. In parallel to the change in resting membrane potential, cerebellar granule neurons began expressing an outward current which when measured at a holding

potential of -30mV was seen to increase in magnitude from 0 ± 5pA to 345 ± 46 pA on days 2 and 13 after culturing, respectively (Watkins and Mathie, 1996).

This current was found to be non-inactivating, outwardly rectifying, active at the resting membrane potential and reversed close to that predicted for a potassium current. It was thus termed IK_{SO} for 'standing-outward' potassium current.
One distinguishing feature of IK_{SO} is that it is inhibited by muscarine. Muscarine is a selective ligand for the muscarinic acetylcholine receptors, members of the seven-transmembrane domain family of receptors. Five subtypes of muscarinic receptors are known, M_1 - M_5 (Caulfield & Birdsall 1998), of which two, M_2 and M_3, are expressed in cerebellar granule neurons, (Fukamauchi *et al.* 1991).
Measured at a holding potential of -30mV, IK_{SO} is concentration-dependently inhibited by muscarine with EC_{50} of 0.17 ± 0.06 μM, via a pertussis toxin insensitive pathway, (Watkins and Mathie 1996). Muscarine (10μM) was shown to increase the input resistance of the cerebellar granule neuron from 480 ± 90 MΩ to 1205 ± 183 MΩ, measured at potentials between -70 and -90 mV, and shifted the zero current potential in the depolarised direction by 15 ± 2mV. The resultant increase in membrane excitability was sufficient to evoke action potentials when cells were held with current clamp and injected with 100pA of current. It has been recently shown that activation of M_3 receptors are responsible for inhibition of IK_{SO} (Boyd *et al.* 2000). M_3 receptors link to the $G_{q/11}$ family of potassium channels which are known to activate phospholipase C.

IK_{SO} has no threshold for activation and was found to be insensitive to TEA (5mM) and 4-AP (10mM), but is inhibited by barium and extracellular acidification. The current voltage relationship for IK_{SO} linearises in the presence of high extracellular potassium in accordance with the Goldman Hodgkin Katz equation for open rectifiers (Millar *et al.* 2000). IK_{SO} is believed to be a member of the two-pore domain family of potassium channel, namely TASK-1 (Millar *et al.*2000).

3.1.4 Ionic selectivity of potassium channels.

It is essential for electrical excitability that different ionic channels are selective for different ions. Many studies have looked into the permeability of a variety of test

ions relative to a reference ion, usually the primary endogenous charge carrier. Permeability studies on potassium channels have, traditionally, used other group I metals, namely lithium, sodium, caesium and rubidium, as well as ammonium and thallium. In snail neurons the A-current has been shown to be twice as permeable to thallium as potassium while Rb^+, NH_4^+, Cs^+, Na^+ and Li^+ have permeabilities of 0.73, 0.18, 0.14, 0.09 and 0.07 respectively, relative to potassium (Taylor, 1987).

Inwardly rectifying channels in the starfish egg have been shown to have the same permeability sequence as the A-current in snail neurons, although the absolute permeability values differ (Hagiwara and Takahashi 1974). Here Cs^+ and Na^+ had very small permeability through the inward rectifier (<0.03 relative to potassium), and lithium had no measurable permeability. It is of interest that Rb^+ and Cs^+ decreased the conductance of potassium through these channels.

Delayed rectifiers in snail neurons are also more permeable to thallium than potassium but unlike the previous examples permeate Cs^+ better than NH_4^+ and Li^+ better than Na^+ (Reuter and Stevens 1980). This is not true for delayed rectifiers in the frog node where NH_4^+ has a higher permeability than Cs^+ (0.13 compared to <0.077; Hille 1973).

	Delayed Rectifier			Kir	A-type	BK_{Ca}
Test Ion	Frog Node	Frog Muscle	Snail Neuron	Starfish Egg	Snail Neuron	Rat muscle
K^+	1.0	1.0	1.0	1.0	1.0	1.0
Tl^+	2.3	--	1.29	1.5	2.04	1.2
Rb^+	0.91	0.95	0.74	0.35	0.73	0.67
NH_4^+	0.13	--	0.15	0.035	0.18	0.11
Cs^+	<0.077	<0.11	0.18	<0.03	<0.14	<0.05
Li^+	<0.018	<0.02	0.09	--	<0.07	<0.02
Na^+	<0.010	<0.03	0.07	<0.03	<0.09	<0.01

Table 3.1. Permeability ratios calculated from reversal potentials.
Adapted from Hille (1992.)

To date very little work has been carried out on the ionic selectivity of leak conductances. Preliminary studies on TASK-1 expressed in oocytes have shown Rb^+ to have a permeability ratio of 0.82 relative to potassium, (Goodwin *et al.* 2000). Na^+ and Li^+ were found to be impermeant. Rb^+ currents were substantially smaller than those carried by potassium, ($I_{Rb}^+/I_K^+ = 0.2$ at -50mV).

The voltage-gated and inwardly rectifying family of potassium channels are homo or heterotetrameric structures with very similar pore forming regions. Two pore domain potassium channels have a dimeric composition and different amino acid sequences within subunits. This unique structure suggests that the mechanics of ion conduction and selectivity will be quite different from the previously characterised potassium channels.

3.2 Aims

This chapter aims to identify potassium currents in primary cultures of cerebellar granule neuons, including the A-current, the delayed rectifier and IK_{SO}. The basic properties of IK_{SO} seen before by Watkins and Mathie (1996) and Millar *et al.* (2000) will also be investigated.

As yet there has been very little work into the selectivity of the two pore domain potassium channels. With such a different molecular structure from the other potassium channels it is important to test the permeability of the both native and expressed channel. This chapter will look into the ability of other ions to carry IK_{SO} and make comparisons with other, well described, potassium channels.

TASK-1 is inhibited by various agonists acting on $G_{q/11}$ linked receptors (Talley *et al.* 2000). Similarly, IK_{SO} has been shown to be inhibited by muscarine and activation of group 1 metabotropic glutamate receptors both linked $G_{q/11}$ coupled receptors. The ability of histamine to inhibit IK_{SO} will also be investigated and the implications of histaminergic inhibition discussed.

3.3 RESULTS

All electrophysiological recordings described in this chapter were performed using the amphotericin perforated patch technique as described in chapter 2.2.1.

3.3.1 Potassium currents in cerebellar granule neurons.

Figure 3.1 shows the three major components to outward potassium current in cerebellar granule neurons. Cells were held at -30mV and stepped to a pre-pulse potential of -120mV for 500ms before stepping to a test potential of 0mV.

3.3.1 (a) The A-type potassium current

The A-type potassium current is a rapidly activating, rapidly inactivating potassium current (Rudy 1988). A-current was induced by holding the cells at -30mV and stepping to a prepulse potential of -120mV before stepping to a test potential of 0mV. The pre-pulse potential is designed to remove the inactivation of the A-current and induce maximal A-current activation when stepping to 0mV.

3.3.1(b) The delayed rectifier

The delayed rectifier is a slowly activating slowly inactivating potassium current (Rudy 1988), in figure 3.1 the delayed rectifier can be observed as the sustained outward current at 0mV after the transient A-current has inactivated

3.3.1(c) IK_{SO}

IK_{SO} is a non-inactivating outward current in cerebellar granule neurons (Watkins and Mathie (1996). IK_{SO} can be observed at the holding potential in figure 3.1 and is in the order of 330pA in magnitude.

3.3.2 Muscarinic Inhibition of IK_{SO}

CGNs were held at -20mV and stepped to -60mV for 800ms before returning to the holding potential. This procedure was repeated every 5 seconds.

As can be seen in panel A of figure 3.2 CGNs possess an outward current which was present at both potentials tested. In control conditions (black line) the standing outward current at -20mV is approximately 415pA (measured before the voltage step after the cell has been at this potential for over 4.6 seconds). Stepping to -60mV

reduces the current to 70pA. Stepping back to -20mV resulted in a rapid increase in current amplitude, back to a similar size as before (420pA).

It is worth noting that under whole cell recording the outward current was observed to undergo a rapid run-down reaching a zero amplitude within a couple of minutes, data not shown. This was also reported by Watkins and Mathie (1996) and suggests that there is a requirement for an intracellular messenger that maintains the constantly active state of IK_{SO}.

Application of 10μM muscarine (figure 3.2 panel A, red line) caused an inhibition of IK_{SO} to approximately 120pA at -20mV resulting in an increased input resistance from 135MΩ in control conditions to approximately 530MΩ in the presence of 10μM muscarine, measured between -20 and -60mV. The current profile was not altered in the presence of muscarine. The time course of muscarinic inhibition is shown in panel B. IK_{SO} is measured at the holding potential after the cells have been at -20mV for 4.6 seconds. Here the data on the graph represent individual measurements of IK_{SO} and the bar indicates application of muscarine. In this cell muscarine can be seen to have induced a rapid and fully reversible inhibition of IK_{SO} of 70.4%. On average 10μM muscarine caused a peak inhibition of IK_{SO} of 70 ± 2 % (n=61) This agrees well with previous reports that 10μM muscarine inhibits IK_{SO} by 68 ± 2% measured at -20mV (Millar *et al.* 2000) and 79 ± 5% measured at -30mV (Watkins and Mathie 1996).

It is worth noting that in the continued presence of muscarine a slight desensitisation of the response can be observed. Also the size of the outward current was often potentiated following washout of muscarine (over-recovery), see figure 3.2B.

Figure 3.3 demonstrates the outwardly rectifying nature of IK_{SO}. Panel A shows the time course of muscarinic inhibition as seen before in figure 3.2B. However, at points (i) and (ii) a current voltage relationship was obtained using the voltage protocol in panel B. Cells were held at a holding potential of -30mV and stepped to voltages ranging from -10mV to -120mV in 10mV increments for 400ms before returning to the holding potential.

Current recordings from this step protocol in (i) control conditions and (ii) the presence of 10μM muscarine are shown. Muscarine reduced the current at all potentials.

Panel C shows the current voltage relationship derived from these recordings. (i) and (ii) represent the current voltage relationship in control conditions and in the presence of muscarine, respectively. A subtracted trace ((i)-(ii)) showing only the muscarine sensitive component of the outward current is shown in red. The muscarine sensitive component of this outward current is clearly outwardly rectifying and reverses at approximately -80mV. It has been shown that the rectifying nature of IK_{SO} is due only to the uneven concentrations of potassium as the current voltage relationship can be seen to linearise as $[K^+]_o = [K^+]_i$ (Millar *et al.* 2000).

3.3.3 Ionic selectivity of IK_{SO}

We have investigated the ability of other ions to carry IK_{SO} by replacing potassium in the extracellular solution with a variety of test ions.

Cells were held at -20mV and slowly ramped down to -100mV at a rate of $0.1 mVms^{-1}$. At -100mV the voltage was stepped back to the holding potential. The ramp protocol was repeated every five seconds. Current voltage relationships from this protocol were determined and plotted, as in figure 3.4b.

Ramps were performed as cells were exposed to an external solution containing 25mM K^+ (monovalent cation concentration was maintaining by reducing extracellular $[Na^+]$) and again after potassium was replaced by the test ion, in this case caesium.

The ionic permeability of the test ion relative to potassium was determined by measuring the zero current potential (reversal potential) and using the equation:

$$E_{RevX} - E_{RevK} = \frac{RT}{zF} \ln \frac{P_X [X^+]_o}{P_K [K^+]_o} \qquad \textbf{Equation 3.1}$$

where $E_{Rev\ X}$ is the reversal potential when the cell is superfused with the test ion, $E_{Rev\ K}$ is the reversal potential when in potassium containing solution. P_X/P_K is the permeability of the test ion relative to potassium. R is the gas constant, T the temperature in Kelvin, z the charge of the ion and F Faraday's constant. RT/zF is a constant and taken as 25.26 at 20°C (Hille 1992).

Figure 3.4 shows the effect of replacing extracellular potassium with caesium. In the example shown the current reverses at -79mV. Increasing the concentration of potassium to 25mM caused a shift in the reversal potential to -31.5mV, and substituting potassium with caesium changes the reversal potential to -62mV. Using the equation 3.1 gives caesium a permeability of 0.30 relative to potassium.
On average caesium was found to have a permeability of 0.22 ± 0.02 (n=6) relative to potassium. The change in reversal potential when increasing the potassium concentration from 2.5mM to 25mM was nearly 10mV less that that predicted by the Nernst equation (48.5mV actual compared to a predicted 58mV). This indicates that the current is not entirely made up by a potassium conductance but is likely to include a significant sodium component.

Figures 3.5a-d show the effects substituting potassium with rubidium, thallium, ammonium or lithium on the reversal potentials in CGNs. Permeabilities relative to potassium are shown in table 3.2.

Test Ion	*Mean Permeability*	*S.E.M.*	*n*	*Ionic Radii*	*ΔH^o hydration*
Potassium	1.00	-	-	1.33	-85
Rubidium	1.02	0.06	5	1.48	-79
Thallium	1.03	0.06	6	1.40	-80
Caesium	0.22	0.02	6	1.69	-71
Ammonium	0.18	0.01	11	-	-
Lithium	0.08	0.01	9	0.60	-131

Table 3.2. Permeabilities of various test ions relative to potassium. Ionic radii (Å) and specific energy of hydration (kcal mol^{-1}) are also shown

It is worth noting that all experiments were carried out using chloride salts of sodium, potassium and the test ion with the exception of that shown in figure 3.5b. Thallium chloride is only soluble up to concentrations of about 3mM, (Cohen & Mulrine 1986) so it was necessary to replace NaCl with Na_2SO_4, KCl with $KC_2H_3O_2$ and $TlC_2H_3O_2$ was used as a source of Tl^+. In this experiment the test ion, thallium,

was used at a concentration of 10mM. The chloride salts of magnesium and calcium were still used giving the total chloride ion concentration of 2.5mM. No sedimentation of TlCl was observed.

3.3.4 Histaminergic Inhibition of IK_{SO}

TASK-1 has been shown to be inhibited by various neurotransmitters that act on $G_{q/11}$ coupled receptors (Talley *et al.* 2000), this study furthers the work done by Watkins and Mathie (1996) on IK_{SO} investigating the effects of histamine on the outward current.

Figure 3.6 shows current recordings in control conditions (black line) and in the presence of 30μM histamine (red line), and below the time course of histaminergic inhibition is shown.

Histamine (30μM) caused a fully reversible inhibition of IK_{SO} with an average peak inhibition of 25.8 ± 7.3% (n=6). However, three more cells (33%) responded to histamine with a decrease in IK_{SO} of less than 5%. The inhibition of IK_{SO} by histamine appears to be much more variable than inhibition by muscarine (see figure 3.2). In the example shown histamine (10μM) caused an increase in input resistance from 307 to 718MΩ, and hence an increase in cellular excitability.

Like muscarinic, histaminergic inhibition desensitised rapidly in the continued presence of agonist and there was also evidence of over-recovery.

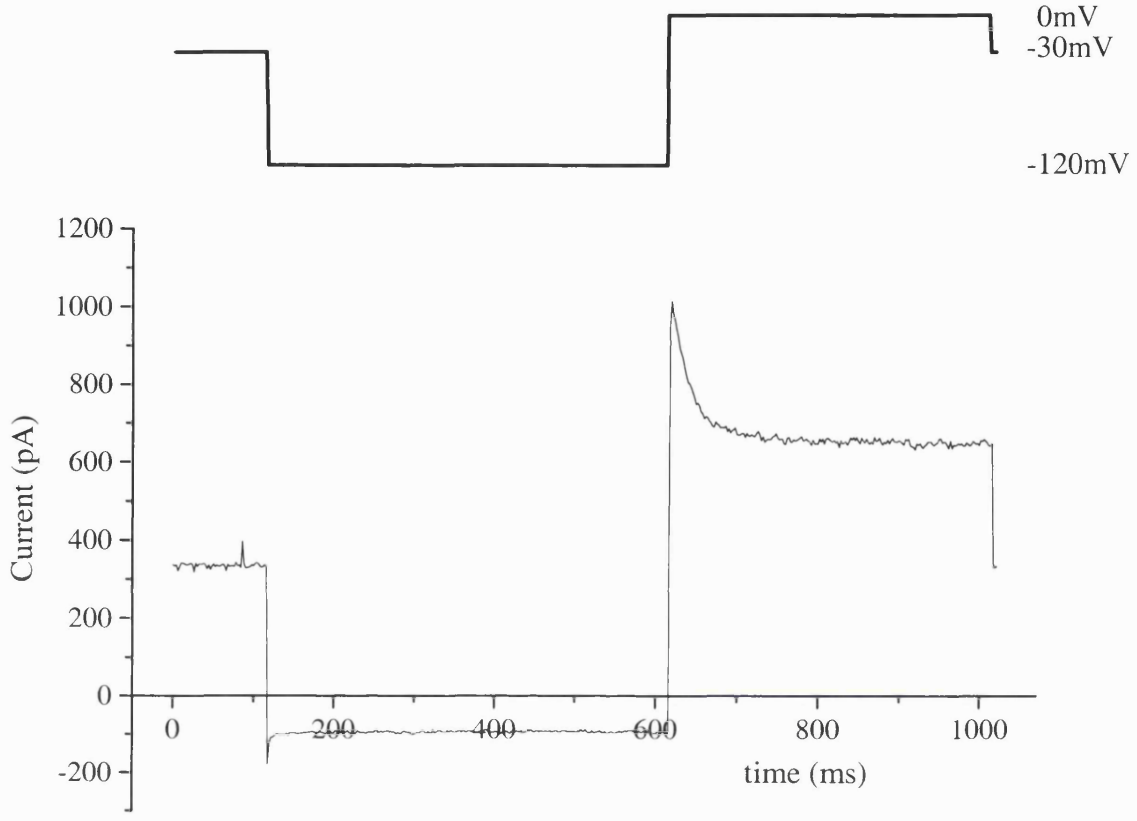

Figure 3.1. Potassium currents in cerebellar granule neurons

Using the amphotericin perforated patch clamp technique the cell was held at -30mV stepped to -120mV for 500ms before stepping to a test potential of 0mV.
The three major potassium conductances are apparent when using this protocol. At -30mV the outward current is IK_{SO} and is approximately 330pA in this cell. Stepping to a pre-pulse potential of -120pA removes the inactivation of A-type potassium channel. The A-current can be observed as the transient peak that appears when the cells are stepped to 0mV. Delayed rectifier current can be observed following inactivation of the A-current while the cell is held at 0mV.

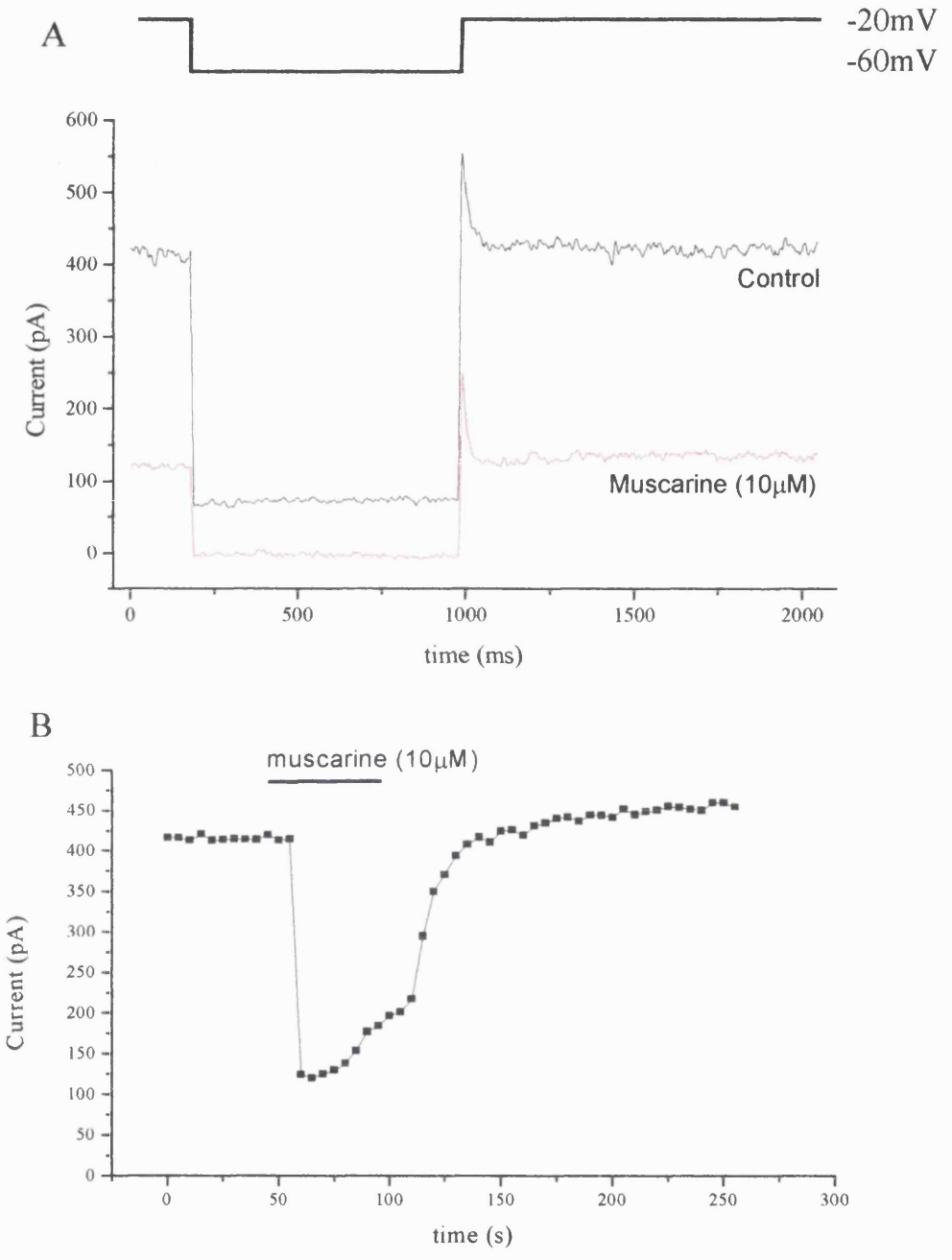

Figure 3.2. Inhibition of IK_{SO} by muscarine (10μM).

Panel A shows the standing outward potassium current, IK_{SO}, in cerebellar granule neurons. Cells were held at -20mV and stepped to -60mV for 400ms before returning to the holding potential, this protocol was repeated every 5s. Muscarine (10μM) causes a significant reduction in the current, shown in red. Panel B shows the time course of muscarinic inhibition. IK_{SO} was measured at -20mV after the cell had been at the holding potential for 4.6 seconds. Muscarinic application is indicated by the bar.

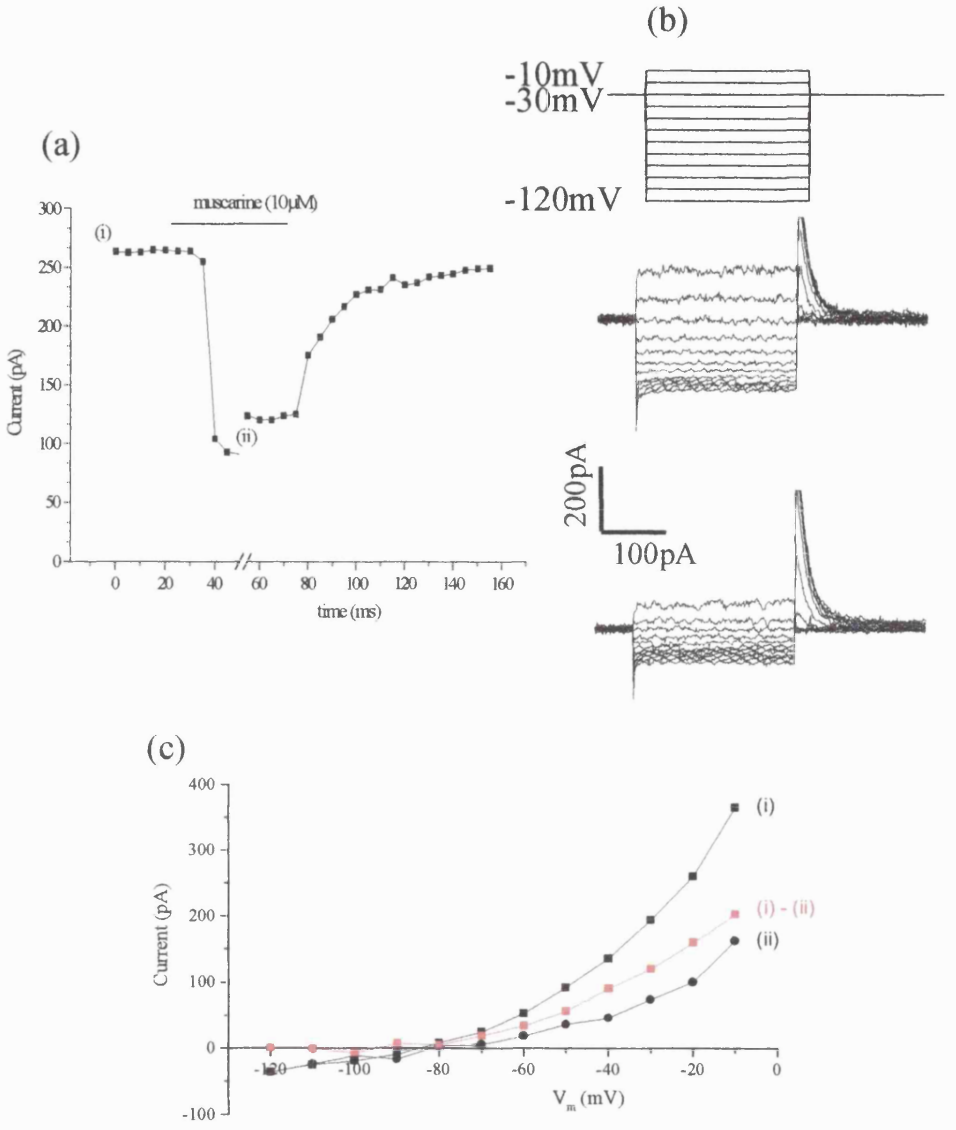

Figure 3.3. IK_{SO} is outwardly rectifying.

Panel (a) shows the time course for muscarinic inhibition (10μM). At points (i) and (ii) the step protocol shown in (b) was performed. Cells were held at held at -30mV and stepped to voltages ranging from -10mV to -120mV in 10mV increments for 250ms before returning to the holding potential. (i) and (ii) in (b) show the resultant current recordings in the absence and presence of muscarine (10μM), respectively. (c) shows the current voltage relationship in the presence and absence of muscarine and the muscarine sensitive component derived from subtracting (ii) from (i). The muscarinic sensitive component is shown in red and is clearly outwardly rectifying.

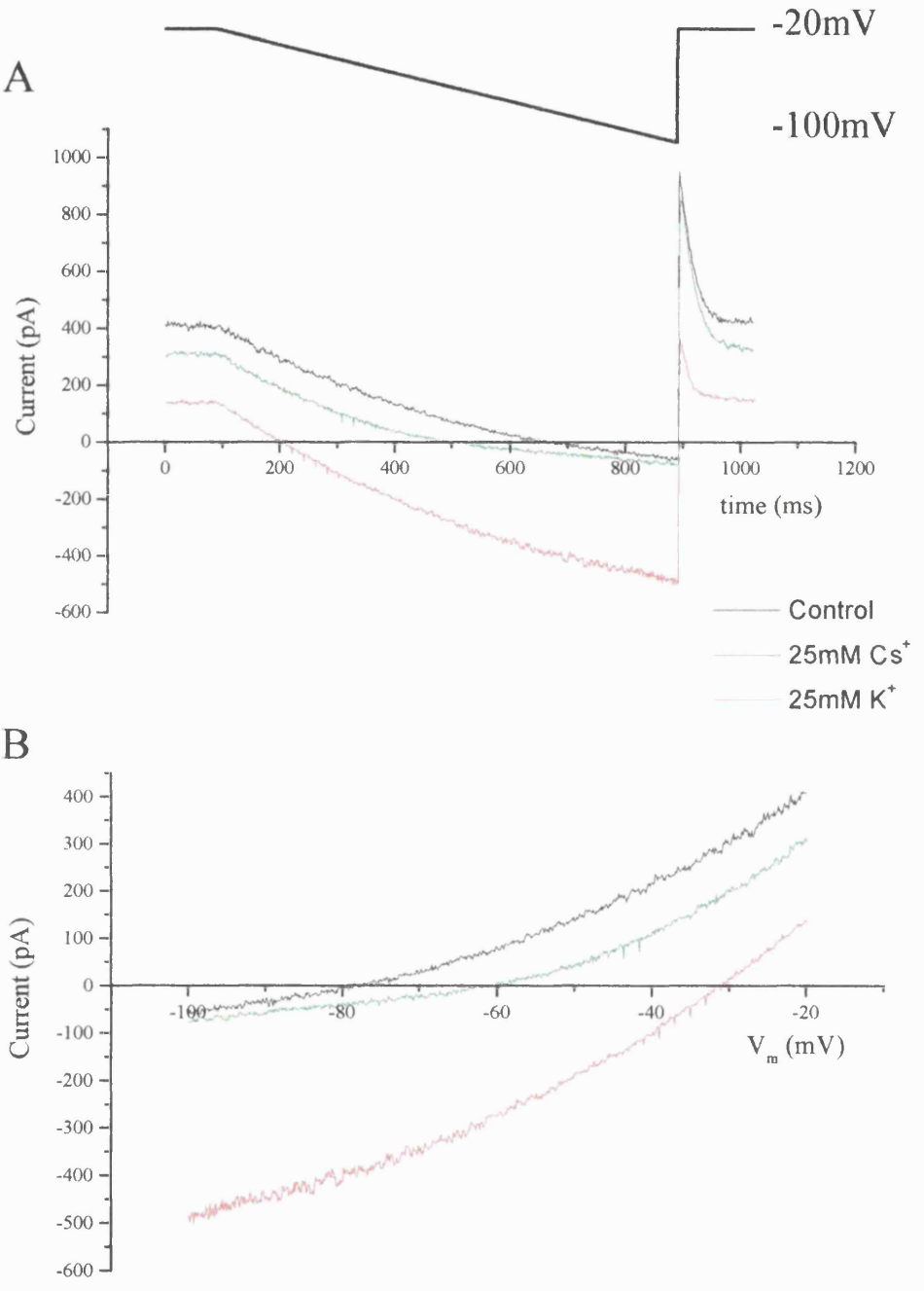

Figure 3.4 Permeability of caesium ions through IK_{SO}.

Voltage ramps were performed, as illustrated in panel A, in control conditions and in the presence of 25mM K^+ and 25mM Cs^+. Cells were held at -20mV and ramped down to -100mV over 800ms ($0.1mVms^{-1}$), ramps were performed every 5s. Panel B shows the current - voltage relationships derived from the current traces shown in panel A.

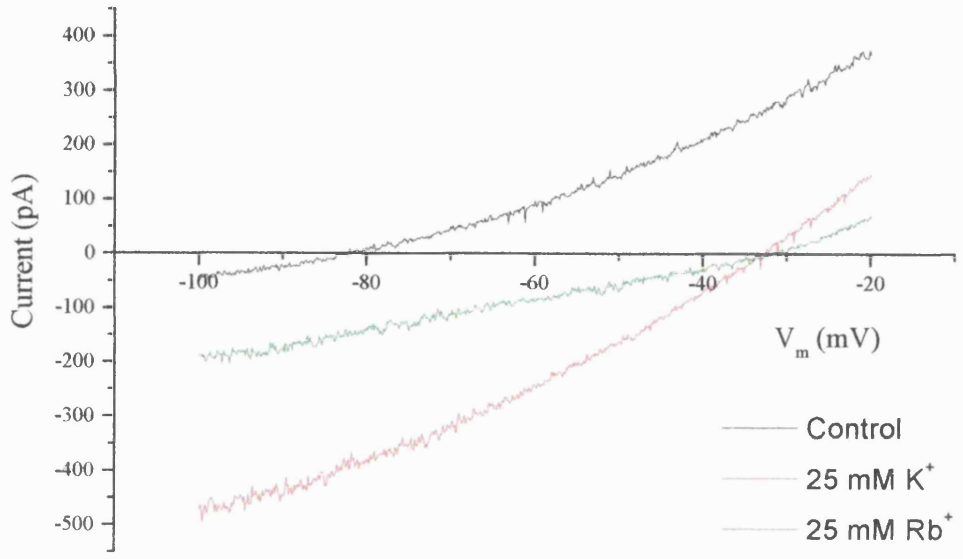

Figure 3.5a. Rb^+ permeability

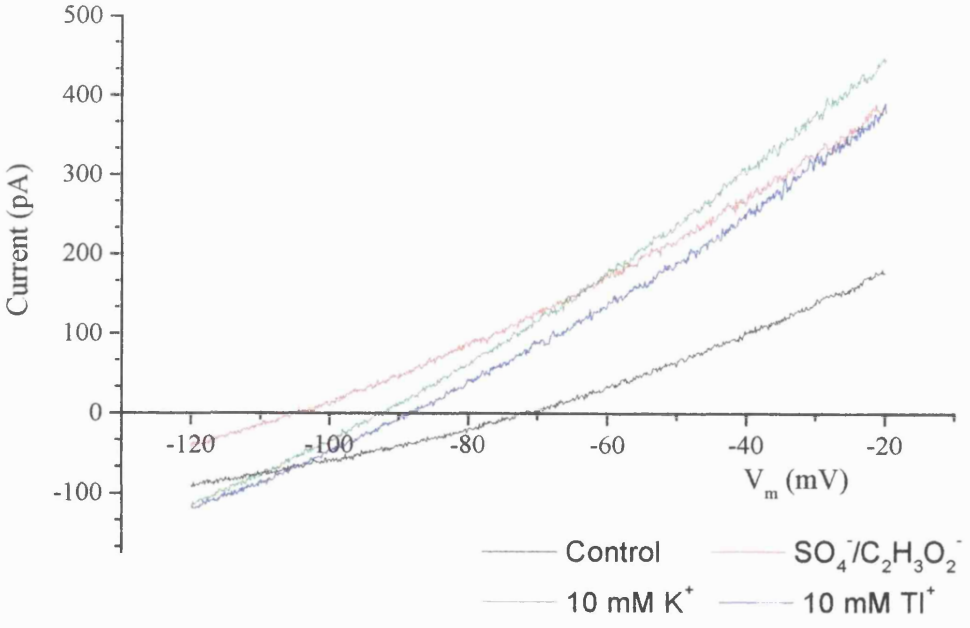

Figure 3.5b Thallium permeability

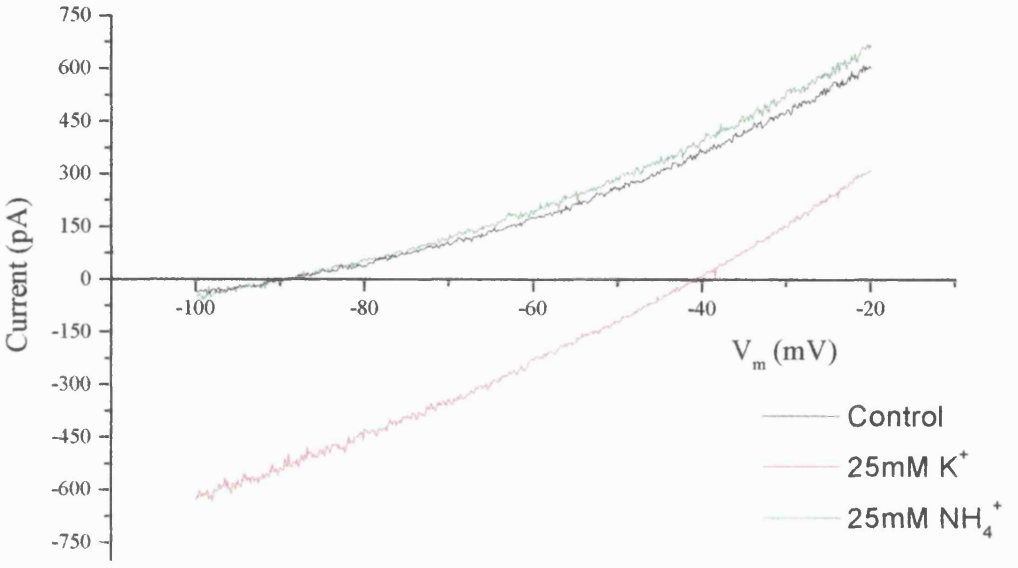

Figure 3.5c. Ammonium permeability

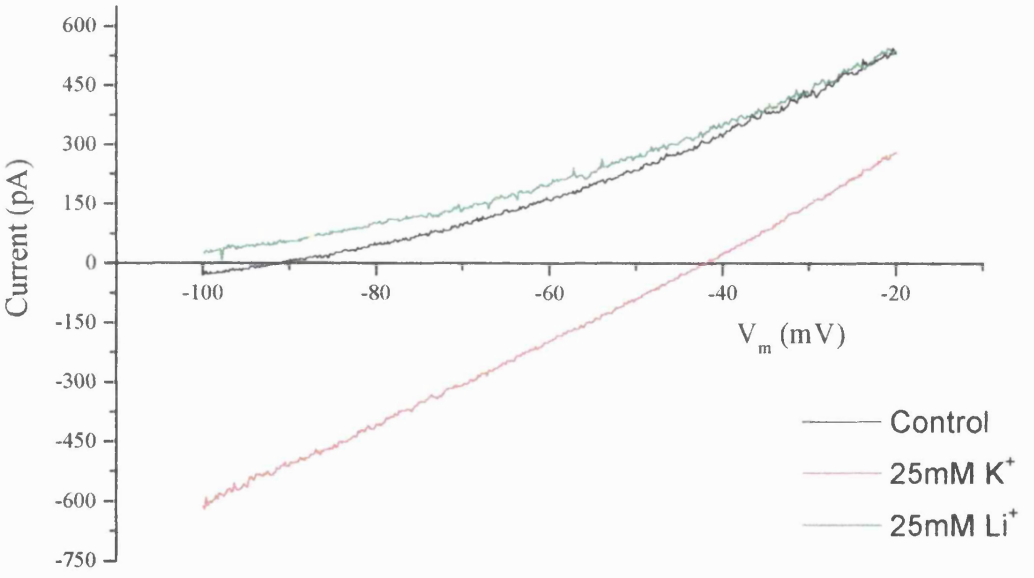

Figure 3.5d. Lithium permeability

Figure 3.5

The effect of exchanging external potassium ions with (a) rubidium, (b) thallium, (c) ammonium and (d) lithium ions on the reversal potential of IK_{SO}. Current voltage relationships were derived using the protocol from figure 3.4. As TlCl is insoluble NaCl was replaced with Na_2SO_4 and KCl with $KC_2H_3O_2$, $TlC_2H_3O_2$ was used as a source of Tl^+, see text

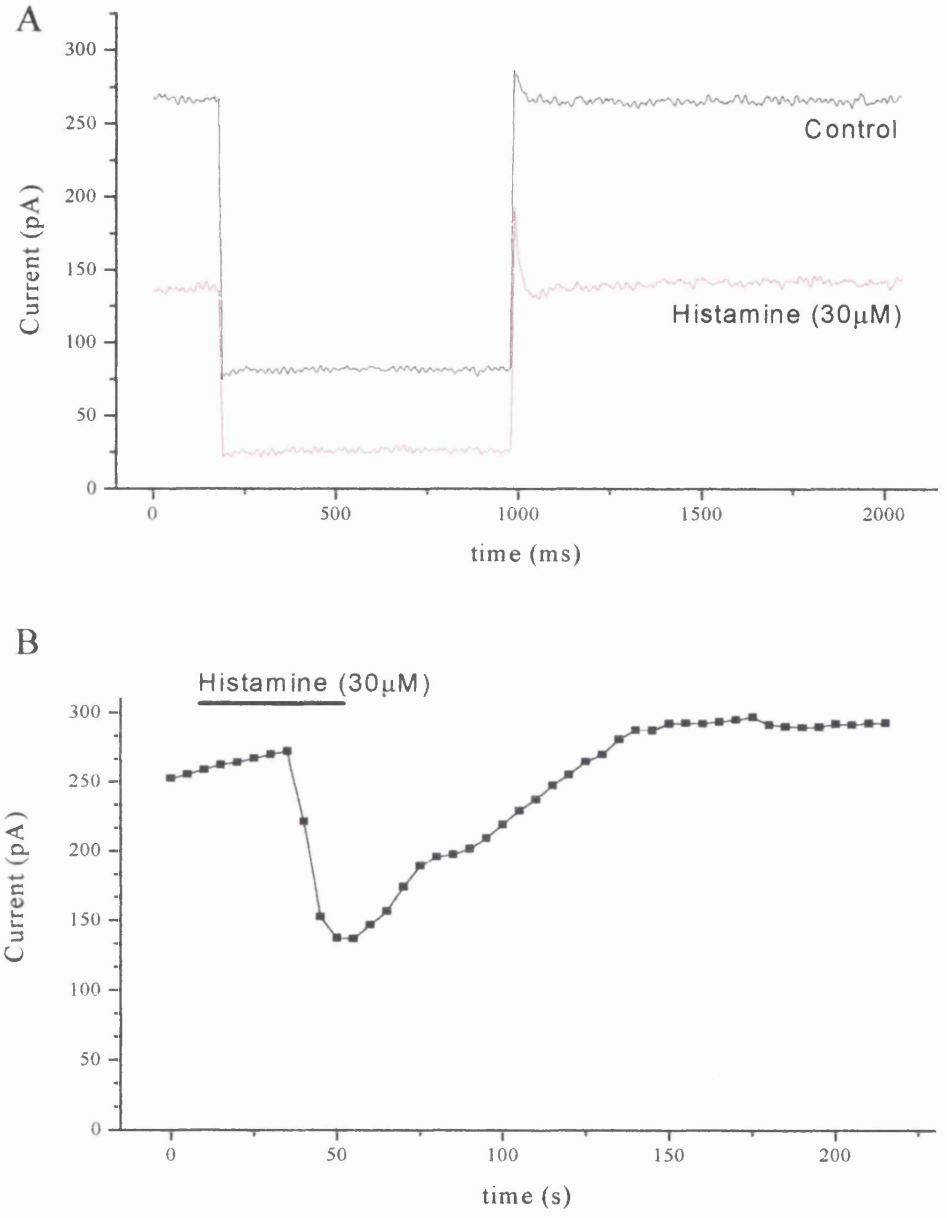

Figure 3.6. Inhibition of IK_{SO} by histamine (30μM).

Panel A shows current traces for IK_{SO} in control conditions (black) and in the presence of histamine (30μM, red line). The time course of histaminergic inhibition is shown in panel B, bar indicates histamine application.

3.4 DISCUSSION

This chapter provides evidence of the existence of A-type and delayed rectifier potassium currents in cerebellar granule neurons as previously reported by many groups, (Hirano *et al.* 1986; Hockburger *et al.* 1987; Cull-Candy *et al.* 1989; Watkins and Mathie 1994). The presence of IK_{SO} was also established and the basic properties of outward rectification and muscarine sensitivity matched well those that had been previously characterised (Watkins and Mathie 1996; Millar *et al.* 2000). The ionic permeability of IK_{SO} was investigated here, and is discussed below, and finally the ability of histamine to inhibit IK_{SO} was also noted

3.4.1 Muscarinic Inhibition of IK_{SO}

This chapter describes the presence of IK_{SO} in cerebellar granule neurons and its inhibition by muscarine. The mechanism underlying inhibition by muscarine has not been resolved although is known to mediate its actions via the M_3 muscarinic receptor (Boyd *et al.* 2000). Activation of M_3 muscarinic receptors in cerebellar granule neurons leads to activation of $G_{q/11}$ G-proteins (Whitman *et al.* 1991). Downstream effectors following $G_{q/11}$ stimulation are multiple, however the most obvious is activation of phospholipase C (PLC). Phospholipase C catalyses the hydrolysis of PIP_2 to DAG and IP_3. DAG is a membrane-bound activator of protein kinase C (PKC; Liu *et al.* 1996) and IP_3 is free to diffuse across the cytoplasm and activate specific IP_3 receptors on the endoplasmic reticulum (Berridge, 1993).

IK_{SO} is not unique in its inhibition by activation of $G_{q/11}$ coupled receptors. Several of the inward rectifiers are regulated by the actions of G-proteins, some being both inhibited and activated (Velimirovic *et al.* 1995). As a general rule the voltage-gated family of potassium channels is not sensitive to muscarinic stimulation, however there are exceptions, the most obvious of which is the M-current.

Due to its muscarine sensitivity IK_{SO} has often been likened to the M-current ($I_{K(M)}$, Brown 1988). $I_{K(M)}$ is a voltage dependent current found in various peripheral and central neurons that shows slow activation and deactivation kinetics and is open close to the membrane potential, hence muscarinic inhibition of $I_{K(M)}$, like muscarinic inhibition of IK_{SO}, increases cellular excitability. $I_{K(M)}$ is inhibited by activation of muscarinic M_1 (Marrion *et al.*1995) and bradykinin B2 (Jones *et*

*al.*1995) receptors. M_1 and B_2 receptors, like M_3, link to activation of $G_{q/11}$ proteins, and like IK_{SO}, the second messenger systems underlying inhibition of $I_{K(M)}$ following $G_{q/11}$ activation are not fully understood. In rat superior cervical ganglion (SCG) neurons $I_{K(M)}$ has been shown to be inhibited by activation of $G_{\alpha q}$ but not $G_{\alpha 11}$, or $\beta\gamma$ subunits of the G-protein (Haley *et al.* 1998). However, recent studies on mouse SCG lacking $G_{\alpha q}$ has shown that the majority of M_1 mediated inhibition of $I_{K(M)}$ is via G_{11} with a lesser proportion coming from activation of $G_{\alpha q}$ and PTX-sensitive G-proteins, and that B_2 mediated inhibition of $I_{K(M)}$ is solely via activation of G_{11}, (Haley *et al.* 2000). Inhibition of the M-current in rat SCG following B_2, but not M_1, receptor stimulation is due to activation of phospholipase C and, IP_3 generation and release of calcium from the intracellular stores (Selyanko & Brown, 1996; Cruzblanca *et al.*1998). Inhibition of the M-current can not therefore be explained by a direct action on a single G-protein subtype and is mediated via different second messenger pathways depending upon the receptor subtype.

Comparisons with $I_{K(M)}$ and IK_{SO} could lead to a better understanding of leak current modulation, but the phenomenon of how two different receptors can couple to the same G-protein to produce different effects is yet to be resolved.

The most obvious starting point when looking for a second messenger system coupling muscarinic M_3 receptor stimulation to IK_{SO} inhibition is to look at intracellular calcium. Stimulation of B_2 receptors induces a rise in calcium in rat SCG neurons and it is this rise in intracellular calcium that underlies bradykinin induced inhibition of $I_{K(M)}$, (Cruzblanca *et al.* 1998). However, the same cannot be said for muscarinic M_1 receptor mediated inhibition of $I_{K(M)}$. Muscarine does not produce a detectable rise in intracellular calcium in this system (Marsh *et al.* 1995) and inhibitors of PLC and calcium release do not affect the muscarinic inhibition (Cruzblanca *et al.* 1998).

Subsequent chapters investigate the properties of muscarinic activation on intracellular calcium and attempt to determine whether rises in intracellular calcium are responsible for M_3 mediated inhibition of IK_{SO}.

3.4.2 Ionic permeability of IK_{SO}

The results presented in this chapter may be the first selectivity measurements of a native two-pore domain potassium channels in mammalian neurons. The selectivity sequence is: $Tl^+ = Rb^+ = K^+ >> Cs^+ > NH_4^+ > Li^+$ and exhibits large differences from the voltage-gated and inward rectifying potassium channels previously observed. The distinct difference in the channel assembly combined with the subtly different amino acid sequence invite the proposal that these channels exhibit quite different permeability sequences. The biggest difference between the data present here and previous work is with the permeability of the transition metal thallium. Tl^+ possess a similar size to that of a potassium ion (Pauling radii of 1.40Å for thallium compared to 1.33Å for potassium) and lower energy of hydration allowing to permeate many potassium channels better than potassium (Hille 1992). In this study Tl^+ has the same permeability as potassium. A narrower pore of this channel compared to other characterised potassium channels might explain why Tl^+ is not more permeant. However, that would not explain the relatively high permeability of Rb^+ which is of a similar order to both K^+ and Tl^+ and has similar dehydration energies. An alternative explanation would be that Tl^+ is maintaining tight electrostatic interactions with acetate ($C_2H_3O_2$). If the energy required to dissociate Tl^+ from $C_2H_3O_2^-$ is significantly higher than the energy released when Tl^+ forms a complex with water then some $TlC_2H_3O_2$ is likely to remain, distorting the assumed concentration of Tl^+ ions in solution.

In this study, Rb^+ permeates this channel better than observed for TASK-1 (0.82; Goodwin *et al.* 2000) and other potassium channels (Hille 1992, see also table 3.1.). This may suggest that the in the native tissue TASK-1 is subject to modulation that changes the properties of the selectivity filter.

The A-current of the snail neuron displays a permeability sequence where Cs^+ is less permeable than NH_4^+ (Taylor 1986) whereas this data would clearly suggest the opposite. Here, caesium is more permeable than it is in many other potassium channels studied . In addition, this study suggests that Li^+ permeates the channel better than other potassium channels (with the exception of the delayed rectifier of the snail neuron). However, as discussed below as much as 10% of the outward current may not be IK_{SO}, and, as the relative permeability of lithium is less than 10% of that of potassium lithium may be permeating through a different channel.

These data suggest that the large differences in the pore composition are reflected in the permeability sequence of the test ions examined.

The differences in the predicted change in reversal potential and that actually observed in this study may indicate that the outward current is not carried entirely by potassium ions. This could be due to two factors, firstly that IK_{SO} is carried in part by some other ion, probably sodium, or that there are other channels open during recording. With regards to the latter possibility the outward current has been shown to be inhibited by as much as 90% by extracellular acidification, and by up to 85% by muscarinic receptor stimulation. If there is another channel contributing to the outward component then its contribution is small (approximately 10%). The ionic selectivity of the muscarinic sensitive component of this current has been investigated. In these studies lithium was found to be impermeant but permeability ratios for other ions showed little or no difference to those reported here. It was therefore concluded that the protocol used here, although not being ideal, was sufficiently accurate.

3.4.3 Histaminergic Inhibition of IK_{SO}

Talley *et al.* (2000) showed that 5-HT, noradrenaline, substance P, thyrotrophin-releasing hormone and 3,5-dihydroxyphenylglycine (a group 1 metabotropic glutamate receptor agonist) were all able to fully inhibit TASK-1 expressed in HEK 293 cells. Further Millar *et al* (2000) showed that activation of muscarinic receptors in oocytes expressing TASK-1 by carbachol also causes leak current inhibition. Modulation of TREK-2 currents by G-protein coupled receptors has recently been demonstrated. Lesage *et al.* (2000) showed that TREK-2 currents could be inhibited by stimulation of the G_S coupled 5-HT_4 or the $G_{q/11}$ coupled mGluR1 receptor, while activation of the G_i-coupled receptor, mGluR2 increases TREK-2 currents in COS cells. It appears therefore that leak currents may be subject to extensive modulation by neurotransmitters and hormones.

Li *et al.* 1999 reported that histamine acting mainly upon H_1 receptors increased spontaneous firing of CGNs. The authors attributed this to an input from the hypothalamocerebellar histaminergic fibres. However, H_1 receptors present on CGNs activate G_q/G_{11} in a similar way to muscarine. Our studies showed that direct application of histamine on CGNs was able to inhibit IK_{SO}, and cause cellular

excitability. However, the inhibition by histamine was less potent than that seen by muscarine and not seen in every cell examined.

The ability of other neurotransmitters to inhibit IK_{SO} has previously been examined. Watkins and Mathie (1996) showed that IK_{SO} was 'not obviously affected' by 5-HT, noradrenaline and 2-chloroadenosine. However, as mentioned TASK-1 is reported to be fully inhibited by 5-HT, noradrenaline, substance P, thyrotropin-releasing hormone and 3,5-dihydroxyphenylglycine (a group 1 metabotropic glutamate receptor agonist; Talley *et al.* 2000), and by muscarine (Millar *et al.* 2000). The apparent discrepancy between the findings for IK_{SO} and TASK-1 may indicate a loss of membrane receptors during the culturing process. A similar loss of histaminergic receptors may explain why histaminergic inhibition of IK_{SO} is much more variable and less potent that muscarinic. Also in the cerebellar slices used by Li *et al.* there may have been more histaminergic receptors present leading to a larger increase in cell excitability than seen here. The increase in spontaneous firing seen by Li *et al.* may therefore be attributed, at least in part, to increased membrane excitability due to inhibition of IK_{SO}.

Chapter 4. Results.

Intracellular calcium regulation in cerebellar granule neurons.

4.1. INTRODUCTION

The elementary aspects of calcium signalling in cerebellar granule neurons remain to be fully classified. However, advances in imaging technology over the last fifteen years have helped to elucidate the global aspects of calcium signalling in cerebellar granule neurons and despite their small size has given an insight into the properties of calcium influx, storage and release.

4.1.1. Voltage-gated calcium channels

As described in the last chapter cerebellar granule neurons have been shown to possess L-, N-, P-, and Q-type calcium currents although a significant proportion that remains to be classified, (the R-type) (Amico *et al.*, 1995; Pearson *et al.*, 1995; Randall & Tsien 1995). These channels have been shown to be functionally active in a number of studies by cell depolarisation induced either by voltage clamp or exposing the cells to high concentrations of extracellular potassium.

Addition of 25mM potassium to the bathing solution of cerebellar granule neurons results in a biphasic $[Ca^{2+}]_i$ response. The $[Ca^{2+}]_i$ response has been observed by calcium imaging using fura-2 fluorescence (Masgrau *et al.*, 2000) and by manganese quench of fura-2 fluorescence (Simpson *et al.*, 1995). Application of 25mM potassium in this way evoked an increase in $[Ca^{2+}]_i$ which rapidly reached a peak before decaying to a plateau. The response was unaffected by NMDA antagonists and was deemed to be due to opening of voltage-gated calcium channels (Simpson *et al.*, 1995). However, only the plateau phase was inhibited by application of the dihydropyridine (-)PN 202 791 suggesting that although calcium influx was responsible for the 25mM potassium evoked $[Ca^{2+}]_i$ response the peak and plateau phases are mediated via different pathways. Incubation in thapsigargin, dantrolene (an inhibitor of calcium mobilisation) or ryanodine reduced the size of the plateau in response to 25mM potassium suggesting that calcium induced calcium release plays an important part in the response (Simpson *et al.*, 1993). The peak calcium response to high extracellular calcium does not appear to facilitated by calcium release from intracellular stores (Simpson *et al.*, 1993). In contrast however, Irving *et al.*, (1992a) did not observe any effect of thapsigargin or ryanodine on the $[Ca^{2+}]_i$ response to 25mM potassium suggesting that CICR is not functionally important in these cells.

4.1.2. Ligand gated calcium channels

NMDA and non NMDA receptor channels have been identified in cerebellar granule neurons. Application of NMDA to cerebellar granule neurons evokes a transient rise in $[Ca^{2+}]_i$ followed by a sustained plateau which, like the response to 25mM potassium, was dependent upon extracellular calcium (Simpson *et al.*, 1993). Also like the response to 25mM potassium, NMDA evoked increases in $[Ca^{2+}]_i$ were diminished by thapsigargin, ryanodine, thapsigargin and ryanodine and by dantrolene (Simpson *et al.*, 1993). It was concluded that a significant proportion of the rise in $[Ca^{2+}]_i$ in response to NMDA receptor stimulation is due to release of calcium from intracellular stores by CICR.

Calcium permeable AMPA receptors have been shown to be present in cerebellar granule neurons (Savidge & Bristow 1997). AMPA has been shown to evoke a small monophasic rise in intracellular calcium (Simpson *et al.*, 1995) which was attributed to release of calcium from intracellular stores, not influx across the plasma membrane. AMPA receptor stimulation has also been shown to be able to couple to activation of $G\alpha_i$ proteins (Wang *et al.*, 1997). It remains to be seen whether AMPA mediated $G\alpha_i$ activation can mobilise calcium from intracellular stores of cerebellar granule neurons as observed by Simpson *et al.*, (1995). AMPA stimulated calcium influx into cerebellar granule neurons has also be demonstrated, Hack & Balázs (1995) showed that while much of calcium influx following AMPA receptor stimulation was via NMDA receptors, voltage-gated calcium channels and the sodium-calcium exchanger, a significant proportion was due to calcium flux through the AMPA receptor channel.

4.1.3. Intracellular stores and calcium mobilisation in CGN.

Calcium can be released from the intracellular stores of cerebellar granule neurons following calcium entry across the plasma membrane, as described above. However in addition, calcium can be released from internal, IP_3 sensitive stores by ligands acting on $G\alpha_q$ receptors on the cell surface.

Both acetylcholine and 1-aminocyclo-pentane-1S, 3R-dicarboxylic acid (1S,3R ACPD; a group 1 mGluR agonist) have been shown to induce a transient rise in intracellular calcium in cerebellar granule neurons, (Irving *et al.*, 1992a) but in all

cases exposure of the cells to $G\alpha_q$ stimulating agonists was preceded by a 25mM potassium depolarisation which was used to replenish Ca^{2+} stores. Similarly, Masgrau *et al.*, (2000) showed that calcium responses to carbachol could only be evoked after exposure to 40mM potassium which acts to charge the internal stores. del Rio *et al.*, (1999) showed that while carbachol was able to evoke a small rise in $[Ca^{2+}]_i$ in about 50% of the cells the response was augmented by a prior depolarisation with 20mM potassium. Activation of histamine, α-adrenergic and metabotropic glutamate receptors failed to evoke a rise in $[Ca^{2+}]_i$ in over 90% of cells examined but the response to histamine and 1S,3R ACPD but not noradrenaline could be enhanced by the potassium depolarisation (del Rio *et al.*, 1999).

4.2. AIMS.

Muscarine has been shown to cause an inhibition in amplitude of IK_{SO} (this study, Boyd *et al.*, 2000; Millar *et al.*, 2000; Watkins & Mathie, 1996). The second messenger system that underlies this inhibition is unknown. Due to the similar muscarinic sensitivity of IK_{SO} and the M-current these two currents have been compared. Bradykinin mediated inhibition of the M-current has been shown to be mediated via a rise in intracellular calcium (Cruzblanca *et al.*, 1998). This chapter aims to further investigate the properties of agonist induced rises in intracellular calcium. Using the fluorescence dye fura-2 the basic properties of calcium signalling and the ability of agonists to $G\alpha_q$ coupled receptors, in particular muscarine, to evoke increases in $[Ca^{2+}]_i$ will be investigated.

4.3 RESULTS

Cells were incubated in fura-2AM for 20 minutes, washed and then incubated for a further 10 minutes as previously described. Once a suitable field had been identified cells were exposed to light of 340 and 380nm wavelengths. Emitted fluorescence following stimulation with light of 340nm was divided by fluorescent intensity following stimulation at 380nm.

From the calibration curves (figure 2.7) the resting calcium concentration in cerebellar granule neurons was estimated to be 20 - 60nM (but see measurement limitations, chapter 4.4). This agrees well with other studies, (e.g. ~50nM Irving *et al.*, 1992a; ~60nM Toescu, 1998; ~70nM Masgrau *et al.*, 2000; 30 ± 10nM Chen *et al.* 1999).

4.3.1. Calcium influx across the plasma membrane.

The ability of cerebellar granule neurons to respond to a potassium induced depolarisation was examined. Figure 4.1 shows the change in F_{340} / F_{380} ratio evoked by increasing the concentration of potassium in the bathing solution to 25mM. As can been seen the F_{340}/F_{380} ratio (and hence $[Ca^{2+}]_i$) increased rapidly in the presence of 25mM potassium. The F_{340}/F_{380} ratio reached a peak before decaying to a plateau phase which persisted throughout the duration of the exposure to the high potassium. Removal of potassium from the bathing solution resulted in a return of the $[Ca^{2+}]_i$ towards basal levels.

Figure 4.2 shows the effect of activating AMPA receptors with kainic acid (kainate). Kainate was used because it will activate AMPA receptors without causing the rapid receptor desensitisation seen with AMPA. The experiment was performed in sodium free (replaced with choline) conditions because sodium influx through the AMPA receptors could induced cellular depolarisation and hence calcium influx through voltage-gated calcium channels. Parallel experiments with cadmium in the extracellular solution (to block voltage-gated calcium channels) showed that in sodium free conditions there was no significant influx through voltage-gated calcium channels. As can be see kainate (250μM) caused a rapid increase in the F_{340}/F_{380} ratio to a plateau of 0.93 ± 0.03. Removal of the stimulating agonist caused

a reduction in the F_{340}/F_{380} ratio towards basal levels. Re-introduction of sodium to the bathing solution during washout of kainate did not alter the rate of calcium removal from the cytoplasm. Stimulation of AMPA receptors has been shown to induce activation of $G\alpha_i$ (Wang *et al.*, 1997). In a series of paired experiments cells were incubated in pertussis toxin (PTX; 500ng/ml) for >18hours. PTX caused a slight (but statistically insignificant $0.1<p<0.5$) reduction in the resting F_{340}/F_{380} ratio from 0.60 ± 0.03 to 0.56 ± 0.02 in PTX. Incubation in PTX did not significantly ($0.1<p<0.5$) alter the magnitude of the response to kainate (F_{340}/F_{380} of 0.39 ±0.03 in control and 0.31 ± 0.03 in PTX, figure 4.2b).

4.3.2. Release of calcium from intracellular stores.

Figures 4.3 - 4.4 show the effect of agonists that activate $G\alpha_q$ on intracellular calcium.

As shown previously, muscarine, (via M3 receptors) is able to inhibit the amplitude of IK_{SO} in every cell examined and would therefore be expected to cause a rise in intracellular calcium in all cells. Figure 4.3a shows the effect of muscarine (10μM) on $[Ca^{2+}]_i$. Muscarine induced a small rise in the F_{340}/F_{380} ratio, from 0.43 ± 0.05 to 0.55 ± 0.08 in a small proportion of cells (9%, 8 out of 87). In the remaining cells no global rise in intracellular calcium was observed. In a series of paired experiments a prior depolarisation with potassium increased the size of the muscarinic response, from a resting F_{340}/F_{380} of 0.67 ± 0.03 to peak of 0.88 ± 0.03 and the proportion of cells responding (51%, 33 out of 65). Here cells were exposed to 25mM potassium for approximately 90 seconds and washed in control external solution before exposure to muscarine. There was no noticeable dependence of the muscarinic response to time in culture. Similar paired experiments showed that the proportion of cells responding to muscarine was variable but in each case the size of the response and proportion of cells responding to muscarine dramatically increased following exposure to high potassium.

The previous results chapter showed that histamine can, in some cells, inhibit IK_{SO} (figure 3.6). Histamine (10, 30 and 100μM; pH 7.4 with NaOH) failed to induce a rise in intracellular calcium in any of the granule neurons examined. Exposing the cells to 25mM potassium prior to histaminergic stimulation did not evoke a change

the F_{340}/F_{380}, figure 4.4a. No response to histamine was observed in any cerebellar granule neurons at any time in culture. However, calcium oscillations were observed in one glial cell (from 7 tested) stimulated with histamine (100μM) see figure 4.4b. No increase in calcium was observed in glial cells when exposed to high potassium containing external solution.

The ability of 1S, 3R ACPD (100μM) to evoke a change in $[Ca^{2+}]_i$ in cerebellar granule neurons was examined. 1S,3R ACPD caused a biphasic response in $[Ca^{2+}]_i$. F_{340}/F_{380} ratios increased from a basal level of 0.50 ± 0.02 to a peak of 0.61 ± 0.03 which then decayed to a plateau level of 0.54 ± 0.02 which was sustained during the presence of the agonist. However, only 35% (26 out of 74) of cells examined responded to 1S,3R ACPD (100μM), figure 4.5a. Prior exposure of the cells to 25mM potassium, as before, increased both the size of the response (from a F_{340}/F_{380} of 0.74 ± 0.06 to 1.02 ± 0.09) and the proportion of responding cells (42% 25 out of 60).

Mobilisation of calcium from intracellular stores following $G\alpha_{i/o}$ stimulation, in the presence of a $G\alpha_q$ agonist has been demonstrated in SH-SY5Y human neuroblastoma cells (Connor *et al.*, 1997). Here the $G\alpha_{i/o}$ stimulating agonist baclofen (30μM; a $GABA_B$ agonist) was used in the presence of DHPG (3μM; a group 1 mGluR agonist). DHPG (3μM) failed to evoke a change in $[Ca^{2+}]_i$ in cerebellar granule neurons and glia. However, at a higher concentration DHPG (100μM) evoked a rise in intracellular calcium in 24% (9 out of 37) of cells examined. Application of baclofen in the presence of DHPG evoked a gradual rise in $[Ca^{2+}]_i$ in glial but not cerebellar granule neurons, figure 4.6. The rise in $[Ca^{2+}]_i$ in glial cells did not recover following washout of the agonists during the course of this experiment.

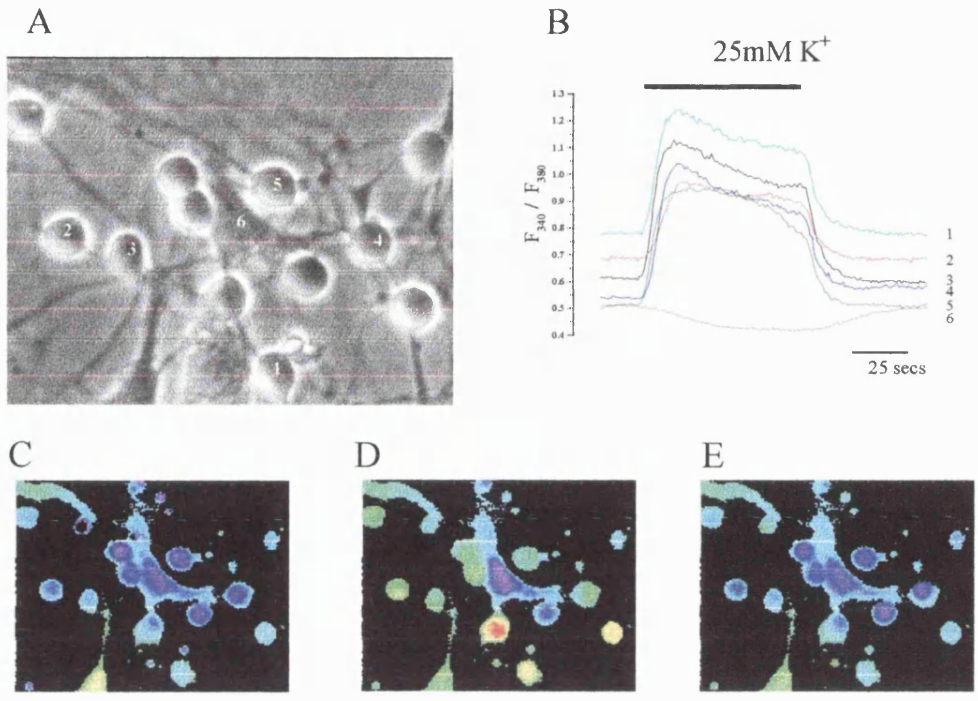

Figure 4.1. $[Ca^{2+}]_i$ elevation evoked by potassium depolarisation.

A typical calcium response of a cerebellar granule neuron to 25mM potassium is shown. Cells were incubated in fura-2AM for 20 minutes at 37°C for 20 minutes as previously described, chapter 2.3.2. Cerebellar granule neurons were exposed to light at 340 and 380nm for 600 and 200ms intervals respectively. Emitted fluorescence was collected at 510nm after stimulation at 340nm was dived by fluorescent intensity follow stimulation at 380nm. This ratio is proportional to the calcium concentration and is plotted in the y axis here.

Panel A shows a phase contrast image of a field of CGNs. B shows the response of 5 CGNs (1-5) and one glia (6) to 25mM potassium. Three pseudocolour images from points along the trace in B are shown in panels C-E. CGNs respond to 25mM potassium with a rise in $[Ca^{2+}]_i$ from a baseline level (panel C) to a peak (D) which is followed by a plateau. Washout of the stimulating potassium returns the F_{340}/F_{380} values towards baseline (panel E). The glia cell does not repsond to 25mM potassium.

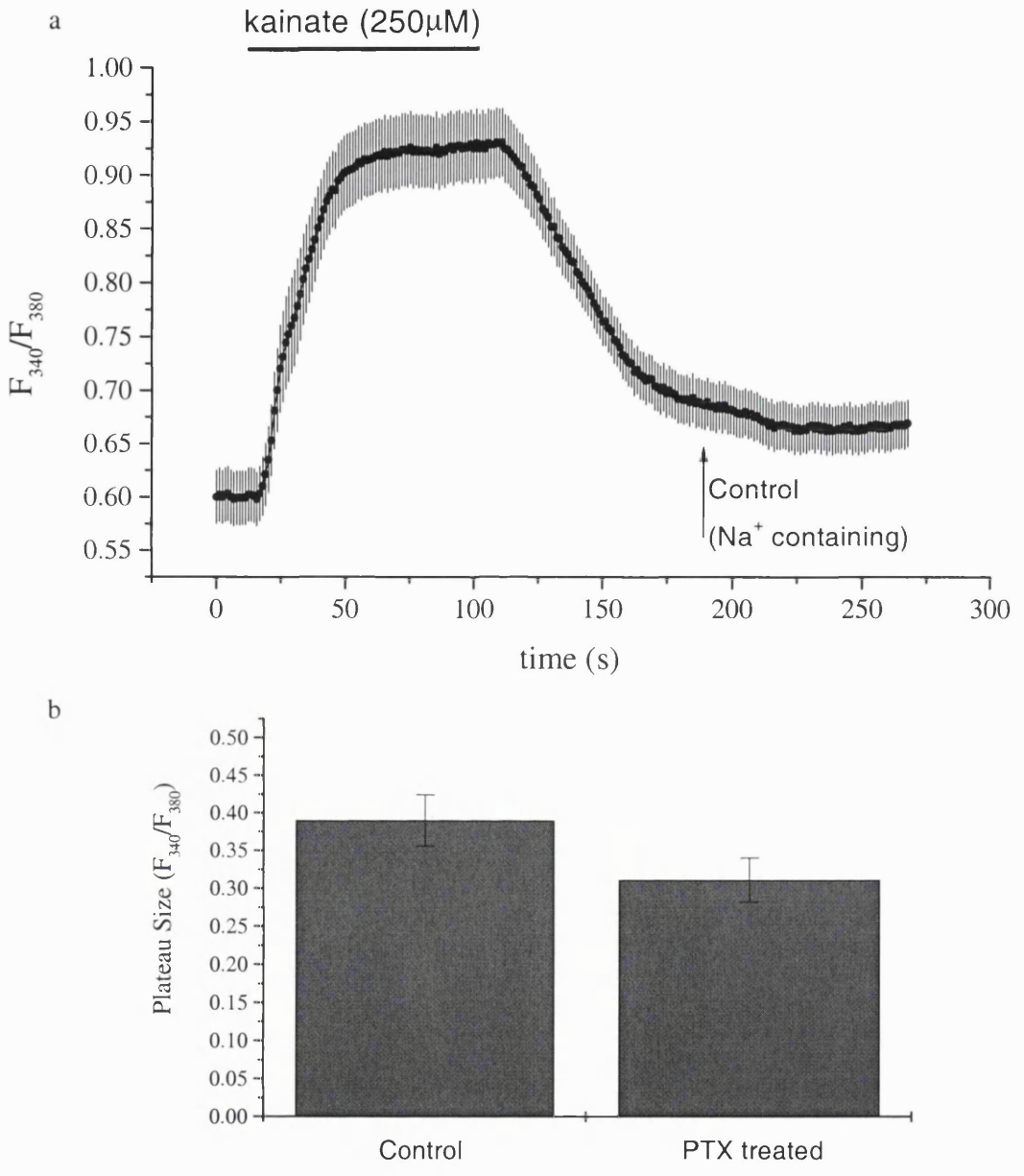

Figure 4.2. $[Ca^{2+}]_i$ elevation evoked by kainate.

a). Kainate induced a large and fully reversible increase in $[Ca^{2+}]_i$ in cerebellar granule neurons. The experiment was performed in sodium free conditions to prevent sodium entry and therefore extensive depolarisation and opening of voltage-gated calcium channels. Re-introduction of sodium to the bathing solution did not hasten the return to baseline. Data, mean ± s.e.mean, n=48

b). Amplitude of the kainate induced increase in $[Ca^{2+}]_i$ in control cells (n=48) and in those incubated in pertussis toxin (PTX; 500ng/ml, >18hours, n=48). Treatment of the cells with pertussis toxin did not significantly change the amplitude of the calcium response to kainate, $0.1<p<0.5$.

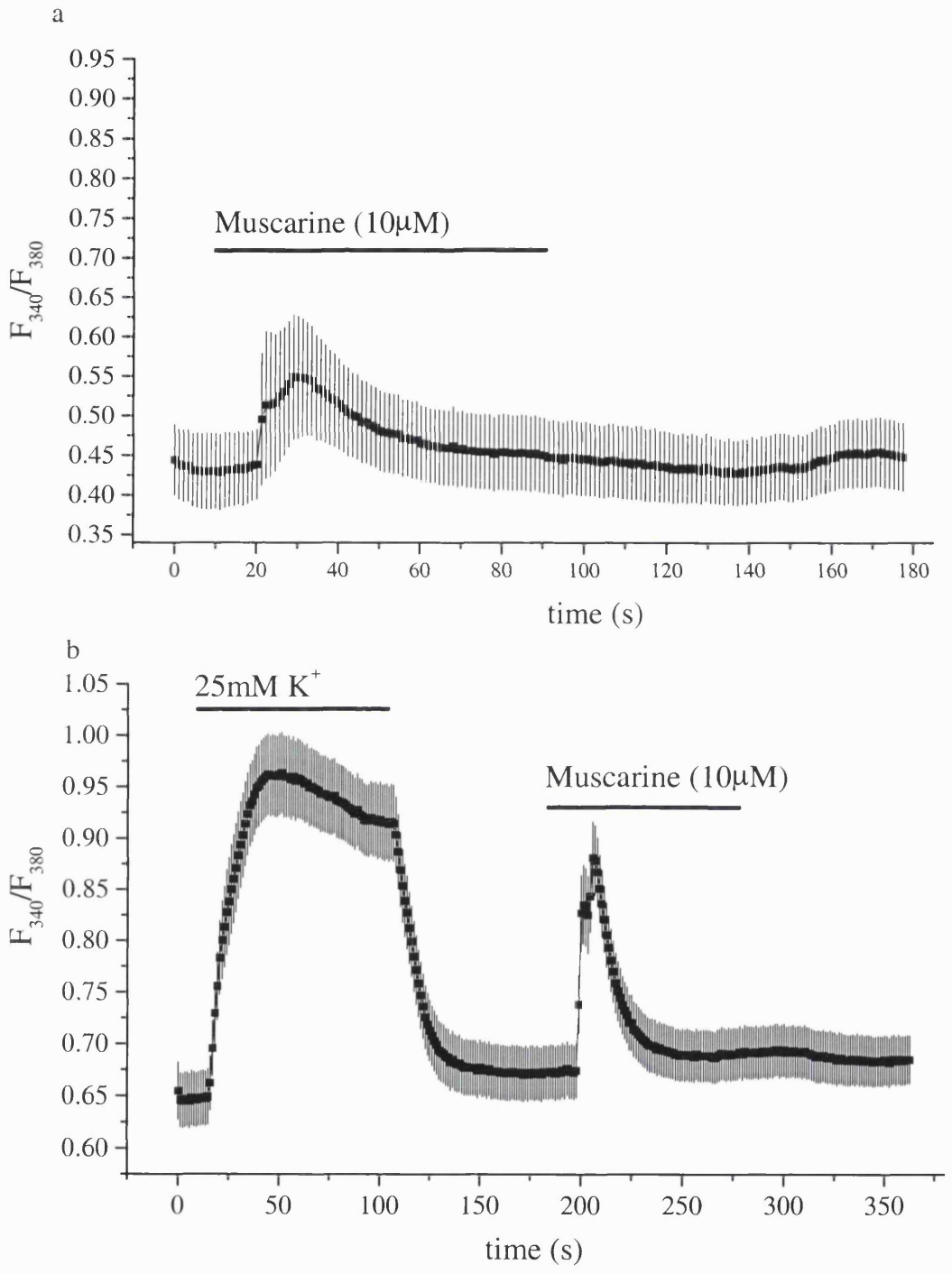

Figure 4.3. Effect of muscarine on $[Ca^{2+}]_i$ in CGN.

a). muscarine (10μM) was bath applied to cerebellar granule neurons. In 8 out of 87 cells (9%) muscarine induced a small transient rise in $[Ca^{2+}]_i$ (data shows mean of responding cells only). In the remainder muscarine evoked no noticeable change in $[Ca^{2+}]_i$.

b). CGN were exposed to a depolarisation (25mM potassium) prior to stimulation with muscarine (10μM). Depolarisation induced a rise in calcium as seen before and increased both the size of the calcium response to muscarine and the proportion of responding cells to 51% (33 out of 65).

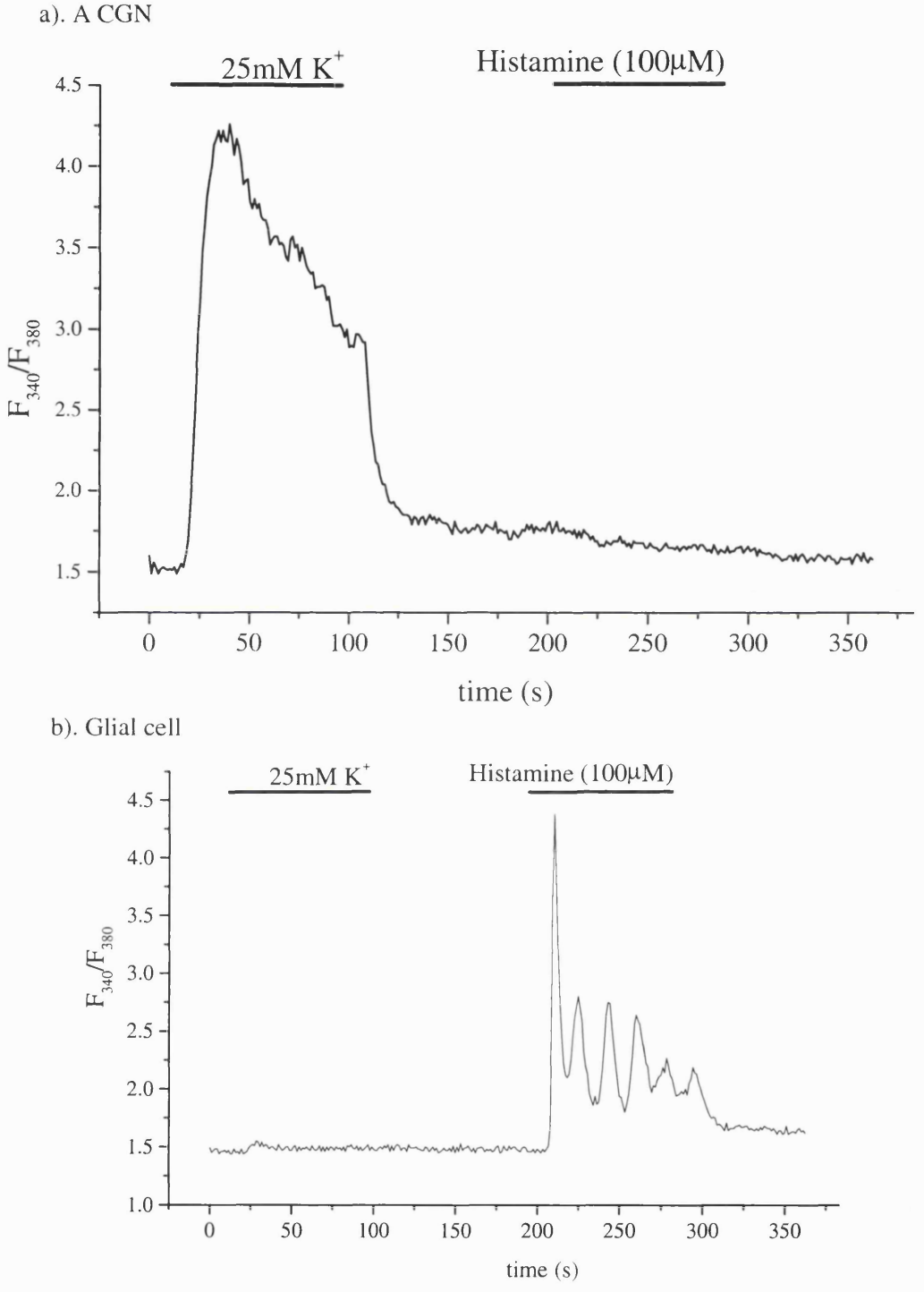

Figure 4.4. Effect of histamine on $[Ca^{2+}]_i$ in CGN and glia.
a). shows the typical response of a CGN to histamine (100μM). Histamine (10, 30 and 100μM) failed to induced a rise in $[Ca^{2+}]_i$ either with or without a prior depolarisation with 25mM potassium.
b). one glial cell (from 7 tested) responded to 100μM histamine (but not to 25mM potassium) with a series of $[Ca^{2+}]_i$ oscillations as shown.

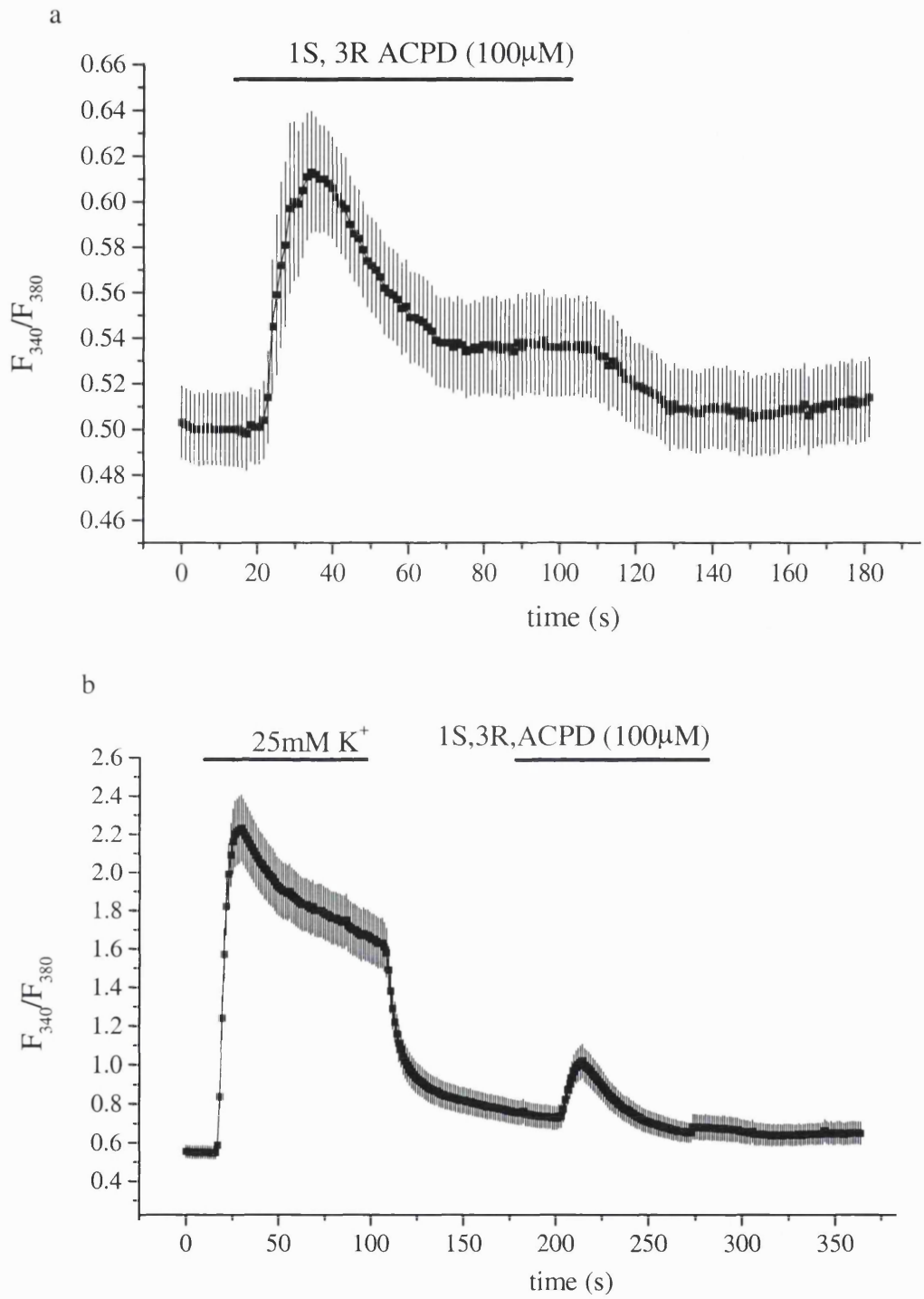

Figure 4.5. The effect of 1S,3R ACPD (100μM) on $[Ca^{2+}]_i$ in CGN.
a). 1S,3R ACPD (100μM) caused a biphasic calcium response in CGN. $[Ca^{2+}]_i$ rapidly reached a transient peak before decaying to a plateau which was sustained during the continued presence of 1S,3R ACPD. 1S,3R ACPD evoked a rise in $[Ca^{2+}]_i$ in 35% of cells examined (26 out of 74). Data shows mean ± s.e.mean of responding cells only.
b). A prior depolarisation with 25mM potassium slightly increase the proportion of cells responding to 1S,3R ACPD to 42% (25 from 60) but did increase the mean amplitude of the transient peak.

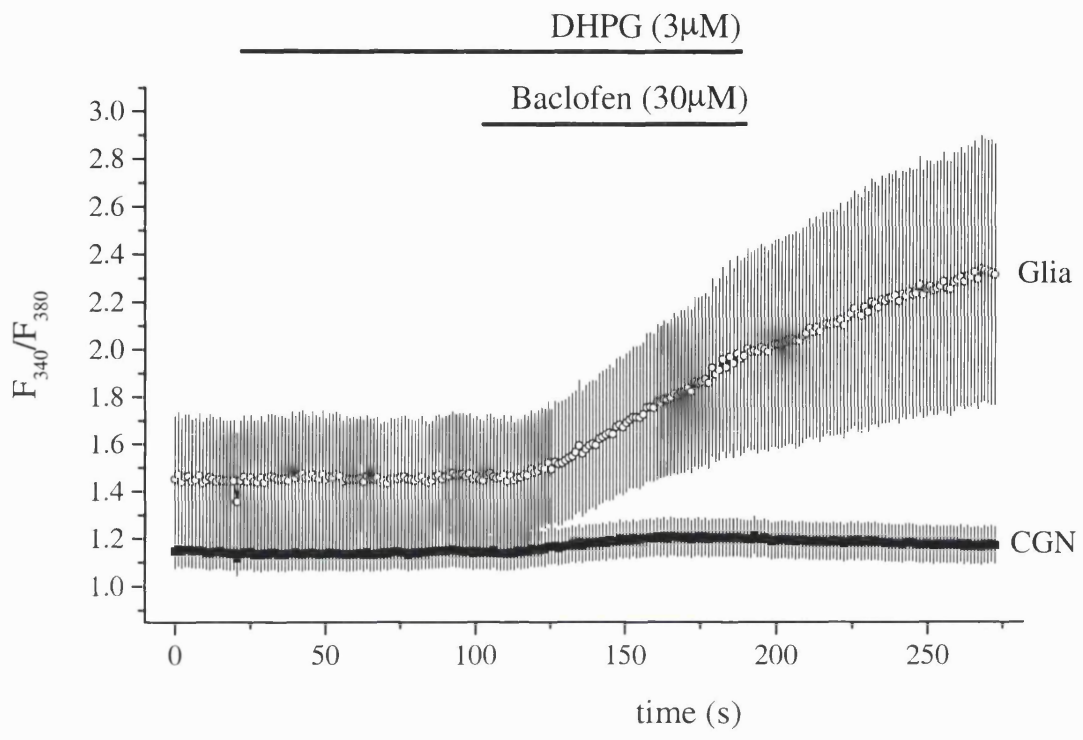

Figure 4.6. Effect of DHPG and baclofen on $[Ca^{2+}]_i$ in CGN and glia.
DHPG did not evoke a rise in intracellular calcium at 3μM, however, at 100μM DHPG induced a transient increase in $[Ca^{2+}]_i$ in 24% (9 out of 37) of cells examined, data not shown. A subsequent application of baclofen (30μM) in the continued presence of DHPG did not increase $[Ca^{2+}]_i$ in cerebellar granule neurons (n=30). However, in glial cells baclofen (30μM) in the presence of DHPG (3μM) evoked a gradual rise in intracellular calcium, which did not wash out upon removal of DHPG and baclofen, (n=5).

4.4. DISCUSSION

This chapter describes the basic aspects of calcium signalling in cerebellar granule neurons. Intracellular calcium can be increased by the opening of voltage-gated or ligand gated ion channel in the plasma membrane. Here 25mM potassium induced depolarisation and kainate (250μM) evoked rises in $[Ca^{2+}]_i$ similar to those previously reported (e.g. Simpson *et al.*, 1996). However, mobilising calcium from intracellular stores was a less reproducible method of inducing a rise in $[Ca^{2+}]_i$. Histaminergic stimulation failed to evoke a change in $[Ca^{2+}]_i$ in granule neurons up to 100μM, a concentration that was observed to evoke calcium oscillations in one glial cell. Muscarinic and metabotropic glutamate receptor stimulation evoked rises in intracellular calcium in a small population of cells examined. The response to both agonists could be augmented by a prior stimulation with 25mM potassium. A $G\alpha_{i/o}$ linked receptor agonist did not induce a rise in $[Ca^{2+}]_i$ in cerebellar granule neurons, but did in glia, in the presence of a $G\alpha_q$ agonist.

4.4.1. Experimental limitations of calcium imaging in this study.

Figure 2.7 shows a calibration curve calculated from experiments which permeabilised the plasma membrane of the cells. However, it became apparent that sometimes resting calcium concentrations in cerebellar granule neurons fell below the calculated 'zero' calcium levels. This is probably due to the 'zero' calcium measurements not being accurate. Due to the abundance of calcium it remains likely that the free concentration could remain in the low nanomolar range even in the presence of EGTA. This could therefore have profound effect on calibration in these experiments because of the very low $[Ca^{2+}]_i$ in cerebellar granule neurons.

Indeed the resting F_{340}/F_{380} changed as the light source (xenon bulb) aged, (e.g. compare resting F_{340}/F_{380} ratios between figures 4.1 and 4.4a). It was therefore decided that where possible experiments would be paired and that only relative changes in F_{340}/F_{380} would be calculated rather that absolute values. Many reports on calcium imaging use uncalibrated data (e.g. Simpson *et al.*, 1996).

4.4.2. Influx of calcium across the plasma membrane.

Calcium influx through voltage-gated and ligand-gated ion channels has been previous described in cerebellar granule neurons, (e.g. Simpson *et al.*, 1996). The results presented here agree well with published reports. Incubation in pertussis toxin did not affect the magnitude of the calcium plateau induced by kainate. In parallel studies kainate induced calcium influx through a PTX-insensitive mechanism, is able to modulate the activity of delayed rectifier potassium currents (Jones *et al.* 2000).

4.4.3. Release of calcium from intracellular stores.

The results presented here indicate that muscarine and 1S,3R ACPD are both able to release calcium from intracellular stores but that the size of the response and the proportion of cells responding are augmented by a prior depolarisation with high concentrations of potassium. In the experiment illustrated in figure 4.3a only 9% of cells responded to muscarine with a rise in calcium. The proportion of cells responding to muscarine was variable (compare with figure 5.1 where 59% of cells responded). The variability observed in this study is reflected in the disparity in published results.

Fohrman *et al.*, (1993) reported that muscarinic (M_3) activation with carbachol failed to evoke a rise in intracellular calcium in cerebellar granule neurons. However, calcium responses could be evoked by a prior stimulation with 40mM potassium. Similar observations were made by Masgrau *et al.*, (2000) where carbachol failed to cause a change in $[Ca^{2+}]_i$ before but not after exposure to 40mM potassium. Whereas, del Rio *et al.*, (1999) found that, under control conditions, approximately 50% of cerebellar granule neurons responded to muscarinic receptor activation with a rise in $[Ca^{2+}]_i$. Other reports have routinely used a prior depolarisation with potassium (e.g. Irving *et al.*, 1992a), however, a further report by Irving *et al.*, (1992b) suggested that potassium depolarisation had no effect on the calcium response to acetylcholine.

This study failed to identify any calcium response following activation of histaminergic receptors, even following prior depolarisation with potassium. These data are not in agreement with the results of del Rio *et al.*, (1999) who found that histamine did evoke small rises in intracellular calcium under control conditions and that these calcium responses could be augmented by a depolarising response. The

difference in results cannot be easily explained. The previous chapter illustrated that histaminergic stimulation was able, at least in most cells examined, to inhibit IK_{SO} suggesting that histaminergic receptors are present in these cultures of cerebellar granule neurons. The most obvious difference between the two studies is the experimental temperature. This study was performed at room temperature whereas the work by del Rio *et al.*, (1999) was performed at 37°C.

In this study stimulation of glutaminergic receptors with 1S,3R ACPD evoke a rise in intracellular calcium in 35% of cells and like muscarine prior depolarisation increased the number of responding cells as well as the size of the response. Like muscarine and histamine the published data concerning the ability of glutaminergic agonists to stimulate a rise in intracellular calcium contains discrepancies. Unlike the calcium responses to muscarine, 1S,3R ACPD failed to increase $[Ca^{2+}]_i$ in control conditions (del Rio *et al.*, 1999) although the response was enhanced by 20mM potassium. Whereas in this study, in Simpson *et al.*, (1996) and in Courtney *et al.*, (1990) 1S,3R ACPD did evoke an increase in $[Ca^{2+}]_i$. As with muscarine Irving *et al.*, (1992a) preceded agonist application with a depolarisation.
The conflicting results that this and other studies have produced indicates that the mechanisms underlying calcium release from intracellular stores are much more complex than previously thought. Different interactions between IP_3 and ryanodine sensitive calcium pools following stimulation with different agonists can only explain some of the results. Subtle differences in experimental techniques could lead to different results. One significant drawback of this and other studies on granule neurons is the inability to look at highly localised calcium signals. This study only concentrated on calcium rises within the somata of the granule neuron. It is possible that synaptic connections onto other granule neurons or even close proximity to them or glial cells may underlie these different results between cells and studies.

In almost all cases a prior depolarisation with potassium increases the response to the $G\alpha_q$ stimulating agonist. Del Rio *et al.*, (1999) found that potassium depolarisation did not markedly enhance the calcium response to noradrenaline). Irving *et al.*, (1992a) suggested that prior exposure to potassium was used to 'charge

the intracellular stores'. As a potassium challenge does increase $[Ca^{2+}]_i$ is seems reasonable to suggest that at least part of the calcium would be sequestered into the intracellular stores hence attenuating the response to $G\alpha_q$ stimulating agonists. It is possible that the increases in calcium during the potassium administration prime the receptor - G protein - PLC complex. del Rio *et al.*, (1996, 1999) showed that IP_3 production was enhanced by mild depolarisation. However, increased IP_3 following α-adrenergic stimulation with noradrenaline levels could not be increased further by mild (20mM potassium) depolarisations (del Rio *et al.*, 1999).

Priming of calcium release has also been demonstrated using $G\alpha_{i/o}$ coupled receptor agonists in SH-SY5Y cells (a human neuroblastoma cell line). Connor & Henderson (1996) showed that calcium could be released from intracellular stores by 9[D-$Pen^{2,5}$]-enkephalin (DPDPE; a δ opioid agonist) in the presence of carbachol but not alone. Similarly a μ opioid receptor agonist DAMGO (Tyr-D-Ala-Gly-N-Me-Phe-Gly-ol) was able to induce a rise in $[Ca^{2+}]_i$ in the presence of carbachol. Both the δ and μ receptors couple to $G\alpha_{i/o}$ and the response could be inhibited by their receptor antagonists. The same response has been observed with neuropeptide Y (at the Y_2 receptor) and somatostatin (at the sst_2 receptor), (Connor *et al.* 1997). The mechanisms underlying $G\alpha_{i/o}$ mediated release of calcium from the stores has not been resolved. In this system a $G\alpha_{i/o}$ stimulating agonist was unable to induce release of calcium from intracellular stores in the presence of a $G\alpha_q$ coupled receptor agonist in cerebellar granule neurons. However, in glial cells a steady rise was observed. This rise was not characteristic of a release from intracellular stores which is fast rising, and therefore may represent an slow influx across the plasma membrane. The differing results in the two studies maybe due to the cell type. The results obtained by Connor & Henderson (1996) were attained with SH-SY5Y cells, and are not reflected in the primary cultures used here. A lack of calcium in the releasable pool may also explain the difference in results.

Furthermore, increases in calcium following potassium induced depolarisation may lead to small highly localised increases in calcium that remain high long after global calcium has returned to baseline levels. As IP_3 and ryanodine receptors have a bell-shaped sensitivity to calcium (see Bezprozvanny *et al.*, 1991 and Galione, 1991)

higher concentrations of calcium at the cytoplasmic face of these receptors may increase their open probability.

It also remains a possibility that all these agonists are evoking a release of calcium from the intracellular stores but that the signal is being rapidly buffered and cannot therefore be observed as a global rise in $[Ca^{2+}]_i$. Calcium binding proteins in the cytoplasm may play a role in such as response. It is also possible that calcium release from the intracellular stores is highly localised. Mitochondria have been shown to be tightly localised to calcium release sites (Jouaville *et al.*, 1995) and it remains a possibility that released calcium is being rapidly taken into the mitochondria and therefore does not evoke a global calcium rise. The following chapter investigates the role of the mitochondria in calcium signalling in cerebellar granule neurons.

As suggested by Irving *et al.*, (1992a) intracellular stores may need to be replenished before they are able to release enough calcium to induce a global rise. Depleted intracellular calcium stores has previously been reported in cerebellar granule neurons (Toescu 1998) and in hippocampal neurons (Irving & Collingridge 1998). Chapter 6 investigates the properties of intracellular calcium stores within these cells.

4.4.4. Physiological Relevance

The results presented here may suggest that there are two populations of cells within the granule cell layer of the cerebellum. One population will readily respond to muscarine and one will not. The ability of each population to survive slightly differing culture procedures may underlie the varying results presented here and by other groups.

Non-excitable cells are dependent upon calcium release from intracellular calcium stores and store-operated calcium channels to evoke rises in $[Ca^{2+}]_i$ (e.g. platelets, Sage 1997). However, as excitable cells have voltage-gated calcium channels which are capable of supplying large quantities of calcium to the cytosol, the role of calcium stores in excitable cells, and in particular neurons, remains to be classified. Irving & Collingridge (1998) suggested that the intracellular calcium stores in hippocampal neurons act as coincidence detectors, responding with a release of calcium only when agonists coupled to $G\alpha_q$ stimulate cells after a depolarisation.

Similarly cerebellar granule neurons may only respond to agonists, such as acetylcholine (at muscarinic receptors), with a release of stored calcium when stimulation follows depolarisation.

Chapter 5. Results

Mitochondrial control of cytoplasmic calcium in CGN

5.1 INTRODUCTION

The ability of mitochondria to take up calcium was first described in the 1960s (Deluca & Engstrom 1961), but it was not until the early 1990s that mitochondria were implicated in calcium signalling. Mitochondria are now know to both sequester calcium prolonging calcium signals and act as buffers for calcium in times of high $[Ca^{2+}]_i$ (Babcock & Hille 1998).

5.1.1 Buffering of the calcium signal by mitochondria.

Thayer and Miller (1990) showed that, in neurons of the dorsal root ganglion, a calcium response to a depolarisation induced by 50mM potassium could be markedly altered by administration of mitochondrial uncouplers. 50mM potassium caused a rapid rise in $[Ca^{2+}]_i$ which decayed to a plateau level upon removal of the stimulant. Although this plateau varied considerably between cells it remained quite consistent within the same cell, and lasted for up to 45 minutes (Thayer *et al.* 1988). Application of CCCP to these neurons caused a small and transient increase in $[Ca^{2+}]_i$ indicating that at rest there was little calcium within the mitochondria. When the cell was stimulated with 50mM potassium again, the peak calcium response was of greater amplitude and duration but the amplitude of the plateau phase decreased dramatically (by 79%). Further, if CCCP was administered during the plateau a rise in intracellular calcium was observed before decaying back to the original baseline level (Thayer and Millar 1990). These results showed that mitochondria are able to strongly affect the calcium signals resulting from a depolarisation.

Similar results were obtained in bullfrog sympathetic neurons (Friel & Tsien 1994) but included the observation that calcium released from intracellular stores by caffeine or ryanodine could also be taken up by mitochondria.

Studies on central mammalian neurons have yielded similar results. In rat forebrain neurons inhibition of mitochondrial uptake reduces the recovery of a calcium load induced by activation of the NMDA receptor by fourfold. Whereas recovery is only slowed twofold by bathing in sodium free conditions which inhibit the plasma membrane Na^+/Ca^{2+} exchanger, (White and Reynolds 1995).

Subsequent reports on a wide variety of cell types have shown that mitochondria both buffer cytosolic calcium and act to prolong calcium signals, and the

mitochondria are now a well established part of cytosolic calcium signalling (Gunter *et al.*1994; Babcock & Hille, 1998; Duchen, 1999).

5.1.2 Localisation of Mitochondria.

As discussed previously (chapter 1.8) release of calcium from IP_3 sensitive stores initiates a process whereby released calcium initiates further release; calcium induced calcium release (CICR). This process results in calcium waves propagating through the cytoplasm of the cell. In 1995 Jouaville *et al.* showed that supplying oxidizable substrates, such as malate, to the cell increased the amplitude of the calcium wave in addition to increasing velocity and interwave period. Application of oxidative substrates caused an increase in oxidative phosphorylation, hyperpolarisation of the mitochondrial membrane and hence an increased capacity to take up calcium. Enhanced calcium uptake into mitochondria results in a higher concentration of calcium required to induce CICR if the mitochondria are in close proximity to the calcium release sites. In addition, local buffering will mean that fewer IP_3 receptors are activated at rest and hence an increased density of excitable receptors are available when a wave propagates, creating the larger amplitude and velocity. This process was termed mitochondrial-generated synchronisation of calcium release (Jouaville *et al.*1995). A similar coupling between mitochondria and IP_3 receptors has been observed in hepatocytes where mitochondria were shown to suppress the positive feedback of CICR, (Hajnóczky *et al.* 1999). Similarly, mitochondrial depolarisation was observed when calcium was released from the SR of rat cardiomyocytes. A tight coupling between mitochondria and the SR would provide sufficiently high calcium release from the SR for calcium uptake into mitochondria, (Duchen *et al.* 1999).

Mitochondria have subsequently been shown by imaging techniques to be highly localised in HeLa cells. Using photoproteins for both the endoplasmic reticulum and mitochondria, Rizzuto *et al.* (1998) demonstrated a highly localised, largely connected tubular network of mitochondria which undergoes continuous re-arrangement. Further, calcium sensitive photoproteins directed to the outer face of the inner mitochondrial membrane showed that the mitochondria are exposed to much higher concentrations of calcium, following activation of IP_3 receptors, than the bulk of the cytoplasm (Rizzuto *et al.* 1998).

5.1.3 Regulation of plasma membrane calcium channels by mitochondria

Store-operated calcium channels open in response to emptying of the endoplasmic reticulum calcium stores, and remain open until they are replenished. In the presence of inhibitors of the SERCA, store-operated channels can remain open for many 10s of minutes. Mitochondria have been shown exhibit a tight control over the state of these channels. Using rhod-1 Hoth *et al.* (1997) showed that mitochondrial calcium uptake is dependent on extracellular calcium in T-cells. This suggested a close proximity to the store operated channels in these cells. Indeed in the presence of mitochondrial uncoupler or sodium free extracellular solution a store-operated calcium influx was not maintained over long periods (>10 mins). The rate of calcium entry under these conditions changed from a high influx to a low influx state. These results demonstrated that mitochondria are responsible for maintaining the activated state of store-operated calcium channels. Mitochondria close to the sites of calcium entry in T-cells are thought to buffer calcium influx thus preventing the build up of high calcium concentrations at the entry points which inactivate the store-operated channels (Hoth *et al.* 1997).

Mitochondria have also been shown to prolong calcium influx through voltage-gated calcium channels and NMDA channels by buffering calcium at the entry points and thus preventing calcium induced inactivation, (Budd & Nicholls 1996a,b; and see below).

5.1.4 Mitochondrial Regulation of calcium in CGN.

Fura-2 imaging of cerebellar granule neurons showed that at rest there was no CCCP releasable pool but that CCCP enhanced the $[Ca^{2+}]_i$ when cells were depolarised by increasing extracellular potassium, (Budd & Nicholls 1996a), although this effect was attributed to a drop in the ATP/ADP ratio. Oligomycin was shown to maintain ATP/ADP ratio when applied in conjunction with rotenone, which dissipates the mitochondrial membrane potential. In the presence of rotenone and oligomycin, CCCP was unable to release a pool of calcium following KCl induced depolarisation. However the magnitude of the rise in $[Ca^{2+}]_i$ induced by high potassium decreased in the presence of oligomycin and rotenone. These results suggest that mitochondria internalise calcium entering through the voltage-gated

calcium channels, and that this uptake prevents calcium induced inactivation of these channels (Budd & Nicholls 1996a).

Similar results were obtained when the $[Ca^{2+}]_i$ was raised by activation of the NMDA receptor, (Kiedrowski & Costa 1995; Budd & Nicholls 1996b). These reports demonstrated that mitochondrial calcium uptake was necessary to prevent glutamate causing large and toxic increases in the $[Ca^{2+}]_i$. It is worth noting, however, that extensive rises in mitochondrial calcium can cause extensive ATP depletion and initiate apoptosis, (Duchen 1999).

5.2 Aims

As described in many cell types mitochondria appear to be highly localised at calcium release sites on the endoplasmic reticulum or near to the plasma membrane calcium channels. Experiments detailed in the previous chapter demonstrate that under normal conditions muscarine and 1S, 3R-ACPD are not efficient at evoking a rise in intracellular calcium. In this chapter the protonophore CCCP was used with the express aim of investigating whether calcium, released from the endoplasmic reticulum, is being rapidly buffered by the mitochondria rather than causing a global rise in $[Ca^{2+}]_i$.

5.3 RESULTS

5.3.1 Effect of abolishing $\Delta\psi_m$ on the muscarine induced rise in $[Ca^{2+}]_i$.

The protonophore CCCP (2μM) was used to dissipate the potential difference across the inner mitochondria membrane. $\Delta\psi_m$ is mainly due to a proton gradient and CCCP causes membranes to become selectively permeable to protons, thus abolishing the electrical gradient, (see Duchen 1999). CCCP has a twofold action on the cell. Firstly, as $\Delta\psi_m$ depolarises so the F_1F_0ATPase attempts to re-establish the proton gradient rapidly using up the cells supply of ATP, and secondly mitochondrial depolarisation will mean that the mitochondria will lose the ability to take up calcium through the mitochondrial calcium uniporter.

In figure 5.1 fura-2 loaded cells were incubated in CCCP (2μM) for approximately 10-15 minutes at 37°C. As can be seen control treated cells (filled squares, n = 68) have a low resting F_{340}/F_{380} ratio of 0.56 ± 0.03 (mean ± s.e.mean) and responded to muscarine with a transient rise in $[Ca^{2+}]_i$ which decayed leaving no obvious plateau in the continued presence of the agonist, similar to previously seen. Surprisingly however, cells treated with CCCP (2μM; open circles n = 70) had a much higher basal F_{340}/F_{380} ratio of 0.89 ± 0.4 and showed no change in $[Ca^{2+}]_i$ in response to muscarine.

Transient rises in intracellular calcium upon treatment with CCCP have been noted in many cell types (e.g. smooth muscle, McCarron & Muir, 1999) including cerebellar granule neurons (Chen *et al.*, 1999), however there are few reports of a sustained rise.

5.3.2 Characterising the CCCP induced rise in $[Ca^{2+}]_i$.

This increase in $[Ca^{2+}]_i$ might not be expected to be due to a sustained release of calcium from the mitochondria as other reports note that at rest mitochondria contain very low levels of calcium, (Babcock & Hille, 1998). The source of the calcium maintaining this sustained rise was investigated by removing extracellular calcium. Figure 5.2 shows the effect of removing extracellular calcium on the plateau established by CCCP. Here cells were incubated in 2μM CCCP as before, calcium was removed from the bathing solution and EGTA (1mM) was used to buffer any residual calcium. Removal of calcium resulted in a drop in the F_{340}/F_{380} ratio from

0.69 ± 0.02 to 0.58 ± 0.01 ($p<0.001$ *t* test) which was fully reversible upon re-administration of calcium.

Thapsigargin treatment in calcium free conditions often evokes a larger rise in $[Ca^{2+}]_i$ when calcium is added back to the external solution, than when cells are treated with thapsigargin in calcium containing solution (e.g. Prothero *et al.* 1998). Here, cells incubated in CCCP in calcium free medium show a larger rise in $[Ca^{2+}]_i$ than those incubated in calcium containing solution (F_{340}/F_{380} of 0.69 ± 0.02, from figure 5.2 compared with 1.39 ± 0.14, figure 5.3). The mechanism for this phenomenon is not understood but it might represent a priming of influx channels in calcium-free conditions.

FCCP, a more potent protonophore than CCCP, induced a similar rise in $[Ca^{2+}]_i$ to CCCP. In figure 5.4 cells were incubated in FCCP (1μM) in calcium-free conditions for at least 10 minutes. Calcium was re-introduced to the bathing solution at the arrow. A subsequent rise in $[Ca^{2+}]_i$ ensued which peaked and decayed to a plateau, F_{340}/F_{380} of 1.17 ± 0.02. Like the CCCP induced plateau, the FCCP induced rise in $[Ca^{2+}]_i$ could be diminished by removal of extracellular calcium. A comparison between cells incubated in either CCCP (2μM) or FCCP (1μM) showed that the amplitude of the calcium plateaus induced these compounds at these concentrations were of the same magnitude, (data not shown).

The sustained rise in $[Ca^{2+}]_i$ would appear to be due to an influx through plasma membrane calcium channels. The identity of the channel responsible for this influx has been investigated by blocking calcium influx with a variety of inorganic ions. Figure 5.5 shows the sensitivity of the sustained rise in $[Ca^{2+}]_i$ to lanthanum. Cells were incubated in CCCP (2μM) in calcium free conditions. Calcium was re-introduced to the bathing medium at the arrow and a resultant large and rapid rise in intracellular calcium was observed, figure 5.3. The sustained calcium plateau was allowed to stabilise for two minutes after which lanthanum (30μM) was introduced to the extracellular solution. As can be seen lanthanum inhibited the calcium influx in a rapid manner to a new plateau (from an F_{340}/F_{380} of 1.13 ± 0.02 to 0.82 ± 0.01, n = 100). A subsequent removal of calcium from the extracellular solution produced a further drop in $[Ca^{2+}]_i$ but not to basal levels.

Figure 5.6a-d shows the effect of other inorganic ions on the plateau induced by incubation in CCCP. Using the same procedure as for lanthanum the ability of nickel, cadmium, cobalt and zinc to block calcium influx was investigated. As can be seen all ions tested had some effect on $[Ca^{2+}]_i$. The magnitude of the inhibition by the inorganic ions was expressed as a percentage inhibition in figure 5.8. Here 100% inhibition is defined as a complete return of the F_{340}/F_{380} ratio to baseline levels, before calcium was re-introduced to the bathing solution. 0% inhibition is defined at the plateau F_{340}/F_{380} ratio.

The comparative lack of inhibition by zinc would suggest that the channel responsible for calcium influx is not a store-operated calcium channel (Prothero *et al.* 1998; Hoth & Penner, 1992). To investigate whether L-type calcium channel activation is responsible for the sustained calcium plateau in the presence of CCCP the L-type channel blocker nifedipine was used. As can be seen from figure 5.7 nifedipine (3μM) caused a strong and reversible reduction in plateau size. Percentage inhibition was calculated to be 53 ± 1%

Figure 5.8 summarises the data shown in figures 5.5 - 5.7. The potency order of block by inorganic ions was $La^{3+} > Cd^{2+} > Co^{2+} > Ni^{2+} > Zn^{2+}$.

5.3.3 Identification of the cause of the CCCP induced rise in $[Ca^{2+}]_i$.

The results detailed above suggest that CCCP in some way induces a rise in intracellular calcium through activation of an L-type 'like' calcium channel on the plasma membrane. However, what causes this activation remains unclear. As mentioned CCCP will cause depletion of intracellular ATP as well as removing the ability of the mitochondria to take up calcium. Oligomycin is a blocker of the F_1F_0ATPase, inhibition of which will not cause rapid cellular depletion because ATP synthesis by glycolysis will provide sufficient ATP under normal conditions. However, if oligomycin is applied at the same time as CCCP it will prevent the F_1F_0ATPase from pumping protons out of the matrix and hence prevent CCCP induced ATP depletion.

Here oligomycin did not induce a rise in intracellular calcium *per se*, and was unable to prevent the CCCP induced rise in $[Ca^{2+}]_i$, figure 5.9. This suggests that either oligomycin is ineffective at preventing ATP hydrolysis by the F_1F_0ATPase or that

cellular ATP depletion is not responsible for the calcium rise observed after incubation in CCCP.

Activation of voltage-gated L-type calcium channels appear to be responsible for the calcium influx observed here. However, current clamp recording of CGNs showed that acute application of CCCP induced only a small and transient depolarisation of the cell membrane. Addition of muscarine, for comparison, produced a much larger transient depolarisation, figure 5.10. Imaging studies have shown that muscarine does not cause activation of voltage-gated calcium channels. Therefore despite CCCP incubation causing activation of L-type calcium channels, it does not appear to be mediated through a cellular depolarisation.

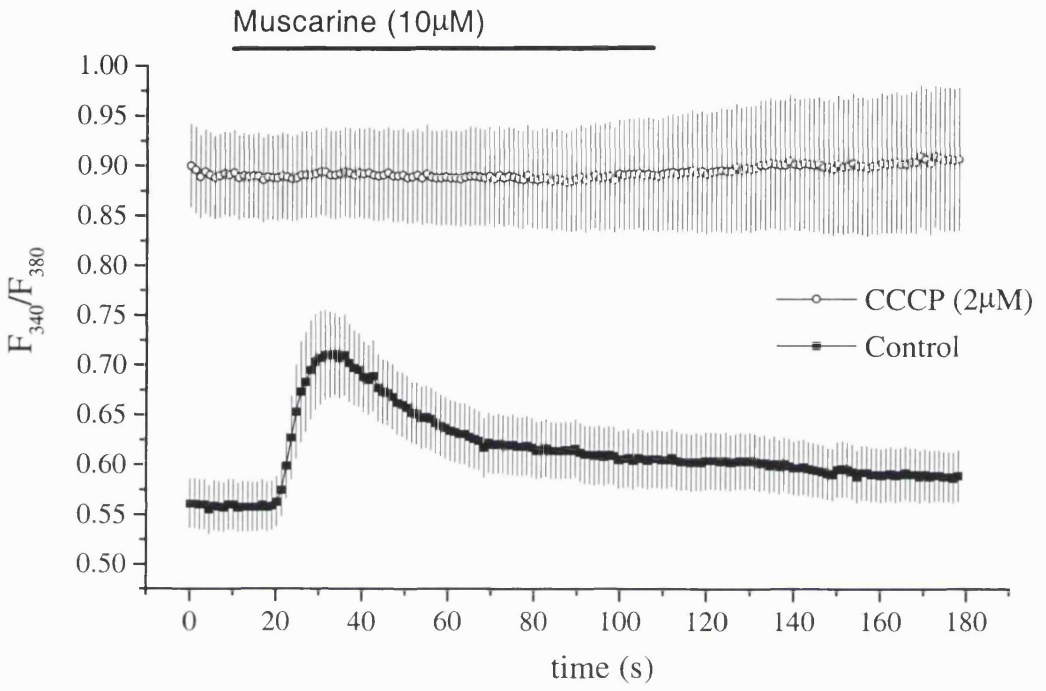

Figure 5.1 Effect of CCCP on the muscarinic calcium response.

Cells were incubated in either control conditions (filled squares, n = 68) or CCCP (2μM; open circles n = 70). 10μM muscarine was bath applied for the duration represented by the bar. A marked difference in the basal calcium concentration can be observed between the two treatment groups. None of the cells treated with CCCP responded to muscarine. 59% (40 out of 68) of control treated cells responded to muscarine. Data includes all cells examined.

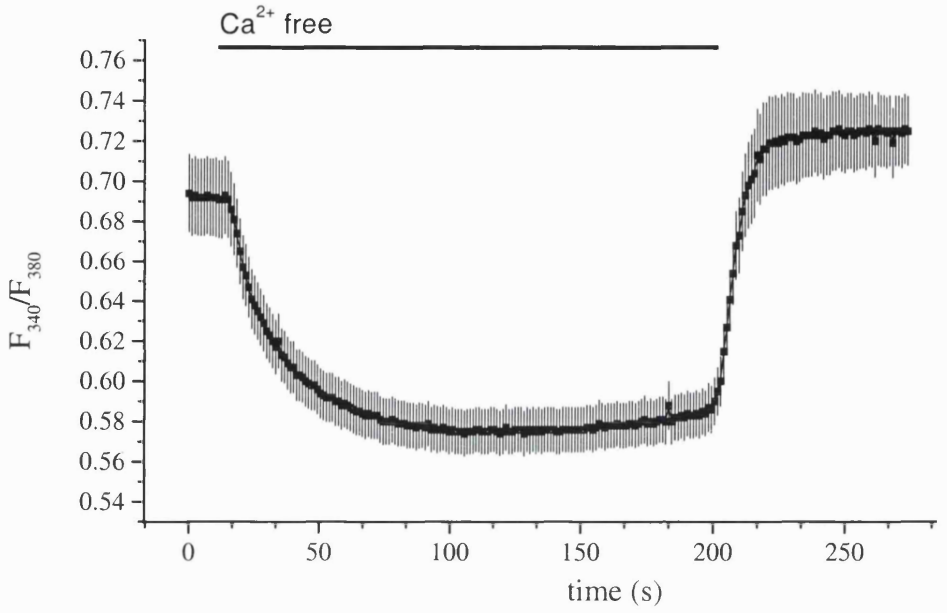

Figure 5.2. The sustained rise in $[Ca^{2+}]_i$ after incubation in CCCP is dependent on extracellular calcium.

Cells were incubated in CCCP (2μM) are before. The subsequent high basal calcium concentration was diminished by the removal of extracellular calcium, n = 61. Calcium free external solution also contained 1mM EGTA.

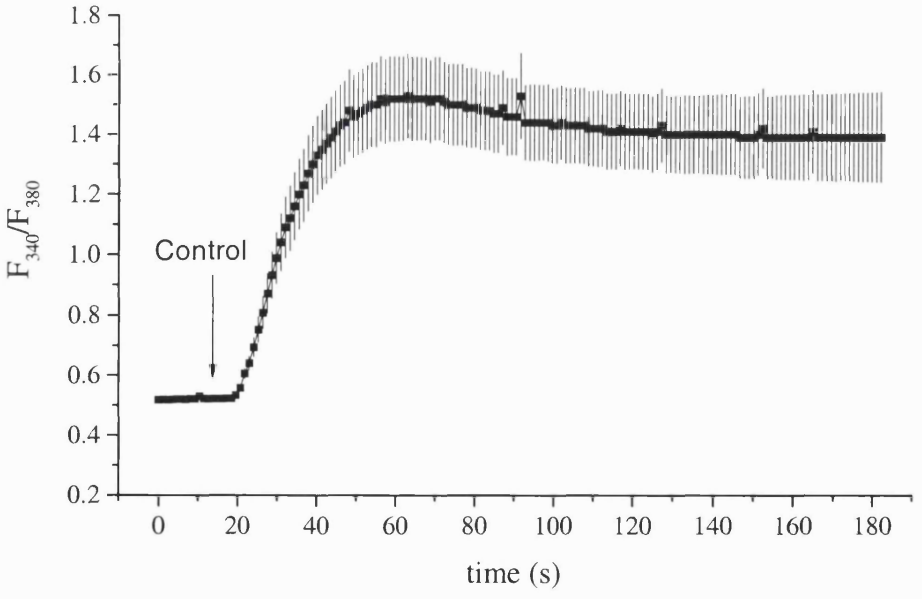

Figure 5.3. Effect of calcium re-administration to cells incubated in calcium free solution containing CCCP (2μM).

Cell were incubated in calcium free external solution containing CCCP (2μM). When calcium was re-introduced to the bathing solution a plateau formed that was larger in size to that seen when cells were incubated in a calcium containing solution with CCCP (2μM; see figure 5.2). n = 13.

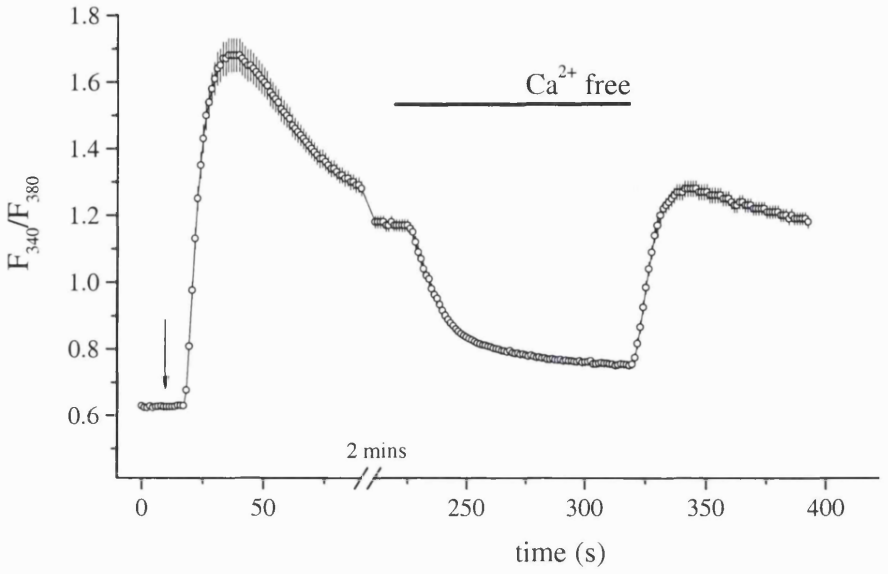

Figure 5.4. FCCP (1μM) also induces a rise in intracellular calcium.
Cells were incubated in FCCP in calcium free conditions for ~10 minutes. Calcium was reintroduced to the bathing solution at the arrow. A subsequent rise in intracellular calcium was observed which was allowed to stabilise for 2 mins. The resultant calcium plateau was sensitive to the removal of extracellular calcium, as with CCCP. n = 63.

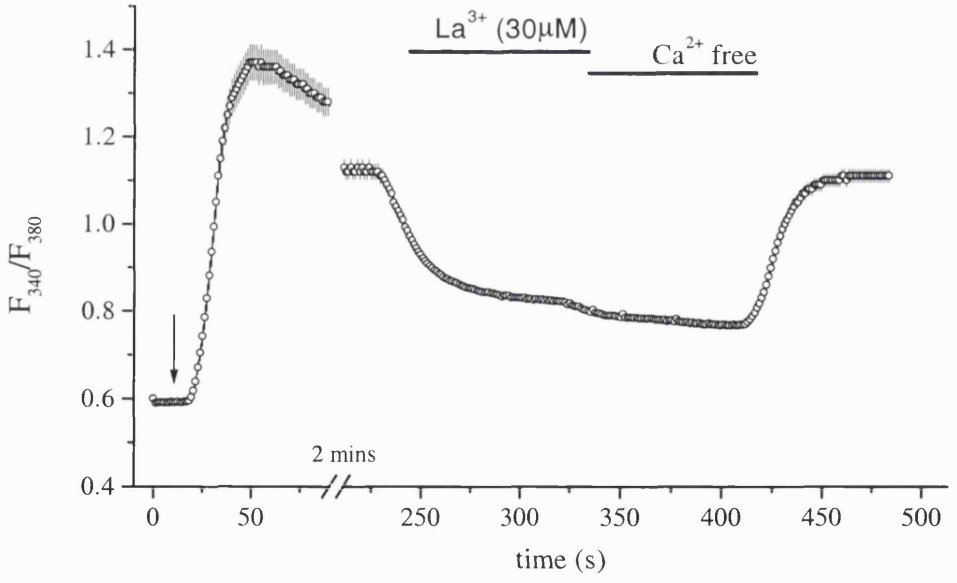

Figure 5.5. The CCCP induced calcium influx is sensitive to lanthanum.
Cells were incubated in calcium free extracellular containing CCCP (2μM), as in figure 5.3. Calcium containing solution was perfused at the arrow. After the $[Ca^{2+}]_i$ had stabilised 30μM lanthanum was applied to the extracellular solution. $[Ca^{2+}]_i$ can be seen to fall to a new level. Subsequent removal of calcium decreased $[Ca^{2+}]_i$ further. Recovery to the plateau levels of was achieved by re-administering calcium to the extracellular solution. n = 100.

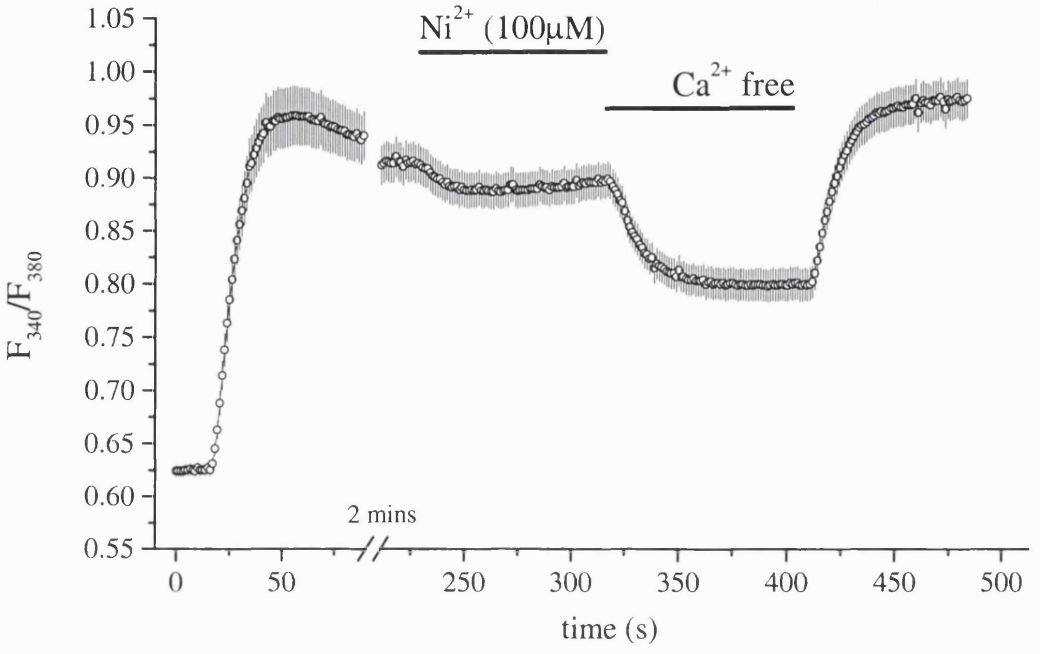

Figure 5.6a. Nickel, n = 141.

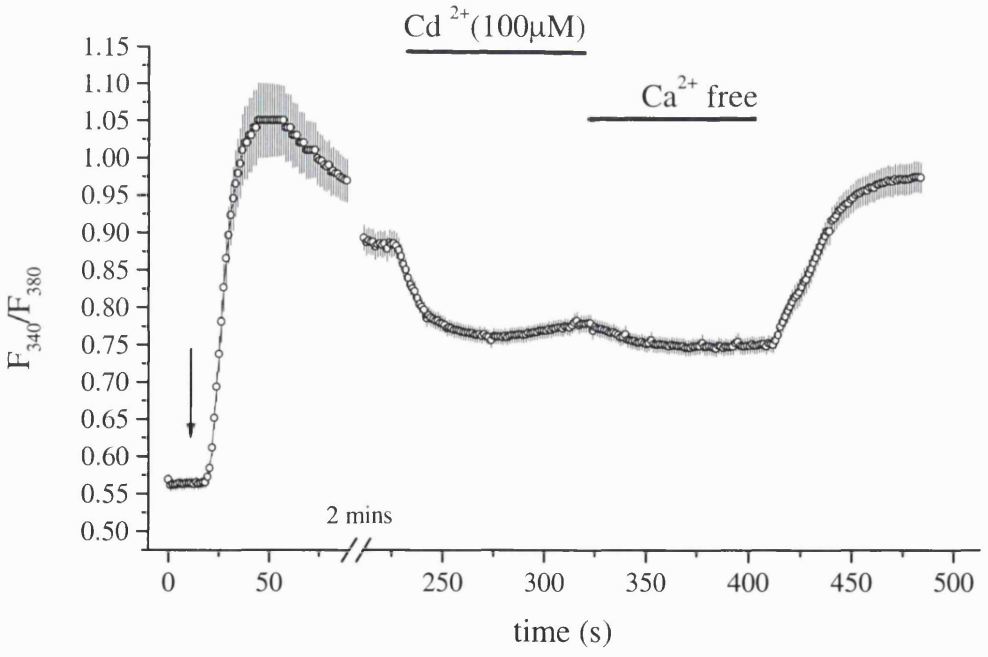

Figure 5.6b Cadmium (n = 53)

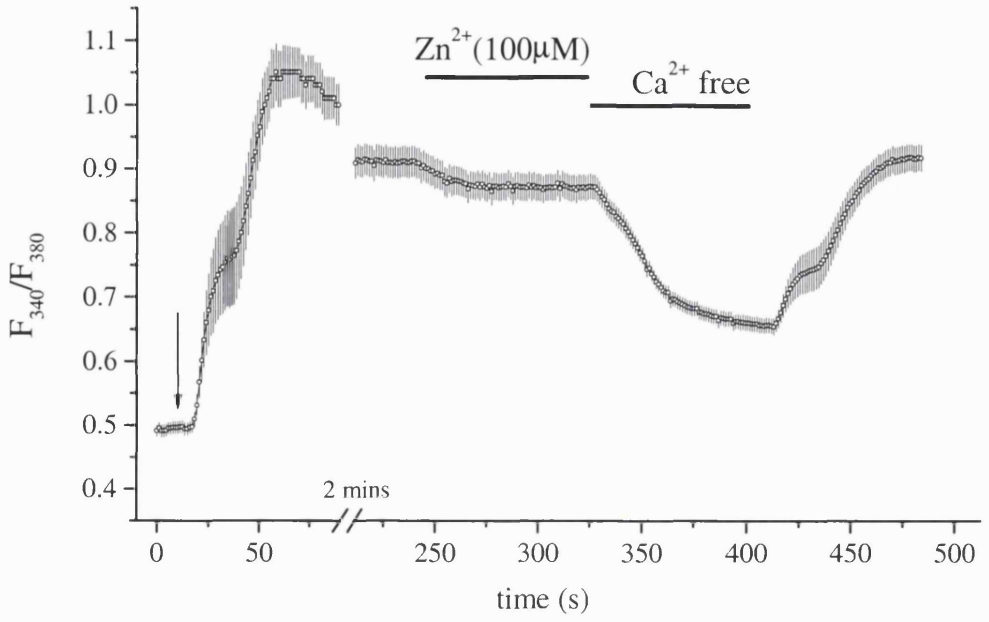

Figure 5.6c. Zinc, n = 33

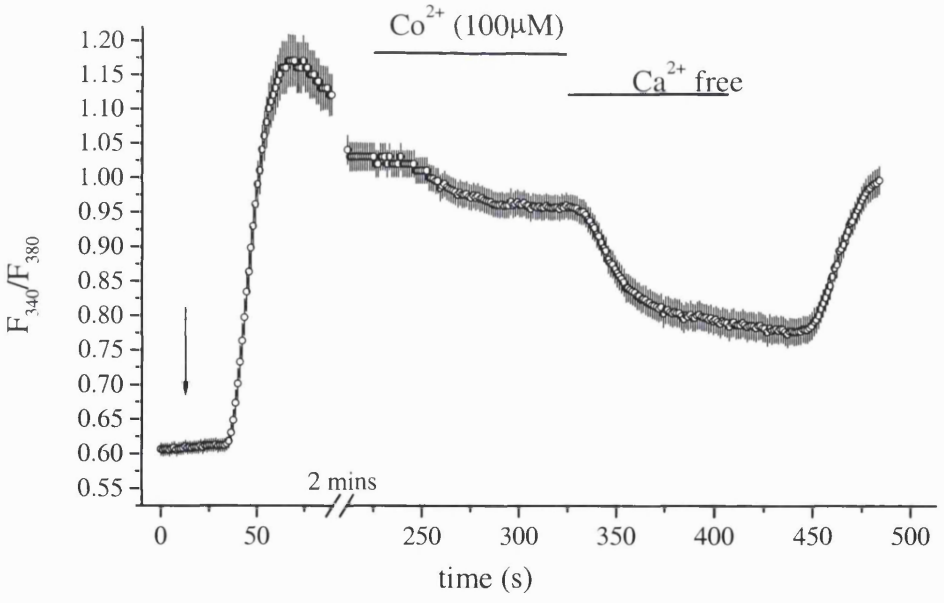

Figure 5.6d Cobalt, n = 32

Figure 5.6 a-d Sensitivity of the CCCP induced rise in $[Ca^{2+}]_i$ to various inorganic ions. Cells were incubated in CCCP (2μM) in calcium free conditions, as in figure 5.5. Calcium was re-administered to the bathing solution at the arrow, and after the plateau had stabilised various in organic ions were applied to the bathing solution. A subsequent removal of calcium from the bathing produced further reductions in $[Ca^{2+}]_i$ which was fully reversible upon calcium re-introduction.

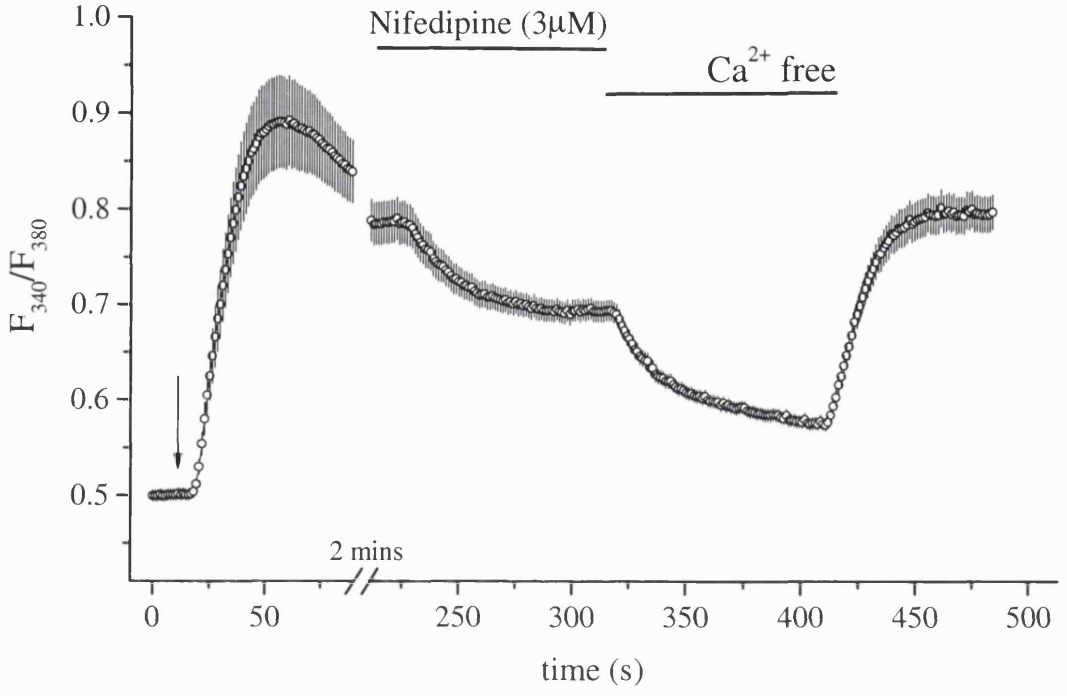

Figure 5.7 Nifedipine blocks the calcium influx initiated by CCCP.
The L-type calcium channel blocker nifedipine (3μM) diminished the size of the calcium plateau established by incubation of the cells in CCCP (2μM) in calcium free solution. Methods are the same as figures 5.5 and 5.6. n = 85

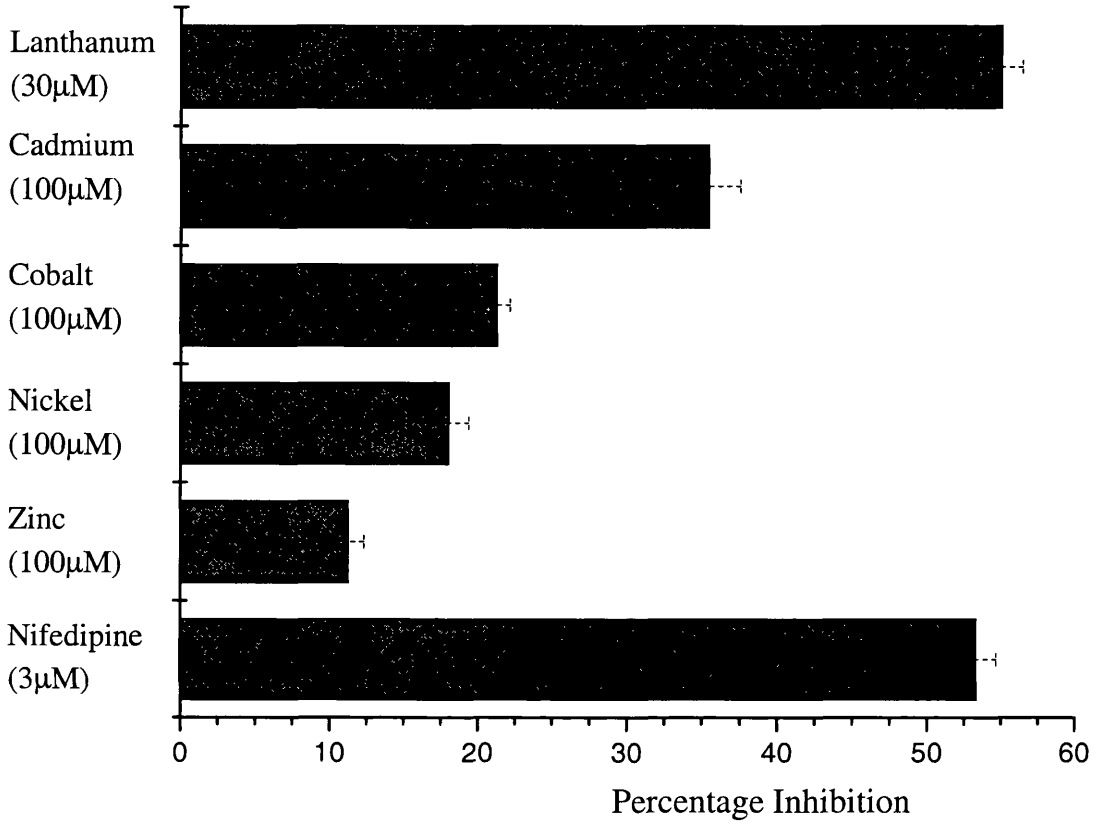

Figure 5.8. Plateau inhibition by inorganic ions and nifedipine.
Percentage inhibitions of the CCCP induced calcium plateau by La^{3+}, Cd^{2+}, Co^{2+}, Ni^{2+}, Zn^{2+} and nifedipine are shown. Values are calculated from data in figures 5.5 - 5.7.

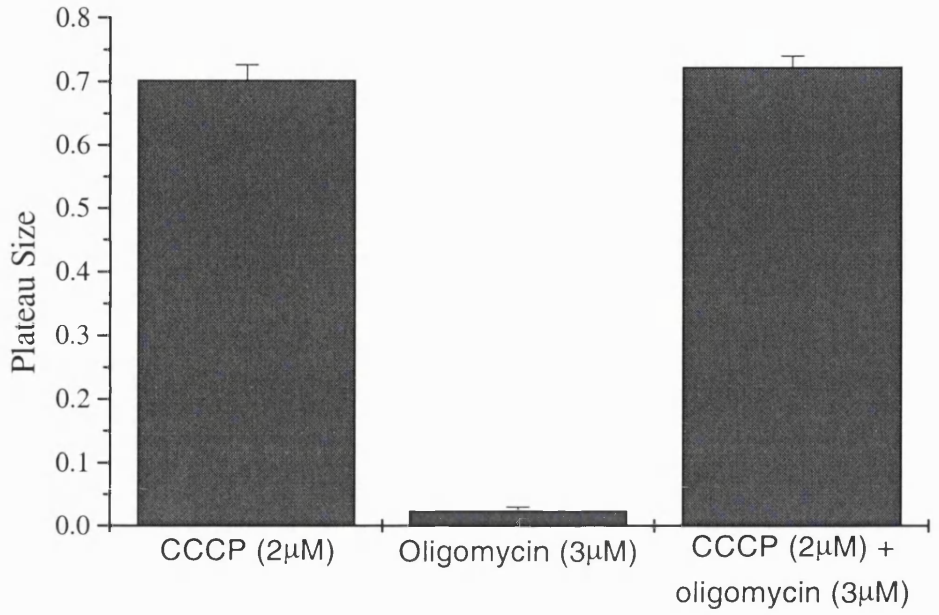

Figure 5.9. Oligomycin does not prevent the CCCP induced rise in $[Ca^{2+}]_i$.
Incubation in oligomycin (3μM), an inhibitor of the F_1F_0-ATPase, does not induce a rise in $[Ca^{2+}]_i$ but is ineffective at preventing the increase in $[Ca^{2+}]_i$ induced by CCCP (2μM).
n = 26 (CCCP 2μM); 57 (oligomycin 3μM); 47 (CCCP 2μM and oligomycin 3μM)

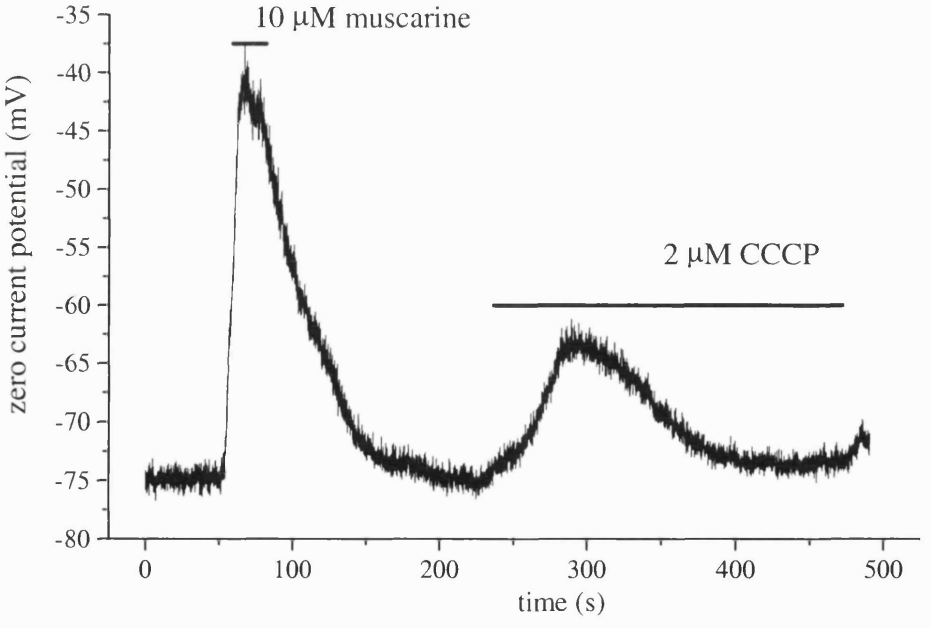

Figure 5.10. CCCP does not cause sustained depolarisation of the cell membrane.
Under current clamp recording CCCP caused only a small and transient depolarisation of the cell. Muscarine however caused a much larger depolarisation. Figure courtesy of Dr J.A. Millar.

5.4 DISCUSSION

This chapter aimed to investigate the role of the mitochondria in calcium signalling in cerebellar granule neurons. The protonophore CCCP was used to dissipate the mitochondrial membrane potential and thus prevent mitochondrial calcium uptake. However, surprisingly CCCP induced a rise in intracellular calcium that was due to an influx, from the extracellular space, though L-type calcium channels. The rise in $[Ca^{2+}]_i$ was not abolished by oligomycin which would be expected to prevent cellular ATP depletion and appeared not to be due to depolarisation of the plasma membrane.

5.4.1 CCCP induced rises in $[Ca^{2+}]_i$.

Metabolic inhibition of cerebellar granule neurons, by sodium cyanide and glucose free medium, caused a rise in intracellular calcium similar to that seen in this study (Chen *et al.*, 1999). However, attempts to characterise the source of the calcium influx in that study were inconclusive. Increased calcium concentrations were found to be unaffected by blockers of NMDA and non-NMDA receptors and nifedipine. This is clearly very different to the findings in this study where the CCCP induced rise in intracellular calcium was inhibited by the L-type calcium channel blocker, nifedipine. Furthermore, Chen *et al.* (1999) found that the metabolic inhibition induced $[Ca^{2+}]_i$ increases were highly sensitive to the inorganic ions, Ni^{2+} and Co^{2+} whereas these ions only caused a weak inhibition of calcium influx, in this study.

When CCCP (100μM) was administered during metabolic inhibition it caused a transient large increase in $[Ca^{2+}]_i$ which decayed leaving no sustained plateau, (Chen *et al.*, 1999). This suggests that CCCP was releasing a pool of calcium stored in the mitochondria during metabolic inhibition. This study does not appear to correlate well with the results presented here which clearly suggest CCCP induces a sustained calcium influx into cerebellar granule cells. The large difference between the concentrations of CCCP used in these studies (2μM here compared with 100μM by Chen *et al.*) seems unlikely to explain the mismatch of results. Chen *et al.* (1999) found that increases in intracellular calcium following metabolic inhibition can be reduced with an inhibitor of PLA_2 activity, it remains to be determined whether a similar pathway is responsible for the $[Ca^{2+}]_i$ increases seen here. Cellular ATP

depletion would appear to be the most likely cause for increased $[Ca^{2+}]_i$ as both metabolic inhibition (Chen *et al.*, 1999) and prolonged CCCP exposure (this study) increase $[Ca^{2+}]_i$. However in this study, oligomycin which would be expected to prevent cellular ATP depletion by inhibition of the F_1F_0ATPase did not prevent the CCCP induced $[Ca^{2+}]_i$ increases.

In dissociated rat hippocampal neurons application of NaCN, or FCCP increased intracellular calcium and caused membrane hyperpolarisation (Nowicky & Duchen 1998). Increases in $[Ca^{2+}]_i$ were attributed to calcium influx through voltage-gated calcium channels and did not appear to be dependent on membrane potential. Hyperpolarisation of hippocampal neurons in response to FCCP was attributed to activation of calcium activated potassium currents (Nowicky & Duchen, 1998). The results presented here correlate well with the findings of Nowicky & Duchen (1998). However in this study, a transient depolarisation was observed under current clamp in response to CCCP, whereas in hippocampal neurons FCCP caused a hyperpolarisation. In both studies $[Ca^{2+}]_i$ increases in response to mitochondrial inhibition were attributed to calcium influx through voltage-gated calcium channels, resolved by block by nifedipine (this study) and by D600 (Nowicky & Duchen 1998). Neither study has shown how opening of voltage-gated calcium channels occurs in the absence of depolarisation, or even in the presence of hyperpolarisation. A shift in the voltage activation curve might explain how the channels can open under these circumstances, a similar effect was observed in sensory neurons in response to cyanide (Duchen 1990). Opening of voltage-gated calcium channels (both L and N-type) in absence of membrane depolarisation has recently been reported (Archer *et al.*, 1999). Activation of fibroblast growth factor receptors activated calcium influx via L- and N-type calcium channels but did not cause membrane depolarisation, rather voltage-gated calcium channel opening was attributed to the generation of polyunsaturated fatty acids (Archer *et al.*, 1999). It remains possible that under these conditions nifedipine is inhibiting a calcium entry pathway that is not voltage-gated although this pathway is not store-operated because of the lack of inhibition by zinc.

A further possibility is that, in cerebellar granule neurons, dihydropryidine sensitive calcium channels are open at rest and calcium influx through these channel is rapidly absorbed by the mitochondria. This hypothesis required a close interaction

between the mitochondria and the calcium channels, similar to that previously described (Budd & Nicholls 1996a). Also as mitochondria have a finite capacity for calcium they would also have a close localisation with efflux pathways. The previous chapter suggests that $G\alpha_q$ linked agonists do not reliably evoke a rise in $[Ca^{2+}]_i$. Constantly open voltage-gated calcium channels may, therefore, provide a constant supply of calcium for the calcium dependent metabolic enzymes of the mitochondria.

The compounds used to inhibit mitochondria in this study and others can have numerous effects on cytosolic processes. Abolition of the mitochondrial membrane potential will prevent uptake of many compounds, such as NADH and ADP. Increased cytosolic concentrations of such compounds may play a role in modulating the properties of plasma membrane ion channels.

5.4.2. Effect of abolishing $\Delta\psi_m$ on the muscarine induced rise in $[Ca^{2+}]_i$.

In the presence of CCCP, muscarine did not evoke a calcium response in any of the cells tested, whereas the data from a paired experiment showed an high response rate to muscarine. It is possible that the high calcium concentrations seen in the presence of CCCP are sufficient to either mask an IP_3 mediated release of calcium from the internal stores or that IP_3 receptors themselves have undergone calcium induced desensitisation. In this regard, studies on mitochondria control of calcium signalling showed that mitochondrial calcium uptake at sites close to the IP_3 receptors on the endoplasmic reticulum facilitates IP_3 mediated calcium signalling (Jouaville *et al.*1995). It therefore remains possible that in the absence of mitochondrial calcium uptake IP_3 receptors are unable to open to release stored calcium. CCCP induced depletion cellular ATP may lead to reduced calcium uptake into the endoplasmic reticulum and hence depleted stores or calcium induced desensitisation of the receptor, G- protein or phospholipase C may be responsible for the lack of calcium response to muscarine.

5.4.3. Mitochondrial control of calcium signalling.

The unexpected rise in intracellular calcium has made direct measurements of the mitochondrial control of calcium signalling difficult. However, some of the

experiments described here do provide an insight into the role of calcium extrusion from the cell.

Removing calcium from the extracellular solution resulted in a decrease in the plateau evoked by incubation in FCCP or CCCP (figures 5.4 - 5.7). However, in all cases the calcium concentration did not fall back to its original levels observed before calcium re-administration, at most calcium levels diminished by about 60%. This may indicate that the mitochondria are critical components of calcium extrusion in cerebellar granule neurons or that ATP depletion severely impairs other extrusion mechanisms, for example the plasma membrane and endoplasmic reticulum Ca^{2+}ATPases.

Further characterisation of the role of mitochondria in calcium homeostasis in cerebellar granule neurons is required. Concurrent measurements of membrane potential and $[Ca^{2+}]_i$ would give a better indication into the whole cell effects of toxic compounds such as mitochondrial uncouplers. Future experiments must include more selective inhibitors of mitochondrial function. Studies investigating the reasons for voltage-gated calcium channel opening in response to mitochondrial uncouplers may provide an insight into properties of these channels.

Chapter 6. Results.

Properties of intracellular calcium stores in CGN.

6.1 INTRODUCTION

6.1.1. Intracellular calcium stores in CGN.

The existence of two separate calcium pools one that is sensitive to thapsigargin and IP_3 and the other being sensitive to caffeine and ryanodine has previously been suggested (e.g. adrenal chromaffin cells Robinson & Burgoyne 1991; or *xenopus* oocytes Shapira *et al.* 1990). Whereas in many cell types including muscle cells ryanodine and IP_3 release calcium from the same internal store (Kanmura *et al.*, 1988). Incubation in thapsigargin or ryanodine has been shown to reduce the size of the calcium plateau evoked by either 25mM potassium or NMDA and that their actions were partially additive, (Simpson *et al.*, 1993). This would indicate that there is a functional interaction between the thapsigargin sensitive and ryanodine sensitive stores in cerebellar granule neurons, or that two discrete stores both have thapsigargin sensitive pumping mechanisms.

Thapsigargin and caffeine, at low concentrations, inhibit acetylcholine or 1S,3R ACPD induced rises in $[Ca^{2+}]_i$, and conversely, acetylcholine and ACPD inhibit caffeine induced $[Ca^{2+}]_i$ increases, (Irving *et al.*, 1992a). Furthermore, ryanodine inhibited the rise in $[Ca^{2+}]_i$ induced by caffeine, acetylcholine and ACPD although the block of IP_3 mediated calcium release was varied. These data promote the view that the ryanodine sensitive and the IP_3 sensitive calcium stores interact in some way. However, more recently Simpson *et al.*, (1996) have shown that the SERCA inhibitor 2,5-di(*tert*-butyl)-1,4-benzohydroquinone (BHQ) is selective between the two proposed calcium pools. They propose that cerebellar granule neurons do possess two anatomically distinct calcium pools one sensitive to IP_3 the other to ryanodine. Calcium release from the IP_3 sensitive store, mediated via activation of $G\alpha_q$ linked receptors, induces a much larger calcium release from the ryanodine sensitive pool by CICR, (Simpson *et al.*, 1996).

The relative contribution of the two intracellular calcium stores to calcium signalling appears to vary with the stimulating agonist. For example, del Rio *et al.*, (1999) showed that ryanodine inhibited the calcium rise induced by 1S,3R ACPD by more than 90% whereas the responses to carbachol and histamine were only inhibited by about 60%.

The thapsigargin sensitive calcium store has also been implicated to act as a calcium 'sink' in cerebellar granule neurons. The amplitude of the rise in $[Ca^{2+}]_i$ induced by large (>30mM) concentrations of extracellular potassium was enhanced by blocking the SERCA pumps of the endoplasmic reticulum with thapsigargin (Toescu, 1998). These data suggest that the intracellular stores act to take up calcium rather than release it (as with Simpson *et al.*, 1993) in the presence of high calcium loads.

6.1.2 Store-operated calcium channels.

Exposure to agonists that couple to the generation of IP_3 and consequently cause a rise in $[Ca^{2+}]_i$ are often observed to induce a calcium influx across the plasma membrane due to store depletion, as already described. This calcium influx is often seen as a plateau following the transient rise in $[Ca^{2+}]_i$ (e.g. cortical neurons, Prothero *et al.*, 1998). A similar but very small plateau was observed following carbachol stimulation (Simpson *et al.*, 1995) but not by Irving *et al.*, (1992a).

6.2 Aims

Despite the presence of muscarinic receptors on all cells tested electrophysiologically, muscarine induces a rise in intracellular calcium in only a small proportion of cells. Similarly, glutaminergic and histaminergic receptor stimulation does not consistently induce a rise in intracellular calcium, see chapter 4. Investigations into the role of mitochondria in buffering calcium release was complicated by an influx of calcium through voltage-gated calcium channels. This chapter aims to investigate the properties of the intracellular calcium stores in cerebellar granule neurons, and in particular, to investigate whether the lack of effect of muscarine is due to depleted intracellular calcium stores, as has been previously suggested (in cerebellar granule neurons, Irving *et al.*, 1992a; and hippocampal neurons Irving & Collingridge 1998).

6.3 RESULTS

6.3.1 Calcium source in the muscarinic response.

Muscarinic induced increases in $[Ca^{2+}]_i$ are assumed to be due to IP_3 induced release of calcium from intracellular stores, following $G\alpha_q$ mediated activation of PLC. Figures 6.1 and 6.2 attempt to confirm the source of the calcium observed in the muscarinic calcium response.

Figure 6.1 shows the effect of a PLC inhibitor, U 73122 (10μM), on muscarine induced increased in $[Ca^{2+}]_i$. Cells were incubated in 10μM U 73122 or vehicle (DMSO) for at least 4 minutes prior to recording. The cells were first stimulated with 25mM potassium to provoke a larger calcium response to muscarine (figure 4.3). Incubation in U 73122 caused a small, but statistically insignificant (*t* test), increase in the resting F_{340}/F_{380} ratio, from 0.36 ± 0.04 in control to 0.43 ± 0.05 in U 73122. Following washout of 25mM potassium muscarine (1μM) applied to evoke a rise in the F_{340}/F_{380} ratio. In vehicle treated cells, muscarine induced an increase in the F_{340}/F_{380} ratio from 0.45 ± 0.05 to a peak of 0.74 ± 0.09, data represents all cells examined. In this group 85% (17 out of 20) of cerebellar granule neurons responded with an increase in the F_{340}/F_{380} ratio. In cells treated with U 73122 (10μM), muscarine (1μM) did not evoke a change in the mean $F_{340}/F380$ ratio from a ratio of 0.53 ± 0.06. However, 1 cell from 20 examined (5%) did respond with an increase in the F_{340}/F_{380} ratio. The two treatment groups described here are shown on separate axes in figure 6.1 for clarity.

The rise in calcium observed during muscarinic stimulation appears to be dependent upon PLC stimulation. Figure 6.2 investigates whether extracellular calcium is required for muscarine induced increases in $[Ca^{2+}]_i$. Here cerebellar granule neurons were stimulated with muscarine after calcium had been removed from the bathing solution. The size of the peak response (F_{340}/F_{380} ratio) to muscarine was plotted against the time in calcium free conditions. Data presented here represents all cells examined and is not paired within the same cells but is within the same cultures. The magnitude of the response to muscarine can be seen to diminish with increasing time in calcium free conditions. In control conditions the mean magnitude of the peak response to muscarine was found to be 0.40 ± 0.08 whereas after 3 minutes in

calcium free conditions peak responses were significantly ($0.02<p<0.05$) diminished to 0.19 ± 0.04. For n numbers see figure 6.2.

6.3.2. Store-operated calcium entry.

The amount of stored calcium and the properties of store-operated calcium entry were investigated using the SERCA inhibitor thapsigargin. Cells were incubated in calcium free conditions with thapsigargin (1μM) at 37°C prior to recording. Calcium was re-introduced into the bathing solution and a plateau allowed to stabilise. Figure 6.3 shows the thapsigargin induced increase in the F_{340}/F_{380} ratio in both cerebellar granule neurons and glia. As can be seen cerebellar granule neurons respond to the re-introduction of calcium with a small but sustained increase in the F_{340}/F_{380} ratio, from 0.50 ± 0.01 to a plateau level of 0.60 ± 0.01, (n = 35). Whereas glial cells in the same fields showed a much larger increase in the F_{340}/F_{380} ratio from 0.54 ± 0.06 to 0.94 ± 0.09, (n = 5). In both cerebellar granule neurons and glia the plateau was diminished by subsequent removal of calcium from the extracellular solution.

The thapsigargin induced calcium plateau in cerebellar granule neurons and glia was found to be sensitive to lanthanum in the extracellular solution, figure 6.4. Cells were incubated in thapsigargin (1μM) in calcium free conditions as before. Once the calcium plateau had stabilised, lanthanum (30μM) was added to the extracellular solution. As can been seen lanthanum caused a decrease in the F_{340}/F_{380} ratio in cerebellar granule neurons from 0.64 ± 0.02 to 0.59 ± 0.02, (n = 35). In the continued presence of lanthanum the F_{340}/F_{380} ratio could be seen to increase gradually. In glia cells the plateau size was much larger than the cerebellar granule neurons, as previously seen, 0.86 ± 0.02. Lanthanum (30μM) diminished the magnitude of this plateau to an F_{340}/F_{380} of 0.72 ± 0.02, (n = 16).

The ability of zinc to inhibit the size of the plateau was also investigated. Cells were incubated in calcium free external solution and thapsigargin as before. Once a calcium plateau had established zinc (30μM) was applied to the bathing solution, figure 6.5. In glia cells zinc caused an inhibition of the plateau from an F_{340}/F_{380} of 0.85 ± 0.08 to 0.65 ± 0.05, (n = 18). In the continued presence of zinc the F_{340}/F_{380} can be seen to gradually increase similar to that previously seen in granule neurons. Cerebellar granule neurons responded to zinc in a much more varied fashion. In a

large proportion of cerebellar granule neurons, zinc caused an almost instantaneous increase in the F_{340}/F_{380} ratio, this could be due to zinc interacting with the calcium binding domain on fura-2 (see discussion). In the example shown in figure 6.5b zinc caused an inhibition of the thapsigargin induced plateau.

Direct comparison between the inhibition of the thapsigargin induced plateau in cerebellar granule neurons is difficult due to unpaired experiments, the variability of the zinc data and the very small size of the response being measured.

6.3.3. Properties of intracellular calcium stores.

A prior depolarisation with potassium has been shown to increase the proportion of cells responding and the magnitude of the calcium response to stimulation number of $G\alpha_q$ coupled receptors, (this study and Masgrau *et al.*, 2000; del Rio *et al.*, 1999; Irving *et al.*, 1992a). The depolarisation with potassium has both been suggested to charge or fill the intracellular stores with calcium (Irving *et al.*, 1992a) and prime the receptor, G-protein, PLC complex (del Rio *et al.*, 1996; 1999).

The ability of potassium induced depolarisations to bring about filling of the intracellular stores was investigated using ionomycin in calcium free conditions as a measure of total stored calcium. Ionomycin will make lipid membranes become permeable to calcium, and will therefore release calcium from all intracellular storage compartments. As calcium leaves intracellular compartments it will pass through the cytoplasm and hence will be detected as a change in fluorescence of the fura-2. Figure 6.6 shows the calcium response to ionomycin in cerebellar granule neurons either with or without a prior exposure to potassium. Cells were either exposed to 25mM potassium or control solution. Calcium was removed from the bathing solution upon washout of the high potassium, after which ionomycin (1μM) was perfusion applied and the magnitude of the resultant transient peak calculated. In control treated cells ionomycin induced a transient rise in the F_{340}/F_{380} ratio from 0.49 ± 0.02 to 0.68 ± 0.04 ($n = 51$). However, in cells pre-treated with potassium the transient peak was larger, a change in the F_{340}/F_{380} ratio from 0.64 ± 0.02 to 0.97 ± 0.04 ($n = 92$). Direct comparison of the absolute size of the peak is complicated by the different baselines (due to incomplete removal of calcium following exposure to potassium), however, statistical analysis of the size of the peaks shows that following exposure to potassium the ionomycin induced transient rise in the

F_{340}/F_{380} is significantly larger, ($p < 0.01$). Figure 6.6a shows the whole recording including the rise in $[Ca^{2+}]_i$ following application of high potassium. For clarity figure 6.6b shows an enlarged area of 6.6a boarded by the dotted line.

To investigate the relative sizes of the ionomycin releasable and thapsigargin sensitive store the two compounds were used together. Cells were incubated either in control conditions or in thapsigargin (1μM), prior to recording. Ionomycin (5μM) was applied to the cells and the magnitude of the transient peak analysed. Incubation of cerebellar granule neurons in thapsigargin had no effect on the size of the peak induced by ionomycin in calcium free conditions (peak F_{340}/F_{380} ratio 1.37 ± 0.05 (n = 50) in thapsigargin treated and 1.40 ± 0.05 (n = 46) in control). However, glia cells in the same field showed marked differences between the two treatment groups. In control conditions the peak F_{340}/F_{380} was much larger than in cerebellar granule neurons, 3.60 ±1.36 (n = 5), whereas incubation in thapsigargin greatly reduced the size of the peak to 1.37 ± 0.18 (n = 8).

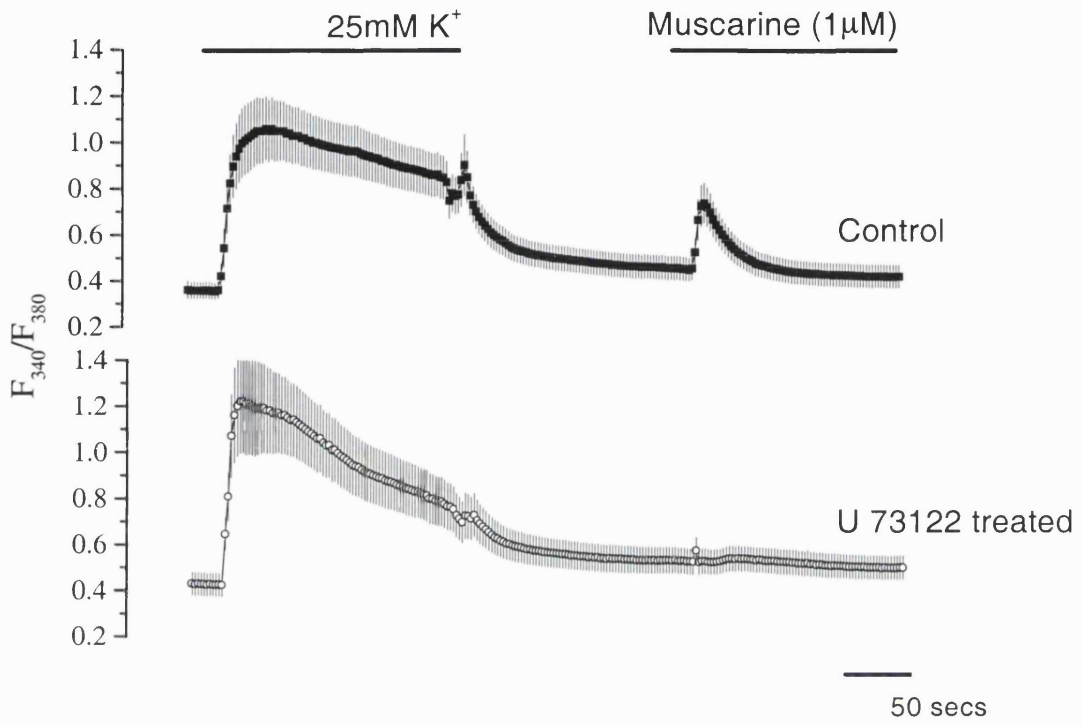

Figure 6.1. Muscarine induced rises in $[Ca^{2+}]_i$ are U 73122 sensitive.
Cells were incubated in either U 73122 (10μM) or vehicle (DMSO) for at least 4 minutes prior to the start of the experiment. U 73122 had no significant effect on the resting F_{340}/F_{380}, but did prevent the muscarine induced increase in F_{340}/F_{380}. Muscarine (1μM) induced a rise in F_{340}/F_{380} in 85% of cells tested (17 out of 20), only 1 cell (from 20, 5%) responded to muscarine in the presence of U 73122. Data shown includes all cells examined, mean ± s.e.mean.

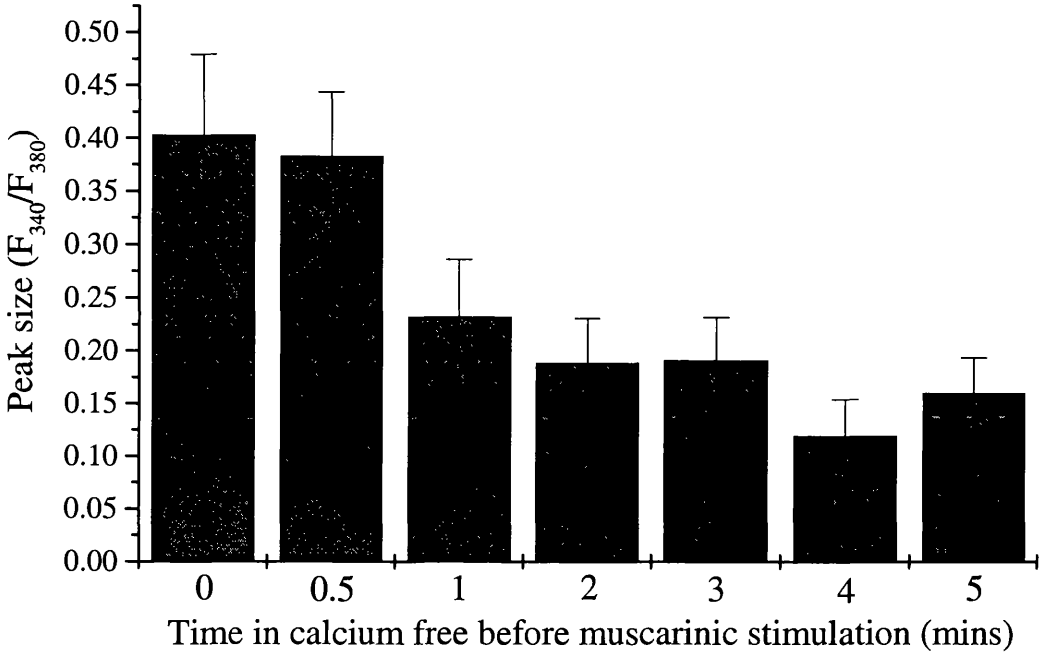

Figure 6.2 Exposure to calcium free conditions diminishes the calcium response to muscarine.

Cells were exposed to calcium free conditions for times indicated. Mean amplitude of the calcium response to muscarine (1μM) is shown. Data includes all cells tested. n = 45 (0 mins), 55 (0.5 mins), 29 (1 min), 36 (2 mins), 29 (3mins), 37 (4mins), 33 (5 mins).

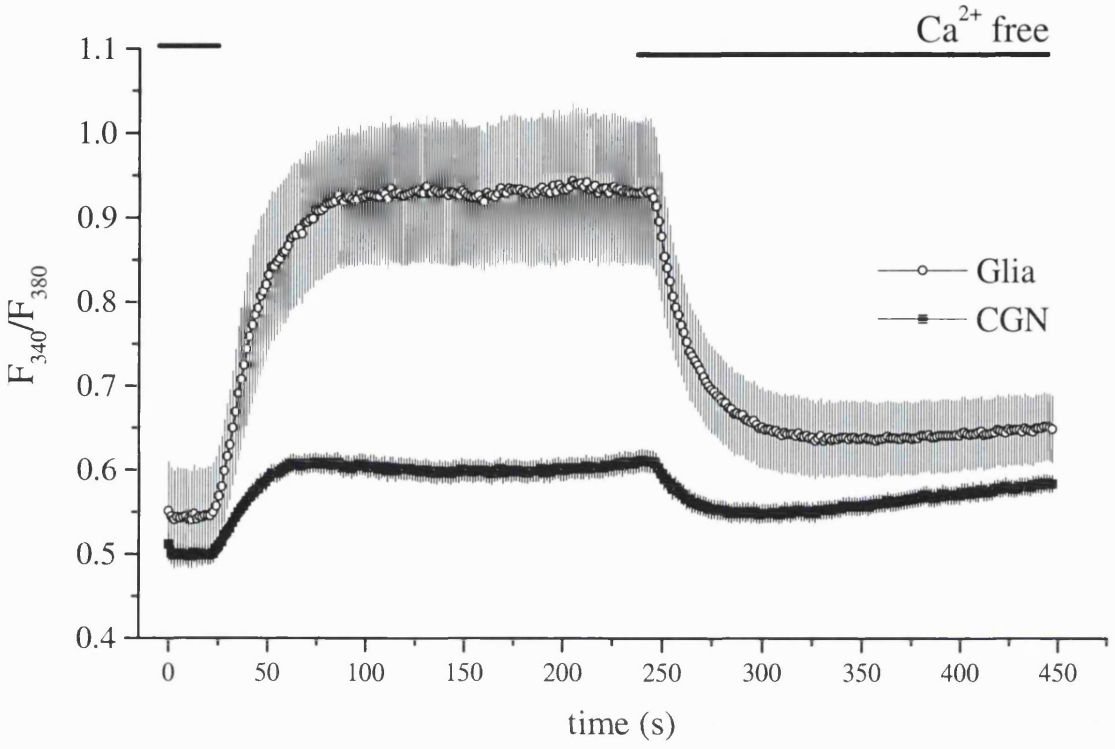

Figure 6.3. Thapsigargin induced rises in $[Ca^{2+}]_i$ in CGN and glia.
Cells were incubated in thapsigargin (1μM) for >10 mins in calcium free conditions. Calcium was re-introduced to the bathing solution. Re-administration of calcium induced a large increase in the F_{340}/F_{380} ratio in glia (n = 5) but a much smaller increase in CGN (n = 35).

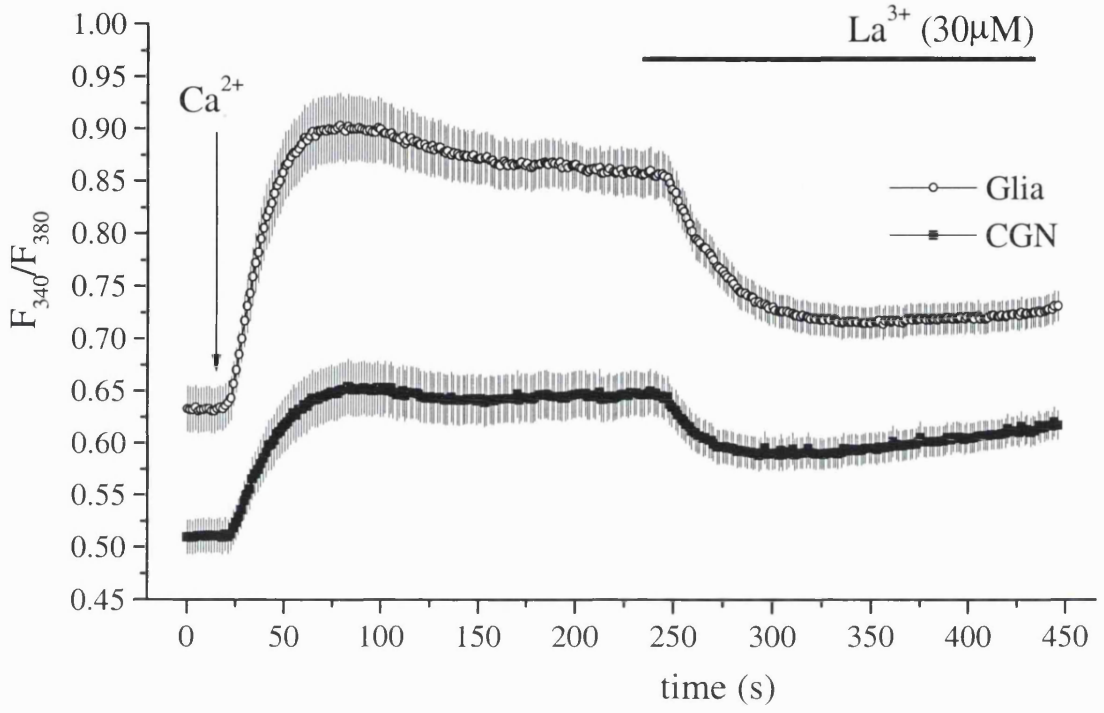

Figure 6.4. Thapsigargin induced rises in $[Ca^{2+}]_i$ are sensitive to lanthanum (30μM) . Cells were incubated in thapsigargin (1μM) in calcium free condition as before. Calcium was re-administered to the bathing solution at the arrow $[Ca^{2+}]_i$ increase as previously seen. Lanthanum (30μM) added to the bathing solution inhibited the plateau in both glia (n = 16) and CGN (n = 35).

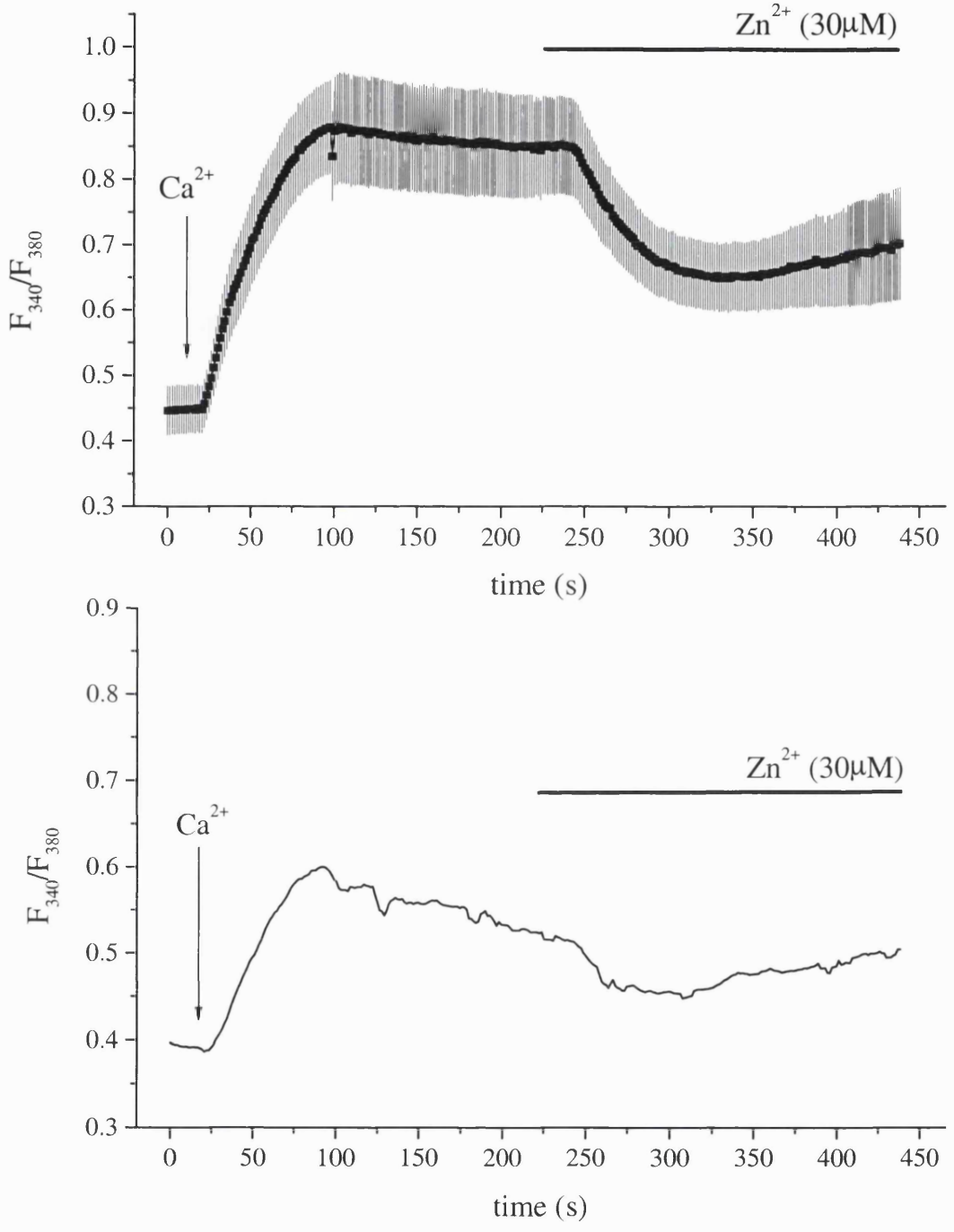

Figure 6.5. Zinc inhibits the thapsigargin induced plateau in glia and CGN.
a). Cells were incubated in thapsigargin (1μM) in calcium free conditions as before. Calcium was re-administered to the bathing solution at the arrow. Once a calcium plateau had established zinc (30μM) was added to the extracellular solution. Zinc caused a decrease in plateau size in glia (n = 18). b) Zinc also reduced plateau size in CGN (one cell shown) but the response was much more varied, see text.

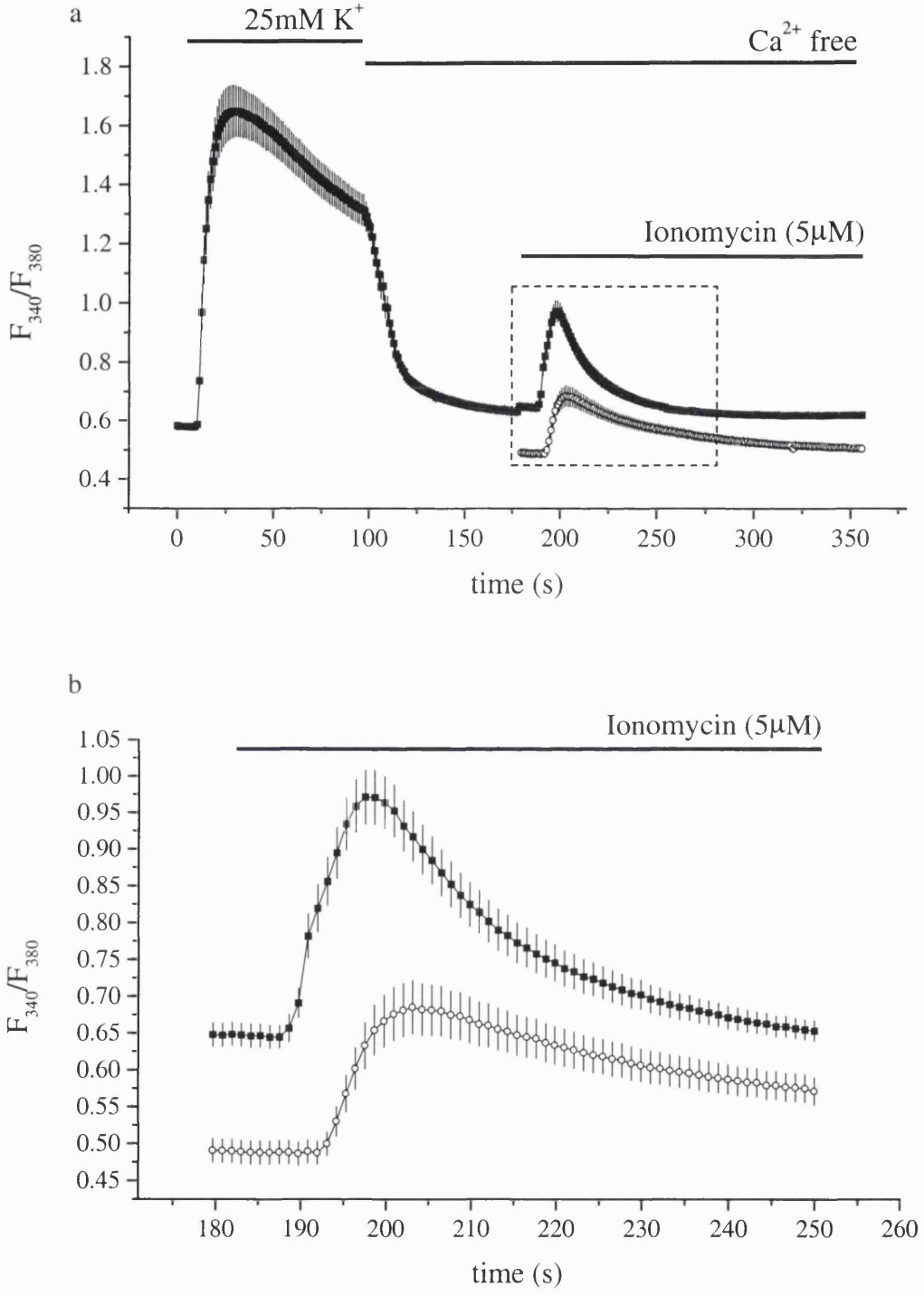

Figure 6.6. Potassium stimulation attenuates the calcium response to ionomycin.
Cells were exposed to ionomycin (5µM) in calcium free external solution either with or without a prior depolarisation with 25mM potassium. The response to the ionomycin was larger following potassium treatment ($p < 0.01$, $n = 92$) than control treated cells, ($n = 51$). Panel b represents an enlarged section of panel a indicated by the dotted rectangle.

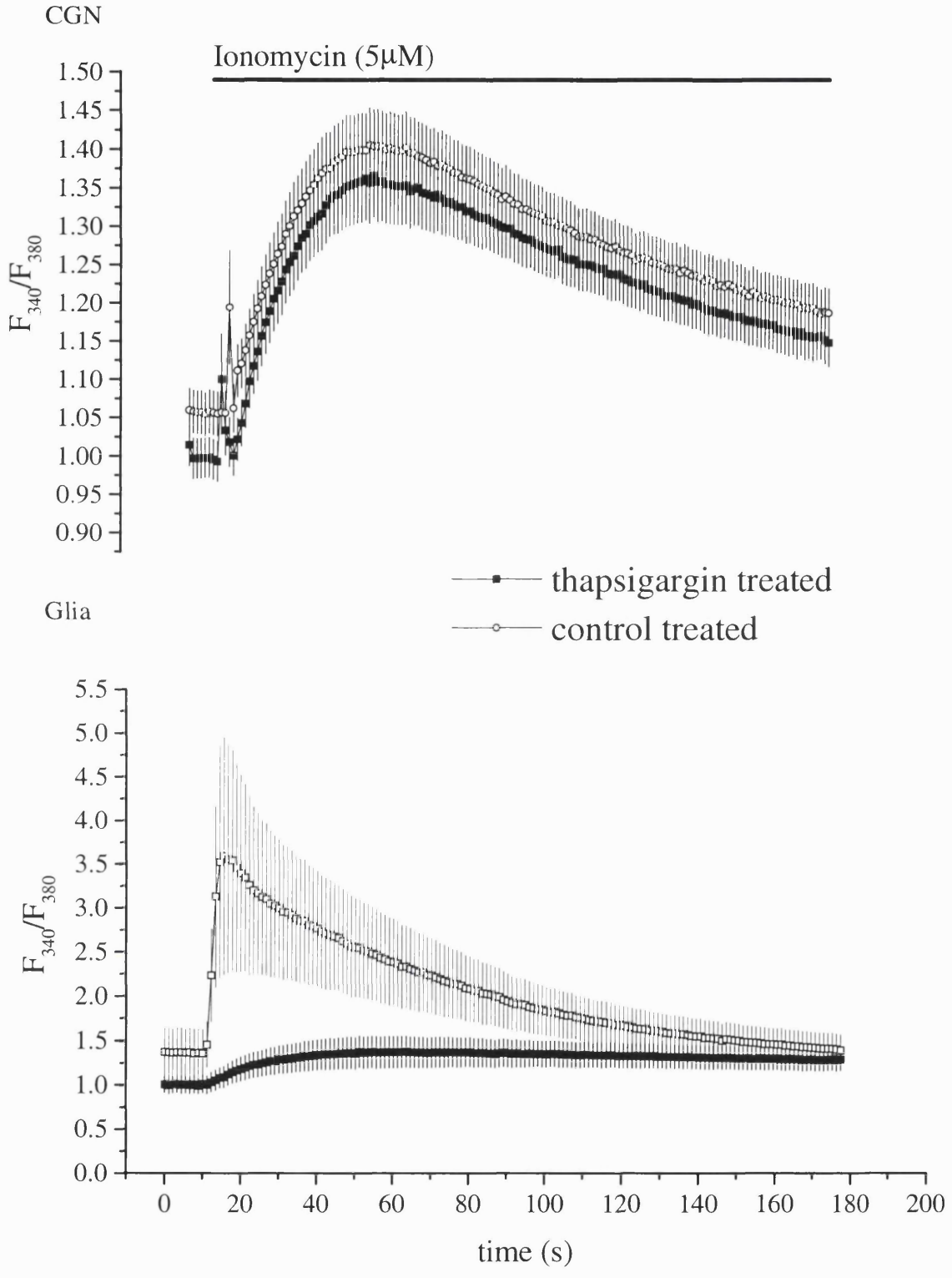

Figure 6.7. Thapsigargin diminishes the ionomycin releasable calcium pool in glia but not in CGN.

Cells were incubated in either thapsigargin (1μM) or control. Ionomycin (5μM) was added to the extracellular solution and the magnitude of the resultant peak analysed. Thapsigargin treatment did not diminish the calcium amount of calcium released by ionomycin in CGN (n =, 50 thapsigargin treated; 46 control) but did in glia (n =, 8 thapsigargin treated; 5 control).

6.4 DISCUSSION

It has previously been shown that muscarine is unable to evoke a calcium response in a large proportion of cerebellar granule neurons examined and that the size of the response and the proportion of responding cells is increased by prior exposure to 25mM potassium. The results presented here suggested that exposure to 25mM potassium does result in 'charging' of the intracellular stores. In addition, these results suggest that there is not a significant thapsigargin releasable calcium store in cerebellar granule neurons whereas there is a substantial one in cerebellar glial cells.

6.4.1. Calcium source in the muscarinic response

U 73122 has been used in cerebellar granule neurons as a specific inhibitor of PLC, (e.g. Netzeband *et al.*, 1999). In this study PLC inhibition prevented muscarine induced rises in $[Ca^{2+}]_i$. This suggests that, as expected, muscarine induces a rise in $[Ca^{2+}]_i$ via activation of PLC and generation of IP_3. U 73122 has been shown to reduce, but not inhibit, the muscarine induced inhibition of IK_{SO}, (Boyd *et al.*, 2000). This suggests that muscarine induced rises in intracellular calcium are not responsible for muscarinic inhibition of IK_{SO}, (see also chapter 7). However, there are reports suggesting that U 73122 is not specific for PLC. For example, Alter *et al.*, (1994) showed that U 73122 and its inactive (at PLC) analogue, U-73343, were able to inhibit the release of insulin from insulin secreting cells of the islets of Langerhans. It therefore remains a possibility that U 73122 is acting a site distinct of PLC to prevent muscarine induced increases in $[Ca^{2+}]_i$. Further studies which include the use of the IP_3 receptor antagonist, xestospongin C, may be useful to further this set of experiments.

Calcium removal from the extracellular solution did not completely inhibit the calcium response to muscarine. After 30 seconds in calcium free conditions the response to muscarine is not significantly different from the response in control conditions. This would suggest that extracellular calcium is not required for muscarine induced calcium responses. As all solutions are bath applied it remains a possibility that there is residual calcium in the bathing solution. However, total exchange of the bath solution is estimated to occur within 40 seconds and the calcium free solution contains the calcium buffer EGTA (1mM). It therefore seems likely that the calcium response to muscarine is due entirely to release of calcium

from intracellular stores. Longer exposure to calcium free conditions reduces further the average magnitude of the calcium response to muscarine. This could be due to a number of factors. Firstly, exposure to calcium free conditions reduces free calcium concentration in the cytoplasm. This reduced calcium concentration may fall below that required to activate IP_3 receptors even in the presence of IP_3 (Bezprozvanny *et al.*, 1991). Secondly, reduced cytosolic calcium may lead to reduced calcium in the stores if intracellular stores are sufficiently 'leaky'. Depleted calcium stores at rest in cerebellar granule neurons have been implicated in the lack of response to $G\alpha_q$ stimulating agonists, and further depletion would lead to greatly diminished responses to muscarine in this system. Finally, reduction in cytoplasmic calcium concentration following prolonged exposure to calcium free conditions may have a negative effect on the activity of the receptor- G-protein - PLC complex. In this respect del Rio *et al.*, (1994) suggested that mild depolarisation could cause potentiation of PLC activation. This effect was found to be dependent on extracellular calcium and therefore could indicate a calcium sensitive component leading to PLC activation. Diminished $[Ca^{2+}]_i$ due to prolonged exposure to calcium free extracellular solutions may therefore lead to reduced PLC activation.

6.4.2. Store-operated calcium entry.

Store-operated calcium entry provides an important pathway for calcium influx into many cells, (e.g. platelets Sage 1997). In neurons store-operated calcium entry has been reported to provide a significant influx pathway for calcium (e.g. Prothero *et al.*, 1998). In this study thapsigargin evoked only small increases in the $[Ca^{2+}]_i$ of cerebellar granule neurons whereas in glia cells in the same field large increases in $[Ca^{2+}]_i$ were apparent. This agrees well with earlier experiments that shows that prolonged exposure to muscarine did not result in the classical 'peak and plateau' calcium response seen in other cell types. The ionic sensitivity of the thapsigargin induced calcium entry into cerebellar granule and glial cells was investigated using lanthanum and zinc, two known inhibitors of store-operated calcium entry. Lanthanum, caused inhibition of the thapsigargin induced calcium entry in both cell types. In cerebellar granule neurons the F_{340}/F_{380} ratio could be observed to increase gradually in the continued presence of lanthanum, this is thought to be due to photobleaching of fura-2. Application of zinc to the extracellular solution caused a

large decrease in the calcium influx in glia cells. This agrees well with previous studies where zinc has been shown to be a potent blocker of store-operated calcium influx (Prothero *et al* 1998; Hoth & Penner 1992). However, in cerebellar granule neurons the results were less obvious. In many cells the F_{340}/F_{380} was seen to increase immediately upon application of zinc. This may represent an interaction with zinc and fura-2. Previous studies have shown that fura-2 can be used as a fluorophore for zinc, (e.g. Dehaye 1995). Interactions between fura-2 and zinc may mask small changes in calcium concentration in the cytoplasm. The effect may be more pronounced in the cerebellar granule neurons due to an increased uptake of zinc compared to glial cells. The variability of the results observed here may have been due to some cerebellar granule neurons allowing the influx of zinc whilst others did not. This may represent a sub-population of neurons. Measuring the relative inhibition by zinc and lanthanum of store operated calcium entry, in this system, is made difficult if not impossible by the possibility of zinc interacting with fura-2. However comparisons of a selection of cells treated with zinc and those treated with lanthanum suggest that there is little difference between inhibition of the influx by these two ions. In other cell types examined zinc always inhibits store-operated calcium channels much more than lanthanum. Functional coupling of L-type calcium channels and ryanodine receptors has been demonstrated in cerebellar granule neurons (Chavis *et al.*, 1996). The similar potency of inhibition of these two ions might suggest that store-operated calcium entry, in cerebellar granule neurons, could be mediated by more than one pathway (both store-operated channels and L-type calcium channels), although much more work is required to investigate whether this is the case and whether this relatively small influx is a functionally important component in cerebellar granule cell calcium homeostasis and signalling.

6.4.3. Intracellular calcium stores.

Cerebellar granule neurons may have leaky or empty endoplasmic reticulum calcium stores. Depleted intracellular stores may underlie the lack of response to $G\alpha_q$ stimulating compounds. Furthermore, if cerebellar granule neurons have depleted calcium stores at rest then they may serve to function as a temporary store in times of high $[Ca^{2+}]_i$ as suggested by Toescu (1998). This might suggest that cerebellar granule neurons have a constant requirement for store-operated calcium entry.

However, thapsigargin induced calcium entry is very small (compared to glia). The lack of store-operated calcium entry could be due to either a lack of channels in the plasma membrane or a desensitisation of the pathways linking store depletion to calcium entry. Either mechanism would maintain a constant depleted state of the stores, possibly changing their role as a calcium source to a calcium sink.
Figure 6.6 shows that prior depolarisation with 25mM potassium does serve to 'charge' the calcium stores as suggested by Irving *et al.* (1992a) and therefore they may act as a calcium 'sink' (Toescu 1998). This has also been demonstrated recently by Masgrau *et al.*, (2000) who showed an increase in the amount of calcium released by ionomycin following depolarisation with either 10 or 40 mM potassium. In addition, incubation in calcium free conditions, thapsigargin or caffeine reduced the ionomycin releasable pool in cerebellar granule neurons (Masgrau *et al.*, 2000).

The augmented responses to muscarine and other $G\alpha_q$ stimulating agonists, seen here and in other studies, which follow mild depolarisations may be due to a filling of the intracellular store and therefore an increase in the amount of releasable calcium. In support of this, thapsigargin was unable to diminish the amount of calcium released by ionomycin in cerebellar granule neurons, but could in glial cells where the control response was much larger. Thapsigargin has been suggested to be selective for IP_3 sensitive stores, therefore the lack of effect of ionomycin in this experiment may suggest that the IP_3 sensitive stores are depleted which would lead to a lack of effect by $G\alpha_q$ stimulating agonists. However, it has also been suggested that a large proportion of the increase in $[Ca^{2+}]_i$ to carbachol is due to release from caffeine sensitive store (Simpson *et al.*, 1996). If this is indeed the case then IP_3 sensitive stores would only have to release small amounts of calcium to induced CICR in the caffeine sensitive stores. Indeed, if the release sites of the two stores are closely opposed then IP_3 induced calcium release could be so small it would be undetected by monitoring global calcium concentrations. If this was the case the two calcium stores, could therefore act both to release calcium in response to agonist stimulation and take up calcium during high calcium loads (as suggested by Toescu 1998).

This study suggests that the lack of effect of agonists such as muscarine, histamine and 1S,3R ACPD on cerebellar granule neurons is due to depleted thapsigargin sensitive calcium stores. Similar observations have been made in hippocampal neurons (Irving & Collingridge 1998). However, it has been suggested that the stores signal their filling state, in an unknown way, to the receptor - G-protein - PLC complex. del Rio *et al.*, (1994) showed that mild depolarisation (10mM potassium) increased IP_3 accumulation following carbachol stimulation. Increased IP_3 accumulation was dependent upon extracellular calcium and sensitive to the L-type calcium channel blocker nifedipine. However, IP_3 accumulation was not augmented as much when calcium was artificially increased with the ionophore ionomycin. It was concluded that depolarisation and calcium entry via L-type calcium channels was necessary to potentiate IP_3 production by carbachol (del Rio *et al.*, 1994). However, more recently it has been suggested that the intracellular stores are able to regulate the activity of PLC. Measuring both IP_3 accumulation and intracellular calcium concentration, Masgrau *et al.*, (2000) showed that factors that deplete intracellular calcium stores, such as thapsigargin, caffeine, high external potassium and calcium free extracellular solution all modulate PLC activity. The mechanisms underlying such communication between the intracellular stores and membrane bound proteins is unknown. Similar proposed interactions between sarco-endoplasmic reticulum bound proteins and channels on the plasma membrane in store-operated calcium entry activation have proved very difficult to resolve.

Chapter 7. Results.

Regulation of IK_{SO} by intracellular messengers

7.1 INTRODUCTION

Ion channels in the plasma membrane that are open to modification allow the cell to rapidly change resting membrane potential and hence cell excitability or the shape, duration and frequency of action potentials.

IK_{SO} is inhibited by activation of the $G_{q/11}$ coupled receptors, (e.g. M_3 receptors Boyd *et al.* 2000, and histamine, chapter 3). Under whole cell recording IK_{SO} exhibits a rapid run-down in current amplitude. This might suggest that IK_{SO} is closely regulated by diffusible intracellular messengers. However, intracellular pathways responsible for maintaining the open state of IK_{SO} and those mediating channel inhibition following exposure to muscarine have not been determined.
Activation of $G_{q/11}$ linked receptors leads to activation of PLC and phosphoinositide turnover, see chapter 1.8. The downstream effects of PLC stimulation are multiple as calcium is a ubiquitous signalling molecule and PKC, which is activated by DAG, has well over 100 known substrates (Liu, 1996).

7.1.1 Modulation of potassium channels by intracellular calcium.

$I_{K(M)}$ is a voltage dependent outward potassium current which is believe to dampen cell excitability by keeping the resting membrane potential close to E_K, (Brown 1988). It is inhibited by activation of the $G_{q/11}$ coupled muscarinic M_1 and bradykinin B_2 receptors. $I_{K(M)}$ has been shown to be potentiated by low and inhibited by high calcium concentrations (Yu, 1994). In excised inside-out patches from rat SCG neurons Selyanko & Brown (1996) showed that in 28/44 patches, calcium was able to inhibit $I_{K(M)}$ with an IC_{50} of 100nM. However, inhibition by calcium was not sustained unlike muscarinic or bradykinin induced block.
In whole cell recordings of rat SCG neurons, bradykinin induced inhibition of $I_{K(M)}$ was found to be sensitive to U 73122 and buffering of intracellular calcium (Cruzblanca *et al.* 1998). But in NG108-15 cells U 73122 did not diminish $I_{K(M)}$ inhibition by bradykinin but did block the channel *per se* (Hildebrandt *et al.* 1997).
It would appear that inhibition of $I_{K(M)}$ by bradykinin is due to an increase in intracellular calcium but maintained inhibition may be mediated by another process.
Muscarinic inhibition of $I_{K(M)}$ in SCG neurons is likely to be via an alternative pathway. It is unaffected by U 73122 and heparin (Cruzblanca *et al.* 1998).

Furthermore muscarine has been shown to be unable to induce a rise in intracellular calcium in these neurons (Marsh *et al.* 1995).

7.1.2 Modulation of potassium channels via calmodulin.

Although it appears that calcium can modulate the activity of ion channels directly it can also act indirectly. Early studies suggested that inhibitors of calmodulin had no effect on the calcium sensitivity of SK_{Ca} channels (e.g. Xia *et al.* 1998 showed that calmodulin is bound to the α subunit SK_{Ca} channels even at rest). Small rises in intracellular calcium known to activate SK_{Ca} could therefore be mediated via calmodulin. Similar results have been observed with an intermediate conductance calcium activated potassium channel (K_{Ca}), where calmodulin was found to be tightly bound to the channel protein and dominant negative mutants of calmodulin reduced current amplitude (Fanger *et al.* 1999). The tight coupling between channel and calmodulin is thought to explain why inhibitors of calmodulin are ineffective at inhibiting these calcium sensitive channels, (Levitan 1999).

7.1.3 Modulation of potassium channels by phosphorylation.

Activation of protein kinase cascades, downstream of G-protein coupled or tyrosine kinase receptor activation, provides a mechanism for amplification and diversification of a response to the extracellular signal.

The T lymphocyte type *n* (Kv1.3) potassium channel has been implicated in events such as increases in the rate of cell proliferation and DNA protein synthesis. This channel has been shown to be phosphorlyated by PKA and PKC on serine residues (Cai & Douglass 1993). Chung & Schlichter (1997) showed that activation of Kv1.3 changed by +8mV and inactivation by +17mV when phosphorylation by PKC was facilitated by adding ATP. Conversely inhibiting PKC by causing depletion of ATP reduced conductance by 41%. Channel phosphorylation therefore, appeared to upregulate the channel and was proposed by the authors to maintain negative membrane potential, thereby increasing the driving force for calcium influx, through store-operated calcium channels, which is required for cell proliferation (Chung & Schlichter, 1997).

Oocytes expressing cloned human Kv3.4, display voltage dependent rapidly inactivating outward potassium currents, similar to A-currents, (Covarrubias *et al.* 1994). Phosphorylation of this channel by PKC alters the inactivation characteristics such that the current resembles the delayed rectifier, having no inactivation. Phosphorylation of this channel occurs at two serine residues within the inactivation gate at the N-terminus, (Covarrubias *et al.* 1994). Slowed inactivation of the current may serve to shorten action potential spikes.

7.2 Aims

This chapter aims to determine whether rises in intracellular calcium are able to inhibit IK_{SO}. Previous chapters have reported that muscarine is not capable of producing a rise in $[Ca^{2+}]_i$ in every cell but is does inhibit IK_{SO} in every cell examined, also histamine was unable to induce a rise in $[Ca^{2+}]_i$ but in some cells did inhibit IK_{SO}. It would, therefore, appear unlikely that muscarinic inhibition of IK_{SO} is mediated via a rise in intracellular calcium but there remains a possibility that it may be accounted for by small localised increases in $[Ca^{2+}]_i$.

Recently there have been several reports that activation of the M_3 receptor can lead to stimulation of the mitogen activated protein (MAP) kinase signalling cascade, (Kim *et al.* 1999; Rosenblum *et al.* 2000; Slack *et al.* 2000). Using inhibitors of MAP kinase kinase (MEK), this chapter will examine whether this signalling pathway is responsible for muscarinic inhibition of IK_{SO}. The effects of protein kinase C on IK_{SO} will also be examined using the phorbol ester PMA.

7.3 RESULTS

7.3.1 Calcium sensitivity of IK_{SO}

Muscarinic receptor activation causes an inhibition of IK_{SO} in all cells examined, (see chapter 3) but caused a rise in intracellular calcium in a fraction of those studies (chapter 4). So it appeared unlikely that a rise in intracellular calcium was responsible for inhibition of IK_{SO}. However if TASK-1 channels are located close to calcium release sites on the membrane of the endoplasmic reticulum there may have been small local rises in calcium that were sufficient to inhibit IK_{SO} but remained undetected when studying whole cell fluorescence. To test the calcium sensitivity of IK_{SO} the calcium ionophore ionomycin was used. Ionomycin has previously been shown to cause large increases in intracellular calcium when calcium is present in the bathing solution. In this study ionomycin (1μM) caused a fully reversible inhibition in the amplitude of the current (measured at -20mV as previously discussed) from 545 to 440 pA an inhibition of approximately 19.5% (See figure 7.1). On average ionomycin (1μM) caused an inhibition in IK_{SO} of 13.8 ± 4.0 % (n=7). Muscarinic inhibition of IK_{SO} in the same cell is shown for reference. Inhibition by muscarine is substantially larger than that of ionomycin (87%).

7.3.2 Mitogen activated protein (MAP) kinase mediated control of IK_{SO}

Muscarine can activate mitogen activated protein kinase (Rosenblum *et al.* 2000). To investigate whether muscarinic activation of MAP kinase underlies inhibition of IK_{SO} two inhibitors of MAP kinase activation, PD 98059 (Alessi *et al.* 1995) and U 0126 (Favata *et al.* 1998), were used. Figure 7.2 shows the effect of an inhibitor of MAP kinase activation, PD 98059, on muscarinic inhibition of IK_{SO}. Cells were incubated in PD 98059 (10μM) for at least 10 minutes prior to recording. The current recording in (a) shows an inhibition of IK_{SO} by muscarine from an amplitude of 394 to 75 pA (approx. 80%). On average, mean inhibition by muscarine (10μM) in the presence of PD 98059 (10μM) was 78.1 ± 1.5 % (n=9), this is not significantly different from the inhibition by muscarine alone ($p>0.05$, students *t* test).

This experiment was repeated with the more specific inhibitor of activation of MAP kinase, U 0126. Figure 7.3 shows the effect of U 0126 (10μM) on muscarine

induced inhibition of IK_{SO}. In the presence of U 0126 (10μM) muscarine (10μM) produced an inhibition in the cell shown from 322 to 77 pA (~76% inhibition). On average muscarinic inhibition of IK_{SO} in the presence of U 0126 reached 69.3 ± 2.8 % (n=4).

Muscarinic inhibition of IK_{SO} in control conditions and in the presence of PD 98059 and U 0126, is summarised in figure 7.4. Neither U 0126 nor PD 98059 significantly affected the inhibition of IK_{SO} by muscarine. However, a slight reduction in current amplitude was suspected in cells which were pre-treated with these compounds. This is addressed later in this chapter.

7.3.3 Role of protein kinase C in muscarinic inhibition of IK_{SO}.

As mentioned PKC is a ubiquitous enzyme which has many substrates. The phorbol ester, phorbol 12-myristate 13-acetate (PMA) has been used to stimulate PKC. The effect of PKC stimulation on basal current and on muscarinic induced inhibition has been observed. Figure 7.5 shows the time course for a muscarinic inhibition of IK_{SO}, addition of PMA and exposure of the cell to muscarine in the presence of PMA. Muscarine caused an inhibition of IK_{SO} as previously observed. After a large over-recovery the cell is exposed to PMA (100nM). PMA had no noticeable effect on outward current measured at -20mV. A slight reduction is evident in the example shown in figure 7.5 but this was not typical. Addition of muscarine after exposure to PMA caused an inhibition of IK_{SO}. However, this inhibition was not as pronounced as previously seen in control conditions. In this cell muscarine in the presence of PMA caused an inhibition of IK_{SO} by 47.2%. On average muscarine, in the prolonged presence of PMA, caused an inhibition of IK_{SO} by just 32.8 ± 4.8 % (n=5).

7.3.4 Effects of U 0126 and PD 98059 on IK_{SO}

As mentioned above basal IK_{SO} amplitude appeared slightly reduced in the presence of the inhibitors of MAP kinase activation, PD 98059 and U 0126. To investigate whether these compounds could affect IK_{SO} *per se*, they were applied acutely.

Figure 7.6 shows the effect of PD 98059 (30μM) on IK_{SO}. As can be seen PD 98059 caused a fully reversible inhibition of IK_{SO} of 49 % (312 to 158 pA). This represents an increase in input resistance from 163MΩ to 268MΩ. The block by PD 98059 was

slightly slower than that seen by muscarine (approx. 85 seconds compared to about 45 seconds). Application of PD 98059 did not influence subsequent inhibition by muscarine (shown for reference) which produced an reduction in current amplitude by 68%. Average inhibition by PD 98059 (30μM) was found to be 47.9 ± 1.2 % (n=10).

Inhibition of IK_{SO} by PD 98059 was found to be concentration dependent. PD 98059 at concentrations of 3, 10, 30 and 100μM inhibited IK_{SO} amplitude by 7.2 ± 4.1 % (n=4), 16.1 ± 1.9 % (n=5), 47.9 ± 1.2 % (n=10) and 77.0 ± 2.6 % (n=3) respectively. These data are summarised in figure 7.9.

Figure 7.7 shows that IK_{SO} is also inhibited by U 0126 (10μM). In this recording muscarine caused an inhibition of IK_{SO} by 79%. U 0126 (10μM) caused an inhibition of IK_{SO} from an amplitude of 756 pA to 602 pA (~20%), representing an increase in input resistance from 70MΩ in control conditions to 83MΩ in the presence of U 0126 (10μM). On average U 0126 at concentrations of 10 and 30μM caused an inhibition of IK_{SO} by 25.0 ± 2.5 % (n=5) and 46.0 ± 3.0 % (n=7) respectively. As can be seen from the time course of inhibition in (b) inhibition of IK_{SO} by U 0126 was very much slower than by muscarine, or PD 98059, taking up to 5 minutes to reach a steady state.

To investigate into whether these structurally dissimilar compounds (see appendix 2 for structures) are exerting their effects on IK_{SO} via MAP kinase the compound U 0125 was used. U 0125 is a structurally similar compound to U 0126 but it much less potent at inhibiting MAP kinase activation (see Favata *et al.* 1998)

Figure 7.8 shows the effect of U 0125 (30μM) on IK_{SO}. As can be seen from the current recording (a) U 0125 (30μM) caused an inhibition in IK_{SO} from 162 to 80 pA (approximately 51%) and on average by 53.3 ± 6.4% (n=4). Shown for reference is muscarinic inhibition of IK_{SO} in the same cell. From the time course in (b) it is evident that despite being structurally similar to U 0126 the onset of block is much more rapid which a steady state being reached in about 80 seconds.

Figure7.9 summarises all results obtained with these compounds. The column chart in figure 7.9 shows percentage inhibitions of IK_{SO} by PD 98059 (3, 10, 30 and

100μM), U 0126 (10 and 30μM) and U 0125 (30μM).The results clearly indicate the concentration depend block of IK_{SO} by PD 98059 and U 0126 (although only two concentrations of U 0126 were tested). It is also clear that despite the differing potency at MEK all three compounds inhibit IK_{SO} to similar degrees (when comparing block obtained at a concentration of 30μM).

U 0126 and PD 98058 inhibit IK_{SO} to similar degrees and it appears unlikely that their site of action is MEK. To investigate whether these compounds act as channel blockers the voltage sensitivity of inhibition has been investigated. Cells were held at -20mV and ramped to -100mV at a rate of $0.1 mVms^{-1}$ before stepping back to the holding potential. This protocol was repeated every 5 seconds. Percentage inhibition was calculated for each data point on the ramp and was plotted against voltage. Figure 7.10 shows percentage inhibition of IK_{SO} by PD 98059 (30μM) against voltage. Block of IK_{SO} by PD 98059 showed little voltage dependence, in the example shown PD 98059 caused an inhibition of 43% at -20mV and 41% at -50mV. In four cells examined PD 98059 (30μM) inhibited IK_{SO} by 45 ± 2 % at -20 mV and by 55 ± 5 % at -50 mV (n = 4).

Using the same protocol as above the voltage sensitivity of block by U 0126 (30μM) was also investigated. However, here ramp protocols were carried out in the presence of 25mM K^+ to give a broader range of potentials to study. Figure 7.11 shows that U 0126 (30μM) did not show voltage dependence of inhibition, blocking the inward current by 47 % at -50mV and by 47% at -100mV. It is worth noting that here because of the presence of 25mM potassium the current observed is inward, not outward. Despite the altered direction of the current the block by U 0126 (30μM) remained the same as seen previously (figure 7.9).

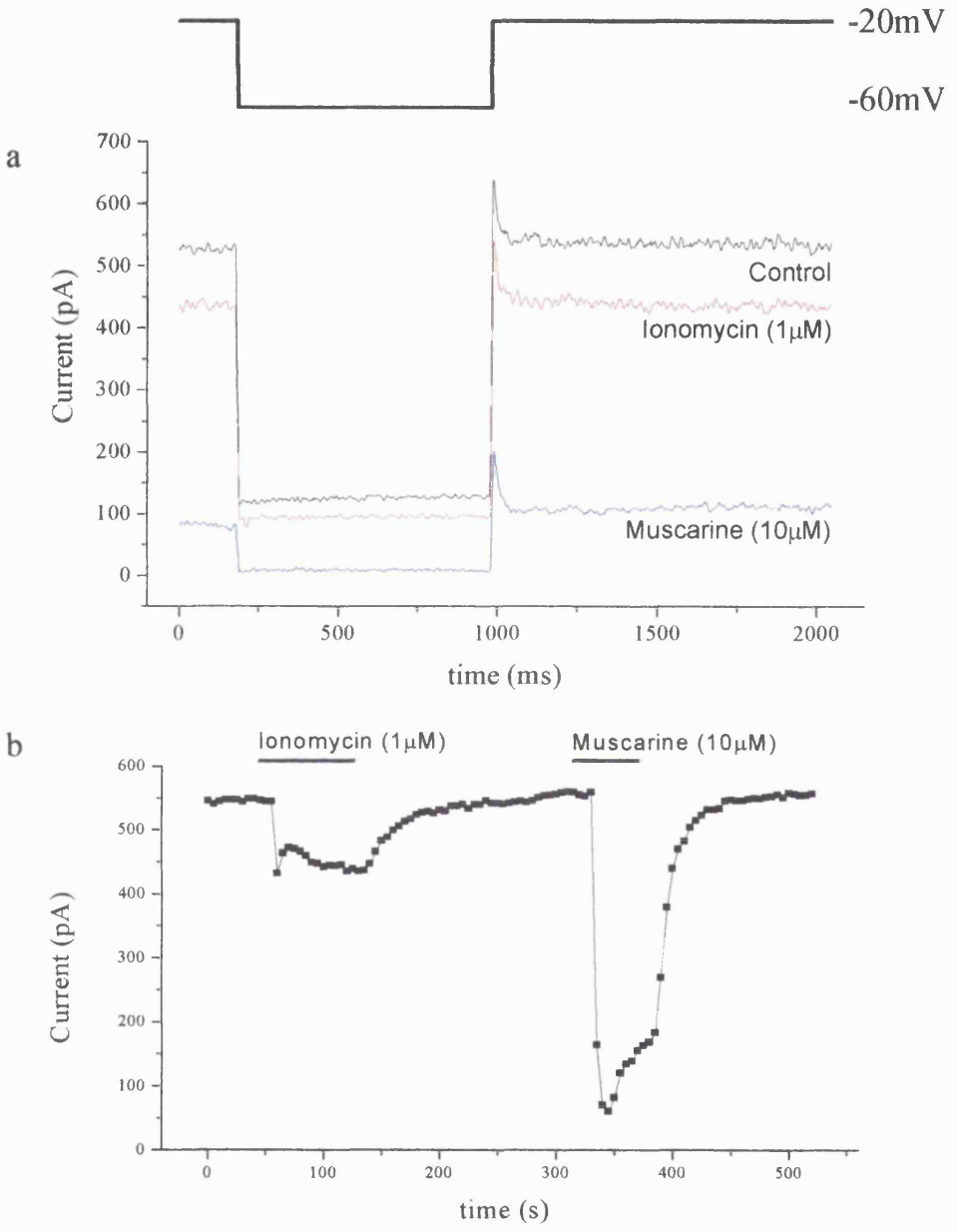

Figure 7.1 Effect of ionomycin on IK_{SO}

Ionomycin (1μM) inhibits IK_{SO}. IK_{SO} was measured as before, (a) shows current recordings from a cell exposed to ionomycin, muscarinic inhibition is shown for reference. (b) shows the time course for ionomycin and muscarinic inhibition of IK_{SO}. Ionomycin (1μM) inhibits IK_{SO} by an average of 13.8 ± 4.0 % (n=7).

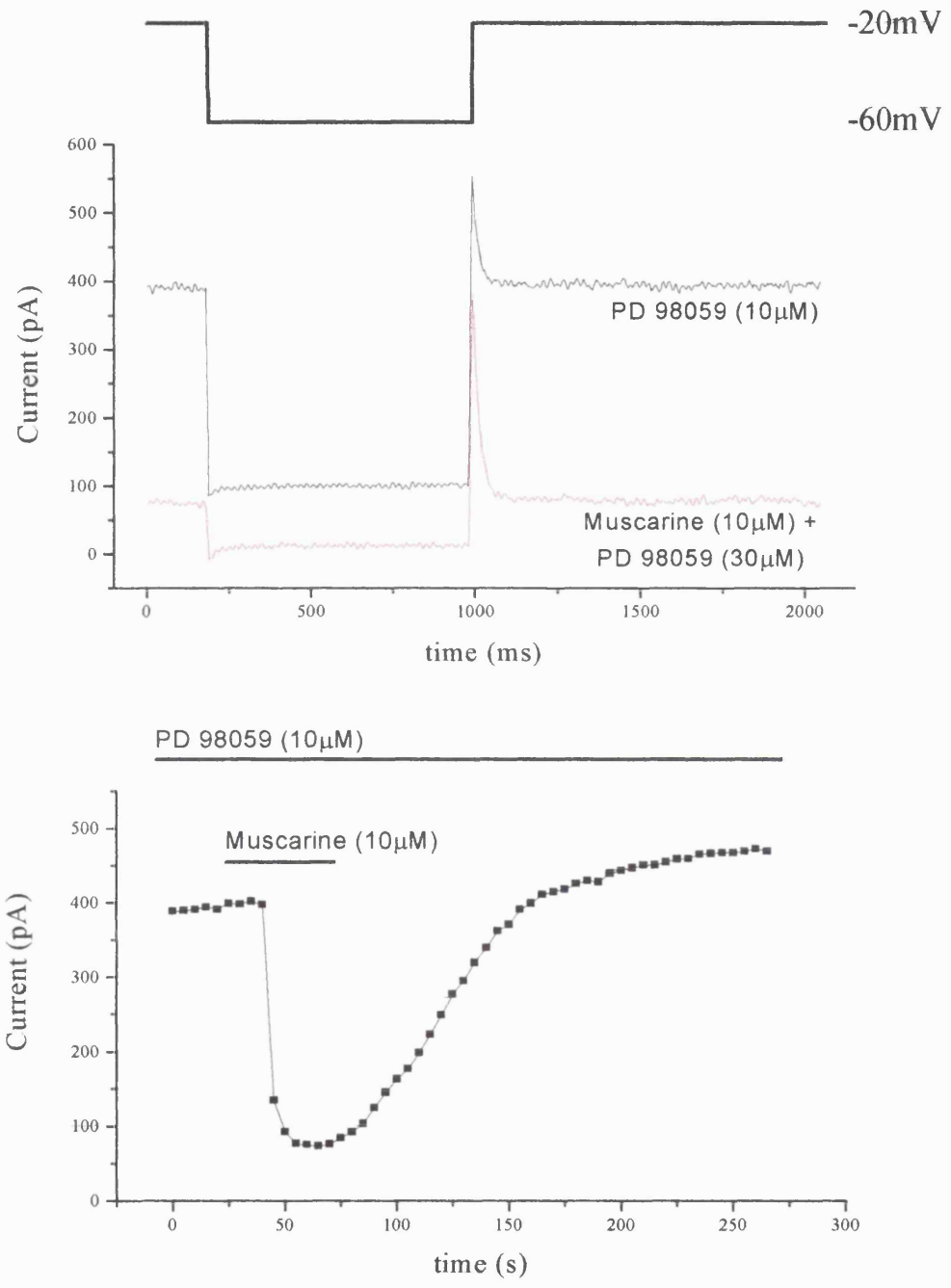

Figure 7.2 Effect of PD 98059 (10μM) on muscarine induced inhibition of IK_{SO}.

Cells were incubated in 10μM PD98059 for a minimum of 10 minutes prior to recording. PD 98059 induced an slightly augmented the inhibition induced by muscarine (10μM), mean inhibition 78.1 ± 1.5 % (n=9).

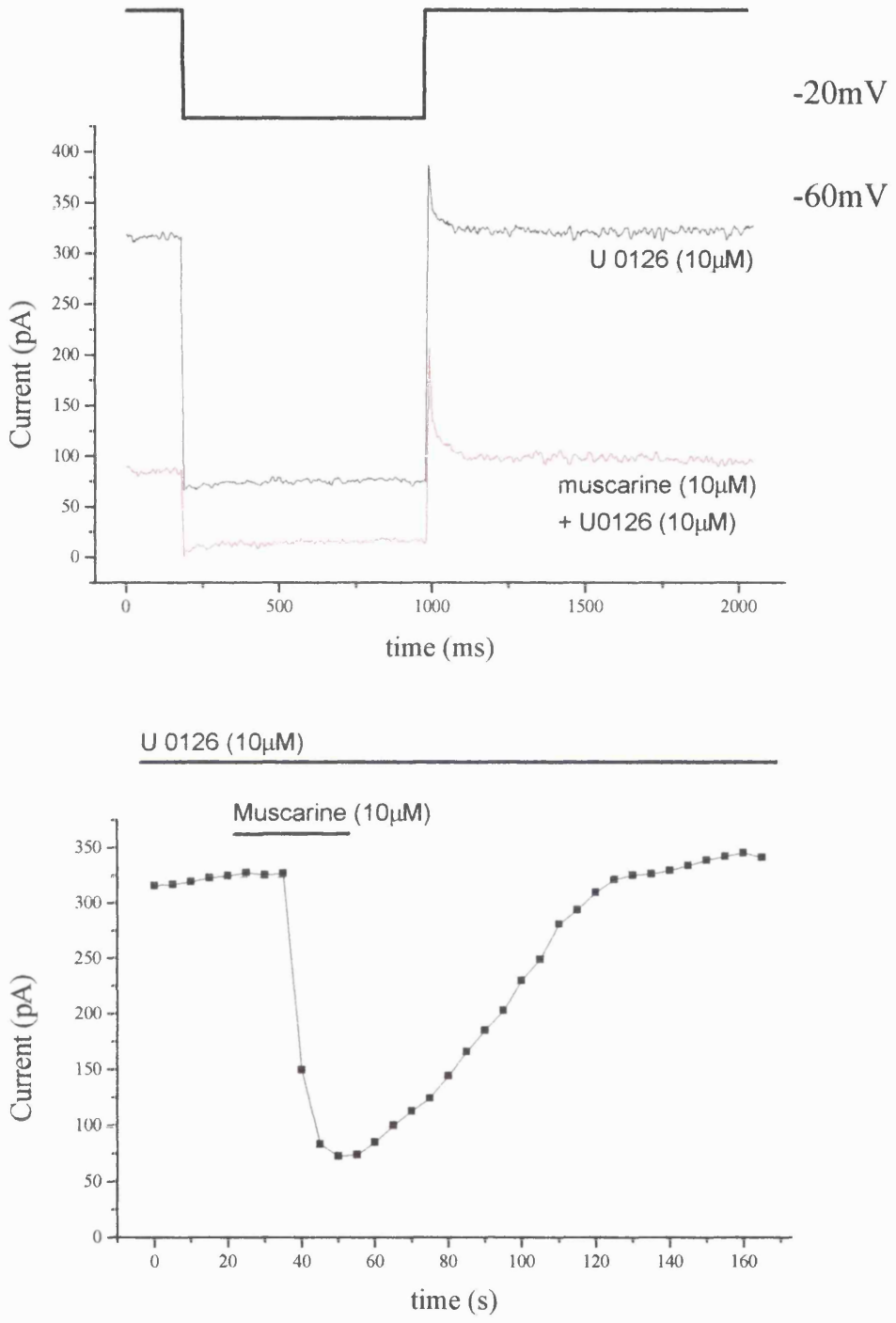

Figure 7.3. Effect of U 0126 (10μM) on muscarine induced inhibition of IK_{SO}.

U 0126 (10μM) did not effect the muscarine (10μM) induced inhibition of IK_{SO}. Mean inhibition 69.3 ± 2.8 % (n=4). Cells were kept in U 0126 (10μM) for at least 15 minutes prior to recording. (a) shows current recordings for muscainic inhibiton in the continued presence of U 0126. (b) shows time course for muscarinic inhibition.

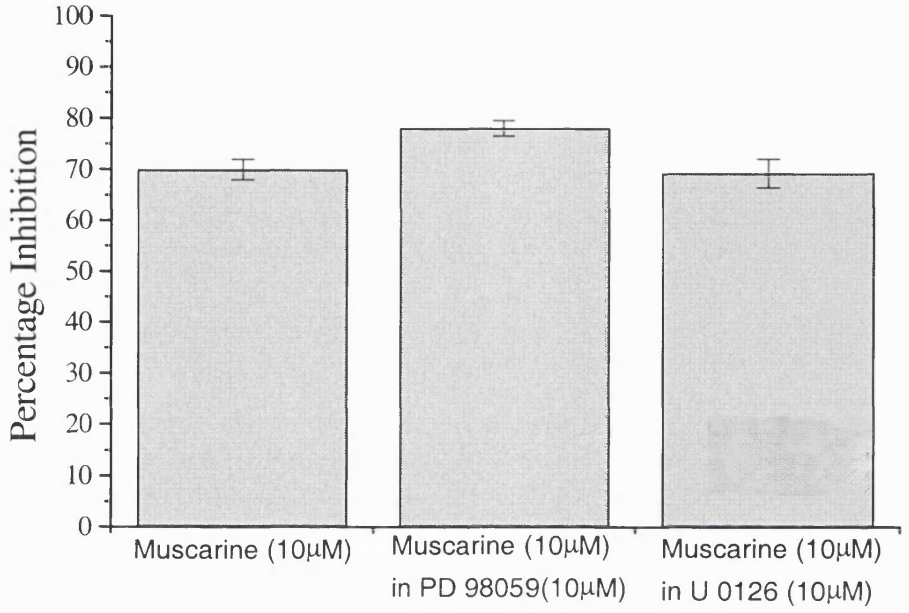

Figure 7.4 Inhibition of IK_{SO} by muscarine in control, PD 98059 and U 0126.

Muscarinic inhibition of IK_{SO} was unaffected by pre-incubation in PD 98059 (10μM) or U 0126 (10μM). Data from figures 3.3, 7.2 and 7.3.

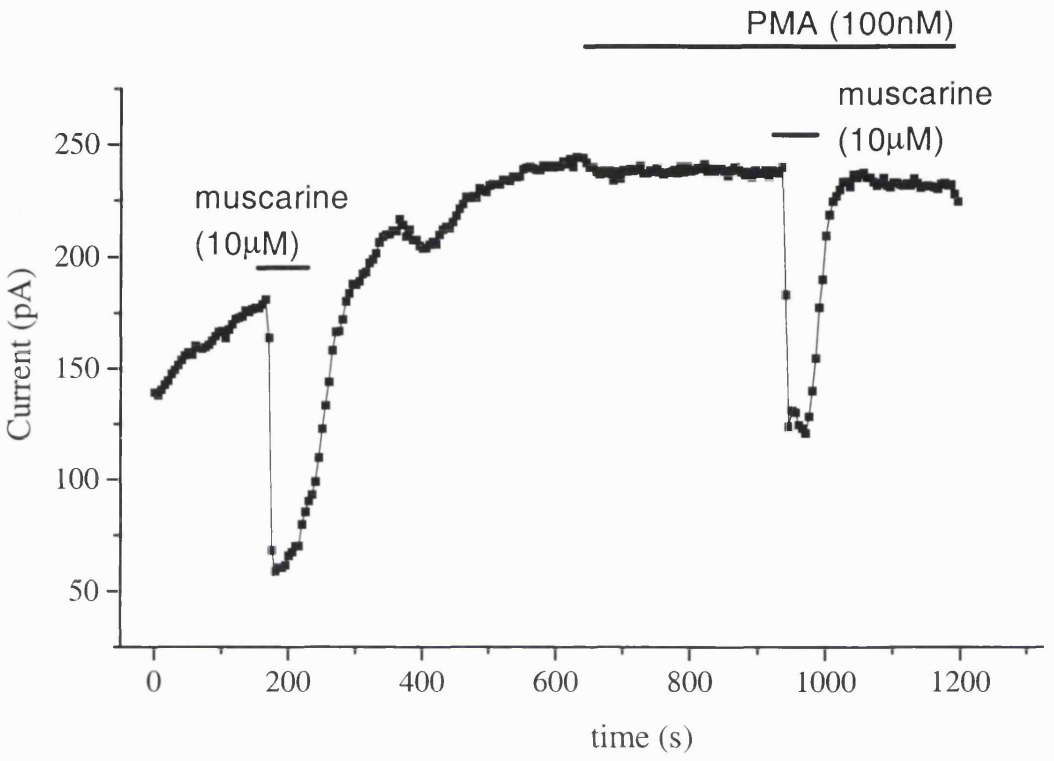

Figure 7.5 Effect of protein kinase C activation on IK_{SO}

IK_{SO} was measured at -20mV as previously discussed. Muscarine caused an inhibition in IK_{SO} of 66.3 %. Application of PMA did no significantly affect IK_{SO} but after prolonged exposure to PMA inhibition of IK_{SO} by muscarine (10μM) was reduced, in the cell shown to 47.2%, on average by 32.8 ± 4.8 (n=5).

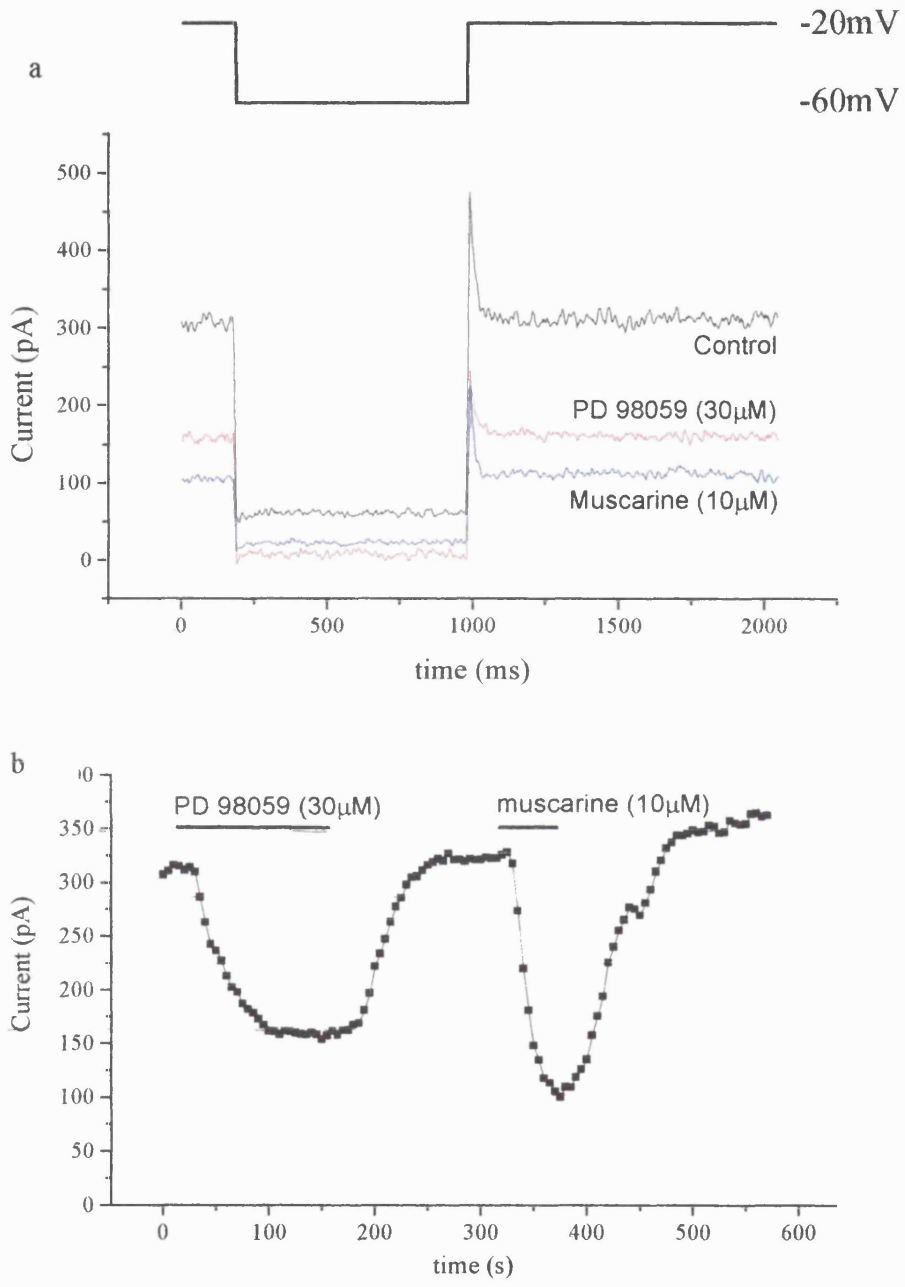

Figure 7.6. IK_{SO} is inhibited by PD 98059.

PD 98059 was found to inhibit IK_{SO} when acutely applied to CGNs. (a) shows current traces for inhibition by PD 98059 (30μM) and muscarine (10μM), (b) shows the time course for the experiment. PD 98059 was found to inhibit IK_{SO} in a concentration dependent manner. PD 98059 at 3, 10, 30 and 100μM inhibited IK_{SO} by 7.2 ± 4.1 % (n=4), 16.1 ± 1.9 % (n=5), 47.9 ± 1.2 % (n=10) and 77.0 ± 2.6 % (n=3) respectively, (see also figure 7.7).

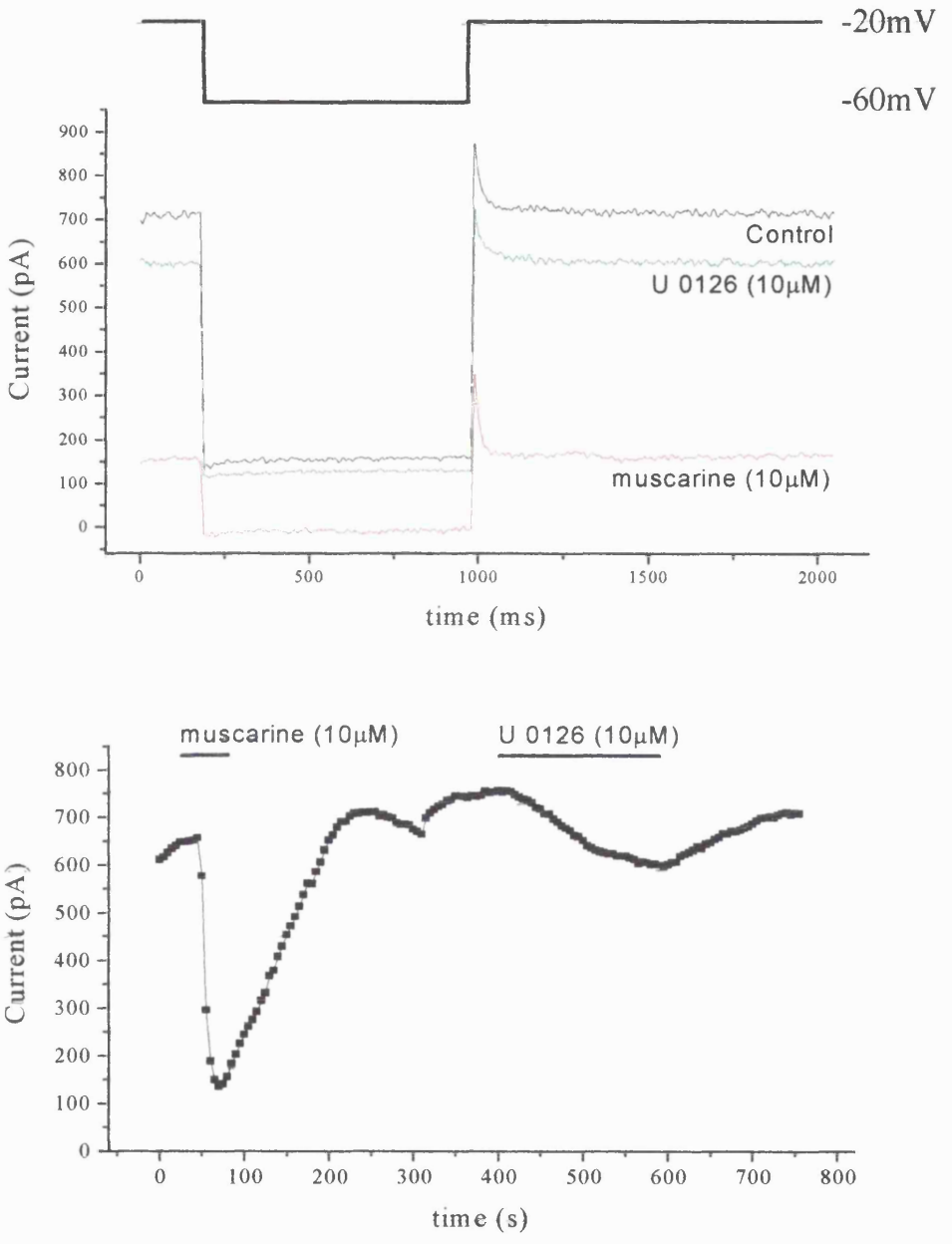

Figure 7.7. Inhibition of IK_{SO} by U 0126

U 0126 was found to inhibit IK_{SO} when applied acutely. Current recordings for inhibition of IK_{SO} by U 0126 (10μM) and muscarine (10μM) are shown in (a). (b) shows the time course for inhibition by muscarine and U 0126. U 0126 10 and 30μM inhibited IK_{SO} by 25.0 ± 2.5 % (n=5) and 46.0 ± 3.0 % (n=7) respectively (see also figure 7.7)

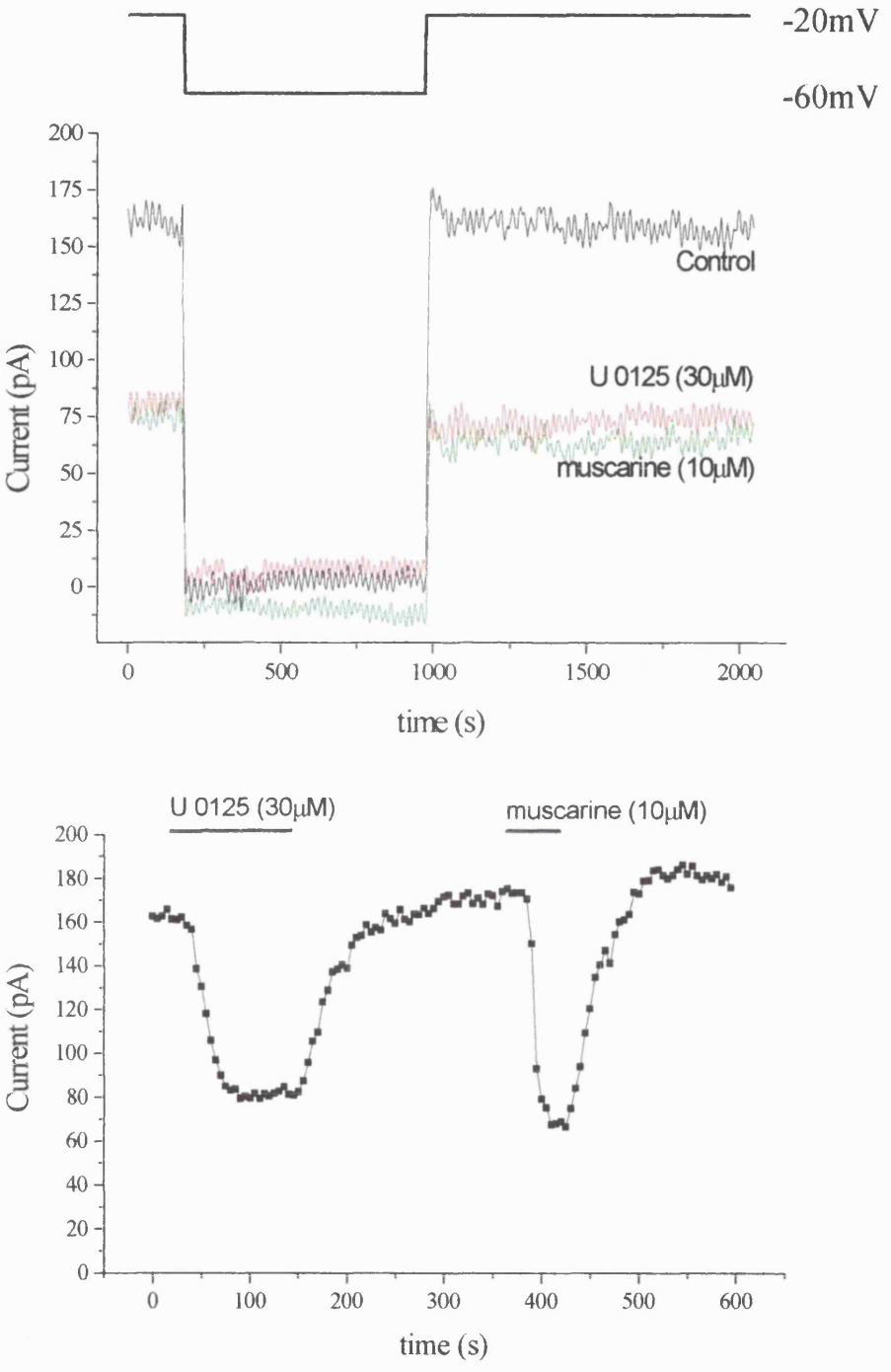

Figure 7.8. Inhibition of IK_{SO} by U 0125 (30μM).

U 0125, a structurely similar compound to U 0126 but with 10-fold less potency for MEK, is able to inhibit IK_{SO} to a similar degree as U 0126. U 0125 (30μM) inhibited IK_{SO} by 53.3 ± 6.4 % (n=4).

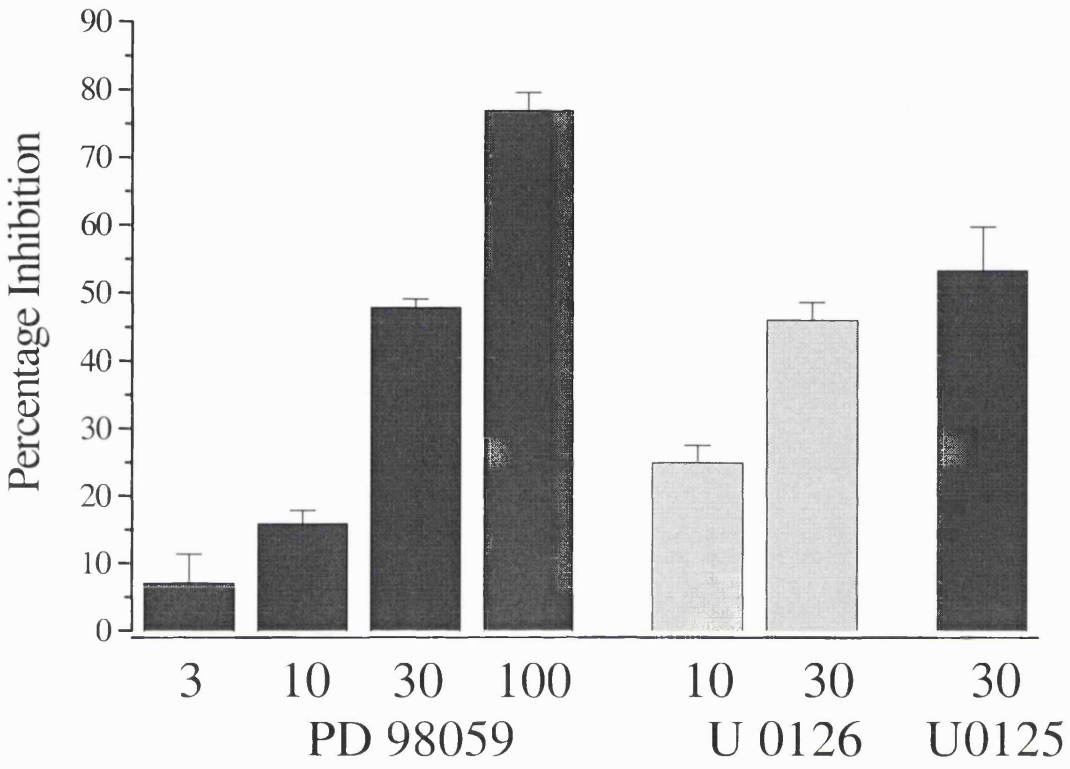

Figure 7.9. Inhibition of IK_{SO} by PD 98059, U 0126 and by U 0125.

IK_{SO} was blocked by the inhibitors of mitogen activated protein kinase, PD 98059 and U 0126. It was also inhibited by U 0125, a compound with structural similarity to U 0126 but with 10 fold less potency for MEK. For structures of PD 98059, U 0126 and U 0125 see appendix 2.

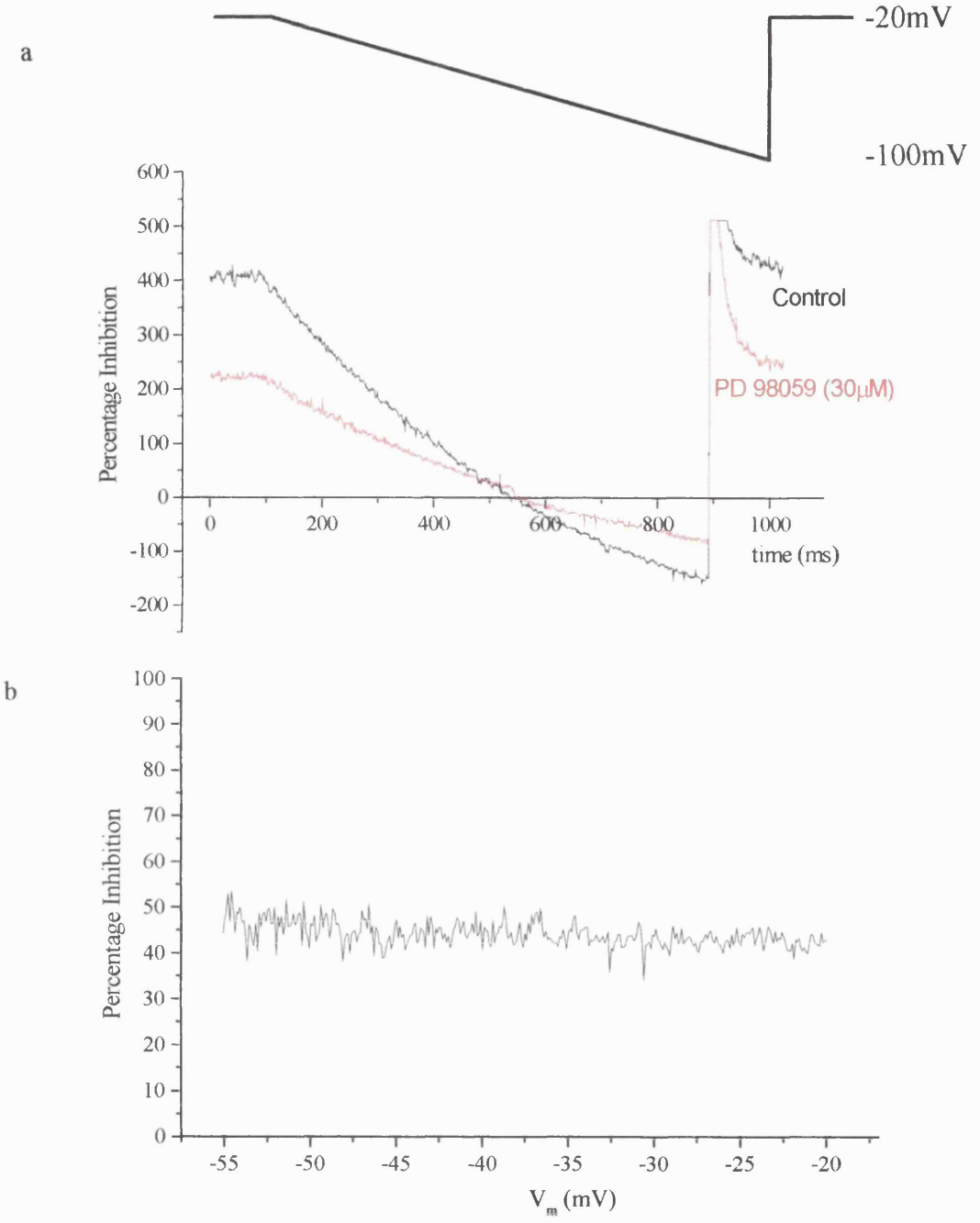

Figure 7.10 Voltage dependency of block of IK_{SO} by PD 98059 (30μM).

(a) shows a current recording from cells held at -20mV and slowly ramped to -100mV at a rate of $0.1 mVms^{-1}$ in control conditions and in the presence of PD 98059 (30μM). (b) shows the percentage inhibition plotted against membrane potential. No voltage dependence of block was observed, PD 98059 caused an inhibition of 43% at -20mV and 41% at -50mV. On average PD 98059 (30μM) inhibited IK_{SO} by 45 ± 2 % at -20 mV and by 55 ± 5 % at -50 mV (n = 4).

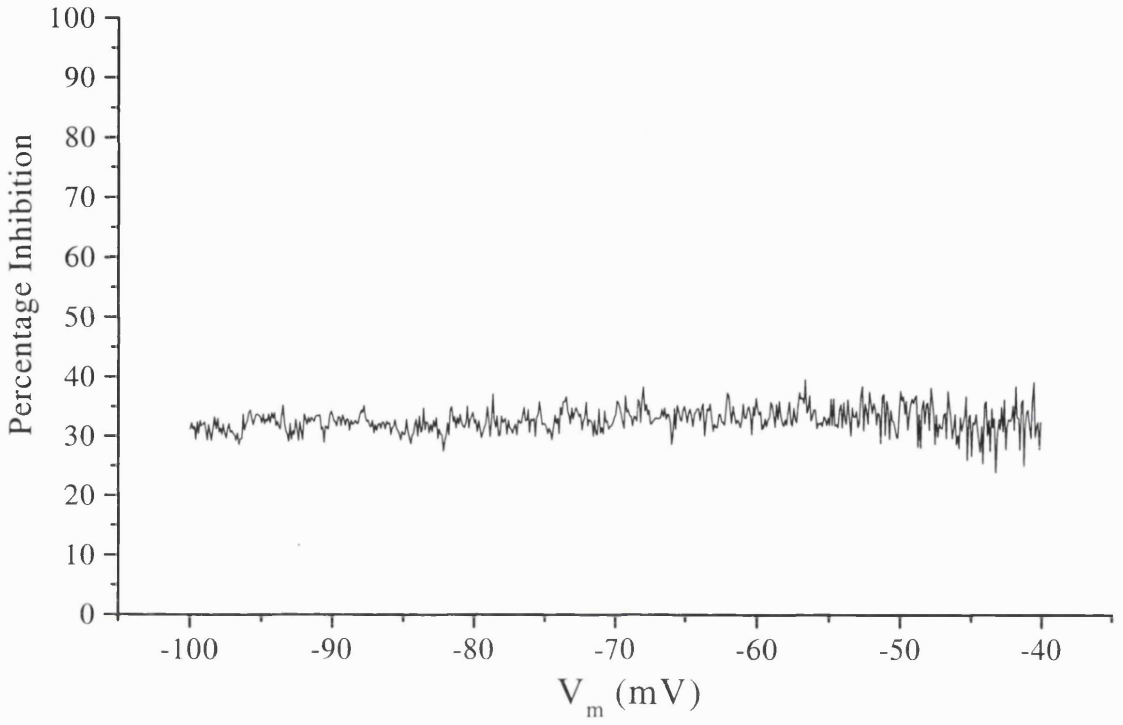

Figure 7.11. Voltage dependence of block by U 0126.

Inhibition of IK_{SO} by U 0126 was found to be independent of voltage. Measurements were taken in the same way as illustrated in fig 7.8. Cells were ramped in external solution containing 25mM potassium to create a shift in the reversal potential and hence a wider voltage range to study.

7.4 DISCUSSION

This chapter has investigated the properties underlying muscarinic inhibition of IK_{SO}. As discussed in chapter 3 IK_{SO} is likely to be inhibited by any receptor that couples to the stimulation of $G_{\alpha q/11}$. However, the downstream signalling pathways that link activated $G_{\alpha q/11}$ to inhibition of this current are not known. These data suggest that calcium is not the second messenger involved in channel inhibition. Stimulation of the MAP kinase signalling cascade does not appear to mediate inhibition of IK_{SO}, but exposure to phorbol esters does. In addition, this chapter identifies three compounds that may act at the same or distinct sites to block IK_{SO}.

7.4.1 Inhibition of IK_{SO} by rises in intracellular calcium.

IK_{SO} is inhibited by agonists that induce the activation of $G_{q/11}$ coupled receptors. Activation of $G_{q/11}$ stimulates PLC and causes a release of calcium from intracellular stores. In a large proportion of cells the rise in intracellular calcium could not be detected using whole cell calcium imaging (see chapter 4), but this does not mean that highly localised rises in intracellular calcium do not underlie muscarinic induced inhibition of IK_{SO}. Here we provide evidence to suggest that IK_{SO} is not inhibited by intracellular calcium rises. These experiments were performed using the perforated patch technique and artificially raising intracellular calcium using the calcium ionophore ionomycin. Other groups have examined calcium sensitivity of a channel more selectively by exposing inside-out patches to varying calcium concentration, (e.g. $I_{K(M)}$ Selyanko & Brown 1996). However this type of recording is not possible here because IK_{SO} experiences run-down under whole-cell recording suggesting that a diffusible second messenger is required for maintaining its continued open state.

In these experiments IK_{SO} was inhibited by a small degree by ionomycin. However, inhibition of IK_{SO} following muscarinic receptor activation was much larger suggesting that calcium rises are at best responsible for only a fraction of the muscarine induced inhibition of IK_{SO}.

7.4.2 Role of the MAP kinase signalling pathway in muscarinic inhibition of IK_{SO}.

Activation of muscarinic M_3 receptors can lead to activation of the MAP kinase signalling cascade (Kim *et al.* 1999; Slack *et al.* 2000). The MAP kinase signalling cascade is a ubiquitous kinase pathway that regulates cell proliferation and differentiation. Activated MAP kinases often translocate to the nucleus but are able to phosphorylate cytosolic proteins. In this study we found no evidence to suggest that activation of MAP kinase was responsible for muscarine induced inhibition of IK_{SO}. This is not all together an unlikely finding as to date there have been very few reports of MAP kinase mediated modulation of ion channels. In rat retinal pigment epithelial cells PD 98059 slowed the activation and reduced the amplitude of a non-selective cation current (Ryan *et al.* 1998) and in rat astrocytes a chloride current has been shown to be inhibited by PD 98059 (Crepel *et al.* 1990). More recently MEK inhibition has been shown to inhibit a voltage-dependent calcium current in dorsal root ganglion neurones (Fitzgerald 2000).

It still remains possible that enzymes further up the MAP kinase signalling cascade, such as Raf-1 (MAP kinase kinase kinase) mediate muscarine induced inhibition of IK_{SO}.

7.4.3 The role of PKC in muscarinic induced inhibition of IK_{SO}.

Protein kinase C is a ubiquitous enzyme with a multitude of substrates. It is therefore an obvious target when attempting to elucidate the signalling mechanisms leading to inhibition of IK_{SO}. The effects of PKC activation on two pore domain potassium channels has been examined. TWIK-1 currents were potentiated by activators of PKC whilst TREK-1 currents were inhibited (Fink *et al.* 1996; Lesage *et al.* 1996). rTASK currents were not found to be affected by PKC activation, (Fink *et al.* 1996; Leonoudakis *et al.* 1998). In this study PMA induced activation of PKC did not affect current amplitude, in accordance with Fink *et al.* (1996). However, what was found was that prolonged PMA activation reduced muscarinic inhibition of IK_{SO}. There are two possible explanations for this phenomenon. Firstly that muscarinic inhibition of IK_{SO} is mediated, in some way, via PKC. However, application of U 73122 did not affect muscarinic inhibition of IK_{SO} (Boyd *et al.* 2000) suggesting that PLC mediated activation of PKC was not responsible for muscarinic inhibition of IK_{SO}. The second possibility is that the activated PKC acts

to desensitise the muscarinic receptor machinery, either the receptor itself, or the G-protein. This method of negative feedback has been reported for many different receptor subtypes including delta opioid receptors in oocytes (Ueda *et al.* 1995), the muscarinic receptors of the rat lacrimal gland cells (Tan & Marty 1991) and the mGluR1 receptor in oocytes (Francesconi & Duvoisin 2000). Until the actions of PKC phosphorylation on IK_{SO} are fully understood these results remain inconclusive. Studies into the mechanisms underlying regulation of IK_{SO} remain hampered by the requirement of the, as yet unidentified, diffusible messenger which maintains the open state of IK_{SO}.

7.4.4 Inhibition of IK_{SO} by PD 98059 and U 0126.

As yet there have been no reports of selective ligands for the two pore domain potassium channels. Although several have been shown to be blocked by various compounds, for example, TWIK-1 and TREK-1 are inhibited by quinidine and quinine and barium and TASK-1 is blocked by barium, zinc and acid pH. Here, it is shown that two compounds PD 98059 and U 0126 inhibit IK_{SO} in a concentration dependent manner and U 0125 inhibits IK_{SO} at a concentration of 30μM. Although the effects of these ligands on the other two pore domain potassium channels has not been fully characterised they may provide a basic structure for more selective ligands to be synthesised.

These two compounds have been used extensively to examine the importance of the MAP kinase signalling pathway in a wide variety of cells. The results presented here show that PD 98059 and U 0126 cause excitation of the plasma membrane. Further, studies that use PD 98059 or U 0126 in intact cells should control for the fact that they are likely to cause cellular depolarisation and that any affects attributed to inhibition of MAP kinase may be due to increased cellular excitation.

The mechanism of action of these compounds remains unclear although it does not appear to be due to either an action on MAP kinase kinase or a direct pore block. The three compounds observed to inhibit IK_{SO}, PD 98059, U 0126 and U 0125, all exhibit differing potencies at MEK inhibition however, as figure 7.9 demonstrates they all inhibit IK_{SO} to similar degrees when applied at a concentration of 30μM. Neither PD 98059 nor U 0126 exhibited any voltage sensitivity of block suggesting

that their site of action is not within the pore of the channel. At this stage there is nothing to suggest that these compounds all act upon the same site, the fact that they all inhibit MEK to some degree may simply be co-incidental. Whether these compounds act on a regulatory protein, the channel itself or even the diffusible messenger that dictates the constantly activated state of IK_{SO}, resolving their site of action is likely to give a valuable insight into how leak currents are regulated by intracellular messengers.

SUMMARY

IK_{SO} is a member of the two-pore domain family of potassium channels which has yet to be fully characterised. It has previously been shown that IK_{SO} is strongly inhibited by stimulation of muscarinic M_3 receptors (Watkins & Mathie 1996; Millar *et al.* 2000; Boyd *et al.* 2000) but the second messenger system underlying the inhibition has not been characterised. This study aimed to investigate some of the properties of IK_{SO} and attempt to elucidate the mechanisms underlying regulation of this potassium current, concentrating on the intracellular calcium as a potential modulator of IK_{SO}.

As with other studies IK_{SO} was detected as a sustained outward current in cerebellar granule neurons that reversed at potentials which suggest potassium as the charge carrier (as with Millar *et al.* 2000). IK_{SO} was also found to be strongly inhibited by muscarine and, albeit less consistently, by histamine. The ability of other ions to carry IK_{SO} was investigated and was found to have a permeability sequence of $Tl^+ = Rb^+ = K^+ >> Cs^+ > NH_4^+ > Li^+$. Many potassium channels have been found to be highly permeable to thallium. These data suggest that the unique structure of the two-pore domain family of potassium channels confer large differences in ionic permeability.

IK_{SO} is inhibited by activation of muscarinic M_3 receptors (Boyd *et al.* 2000). M_3 receptors are known to couple to stimulation of $G\alpha_q$ which in turn is known to induce a rise in intracellular calcium via the generation of IP_3 and the release of calcium from intracellular stores. It was therefore prudent to investigate whether a release of calcium from intracellular stores mediates muscarinic inhibition of IK_{SO}. A similar pathway is known to be responsible for bradykinin mediated inhibition of the M-current in sympathetic neurons (Cruzblanca *et al.* 1998). However, this study found inconsistent elevations in $[Ca^{2+}]_i$ following muscarinic stimulation, but that the size of the calcium response and the proportion of responding cells could be greatly enhanced by depolarising the cells, by increased extracellular potassium concentration, prior to muscarine addition. This phenomenon has been observed in

other studies (Irving *et al.* 1992a, b; Masgrau *et al.* 2000) and in other cell types (e.g. Irving & Collingridge 1998).

The most likely explanation for these results is that the intracellular calcium stores are depleted at rest and require a large rise in cytoplasmic calcium to induce sufficient store loading. Indeed the results presented here show that intracellular, thapsigargin sensitive, calcium stores are not only depleted at rest but can also be charged by a depolarisation. The relative lack of contribution of store operated calcium channels in cerebellar granule neurons may indicate that intracellular stores are not functionally important under 'normal' conditions. However, following periods of intense synaptic activity charging of the intracellular stores would be expected to occur which would dramatically change the cellular response to agonists activating $G\alpha_q$ coupled receptors. Furthermore, depleted calcium stores would contribute to buffering of large calcium loads during periods of intense synaptic activity (Toescu, 1998).

The irreproducibility of a calcium response following muscarinic stimulation would suggest that calcium does not mediate muscarinic inhibition of IK_{SO}. Also BAPTA AM treatment (Watkins & Mathie 1996) and U -73122 (this study; Boyd *et al.* 2000) both abolish any calcium response to muscarine without removing the inhibition of IK_{SO}. However, it remains possible that calcium mediated modulation of IK_{SO} was occurring but the levels were too small or too highly localised to be detected using whole cell calcium imaging. Ionomycin was able to inhibit IK_{SO} but not to the extent observed by muscarine. This suggests that calcium is not the primary second messenger following muscarinic stimulation although it may have a modulatory effect either directly or via an intermediate protein.

The mechanisms underlying the regulation of IK_{SO} remain to be resolved. IK_{SO} is observed to run-down under whole-cell recording suggesting that there is a diffusible messenger that maintains the constant active state of IK_{SO}. Determination and characterisation of this messenger is likely to increase the understanding of these channels and may provide a useful pharmacological target. The primary second messenger system leading to inhibition of IK_{SO} following muscarinic

stimulation also remains to be resolved although it is now not thought to involve intracellular calcium or MAP kinase. However, inhibitors of MAP kinase activation PD 98059 and U 0126 have been found to cause a voltage independent block of IK_{SO}. The mechanisms underlying inhibition of IKSO by these compounds is not known although it is not believe to be due to an action on MAP kinase. Elucidation of the site of action of these drugs might involve one of the second messenger pathways mentioned above or reveal a novel regulatory pathway.

All the above experiments were performed on cultured cerebellar granule neurons. Similar experiments on cerebellar slices have been performed (Millar *et al.* 2000) but need to be extended if the role of these channels in a functional cerebellum is to be resolved.

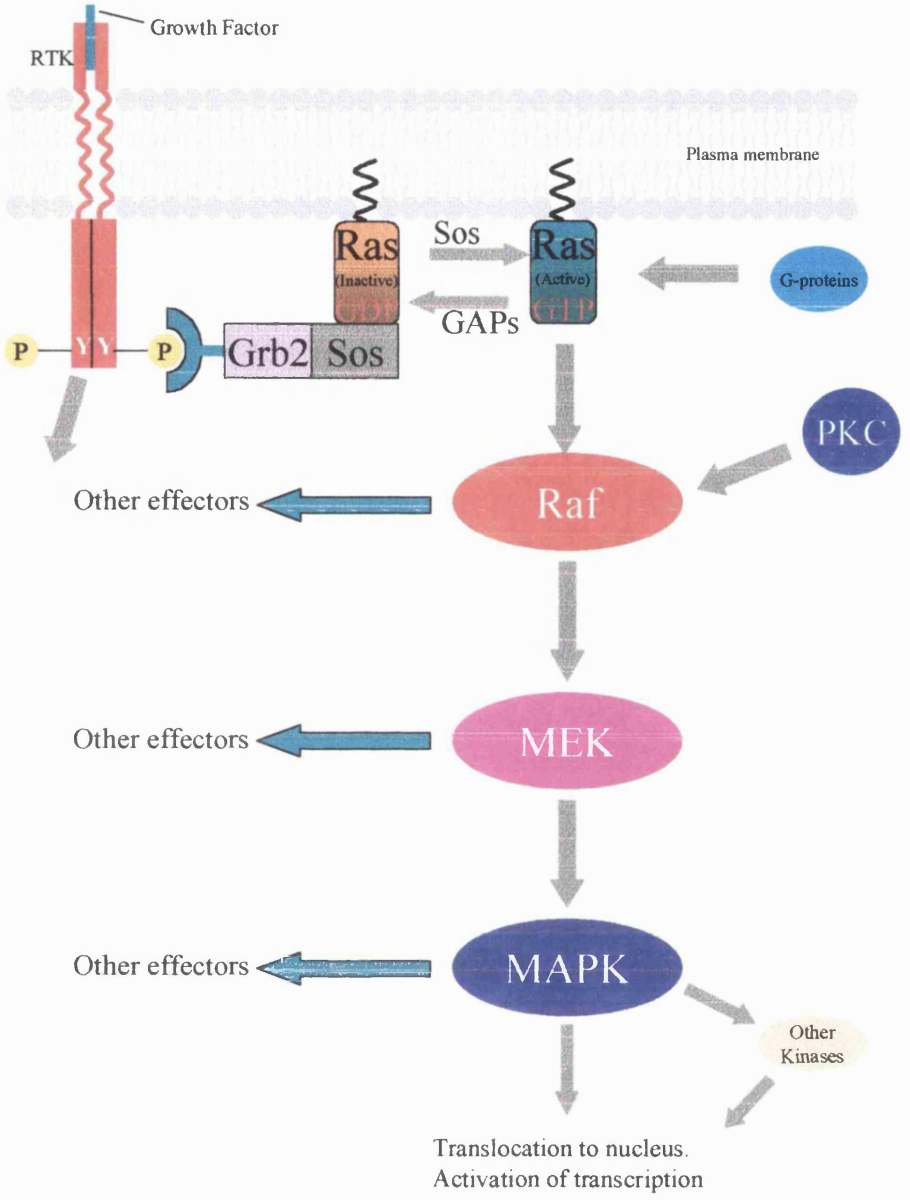

The MAP kinase signalling cascade.

Following stimulation and autophosphorylation of a receptor tyrosine kinase the Grb2 / Sos complex binds and activates. Sos induces the exchange of GDP for GTP on Ras and allows the binding of Raf (or MAPKKK). Raf is a kinase, which can phosphorlyate MEK (MAPKK) activating it to phosphorylate MAPK. Alternative inputs and output to this kinase cascade are shown. Activity is ceased by hydrolysis of the GTP bound to Ras by GADs returning it to its inactive state.

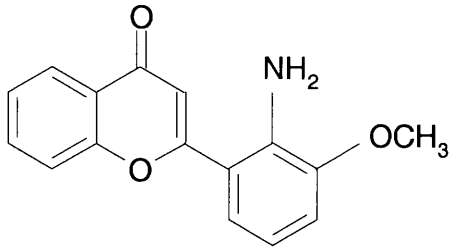

PD 98059

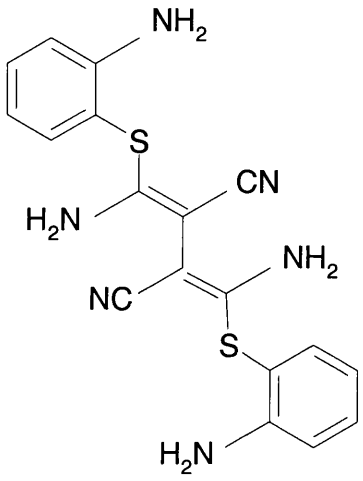

U 0126

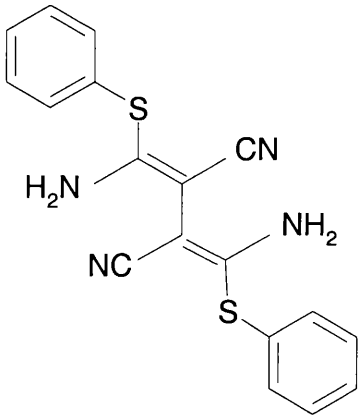

U 0125

Chemical structures of PD 98059, U 0126 and U 0125.

List of References

ADAMS, M.D., CELNIKER, S.E., HOLT, R.A., EVANS, C.A., GOCAYNE, J.D., AMANATIDES, P.G., SCHERER, S.E., LI, P.W., HOSKINS, R.A., GALLE, R.F., GEORGE, R.A., LEWIS, S.E., RICHARDS, S., ASHBURNER, M., HENDERSON, S.N., SUTTON, G.G., WORTMAN, J.R., YANDELL, M.D., ZHANG, Q., CHEN, L.X., BRANDON, R.C., ROGERS, Y.H., BLAZEJ, R.G., CHAMPE, M., PFEIFFER, B.D., WAN, K.H., DOYLE, C., BAXTER, E.G., HELT, G., NELSON, C.R., GABOR, M.G., ABRIL, J.F., AGBAYANI, A., AN, H.J., ANDREWS-PFANNKOCH, C., BALDWIN, D., BALLEW, R.M., BASU, A., BAXENDALE, J., BAYRAKTAROGLU, L., BEASLEY, E.M., BEESON, K.Y., BENOS, P.V., BERMAN, B.P., BHANDARI, D., BOLSHAKOV, S., BORKOVA, D., BOTCHAN, M.R., BOUCK, J., BROKSTEIN, P., BROTTIER, P., BURTIS, K.C., BUSAM, D.A., BUTLER, H., CADIEU, E., CENTER, A., CHANDRA, I., CHERRY, J.M., CAWLEY, S., DAHLKE, C., DAVENPORT, L.B., DAVIES, P., DE PABLOS, B., DELCHER, A., DENG, Z., MAYS, A.D., DEW, I., DIETZ, S.M., DODSON, K., DOUP, L.E., DOWNES, M., DUGAN-ROCHA, S., DUNKOV, B.C., DUNN, P., DURBIN, K.J., EVANGELISTA, C.C., FERRAZ, C., FERRIERA, S., FLEISCHMANN, W., FOSLER, C., GABRIELIAN, A.E., GARG, N.S., GELBART, W.M., GLASSER, K., GLODEK, A., GONG, F., GORRELL, J.H., GU, Z., GUAN, P., HARRIS, M., HARRIS, N.L., HARVEY, D., HEIMAN, T.J., HERNANDEZ, J.R., HOUCK, J., HOSTIN, D., HOUSTON, K.A., HOWLAND, T.J., WEI, M.H., IBEGWAM, C., JALALI, M., KALUSH, F., KARPEN, G.H., KE, Z., KENNISON, J.A., KETCHUM, K.A., KIMMEL, B.E., KODIRA, C.D., KRAFT, C., KRAVITZ, S., KULP, D., LAI, Z., LASKO, P., LEI, Y., LEVITSKY, A.A., LI, J., LI, Z., LIANG, Y., LIN, X., LIU, X., MATTEI, B., MCINTOSH, T.C., MCLEOD, M.P., MCPHERSON, D., MERKULOV, G., MILSHINA, N.V., MOBARRY, C., MORRIS, J., MOSHREFI, A., MOUNT, S.M., MOY, M., MURPHY, B., MURPHY, L., MUZNY, D.M., NELSON, D.L., NELSON, D.R., NELSON, K.A., NEPU, N.A., NIXON, K., NUSSKERN, D.R., PACLEB, J.M., PALAZZOLO, M., PITTMAN, G.S., PAN, S., POLLARD, J., PURI, V., REESE, M.G., REINERT, K., REMINGTON, K., SAUNDERS, R.D., SCHEELER, F., SHEN, H., SHUE, B.C., SIDEN-KIAMOS, I., SIMPSON, M., SKUPSKI, M.P., SMITH, T., SPIER, E., SPRADLING, A.C., STAPLETON, M., STRONG, R., SUN, E., SVIRSKAS, R., TECTOR, C., TURNER, R., VENTER, E., WANG, A.H., WANG, X., WANG, Z.Y., WASSARMAN, D.A., WEINSTOCK, G.M., WEISSENBACH, J., WILLIAMS, S.M., WOODAGE, T., WORLEY, K.C., WU, D., YANG, S., YAO, Q.A., YE, J., YEH, R.F., ZAVERI, J.S., ZHAN, M., ZHANG, G., ZHAO, Q., ZHENG, L., ZHENG, X.H., ZHONG, F.N., ZHONG, W., ZHOU, X., ZHU, S., ZHU, X., SMITH, H.O., GIBBS, R.A., MYERS, E.W., RUBIN, G.M. & VENTER, J.C. (2000). The genome sequence of Drosophila melanogaster. *Science* **287**, 2185-2195.

ALESSI, D.R., CUENDA, A., COHEN, P., DUDLEY, D.T. & SALTIEL, A.R. (1995). PD 098059 is a specific inhibitor of the activation of mitogen-activated protein kinase kinase in vitro and in vivo. *J. Biol. Chem.* **270**, 27489-27494.

ALTER, C.A., AMAGASU, M., SHAH, K., JOLLY, Y.C., MAJOR, C. & WOLF, B.A. (1994). U-73122 does not specifically inhibit phospholipase C in rat pancreatic islets and insulin-secreting beta-cell lines. *Life Sci.* **54**, L107-L112

AMICO, C., MARCHETTI, C., NOBILE, M. & USAI, C. (1995). Pharmacological types of calcium channels and their modulation by baclofen in cerebellar granules. *J. Neurosci.* **15**, 2839-2848.

ARCHER, F.R., DOHERTY, P., COLLINS, D. & BOLSOVER, S.R. (1999). CAMs and FGF cause a local submembrane calcium signal promoting axon outgrowth without a rise in bulk calcium concentration. *Eur. J. Neurosci.* **11**, 3565-3573.

ARMSTRONG, C. (1998). The vision of the pore. *Science* **280**, 56-57.

ARMSTRONG, C.M. & BEZANILLA, F. (1973). Currents related to movement of the gating particles of the sodium channels. *Nature* **242**, 459-461.

ATKINSON, N.S., ROBERTSON, G.A. & GANETZKY, B. (1991). A component of calcium-activated potassium channels encoded by the Drosophila slo locus. *Science* **253**, 551-555.

BABA-AISSA, F., RAEYMAEKERS, L., WUYTACK, F., DE GREEF, C., MISSIAEN, L. & CASTEELS, R. (1996). Distribution of the organellar Ca^{2+} transport ATPase SERCA2 isoforms in the cat brain. *Brain Res.* **743**, 141-153.

BABCOCK, D.F. & HILLE, B. (1998). Mitochondrial oversight of cellular Ca^{2+} signaling. *Curr. Opin. Neurobiol.* **8**, 398-404.

BALSER, J.R. (1999). Structure and function of the cardiac sodium channels. *Cardiovasc. Res.* **42**, 327-338.

BANG, H., KIM, Y. & KIM, D. (2000). TREK-2, a new member of the mechanosensitive tandem-pore K^+ channel family. *J. Biol. Chem.* **275**, 17412-17419.

BARDONI, R. & BELLUZZI, O. (1993). Kinetic study and numerical reconstruction of A-type current in granule cells of rat cerebellar slices. *J Neurophysiol.* **69**, 2222-2231.

BARGMANN, C.I. (1998). Neurobiology of the Caenorhabditis elegans genome. *Science* **282**, 2028-2033.

BARRY, P.H. & LYNCH, J.W. (1991). Liquid junction potentials and small cell effects in patch-clamp analysis [published erratum appears in J Membr Biol 1992 Feb;125(3):286]. *J. Membr. Biol.* **121**, 101-117.

BERRIDGE, M.J. (1993). Inositol trisphosphate and calcium signalling. *Nature* **361**, 315-325.

BERRIDGE, M.J. (1995). Capacitative calcium entry. *Biochem. J.* **312**, 1-11.

BERRIDGE, M.J. (1995). Inositol trisphosphate and calcium signaling. *Ann. N.Y. Acad. Sci.* **766**, 31-43.

BERRIDGE, M.J. (1996). Microdomains and elemental events in calcium signalling. *Cell Calcium* **20**, 95-96.

BERRIDGE, M.J. (1998). Neuronal calcium signaling. *Neuron* **21**, 13-26.

BETTLER, B. & MULLE, C. (1995). Review: neurotransmitter receptors. II. AMPA and kainate receptors. *Neuropharmacology* **34**, 123-139.

BEZPROZVANNY, I., WATRAS, J. & EHRLICH, B.E. (1991). Bell-shaped calcium-response curves of Ins(1,4,5)P3- and calcium-gated channels from endoplasmic reticulum of cerebellum. *Nature* **351**, 751-754.

BHAVE, S.V., SNELL, L.D., TABAKOFF, B. & HOFFMAN, P.L. (2000). Chronic ethanol exposure attenuates the anti-apoptotic effect of NMDA in cerebellar granule neurons. *J. Neurochem.* **75**, 1035-1044.

BIRD, G.S., ROSSIER, M.F., HUGHES, A.R., SHEARS, S.B., ARMSTRONG, D.L. & PUTNEY, J.W.J. (1991). Activation of Ca^{2+} entry into acinar cells by a non-phosphorylatable inositol trisphosphate. *Nature* **352**, 162-165.

BIRNBAUMER, L., QIN, N., OLCESE, R., TAREILUS, E., PLATANO, D., COSTANTIN, J. & STEFANI, E. (1998). Structures and functions of calcium channel beta subunits. *J. Bioenerg. Biomembr.* **30**, 357-375.

BLEAKMAN, D. & LODGE, D. (1998). Neuropharmacology of AMPA and kainate receptors. *Neuropharmacology* **37** , 1187-1204.

BOYD, D.F., MILLAR, J.A., WATKINS, C.S. & MATHIE, A. (2000). The role of Ca^{2+} stores in the muscarinic inhibition of the K^+ current, IK_{SO}, in neonatal rat cerebellar granule cells. *J.Physiol.(Lond.)* **529**, 321-331.

BRANN, M.R., ELLIS, J., JORGENSEN, H., HILL-EUBANKS, D. & JONES, S.V. (1993). Muscarinic acetylcholine receptor subtypes: localization and structure/function. *Prog. Brain. Res.* **98**, 121-127.

BROWN D.A. (1988). M currents. In Narahashi, T. (ed), Ion channels, vol 1. Plenum Publishing Corporation, New York, 55-94.

BUDD, S.L. & NICHOLLS, D.G. (1996). A reevaluation of the role of mitochondria in neuronal Ca^{2+} homeostasis. *J. Neurochem.* **66**, 403-411.

BUDD, S.L. & NICHOLLS, D.G. (1996). Mitochondria, calcium regulation, and acute glutamate excitotoxicity in cultured cerebellar granule cells. *J. Neurochem.* **67**, 2282-2291.

BUTTERWORTH, J.F. & STRICHARTZ, G.R. (1990). Molecular mechanisms of local anesthesia: a review. *Anesthesiology* **72**, 711-734.

CAI, Y.C. & DOUGLASS, J. (1993). In vivo and in vitro phosphorylation of the T lymphocyte type n (Kv1.3) potassium channel. *J. Biol. Chem.* **268**, 23720-23727.

CARAFOLI, E. (1987). Intracellular calcium homeostasis. *Annu. Rev. Biochem.* **56**, 395-433.

CARIGNANI, C., ROBELLO, M., MARCHETTI, C. & MAGA, L. (1991). A transient outward current dependent on external calcium in rat cerebellar granule cells. *J. Membr. Biol.* **122**, 259-265.

CARLIER, E., DARGENT, B., DE WAARD, M. & COURAUD, F. (2000). Na(+) channel regulation by calmodulin kinase II in rat cerebellar granule cells. *Biochem. Biophys. Res. Commun.* **274**, 394-399.

CATTERALL, W.A. (1999). Molecular properties of brain sodium channels: an important target for anticonvulsant drugs. *Adv. Neurol.* **79**, 441-456.

CATTERALL, W.A. (2000). From ionic currents to molecular mechanisms: the structure and function of voltage-gated sodium channels. *Neuron* **26**, 13-25.

CAULFIELD, M.P. & BIRDSALL, N.J. (1998). International Union of Pharmacology. XVII. Classification of muscarinic acetylcholine receptors. *Pharmacol. Rev.* **50**, 279-290.

CHA, A., SNYDER, G.E., SELVIN, P.R. & BEZANILLA, F. (1999). Atomic scale movement of the voltage-sensing region in a potassium channel measured via spectroscopy. *Nature* **402**, 809-813.

CHAVEZ, R.A., GRAY, A.T., ZHAO, B.B., KINDLER, C.H., MAZUREK, M.J., MEHTA, Y., FORSAYETH, J.R. & YOST, C.S. (1999). TWIK-2, a new weak inward rectifying member of the tandem pore domain potassium channel family [published erratum appears in J Biol Chem 1999 Aug 20;274(34):24440]. *J. Biol. Chem.* **274**, 7887-7892.

CHAVIS, P., FAGNI, L., LANSMAN, J.B. & BOCKAERT, J. (1996). Functional coupling between ryanodine receptors and L-type calcium channels in neurons. *Nature* **382**, 719-722.

CHEN, W.H., CHU, K.C., WU, S.J., WU, J.C., SHUI, H.A. & WU, M.L. (1999). Early metabolic inhibition-induced intracellular sodium and calcium increase in rat cerebellar granule cells. *J Physiol (Lond)* **515**, 133-146.

CHUNG, I. & SCHLICHTER, L.C. (1997). Native Kv1.3 channels are upregulated by protein kinase C. *J. Membr. Biol.* **156**, 73-85.

COETZEE, W.A., AMARILLO, Y., CHIU, J., CHOW, A., LAU, D., MCCORMACK, T., MORENO, H., NADAL, M.S., OZAITA, A., POUNTNEY, D., SAGANICH, M., VEGA-SAENZ, d.M. & RUDY, B. (1999). Molecular diversity of K^+ channels. *Ann. N.Y. Acad. Sci.* **868**, 233-285.

COHEN, I.S. & MULRINE N.K. (1986). Effects of thallium on membrane currents at diastolic potentials in canine cardiac purkinje strands. *J. Physiol. (Lond.)* **370**, 298

COLE K.S. (1949). Dynamic electrical characteristics of the squid axon membrane. *Arch. Sci. Physiol.* **3**, 253-258.

COLLINGRIDGE, G.L. & LESTER, R.A. (1989). Excitatory amino acid receptors in the vertebrate central nervous system. *Pharmacol. Rev.* **41**, 143-210.

CONNOR, M. & HENDERSON, G. (1996). delta- and mu-opioid receptor mobilization of intracellular calcium in SH-SY5Y human neuroblastoma cells. *Br. J. Pharmacol.* **117**, 333-340.

CONNOR, M., YEO, A. & HENDERSON, G. (1997). Neuropeptide Y Y2 receptor and somatostatin sst2 receptor coupling to mobilization of intracellular calcium in SH-SY5Y human neuroblastoma cells. *Br. J. Pharmacol.* **120**, 455-463.

COSENS, D.J. & MANNING, A. (1969). Abnormal electroretinogram from a Drosophila mutant. *Nature* **224**, 285-287.

COURTNEY, K.R. (1988). Local anesthetics. *Int. Anesthesiol. Clin.* **26**, 239-247.

COURTNEY, M.J., LAMBERT, J.J. & NICHOLLS, D.G. (1990). The interactions between plasma membrane depolarization and glutamate receptor activation in the regulation of cytoplasmic free calcium in cultured cerebellar granule cells. *J. Neurosci.* **10**, 3873-3879.

COVARRUBIAS, M., WEI, A., SALKOFF, L. & VYAS, T.B. (1994). Elimination of rapid potassium channel inactivation by phosphorylation of the inactivation gate. *Neuron* **13**, 1403-1412.

CREPEL, V., PANENKA, W., KELLY, M.E. & MACVICAR, B.A. (1998). Mitogen-activated protein and tyrosine kinases in the activation of astrocyte volume-activated chloride current. *J. Neurosci.* **18**, 1196-1206.

CRUZBLANCA H, KOH D-S & HILLE, B. (1998). Bradykinin inhibits M current via phospholipase C and Ca^{2+} release from IP_3-sensitive Ca^{2+} stores in rat sympathetic neurones. *Proc. Natl. Acad. Sci.U.S.A.* **95**, 7151-7156.

CULL-CANDY S.G., HOWE J.R. & OGDEN D. (1988). Noise and single channels activatd by excitatiry amino acids in rat cerebellar granule neurones. *J. Physiol. (Lond.)* **400**, 189-222.

CULL-CANDY S.G., MARSHALL C.G. & OGDEN D. (1989). Voltage-activated membrane currents in rat cerebellar granule neurones. *J. Physiol. (Lond.)* **414**, 179-199.

CURTIS H.J. & COLE K.S. (1940). Membrane action potentials from the squid giant axon. *J. Cell Comp. Physiol.* **15**, 147

CURTIS H.J. & COLE K.S. (1942). Membrane resting and action potentials from the squid giant axon. *J. Cell Comp. Physiol.* **19**, 135-144.

CURTIS, D.R., DUGGAN, A.W., FELIX, D., JOHNSTON, G.A., TEB, e.A. & WATKINS, J.C. (1972). Excitation of mammalian central neurones by acidic amino acids. *Brain Res.* **41**, 283-301.

DASCAL, N., LIM, N.F., SCHREIBMAYER, W., WANG, W., DAVIDSON, N. & LESTER, H.A. (1993). Expression of an atrial G-protein-activated potassium channel in Xenopus oocytes. *Proc. Natl. Acad. Sci. U.S .A.* **90**, 6596-6600.

DAWSON, A.P. (1997). Calcium signalling: how do IP3 receptors work? *Curr. Biol.* **7**, R544-R547

DEHAYE, J.P. (1995). Regulation by purinergic agonists of zinc uptake by rat submandibular glands. *J. Trace Elem. Med. Biol.* **9**, 94-101.

DEL RIO, E., MCLAUGHLIN, M., DOWNES, C.P. & NICHOLLS, D.G. (1999). Differential coupling of G-protein-linked receptors to Ca^{2+} mobilization through inositol(1,4,5)trisphosphate or ryanodine receptors in cerebellar granule cells in primary culture. *Eur. J. Neurosci.* **11**, 3015-3022.

DEL RIO, E., NICHOLLS, D.G. & DOWNES, C.P. (1994). Involvement of calcium influx in muscarinic cholinergic regulation of phospholipase C in cerebellar granule cells. *J. Neurochem.* **63**, 535-543.

DEL RIO, E., NICHOLLS, D.G. & DOWNES, C.P. (1996). Characterization of the effects of lithium and inositol on phosphoinositide turnover in cerebellar granule cells in primary culture. *J. Neurochem.* **66**, 517-524.

DELUCA, H.F. & ENGSTROM, G.W. (1961). Calcium uptake by rat kidney mitochondria. *Proc. Natl. Acad. Sci. U.S.A.* **47**, 1744-1750.

DOYLE, D.A., MORAIS, C.J., PFUETZNER, R.A., KUO, A., GULBIS, J.M., COHEN, S.L., CHAIT, B.T. & MACKINNON, R. (1998). The structure of the potassium channel: molecular basis of K^+ conduction and selectivity [see comments]. *Science* **280**, 69-77.

DUCHEN, M.R. (1990). Effects of metabolic inhibition on the membrane properties of isolated mouse primary sensory neurones. *J. Physiol. (Lond.)* **424**, 387-409.

DUCHEN, M.R. (1999). Contributions of mitochondria to animal physiology: from homeostatic sensor to calcium signalling and cell death. *J. Physiol. (Lond.)* **516 (Pt 1)**, 1-17.

DUPRAT, F., LESAGE, F., FINK, M., REYES, R., HEURTEAUX, C. & LAZDUNSKI, M. (1997). TASK, a human background K^+ channel to sense external pH variations near physiological pH. *EMBO J.* **16**, 5464-5471.

ECKERT, R. & CHAD, J.E. (1984). Inactivation of Ca channels. *Prog. Biophys. Mol. Biol.* **44**, 215-267.

ERTEL, E.A., CAMPBELL, K.P., HARPOLD, M.M., HOFMANN, F., MORI, Y., PEREZ-REYES, E., SCHWARTZ, A., SNUTCH, T.P., TANABE, T., BIRNBAUMER, L., TSIEN, R.W. & CATTERALL, W.A. (2000). Nomenclature of voltage-gated calcium channels. *Neuron* **25**, 533-535.

FAGNI, L., BOSSU, J.L. & BOCKAERT, J. (1994). Inhibitory effects of dihydropyridines on macroscopic K^+ currents and on the large-conductance $Ca(^{2+})$-activated K^+ channel in cultured cerebellar granule cells. *Pflugers Arch.* **429**, 176-182.

FATT, P. & KATZ B. (1953). The electrical properties of crustacean muscle fibres. *J. Physiol. (Lond).* **120**, 171-204.

FANGER, C.M., HOTH, M., CRABTREE, G.R. & LEWIS, R.S. (1995). Characterization of T cell mutants with defects in capacitative calcium entry: genetic evidence for the physiological roles of CRAC channels. *J. Cell Biol.* **131**, 655-667.

FAVATA, M.F., HORIUCHI, K.Y., MANOS, E.J., DAULERIO, A.J., STRADLEY, D.A., FEESER, W.S., VAN DYK, D.E., PITTS, W.J., EARL, R.A., HOBBS, F., COPELAND, R.A., MAGOLDA, R.L., SCHERLE, P.A. & TRZASKOS, J.M. (1998). Identification of a novel inhibitor of mitogen-activated protein kinase kinase. *J. Biol. Chem.* **273**, 18623-18632.

FICKER, E., TAGLIALATELA, M., WIBLE, B.A., HENLEY, C.M. & BROWN, A.M. (1994). Spermine and spermidine as gating molecules for inward rectifier K^+ channels. *Science* **266**, 1068-1072.

FINCH, E.A., TURNER, T.J. & GOLDIN, S.M. (1991). Calcium as a coagonist of inositol 1,4,5-trisphosphate-induced calcium release. *Science* **252**, 443-446.

FINK, M., DUPRAT, F., LESAGE, F., REYES, R., ROMEY, G., HEURTEAUX, C. & LAZDUNSKI, M. (1996). Cloning, functional expression and brain localization of a novel unconventional outward rectifier K^+ channel. *EMBO J.* **15**, 6854-6862.

FINK, M., LESAGE, F., DUPRAT, F., HEURTEAUX, C., REYES, R., FOSSET, M. & LAZDUNSKI, M. (1998). A neuronal two P domain K^+ channel stimulated by arachidonic acid and polyunsaturated fatty acids. *EMBO J.* **17**, 3297-3308.

FITZGERALD, E.M. (2000). Regulation of voltage-dependent calcium channels in rat sensory neurones involves a ras-mitogen-activated protein kinase pathway. *J. Physiol. (Lond.)* **527**, 433-444.

FOHRMAN, E.B., DE ERAUSQUIN, G., COSTA, E. & WOJCIK, W.J. (1993). Muscarinic m3 receptors and dynamics of intracellular Ca^{2+} cerebellar granule neurons. *Eur. J. Pharmacol.* **245**, 263-271.

FORTI, L., TOTTENE, A., MORETTI, A. & PIETROBON, D. (1994). Three novel types of voltage-dependent calcium channels in rat cerebellar neurons. *J. Neurosci.* **14**, 5243-5256.

FOZZARD, H.A. & HANCK, D.A. (1996). Structure and function of voltage-dependent sodium channels: comparison of brain II and cardiac isoforms. *Physiol. Rev.* **76**, 887-926.

FRANCESCONI, A. & DUVOISIN, R.M. (2000). Opposing effects of protein kinase C and protein kinase A on metabotropic glutamate receptor signaling: selective desensitization of the inositol trisphosphate/Ca^{2+} pathway by phosphorylation of the receptor-G protein-coupling domain. *Proc. Natl. Acad. Sci. U.S.A.* **97**, 6185-6190.

FRIEL, D.D. & TSIEN, R.W. (1994). An FCCP-sensitive Ca^{2+} store in bullfrog sympathetic neurons and its participation in stimulus-evoked changes in [Ca^{2+}]i. *J. Neurosci.* **14**, 4007-4024.

FUKAMAUCHI, F., HOUGH, C. & CHUANG, D.M. (1991). Expression and agonist-induced down-regulation of mRNAs of m2- and m3-muscarinic acetylcholine receptors in cultured cerebellar granule cells. *J. Neurochem.* **56**, 716-719.

FURUICHI, T., KOHDA, K., MIYAWAKI, A. & MIKOSHIBA, K. (1994). Intracellular channels [published erratum appears in Curr Opin Neurobiol 1994 Oct;4(5):758]. *Curr. Opin. Neurobiol.* **4**, 294-303.

FURUICHI, T., YOSHIKAWA, S., MIYAWAKI, A., WADA, K., MAEDA, N. & MIKOSHIBA, K. (1989). Primary structure and functional expression of the inositol 1,4,5-trisphosphate-binding protein P400. *Nature* **342**, 32-38.

GALIONE, A., LEE, H.C. & BUSA, W.B. (1991). Ca($^{2+}$)-induced Ca^{2+} release in sea urchin egg homogenates: modulation by cyclic ADP-ribose. *Science* **253**, 1143-1146.

GARCIA, M.L. & STREHLER, E.E. (1999). Plasma membrane calcium ATPases as critical regulators of calcium homeostasis during neuronal cell function. *Front Biosci* **4**, D869-D882

GOLDSTEIN, S.A., WANG, K.W., ILAN, N. & PAUSCH, M.H. (1998). Sequence and function of the two P domain potassium channels: implications of an emerging superfamily. *J. Mol. Med.* **76**, 13-20.

GOODWIN P.A., ASHMOLE I. & STANFIELD P.R. (2000). The ionic selectivity of the murine tandem pore potassium channel TASK-1, expressed in *Xenopus laevis* oocytes. *J. Physiol. (Lond.)* **527**, 129P.

GRAY, A.T., WINEGAR, B.D., LEONOUDAKIS, D.J., FORSAYETH, J.R. & YOST, C.S. (1998). TOK1 is a volatile anesthetic stimulated K^+ channel. *Anesthesiology* **88**, 1076-1084.

GREGORY, R.B. & BARRITT, G.J. (1996). Store-activated Ca^{2+} inflow in Xenopus laevis oocytes: inhibition by primaquine and evaluation of the role of membrane fusion. *Biochem. J.* **319**, 755-760.

GRYNKIEWICZ, G., POENIE, M. & TSIEN, R.Y. (1985). A new generation of Ca^{2+} indicators with greatly improved fluorescence properties. *J. Biol. Chem.* **260**, 3440-3450.

GUNTER, T.E., GUNTER, K.K., SHEU, S.S. & GAVIN, C.E. (1994). Mitochondrial calcium transport: physiological and pathological relevance. *Am. J. Physiol.* **267**, C313-C339

HACK, N. & BALAZS, R. (1995). Properties of AMPA receptors expressed in rat cerebellar granule cell cultures: Ca^{2+} influx studies. *J. Neurochem.* **65**, 1077-1084.

HAGIWARA S. & TAKAHASHI K (1974). The anomalous rectification and cation selectivity of the membrane of the starfish egg cell. *J. Membr. Biol.* **18**, 61-80.

HAJNOCZKY, G., ROBB, G.L., SEITZ, M.B. & THOMAS, A.P. (1995). Decoding of cytosolic calcium oscillations in the mitochondria. *Cell* **82**, 415-424.

HAJNOCZKY, G. & THOMAS, A.P. (1994). The inositol trisphosphate calcium channel is inactivated by inositol trisphosphate. *Nature* **370**, 474-477.

HALEY J.E., ABOGADIE F C, DELMAS P, DAYRELL M, VALLIS Y, MILLIGAN G, CAULFIELD, M.P., BROWN, D. & BUCKLEY N J (1998). The α subunit of G_q contributes to muscarinic inhibition of the M-type potassium current in sympathetic neurons. *J. Neurosci.* **18**, 4521-4531.

HALEY J.E., DELMAS P, OFFERMANNS S, ABOGADIE F C, SIMON M I, BUCKLEY N J & BROWN, D. (2000). Muscarinic Inhibition of calcium current and M current in $G\alpha_q$- deficient mice. *J. Neurosci.* **20**, 3973-3979.

HAMILL, O.P., MARTY, A., NEHER, E., SAKMANN, B. & SIGWORTH, F.J. (1981). Improved patch-clamp techniques for high-resolution current recording from cells and cell-free membrane patches. *Pflugers Arch.* **391**, 85-100.

HARNICK, D.J., JAYARAMAN, T., MA, Y., MULIERI, P., GO, L.O. & MARKS, A.R. (1995). The human type 1 inositol 1,4,5-trisphosphate receptor from T lymphocytes. Structure, localization, and tyrosine phosphorylation. *J. Biol. Chem.* **270**, 2833-2840.

HEGINBOTHAM, L., ABRAMSON, T. & MACKINNON, R. (1992). A functional connection between the pores of distantly related ion channels as revealed by mutant K^+ channels. *Science* **258**, 1152-1155.

HEGINBOTHAM, L., LU, Z., ABRAMSON, T. & MACKINNON, R. (1994). Mutations in the K^+ channel signature sequence. *Biophys. J.* **66**, 1061-1067.

HERRUP, K. & KUEMERLE, B. (1997). The compartmentalization of the cerebellum. *Annu. Rev. Neurosci.* **20**, 61-90.

HILLE, B. (1992) "Ionic Channels of excitable membranes." 2nd edition. Sinauer Associates, Sunderland, MA.

HILLE, B. (1973). Potassium channels in myelinated nerve. Selective permeability to small cations. *J. Gen. Physiol.* **61**, 669-686.

HIRANO, T., KUBO, Y. & WU, M.M. (1986). Cerebellar granule cells in culture: monosynaptic connections with Purkinje cells and ionic currents. *Proc. Natl. Acad. Sci. U.S.A.* **83**, 4957-4961.

HO, K., NICHOLS, C.G., LEDERER, W.J., LYTTON, J., VASSILEV, P.M., KANAZIRSKA, M.V. & HEBERT, S.C. (1993). Cloning and expression of an inwardly rectifying ATP-regulated potassium channel. *Nature* **362**, 31-38.

HOCKBERGER P.E., TSENG H-Y. & CONNOR J.A. (1987). Immunocytochemicaland electrophysiological differentiation of rat cerebellar granule cells in explant cultures. *J. Neurosci.* **7**, 1370-1383.

HODGKIN A.L. & HUXLEY A.F. (1939). Action potentials recorded from inside a nerve fibre. *Nature* **144**, 710-711.

HODGKIN A.L., HUXLEY A.F. & KATZ B. (1952). Measurements of current-voltage relations in the membrane of the giant squid axonof Loligo. *J. Physiol. (Lond.)* **116**, 424-448.

HODGKIN A.L. & KATZ B. (1949). The effect of sodium ions on the electrical activity of the giant axon of the squid. *J. Physiol. (Lond.)* **108**, 37-77.

HOLLMANN, M., HARTLEY, M. & HEINEMANN, S. (1991). Ca^{2+} permeability of KA-AMPA--gated glutamate receptor channels depends on subunit composition. *Science* **252**, 851-853.

HOTH, M., FANGER, C.M. & LEWIS, R.S. (1997). Mitochondrial regulation of store-operated calcium signaling in T lymphocytes. *J. Cell Biol.* **137**, 633-648.

HOTH, M. & PENNER, R. (1992). Depletion of intracellular calcium stores activates a calcium current in mast cells. *Nature* **355**, 353-356.

HUME, R.I., DINGLEDINE, R. & HEINEMANN, S.F. (1991). Identification of a site in glutamate receptor subunits that controls calcium permeability. *Science* **253**, 1028-1031.

IRVINE, R.F. (1990). 'Quantal' Ca^{2+} release and the control of Ca^{2+} entry by inositol phosphates--a possible mechanism. *FEBS Lett.* **263**, 5-9.

IRVING, A.J. & COLLINGRIDGE, G.L. (1998). A characterization of muscarinic receptor-mediated intracellular Ca^{2+} mobilization in cultured rat hippocampal neurones. *J. Physiol. (Lond.)* **511** , 747-759.

IRVING, A.J., COLLINGRIDGE, G.L. & SCHOFIELD, J.G. (1992a). Interactions between Ca^{2+} mobilizing mechanisms in cultured rat cerebellar granule cells. *J. Physiol. (Lond.)* **456**, 667-680.

IRVING, A.J., COLLINGRIDGE, G.L. & SCHOFIELD, J.G. (1992b). L-glutamate and acetylcholine mobilise Ca^{2+} from the same intracellular pool in cerebellar granule cells using transduction mechanisms with different Ca^{2+} sensitivities. *Cell Calcium* **13**, 293-301.

ISACOFF, E.Y., JAN, Y.N. & JAN, L.Y. (1990). Evidence for the formation of heteromultimeric potassium channels in Xenopus oocytes [see comments]. *Nature* **345**, 530-534.

JALONEN, T., JOHANSSON, S., HOLOPAINEN, I., OJA, S.S. & ARHEM, P. (1990). Single-channel and whole-cell currents in rat cerebellar granule cells. *Brain Res.* **535**, 33-38.

JAYARAMAN, T., ONDRIAS, K., ONDRIASOVA, E. & MARKS, A.R. (1996). Regulation of the inositol 1,4,5-trisphosphate receptor by tyrosine phosphorylation. *Science* **272**, 1492-1494.

JONES S., BROWN D.A., MILLIGAN G, WILLER E, BUCKLEY N J & CAULFIELD, M.P. (1995). Bradykinin excites rat sympathetic neurones by inhibition of M current through a mechanism involving B_2 receptors and $G_{\alpha q/11}$. *Neuron* **14**, 399-405.

JONES, G., BOYD, D.F., YEUNG, S.Y. & MATHIE, A. (2000). Inhibition of delayed rectifier K^+ conductance in cultured rat cerebellar granule neurons by activation of calcium-permeable AMPA receptors. *Eur. J. Neurosci.* **12**, 935-944.

JONGSMA, H.J. (1998). Sudden cardiac death: a matter of faulty ion channels? *Curr. Biol.* **8**, R568-R571

JOUAVILLE, L.S., ICHAS, F., HOLMUHAMEDOV, E.L., CAMACHO, P. & LECHLEITER, J.D. (1995). Synchronization of calcium waves by mitochondrial substrates in Xenopus laevis oocytes. *Nature* **377**, 438-441.

JOUAVILLE, L.S., PINTON, P., BASTIANUTTO, C., RUTTER, G.A. & RIZZUTO, R. (1999). Regulation of mitochondrial ATP synthesis by calcium: evidence for a long-term metabolic priming. *Proc. Natl. Acad. Sci. U.S.A.* **96**, 13807-13812.

KANMURA, Y., MISSIAEN, L., RAEYMAEKERS, L. & CASTEELS, R. (1988). Ryanodine reduces the amount of calcium in intracellular stores of smooth-muscle cells of the rabbit ear artery. *Pflugers Arch.* **413**, 153-159.

KARSCHIN, C., DISSMANN, E., STUHMER, W. & KARSCHIN, A. (1996). IRK(1-3) and GIRK(1-4) inwardly rectifying K^+ channel mRNAs are differentially expressed in the adult rat brain. *J. Neurosci.* **16**, 3559-3570.

KETCHUM, K.A., JOINER, W.J., SELLERS, A.J., KACZMAREK, L.K. & GOLDSTEIN, S.A. (1995). A new family of outwardly rectifying potassium channel proteins with two pore domains in tandem. *Nature* **376**, 690-695.

KIEDROWSKI, L. & COSTA, E. (1995). Glutamate-induced destabilization of intracellular calcium concentration homeostasis in cultured cerebellar granule cells: role of mitochondria in calcium buffering. *Mol. Pharmacol.* **47**, 140-147.

KIM, J.Y., YANG, M.S., OH, C.D., KIM, K.T., HA, M.J., KANG, S.S. & CHUN, J.S. (1999). Signalling pathway leading to an activation of mitogen-activated protein kinase by stimulating M3 muscarinic receptor. *Biochem. J.* **337**, 275-280.

KIM, Y., BANG, H. & KIM, D. (2000). TASK-3, a new member of the tandem pore $K(^+)$ channel family. *J. Biol. Chem.* **275**, 9340-9347.

KISELYOV, K., MIGNERY, G.A., ZHU, M.X. & MUALLEM, S. (1999). The N-terminal domain of the IP3 receptor gates store-operated hTrp3 channels. *Molecular Cell.* **4**, 423-429.

KISELYOV, K., XU, X., MOZHAYEVA, G., KUO, T., PESSAH, I., MIGNERY, G., ZHU, X., BIRNBAUMER, L. & MUALLEM, S. (1998). Functional interaction between InsP3 receptors and store-operated Htrp3 channels. *Nature* **396**, 478-482.

KRAPIVINSKY, G., GORDON, E.A., WICKMAN, K., VELIMIROVIC, B., KRAPIVINSKY, L. & CLAPHAM, D.E. (1995). The G-protein-gated atrial K^+ channel IKACh is a heteromultimer of two inwardly rectifying $K(^+)$-channel proteins. *Nature* **374**, 135-141.

KUBO, Y., BALDWIN, T.J., JAN, Y.N. & JAN, L.Y. (1993). Primary structure and functional expression of a mouse inward rectifier potassium channel [see comments]. *Nature* **362**, 127-133.

LEONOUDAKIS, D., GRAY, A.T., WINEGAR, B.D., KINDLER, C.H., HARADA, M., TAYLOR, D.M., CHAVEZ, R.A., FORSAYETH, J.R. & YOST, C.S. (1998). An open rectifier potassium channel with two pore domains in tandem cloned from rat cerebellum. *J. Neurosci.* **18**, 868-877.

LESAGE, F., GUILLEMARE, E., FINK, M., DUPRAT, F., LAZDUNSKI, M., ROMEY, G. & BARHANIN, J. (1996). TWIK-1, a ubiquitous human weakly inward rectifying K^+ channel with a novel structure. *EMBO J.* **15**, 1004-1011.

LESAGE, F. & LAZDUNSKI, M. (1998). Mapping of human potassium channel genes TREK-1 (KCNK2) and TASK (KCNK3) to chromosomes 1q41 and 2p23. *Genomics* **51**, 478-479.

LESAGE, F., TERRENOIRE, C., ROMEY, G. & LAZDUNSKI, M. (2000). Human TREK2, a 2P domain mechano-sensitive K^+ channel with multiple

regulations by polyunsaturated fatty acids, lysophospholipids and Gs-, Gi- and Gq-protein-coupled receptors. *J. Biol. Chem.* **275**, 28398-28405

LEUNG, Y.M., ZENG, W.Z., LIOU, H.H., SOLARO, C.R. & HUANG, C.L. (2000). Phosphatidylinositol 4,5-bisphosphate and intracellular pH regulate the ROMK1 potassium channel via separate but interrelated mechanisms. *J. Biol. Chem.* **275**, 10182-10189.

LEVITAN, I.B. (1999). It is calmodulin after all! Mediator of the calcium modulation of multiple ion channels. *Neuron* **22**, 645-648.

LEYSSENS, A., NOWICKY, A.V., PATTERSON, L., CROMPTON, M. & DUCHEN, M.R. (1996). The relationship between mitochondrial state, ATP hydrolysis, [Mg^{2+}], and [Ca^{2+}](i) studied in isolated rat cardiomyocytes. *J. Physiol. (Lond.)* **496**, 111-128.

LI, W.-C., TANG X-H, LI H-Z & WANG J-J (1999). Histamine excites rat cerebellar granule cells in vitro through H_1 and H_2 receptors. *J. Physiol. (Paris.)* **93**, 239-244.

LIU L-P (1996). Protein Kinase C and its Substrates. *Mol. Cell. Endo.* **116**, 1-29.

LLINAS, R., SUGIMORI, M., LIN, J.W. & CHERKSEY, B. (1989). Blocking and isolation of a calcium channel from neurons in mammals and cephalopods utilizing a toxin fraction (FTX) from funnel-web spider poison. *Proc. Natl. Acad. Sci. U.S.A.* **86**, 1689-1693.

LLINAS, R., SUGIMORI, M. & SILVER, R.B. (1992). Microdomains of high calcium concentration in a presynaptic terminal. *Science* **256**, 677-679.

LOPATIN, A.N., MAKHINA, E.N. & NICHOLS, C.G. (1994). Potassium channel block by cytoplasmic polyamines as the mechanism of intrinsic rectification. *Nature* **372**, 366-369.

MACKINNON, R. (1991). Determination of the subunit stoichiometry of a voltage-activated potassium channel. *Nature* **350**, 232-235.

MACKINNON, R. & MILLER, C. (1989). Mutant potassium channels with altered binding of charybdotoxin, a pore-blocking peptide inhibitor. *Science* **245**, 1382-1385.

MAINGRET, F., LAURITZEN, I., PATEL, A.J., HEURTEAUX, C., REYES, R., LESAGE, F., LAZDUNSKI, M. & HONORE, E. (2000). TREK-1 is a heat-activated background $K(^+)$ channel. *EMBO J.* **19**, 2483-2491.

MAINGRET, F., PATEL, A.J., LESAGE, F., LAZDUNSKI, M. & HONORE, E. (2000). Lysophospholipids open the two-pore domain mechano-gated $K(^+)$ channels TREK-1 and TRAAK. *J. Biol. Chem.* **275**, 10128-10133.

MANNUZZU, L.M., MORONNE, M.M. & ISACOFF, E.Y. (1996). Direct physical measure of conformational rearrangement underlying potassium channel gating. *Science* **271**, 213-216.

MANO, I. & TEICHBERG, V.I. (1998). A tetrameric subunit stoichiometry for a glutamate receptor-channel complex. *Neuroreport* **9**, 327-331.

MARBAN, E., YAMAGISHI, T. & TOMASELLI, G.F. (1998). Structure and function of voltage-gated sodium channels. *J. Physiol. (Lond.)* **508,** 647-657.

MARCHETTI, C., CARIGNANI, C. & ROBELLO, M. (1991). Voltage-dependent calcium currents in dissociated granule cells from rat cerebellum. *Neuroscience* **43**, 121-133.

MARKS, A.R., TEMPST, P., HWANG, K.S., TAUBMAN, M.B., INUI, M., CHADWICK, C., FLEISCHER, S. & NADAL-GINARD, B. (1989). Molecular cloning and characterization of the ryanodine receptor/junctional channel complex cDNA from skeletal muscle sarcoplasmic reticulum. *Proc. Natl. Acad. Sci. U.S.A.* **86**, 8683-8687.

MARRION N.V., SMART T.G., MARSH S.J. & BROWN, D. (1989). Muscarinic supression of the M-current in the rat sympathetic ganglion is mediated by receptors of the M_1-subtype. *Br. J. Pharmacol.* **98**, 557-573.

MARSH, S.J., TROUSLARD, J., LEANEY, J.L. & BROWN, D.A. (1995). Synergistic regulation of a neuronal chloride current by intracellular calcium and muscarinic receptor activation: a role for protein kinase C. *Neuron* **15**, 729-737.

MASGRAU, R., SERVITJA, J.M., SARRI, E., YOUNG, K.W., NAHORSKI, S.R. & PICATOSTE, F. (2000). Intracellular Ca^{2+} stores regulate muscarinic receptor stimulation of phospholipase C in cerebellar granule cells. *J. Neurochem.* **74**, 818-826.

MCCARRON, J.G. & MUIR, T.C. (1999). Mitochondrial regulation of the cytosolic Ca^{2+} concentration and the InsP3-sensitive Ca^{2+} store in guinea-pig colonic smooth muscle. *J. Physiol. (Lond.)* **516**, 149-161.

MCCORMACK, J.G., HALESTRAP, A.P. & DENTON, R.M. (1990). Role of calcium ions in regulation of mammalian intramitochondrial metabolism. *Physio. Rev.* **70**, 391-425.

MEERA, P., WALLNER, M., SONG, M. & TORO, L. (1997). Large conductance voltage- and calcium-dependent K^+ channel, a distinct member of voltage-dependent ion channels with seven N-terminal transmembrane segments (S0-S6), an extracellular N terminus, and an intracellular (S9-S10) C terminus. *Proc. Natl. Acad. Sci. U.S.A* **94**, 14066-14071.

MEIR, A. & DOLPHIN, A.C. (1998). Known calcium channel alpha1 subunits can form low threshold small conductance channels with similarities to native T-type channels. *Neuron* **20**, 341-351.

MIKOSHIBA, K., FURUICHI, T. & MIYAWAKI, A. (1994). Structure and function of IP3 receptors. *Semin. Cell Biol.* **5**, 273-281.

MOLECULAR PROBES product literature. http://www.probes.com/

MILLAR, J.A., BARRATT, L., SOUTHAN, A.P., PAGE, K.M., FYFFE, R.E.W., ROBERTSON, B. & MATHIE, A. (2000). A functional role for the two-pore domain potassium channel TASK-1 in cerebellar granule neurons., *Proc. Natl. Acad. Sci.U.S.A.* **97**, 3614-3618.

MONTELL, C. (1997). New light on TRP and TRPL. *Mol. Pharmacol.* **52**, 755-763.

MONTELL, C., JONES, K., HAFEN, E. & RUBIN, G. (1985). Rescue of the Drosophila phototransduction mutation trp by germline transformation. *Science* **230**, 1040-1043.

MORI, Y., FRIEDRICH, T., KIM, M.S., MIKAMI, A., NAKAI, J., RUTH, P., BOSSE, E., HOFMANN, F., FLOCKERZI, V. & FURUICHI, T. (1991). Primary structure and functional expression from complementary DNA of a brain calcium channel. *Nature* **350**, 398-402.

MYERS, E.W., SUTTON, G.G., DELCHER, A.L., DEW, I.M., FASULO, D.P., FLANIGAN, M.J., KRAVITZ, S.A., MOBARRY, C.M., REINERT, K.H., REMINGTON, K.A., ANSON, E.L., BOLANOS, R.A., CHOU, H.H., JORDAN, C.M., HALPERN, A.L., LONARDI, S., BEASLEY, E.M., BRANDON, R.C., CHEN, L., DUNN, P.J., LAI, Z., LIANG, Y., NUSSKERN, D.R., ZHAN, M., ZHANG, Q., ZHENG, X., RUBIN, G.M., ADAMS, M.D. & VENTER, J.C. (2000). A whole-genome assembly of Drosophila. *Science* **287**, 2196-2204.

NARAHASHI, T. (1996). Neuronal ion channels as the target sites of insecticides. *Pharmacol. Toxicol.* **79**, 1-14.

NEHER, E. (1992). Correction for liquid junction potentials in patch clamp experiments. *Methods Enzymol.* **207**, 123-131.

NETZEBAND, J.G., CONROY, S.M., PARSONS, K.L. & GRUOL, D.L. (1999). Cannabinoids enhance NMDA-elicited Ca^{2+} signals in cerebellar granule neurons in culture. *J. Neurosci.* **19**, 8765-8777.

NODA, M., SHIMIZU, S., TANABE, T., TAKAI, T., KAYANO, T., IKEDA, T., TAKAHASHI, H., NAKAYAMA, H., KANAOKA, Y. & MINAMINO, N. (1984). Primary structure of Electrophorus electricus sodium channel deduced from cDNA sequence. *Nature* **312**, 121-127.

NOWICKY, A.V. & DUCHEN, M.R. (1998). Changes in $[Ca^{2+}](i)$ and membrane currents during impaired mitochondrial metabolism in dissociated rat hippocampal neurons. *J. Physiol. (Lond.)* **507**, 131-145.

OBRENOVITCH, T.P. (1998). Neuroprotective strategies: voltage-gated Na^{+}-channel down-modulation versus presynaptic glutamate release inhibition. *Rev Neurosci* **9**, 203-211.

OLIVER, D., BAUKROWITZ, T. & FAKLER, B. (2000). Polyamines as gating molecules of inward-rectifier K^+ channels. *Eur. J. Biochem.* **267**, 5824-5829.

OPTICAN, L.M. & ROBINSON, D.A. (1980). Cerebellar-dependent adaptive control of primate saccadic system. *J. Neurophysiol.* **44**, 1058-1076.

PAPAZIAN, D.M., SCHWARZ, T.L., TEMPEL, B.L., JAN, Y.N. & JAN, L.Y. (1987). Cloning of genomic and complementary DNA from Shaker, a putative potassium channel gene from Drosophila. *Science* **237**, 749-753.

PAREKH, A.B., TERLAU, H. & STUHMER, W. (1993). Depletion of InsP3 stores activates a Ca^{2+} and K^+ current by means of a phosphatase and a diffusible messenger [see comments]. *Nature* **364**, 814-818.

PARKER, I. & YAO, Y. (1996). Ca^{2+} transients associated with openings of inositol trisphosphate-gated channels in Xenopus oocytes. *J. Physiol. (Lond.)* **491**, 663-668.

PEARSON, H.A., SUTTON, K.G., SCOTT, R.H. & DOLPHIN, A.C. (1995a). Characterization of Ca^{2+} channel currents in cultured rat cerebellar granule neurones. *J. Physiol. (Lond.)* **482**, 493-509.

PEARSON, H.A., SUTTON, K.G., SCOTT, R.H. & DOLPHIN, A.C. (1995b). Characterization of Ca^{2+} channel currents in cultured rat cerebellar granule neurones. *J. Physiol. (Lond.)* **482,** 493-509.

PEREZ-REYES, E., CRIBBS, L.L., DAUD, A., LACERDA, A.E., BARCLAY, J., WILLIAMSON, M.P., FOX, M., REES, M. & LEE, J.H. (1998). Molecular characterization of a neuronal low-voltage-activated T-type calcium channel. *Nature* **391**, 896-900.

PESSIA, M., TUCKER, S.J., LEE, K., BOND, C.T. & ADELMAN, J.P. (1996). Subunit positional effects revealed by novel heteromeric inwardly rectifying K^+ channels. *EMBO J.* **15**, 2980-2987.

PETERSEN, C.C. & BERRIDGE, M.J. (1994). The regulation of capacitative calcium entry by calcium and protein kinase C in Xenopus oocytes. *J. Biol. Chem.* **269**, 32246-32253.

PETERSEN, O.H., GALLACHER, D.V., WAKUI, M., YULE, D.I., PETERSEN, C.C. & TOESCU, E.C. (1991). Receptor-activated cytoplasmic Ca^{2+} oscillations in pancreatic acinar cells: generation and spreading of Ca^{2+} signals. *Cell Calcium* **12**, 135-144.

PETERSEN, O.H., GERASIMENKO, O.V., GERASIMENKO, J.V., MOGAMI, H. & TEPIKIN, A.V. (1998). The calcium store in the nuclear envelope. *Cell Calcium* **23**, 87-90.

PHILIPSON, K.D. & NICOLL, D.A. (2000). Sodium-calcium exchange: a molecular perspective. *Annu. Rev. Physiol.* **62**, 111-133.

PINTON, P., POZZAN, T. & RIZZUTO, R. (1998). The Golgi apparatus is an inositol 1,4,5-trisphosphate-sensitive Ca^{2+} store, with functional properties distinct from those of the endoplasmic reticulum. *EMBO J.* **17**, 5298-5308.

PROTHERO, L.S., RICHARDS, C.D. & MATHIE, A. (1998). Inhibition by inorganic ions of a sustained calcium signal evoked by activation of mGlu5 receptors in rat cortical neurons and glia. *Br. J. Pharmacol.* **125**, 1551-1561.

PUTNEY, J.W.J. (1977). Muscarinic, alpha-adrenergic and peptide receptors regulate the same calcium influx sites in the parotid gland. *J. Physiol. (Lond.)* **268**, 139-149.

PUTNEY, J.W.J. & MCKAY, R.R. (1999). Capacitative calcium entry channels. *Bioessays* **21**, 38-46.

RAE J., COOPER K., GATES P. & WATSKY M. (1991). Low access resistance perforated patch recordings using amphotericin B. *J. Neurosci. Methods* **37**: 15-26.

RAGSDALE, D.S. & AVOLI, M. (1998). Sodium channels as molecular targets for antiepileptic drugs. *Brain Res. Brain. Res. Rev.* **26**, 16-28.

RANDALL, A. & TSIEN, R.W. (1995). Pharmacological dissection of multiple types of Ca^{2+} channel currents in rat cerebellar granule neurons. *J. Neurosci.* **15**, 2995-3012.

RANDRIAMAMPITA, C. & TSIEN, R.Y. (1995). Degradation of a calcium influx factor (CIF) can be blocked by phosphatase inhibitors or chelation of Ca^{2+}. *J. Biol. Chem.* **270**, 29-32.

RETTIG, J., HEINEMANN, S.H., WUNDER, F., LORRA, C., PARCEJ, D.N., DOLLY, J.O. & PONGS, O. (1994). Inactivation properties of voltage-gated K^+ channels altered by presence of beta-subunit. *Nature* **369**, 289-294.

REUTER H & STEVENS C.F. (1980). Ion conductance and ion selectivity of potassium channles in snail neurones. *J. Membr. Biol.* **57**, 103-118.

REYES, R., DUPRAT, F., LESAGE, F., FINK, M., SALINAS, M., FARMAN, N. & LAZDUNSKI, M. (1998). Cloning and expression of a novel pH-sensitive two pore domain K^+ channel from human kidney. *J. Biol. Chem.* **273**, 30863-30869.

RIZZUTO, R., PINTON, P., CARRINGTON, W., FAY, F.S., FOGARTY, K.E., LIFSHITZ, L.M., TUFT, R.A. & POZZAN, T. (1998). Close contacts with the endoplasmic reticulum as determinants of mitochondrial Ca^{2+} responses. *Science* **280**, 1763-1766.

ROBB-GASPERS, L.D., BURNETT, P., RUTTER, G.A., DENTON, R.M., RIZZUTO, R. & THOMAS, A.P. (1998). Integrating cytosolic calcium signals into mitochondrial metabolic responses. *EMBO J.* **17**, 4987-5000.

ROBINSON, I.M. & BURGOYNE, R.D. (1991). Characterisation of distinct inositol 1,4,5-trisphosphate-sensitive and caffeine-sensitive calcium stores in digitonin-permeabilised adrenal chromaffin cells. *J. Neurochem.* **56**, 1587-1593.

RODEN, D.M. & GEORGE, A.L.J. (1997). Structure and function of cardiac sodium and potassium channels. *Am. J. Physiol.* **273**, H511-H525

ROSENBLUM, K., FUTTER, M., JONES, M., HULME, E.C. & BLISS, T.V. (2000). ERKI/II regulation by the muscarinic acetylcholine receptors in neurons. *J. Neurosci.* **20**, 977-985.

RUDY, B. (1988). Diversity and ubiquity of K channels. *Neuroscience* **25**, 729-749.

RYAN, J.S. & KELLY, M.E. (1998). Activation of a nonspecific cation current in rat cultured retinal pigment epithelial cells: involvement of a G(alpha i) subunit protein and the mitogen-activated protein kinase signalling pathway. *Br. J. Pharmacol.* **124**, 1115-1122.

SAGE, S.O. (1997). The Wellcome Prize Lecture. Calcium entry mechanisms in human platelets. *Exp. Physiol.* **82**, 807-823.

SAH, P. (1996). $Ca^{(2+)}$-activated K^+ currents in neurones: types, physiological roles and modulation. *Trends Neurosci.* **19**, 150-154.

SALINAS, M., REYES, R., LESAGE, F., FOSSET, M., HEURTEAUX, C., ROMEY, G. & LAZDUNSKI, M. (1999). Cloning of a new mouse two-P domain channel subunit and a human homologue with a unique pore structure. *J. Biol. Chem.* **274**, 11751-11760.

SAVIDGE, J.R. & BRISTOW, D.R. (1997). Distribution of $Ca^{(2+)}$-permeable AMPA receptors among cultured rat cerebellar granule cells. *Neuroreport* **8**, 1877-1882.

SCHREIBER, M. & SALKOFF, L. (1997). A novel calcium-sensing domain in the BK channel. *Biophys. J.* **73**, 1355-1363.

SCHREMPF, H., SCHMIDT, O., KUMMERLEN, R., HINNAH, S., MULLER, D., BETZLER, M., STEINKAMP, T. & WAGNER, R. (1995). A prokaryotic potassium ion channel with two predicted transmembrane segments from Streptomyces lividans. *EMBO J.* **14**, 5170-5178.

SELYANKO, A.A. & BROWN, D.A. (1996). Intracellular calcium directly inhibits potassium M channels in excised membrane patches from rat sympathetic neurons. *Neuron* **16**, 151-162.

SEOH, S.A., SIGG, D., PAPAZIAN, D.M. & BEZANILLA, F. (1996). Voltage-sensing residues in the S2 and S4 segments of the Shaker K^+ channel. *Neuron* **16**, 1159-1167.

SHAPIRA, H., LUPU-MEIRI, M., GERSHENGORN, M.C. & ORON, Y. (1990). Activation of two different receptors mobilizes calcium from distinct stores in Xenopus oocytes. *Biophys J.* **57**, 1281-1285.

SHENG, M. (1996). PDZs and receptor/channel clustering: rounding up the latest suspects. *Neuron* **17**, 575-578.

SIMPSON, P.B., CHALLISS, R.A. & NAHORSKI, S.R. (1993). Involvement of intracellular stores in the Ca^{2+} responses to N-Methyl-D-aspartate and depolarization in cerebellar granule cells. *J. Neurochem.* **61**, 760-763.

SIMPSON, P.B., CHALLISS, R.A. & NAHORSKI, S.R. (1995). Divalent cation entry in cultured rat cerebellar granule cells measured using Mn^{2+} quench of fura 2 fluorescence. *Eur. J. Neurosci.* **7**, 831-840.

SIMPSON, P.B., NAHORSKI, S.R. & CHALLISS, R.A. (1996). Agonist-evoked Ca^{2+} mobilization from stores expressing inositol 1,4,5-trisphosphate receptors and ryanodine receptors in cerebellar granule neurones. *J. Neurochem.* **67**, 364-373.

SINGER, D., BIEL, M., LOTAN, I., FLOCKERZI, V., HOFMANN, F. & DASCAL, N. (1991). The roles of the subunits in the function of the calcium channel. *Science* **253**, 1553-1557.

SITSAPESAN, R., MCGARRY, S.J. & WILLIAMS, A.J. (1995). Cyclic ADP-ribose, the ryanodine receptor and Ca^{2+} release. *Trends Pharmacol. Sci.* **16**, 386-391.

SLACK, B.E. (2000). The m3 muscarinic acetylcholine receptor is coupled to mitogen-activated protein kinase via protein kinase C and epidermal growth factor receptor kinase. *Biochem. J.* **348**, 381-387.

STARR, T.V., PRYSTAY, W. & SNUTCH, T.P. (1991). Primary structure of a calcium channel that is highly expressed in the rat cerebellum. *Proc. Natl. Acad. Sci. U.S.A.* **88**, 5621-5625.

STUHMER, W., STOCKER, M., SAKMANN, B., SEEBURG, P., BAUMANN, A., GRUPE, A. & PONGS, O. (1988). Potassium channels expressed from rat brain cDNA have delayed rectifier properties. *FEBS Lett.* **242**, 199-206.

SUGAWARA, H., KUROSAKI, M., TAKATA, M. & KUROSAKI, T. (1997). Genetic evidence for involvement of type 1, type 2 and type 3 inositol 1,4,5-trisphosphate receptors in signal transduction through the B-cell antigen receptor. *EMBO J.* **16**, 3078-3088.

SUTTON, K.G., MCRORY, J.E., GUTHRIE, H., MURPHY, T.H. & SNUTCH, T.P. (1999). P/Q-type calcium channels mediate the activity-dependent feedback of syntaxin-1A. *Nature* **401**, 800-804.

TALLEY, E.M., LEI, Q.B., SIROIS, J.E. & BAYLISS, D.A. (2000). TASK-1, a two-pore domain K^+ channel, is modulated by multiple neurotransmitters in motoneurons. *Neuron* **25**, 399-410.

TAN, Y.P. & MARTY, A. (1991). Protein kinase C-mediated desensitization of the muscarinic response in rat lacrimal gland cells. *J. Physiol. (Lond.)* **433**, 357-371.

TAYLOR P.S. (1987). Selectivity and patch measurement of A-current channels in *helix aspersa* neurones. *J. Physiol. (Lond.)* **388**, 437-447.

TAYLOR, C.P. & MELDRUM, B.S. (1995). Na^+ channels as targets for neuroprotective drugs. *Trends Pharmacol. Sci.* **16**, 309-316.

TEMPEL, B.L., PAPAZIAN, D.M., SCHWARZ, T.L., JAN, Y.N. & JAN, L.Y. (1987). Sequence of a probable potassium channel component encoded at Shaker locus of Drosophila. *Science* **237**, 770-775.

THAYER, S.A., HIRNING, L.D. & MILLER, R.J. (1988). The role of caffeine-sensitive calcium stores in the regulation of the intracellular free calcium concentration in rat sympathetic neurons in vitro. *Mol. Pharmacol.* **34**, 664-673.

THAYER, S.A. & MILLER, R.J. (1990). Regulation of the intracellular free calcium concentration in single rat dorsal root ganglion neurones in vitro. *J. Physiol. (Lond.)* **425**, 85-115.

THOMAS, D. & HANLEY, M.R. (1995). Evaluation of calcium influx factors from stimulated Jurkat T-lymphocytes by microinjection into Xenopus oocytes. *J. Biol. Chem.* **270**, 6429-6432.

TINEL, H., CANCELA, J.M., MOGAMI, H., GERASIMENKO, J.V., GERASIMENKO, O.V., TEPIKIN, A.V. & PETERSEN, O.H. (1999). Active mitochondria surrounding the pancreatic acinar granule region prevent spreading of inositol trisphosphate-evoked local cytosolic $Ca(^{2+})$ signals. *EMBO J.* **18**, 4999-5008.

TOESCU, E.C. (1998). Intraneuronal Ca^{2+} stores act mainly as a 'Ca^{2+} sink' in cerebellar granule neurones. *Neuroreport.* **9**, 1227-1231.

UEDA, H., MIYAMAE, T., HAYASHI, C., WATANABE, S., FUKUSHIMA, N., SASAKI, Y., IWAMURA, T. & MISU, Y. (1995). Protein kinase C involvement in homologous desensitization of delta-opioid receptor coupled to Gi1-phospholipase C activation in Xenopus oocytes. *J. Neurosci.* **15**, 7485-7499.

VACA, L., SINKINS, W.G., HU, Y., KUNZE, D.L. & SCHILLING, W.P. (1994). Activation of recombinant trp by thapsigargin in Sf9 insect cells. *Am. J. Physiol.* **267**, C1501-C1505

VELIMIROVIC, B.M., KOYANO, K., NAKAJIMA, S. & NAKAJIMA, Y. (1995). Opposing mechanisms of regulation of a G-protein-coupled inward rectifier K^+ channel in rat brain neurons. *Proc. Natl. Acad. Sci. U.S.A.* **92**, 1590-1594.

VERGARA, C., LATORRE, R., MARRION, N.V. & ADELMAN, J.P. (1998). Calcium-activated potassium channels. *Curr. Opin. Neurobiol.* **8**, 321-329.

VOILLEY, N., GALIBERT, A., BASSILANA, F., RENARD, S., LINGUEGLIA, E., COSCOY, S., CHAMPIGNY, G., HOFMAN, P., LAZDUNSKI, M. & BARBRY, P. (1997). The amiloride-sensitive Na^+ channel: from primary structure to function. *Comp. Biochem. Physiol. A. Physiol.* **118**, 193-200.

VOOGD, J. & GLICKSTEIN, M. (1998). The anatomy of the cerebellum. *Trends Neurosci.* **21**, 370-375.

WALKER, D., BICHET, D., GEIB, S., MORI, E., CORNET, V., SNUTCH, T.P., MORI, Y. & DE WAARD, M. (1999). A new beta subtype-specific interaction in alpha1A subunit controls P/Q-type Ca^{2+} channel activation. *J. Biol. Chem.* **274**, 12383-12390.

WANG, Y., SMALL, D.L., STANIMIROVIC, D.B., MORLEY, P. & DURKIN, J.P. (1997). AMPA receptor-mediated regulation of a Gi-protein in cortical neurons. *Nature* **389**, 502-504.

WATKINS, C.S. & MATHIE, A. (1994). Modulation of the gating of the transient outward potassium current of rat isolated cerebellar granule neurons by lanthanum. *Pflugers Arch.* **428**, 209-216.

WATKINS, C.S. & MATHIE, A. (1996). A non-inactivating K^+ current sensitive to muscarinic receptor activation in rat cultured cerebellar granule neurons. *J. Physiol. (Lond.)* **491**, 401-412.

WAXMAN, S.G. (1999). The molecular pathophysiology of pain: abnormal expression of sodium channel genes and its contributions to hyperexcitability of primary sensory neurons. *Pain*, S133-S140

WAXMAN, S.G., DIB-HAJJ, S., CUMMINS, T.R. & BLACK, J.A. (1999). Sodium channels and pain. *Proc. Natl. Acad. Sci. U.S.A.* **96**, 7635-7639.

WERTH, J.L. & THAYER, S.A. (1994). Mitochondria buffer physiological calcium loads in cultured rat dorsal root ganglion neurons. *J. Neurosci.* **14**, 348-356.

WES, P.D., CHEVESICH, J., JEROMIN, A., ROSENBERG, C., STETTEN, G. & MONTELL, C. (1995). TRPC1, a human homolog of a Drosophila store-operated channel. *Proc. Natl. Acad. Sci. U.S.A.* **92**, 9652-9656.

WHITE, R.J. & REYNOLDS, I.J. (1995). Mitochondria and Na^+/Ca^{2+} exchange buffer glutamate-induced calcium loads in cultured cortical neurons. *J. Neurosci.* **15**, 1318-1328.

WHITHAM, E.M., CHALLISS, R.A. & NAHORSKI, S.R. (1991). M3 muscarinic cholinoceptors are linked to phosphoinositide metabolism in rat cerebellar granule cells. *Eur. J. Pharmacol.* **206**, 181-189.

XIA, X.M., FAKLER, B., RIVARD, A., WAYMAN, G., JOHNSON-PAIS, T., KEEN, J.E., ISHII, T., HIRSCHBERG, B., BOND, C.T., LUTSENKO, S.,

MAYLIE, J. & ADELMAN, J.P. (1998). Mechanism of calcium gating in small-conductance calcium-activated potassium channels. *Nature* **395** , 503-507.

XU, X.Z.S., LI, H.S., GUGGINO, W.B. & MONTELL, C. (1997). Coassembly of TRP and TRPL produces a distinct store-operated conductance. *Cell* **89**, 1155-1164.

YANG, J., JAN, Y.N. & JAN, L.Y. (1995). Determination of the subunit stoichiometry of an inwardly rectifying potassium channel. *Neuron* **15**, 1441-1447.

YAO, Y., FERRERMONTIEL, A.V., MONTAL, M. & TSIEN, R.Y. (1999). Activation of store-operated Ca^{2+} current in Xenopus oocytes requires SNAP-25 but not a diffusible messenger. *Cell* **98**, 475-485.

YU, S.P., O'MALLEY, D.M. & ADAMS, P.R. (1994). Regulation of M current by intracellular calcium in bullfrog sympathetic ganglion neurons. *J. Neurosci.* **14**, 3487-3499.

ZHU, X., CHU, P.B., PEYTON, M. & BIRNBAUMER, L. (1995). Molecular cloning of a widely expressed human homologue for the Drosophila trp gene. *FEBS Lett.* **373**, 193-198.

ZITT, C., OBUKHOV, A.G., STRUBING, C., ZOBEL, A., KALKBRENNER, F., LUCKHOFF, A. & SCHULTZ, G. (1997). Expression of TRPC3 in Chinese hamster ovary cells results in calcium-activated cation currents not related to store depletion. *J. Cell Biol.* **138**, 1333-1341.

ZWEIFACH, A. & LEWIS, R.S. (1993). Mitogen-regulated Ca^{2+} current of T lymphocytes is activated by depletion of intracellular Ca^{2+} stores. *Proc. Natl. Acad. Sci. U.S.A.* **90**, 6295-6299.

PUBLICATIONS

The following publications have been obtained as a result of some of the work presented in this report.

Abstracts

BOYD, D.F., McMAHON, R., MILLAR, J.A. & MATHIE A. (1999). Characterisation of the calcium influx induced by the protonophore CCCP across the plasma membrane of cultured rat cerebellar granule neurons. *J. Physiol.* **520**, 38-39P.

BOYD, D.F. & MATHIE A. (2000). Characterisation of the role of the endoplasmic reticulum calcium store in cultured rat cerebellar granule neurons. *J.Physiol.* **523,** 29P.

BOYD, D.F. & MATHIE A. (2000). Inhibition of IK_{SO} by the inhibitors of mitogen activated protein kinase activation, PD 98059 and U 0126, in rat cerebellar granule neurons. *J. Physiol.* **528**, 35P.

Articles

JONES, G., BOYD, D.F., YEUNG, S.Y. & MATHIE, A. (2000). Inhibition of delayed rectifier K^+ conductance in cultured rat cerebellar granule neurons by activation of calcium-permeable AMPA receptors. *Eur J Neurosci* **12**, 935-944.

BOYD, D.F., MILLAR, J.A., WATKINS, C.S. & MATHIE A. (2000). The role of Ca^{2+} stores in the muscarinic inhibition of the K+ current IK_{SO} in neonatal rat cerebellar granule cells. *J. Physiol.* **529,** 231-331.